Engineering Geologic, Geophysical, Hydrologic, and Rock-Mechanics Investigations of the Straight Creek Tunnel Site and Pilot Bore, Colorado

---

GEOLOGICAL SURVEY PROFESSIONAL PAPER 815

Engineering Geologic, Geophysical, Hydrologic and Rock-Mechanics Investigations of the Straight Creek Tunnel Site and Pilot Bore, Colorado

GEOLOGICAL SURVEY PROFESSIONAL PAPER 815

UNITED STATES GOVERNMENT PRINTING OFFICE, WASHINGTON : 1974

UNITED STATES DEPARTMENT OF THE INTERIOR

ROGERS C. B. MORTON, *Secretary*

GEOLOGICAL SURVEY

V. E. McKelvey, *Director*

Library of Congress catalog-card No. 73-600330

For sale by the Superintendent of Documents, U.S. Government Printing Office
Washington, D.C. 20402 – Price $5.55 (paper cover)
Stock Number 2401-02477

PREFACE

Tunnels are among the most expensive of engineering structures. They can, and often do, present great difficulties in design and construction. For several decades the techniques used in tunneling have lagged behind those used in other fields of engineering. An engineer, for example, can design a bridge so that it will adequately and economically fulfill its proper function. The design and construction of underground openings commonly is a far different situation. The stresses surrounding a planned underground opening are generally unknown quantities, as are the nature and behavior of the rock mass itself. Therefore, judgment and trial and error prevail; design, in its true sense, becomes impossible; and safety factors can be uneconomically large or dangerously small.

Geological factors exert a decisive influence on the difficulties and costs of tunnel construction. Tunnel hazards — unanticipated sources of expense and delay — are caused largely by the divergence of structural details of a given rock mass from the statistical average for similar rock masses. This variation in rock structure results in erratic tunneling costs; the cost of a tunnel may be considerably higher than the average cost of similar tunnels constructed in similar bodies of rock. A competent experienced geologist usually can predict the kinds of difficulties that would be encountered in different parts of a proposed tunnel, but he seldom can quantitatively evaluate the difficulties. On such a basis, preliminary estimates for materials and equipment for constructing a tunnel commonly involve considerable guesswork. This guesswork usually results in the procurement of unnecessary supplies to offset the possibility of facing an emergency with inadequate provisions.

The present (1972) state of tunnel art combines experience and intuition with theoretical and practical principles to design and construct underground openings. We believe that in the future the fullest use of rock-mass information, together with improved theory, will result in greater economy, safety, and confidence in tunnel construction. It is toward this goal that the present report is directed.

The Straight Creek Tunnel is about 55 miles west of Denver. The proximity of this tunnel to the research center of the U.S. Geological Survey in Denver offered an unusual opportunity to utilize the personnel and facilities of the Survey on the problems of defining the environment of the proposed tunnel. The authors were able to consult with, and have the services of, experts in nearly every field of geology. As a result, research investigations in the tunnel area were conducted by many survey personnel. The investigations performed in conjunction with the basic geologic investigations, such as geophysical and ground-water research, are described in separate chapters by those who directed the research.

At the dedication of the first of the twin bores on March 8, 1973, the Colorado Division of Highways, in accordance with a resolution passed by the General Assembly of Colorado, officially named the tunnel the Eisenhower Memorial Tunnel.

CONTENTS

[Letters in parentheses preceeding titles designate the chapters]

ILLUSTRATIONS

[Plates are in pocket]

TABLES

ENGINEERING GEOLOGIC, GEOPHYSICAL, HYDROLOGIC, AND ROCK-MECHANICS INVESTIGATIONS OF THE STRAIGHT CREEK TUNNEL SITE AND PILOT BORE, COLORADO

By CHARLES S. ROBINSON, FITZHUGH T. LEE, and others

ABSTRACT

The Straight Creek Tunnel, planned as a twin-bore vehicular tunnel, will carry Interstate Highway 70 beneath the Continental Divide about 55 miles west of Denver, Colo. The pilot bore, to be enlarged for the eastbound highway tunnel, is about 8,350 feet long, 13 feet in diameter, and about 11,000 feet above sea level. The final bores will be the highest highway tunnels in the world and the first interstate highway tunnels to cross the Continental Divide. The need for a highway tunnel under the divide has increased in recent years. The Colorado Department of Highways, beginning in 1932, made studies to locate the most feasible tunnel route through the mountains. Independent studies in 1956 and 1960 indicated that the Straight Creek–Loveland basin area was the best of several possible tunnel routes. This route is advantageous because it will eliminate a climb of 990 feet, as well as avoid hazardous avalanche areas, and it will shorten by 10 miles the highway distance between Loveland basin and Dillon. The Colorado Department of Highways estimates savings of $7 million (1964) annually to motorists using the tunnel.

In June 1962 the U.S. Geological Survey with the cooperation of the Colorado Department of Highways began a detailed geological and geophysical study of the Straight Creek–Loveland basin area. Emphasis was placed on the definition of underground conditions for a pilot bore whose location was predetermined. An area of about 6 square miles was mapped geologically at a scale of 1:12,000. Geologic and geophysical logs were made of two diamond-drill holes near the proposed tunnel line, and a seismic survey was made at the surface along the tunnel line. Physical properties tests supplemented the fieldwork. The investigations were concerned mainly with predicting the kinds of conditions, as well as their extent and approximate location, that could be expected at tunnel level.

The tunnel is in the Loveland Pass–Berthoud Pass shear zone, which is about 2 miles wide, trends north-northeast, and is composed of Precambrian granitic and metasedimentary rocks that are moderately to intensely sheared. The granitic rocks are medium to fine grained and consist of about equal parts of quartz, potassium feldspar, and plagioclase feldspar, and 5–15 percent biotite. The metasedimentary rocks consist of various biotite gneisses. Where the bedrock is not faulted or sheared, its strength depends upon the amount and orientation of biotite and chlorite. In shear zones the granite is more competent than the gneisses. Faults and shear zones are the most important structural features from the standpoint of tunnel driving.

By using field and laboratory data, it was possible to construct a statistical model of the geology at pilot-bore level. This model was used to predict rock loads, spacing of sets, amount of lagging and blocking, sections of the tunnel requiring feeler holes, rates of water flows, and amount of grout necessary to seal badly broken ground saturated with water. The Colorado Department of Highways made this information available to prospective bidders. A contract for $1,300,000 was awarded Mid-Valley, Inc., for construction of the pilot bore, and they started construction in October 1963. The pilot bore was holed through in December 1964 at a cost of about $1,400,000.

During construction of the pilot bore, geologic, geophysical, hydrologic, and rock-mechanics instrumentation programs were conducted. The purpose of these studies was to determine the relation between, and to evaluate methods of measuring the relation between, geologic conditions and the engineering practices in the design and construction stages of a tunnel.

The walls of the pilot bore were mapped geologically at 1 inch to 50 feet. The face, as it was advanced, was mapped once during each shift (8 hours) at a scale of 1 inch to 2 feet. In support of the rock-mechanics instrumentation and geophysical programs, geologic maps were made of one wall or the other at 1 inch to 5 feet for a 50-foot distance on each side of an instrument or geophysical station. Samples were systematically collected during the geologic mapping. Hand samples were collected for petrographic analyses; altered wallrock and fault-gouge samples were collected for determination of swelling pressure and clay mineralogy; chip samples were collected over a 5-foot distance on each side of instrument stations for chip-size and mineral analyses; and blocks of wallrocks about 1 foot in largest dimension were collected and cored in the laboratory for determination, by dynamic and static tests, of elastic properties. As the construction of the pilot bore progressed and the results of the rock-mechanics investigations became available, it became apparent that the distribution and amount of wooden blocking between the steel sets and the wallrock directly influenced the loads supported by the sets. As a result, the wooden blocking around each instrumented set was mapped at 1 inch to 2 feet.

Geophysical investigations during construction of the pilot bore consisted of measurements of wallrock temperature, seismic refraction, and electrical resistivity. The wallrock temperatures, which were measured in water-filled drill holes about every 500 feet along the pilot bore, ranged from 4.2°C (39.6°F) to 10.5°C (50.9°F).

Seismic-refraction and electrical-resistivity measurements along the walls of the pilot bore indicated that both a low-velocity layer and a high-resistivity layer exist in the disturbed rock surrounding the excavation. Seismic measurements were analyzed to obtain the thickness and seismic velocity of rock in the low-velocity layer, the velocity of rock behind this layer, and the amplitude of seismic energy received at the detectors. Electrical-resistivity measurements were analyzed to obtain the thickness and electrical resistivity of the high-resistivity layer and the resistivity of rock behind the layer. The electrical resistivity and the seismic velocity correlated well with the following parameters, all of which are important in tunnel construction: Height of tension arch, stable vertical rock load, rock quality, rate of construction and cost per foot, percentage lagging and blocking, set spacing, and type of steel support required. Results indicated the possibility of predicting, from geophysical measurements, economic and engineering aspects of tunnel construction. Further investigation in other tunnels would determine whether similar correlations exist in different geologic environments. The accuracy of predictions based on surface geophysical measurements was tested by making seismic and resistivity surveys on the surface and in holes drilled from the surface along the line of the pilot bore. Results indicated that reasonably accurate predic-

tions are possible from surface measurements. Greater accuracy and more detailed information would be obtained if predictions were based on geophysical logging measurements made in feeler holes drilled ahead of an advancing tunnel face.

Hydrologic investigations consisted of maintenance of a recording flume near the portal of the pilot bore, periodic measurements of flows for different intervals of the tunnel, estimates of water flows from feeler holes and fractures, water-pressure measurements, study of an observation well adjacent to the tunnel line at the surface, and determinations of the chemical characteristics of the water flowing into the tunnel. It was determined that occurrence of water-bearing zones in the granitic and metasedimentary rocks is directly related to fracture spacing. Rocks that have a fracture spacing of 0.1−0.5 foot are major water producers; those that have a spacing of 0.5−1 foot are secondary producers. Shear zones have fracture spacings of less than 0.1 foot and are much less permeable because clay associated with the extensive alteration impedes movement of water. Competent rocks that have a fracture spacing greater than 1 foot lack the necessary porosity and permeability to yield significant quantities of water. Ground water in the pilot bore is in two zones — an active zone and a passive zone. The zones are differentiated on the bases of changes in rate of discharge with changes in season and on differences in the chemical quality of the water. Results of the hydrologic investigations indicate that the following factors should be considered when new bores are driven in similar areas: (1) The tunnel should be started in late fall or early winter, when discharge from the active zone is at a minimum; (2) water pockets in the passive zone should be allowed to drain because of short discharge time; and (3) the active zone, as well as sections in the passive zone having a fracture spacing of 0.1−1 foot, should be grouted.

Rock-mechanics instruments were installed in the pilot bore by Terrametrics, Inc., for the purpose of measuring the loads on the supports and for the determination of strain rates and total strain around the pilot bore. Two types of instruments — electronic load cells and borehole extensometers — were installed at 44 instrument stations. The load cells were placed between the legs of the sets and the foot blocks, and at a few stations they were also placed in horizontal positions in the crown of the sets and between the legs and invert struts to measure horizontal loads. The borehole extensometers, which were of single- and multiple-anchor types, were placed in boreholes, generally 25 feet deep, drilled into the roof and walls of the pilot bore. From the load-cell and extensometer data it was possible to calculate the total maximum and stable loads, in pounds; the maximum and stable geologic rock loads, in pounds per square foot; the wall and arch deflections, in inches; and the height of the tension arch, in feet; and to relate these factors to the geologic conditions and the engineering practices in the pilot bore. Maximum loads developed where the apparent dip of faults and shear zones was about 45°. The loads were less where the apparent dips were either greater or less than 45°.

Elastic theory usually provides an inaccurate description of the mechanics of deformation of the rock mass around a tunnel. A more accurate and complete description of the deformation requires the analysis and interpretation of the controlling geologic and construction conditions. Computer techniques were used to analyze the inelastic geologic and construction controls on tunnel mechanics. Statistical models were constructed which describe the mechanism of load transfer and rock strain associated with the advancing pilot-bore face. The geologic and construction factors that influence and rock-mass stabilization time and the loads carried by the steel sets are (1) average fracture spacing, (2) degree of faulting and shearing, (3) percentage of alteration, (4) thickness of nearest fault zone, (5) rate of ground-water flow, (6) average dip of joints, (7) rock type, (8) average pilot-bore advance rate during the period preceding stabilization, (9) the size and spacing of steel sets, and (10) the composite construction variable of steel section modulus plus number of effective blocking points. Depth of the pilot bore and distance to the nearest fault were not significant to the determination of rock loads. The transfer of rock loads to tunnel walls and the subsequent stabilization of the rock mass adjacent to and along an active tunnel occur at a much later time and at a much greater distance than anticipated by elastic theory.

A comparison of predictions based on the statistical model of the geology and findings from the pilot bore shows satisfactory agreement as to the percentages of different rock types, fracture spacings and faults and shear zones, in percent of pilot-bore length, as well as rock loads, attitudes of foliation, faults, and joints, swell pressures of gouge, spacing of sets, and amount of lagging and blocking. Ground-water quantities agreed with predicted quantities, although hydrologic conditions differed from those predicted. In less satisfactory agreement were the number of linear feet of feeler holes and the amount of grout necessary.

Introduction

By CHARLES S. ROBINSON *and* FITZHUGH T. LEE

ENGINEERING GEOLOGIC, GEOPHYSICAL, HYDROLOGIC, AND ROCK-MECHANICS INVESTIGATIONS OF THE STRAIGHT CREEK TUNNEL SITE AND PILOT BORE, COLORADO

GEOLOGICAL SURVEY PROFESSIONAL PAPER 815–A

ENGINEERING GEOLOGIC, GEOPHYSICAL, HYDROLOGIC, AND ROCK-MECHANICS INVESTIGATIONS OF THE STRAIGHT CREEK TUNNEL SITE AND PILOT BORE, COLORADO

INTRODUCTION

By CHARLES S. ROBINSON and FITZHUGH T. LEE

The Straight Creek Tunnel is being constructed through the Continental Divide about 55 miles west of Denver (figs. 1, 2). The purpose of the tunnel is to carry traffic on Interstate Highway 70 under the Continental Divide, and so eliminate the need to use Loveland Pass on the present U.S. Highway 6. The east portal is in Loveland basin near the head of Clear Creek, in Clear Creek County. The west portal is near the head of Straight Creek, in Summit County. The tunnel will be about 8,400 feet long and will consist of twin bores, each containing two driving lanes. The geologic investigations of the Straight Creek Tunnel site were directly concerned with the construction of a pilot bore, which was driven to determine the feasibility of constructing the twin-bore tunnel at this site.

HISTORY OF TUNNEL LOCATION

The people of Colorado have long wanted an all-weather transportation route from the eastern slope to the western slope of the Continental Divide in Colorado. Since the earliest days of mining in Colorado, the Continental Divide has acted as a barrier to the transportation of raw materials mined and produced on the western slope to the markets on the eastern slope and transportation of supplies and tools from the eastern slope to the producing areas on the western slope. The problem was partly solved by the construction of railroads in the late 1800's and the early 1900's. The first tunnel through the Continental Divide in Colorado was the Alpine Tunnel constructed by the Denver, South Park, and Pacific Railroad (narrow-gage) in 1883 to carry rail traffic

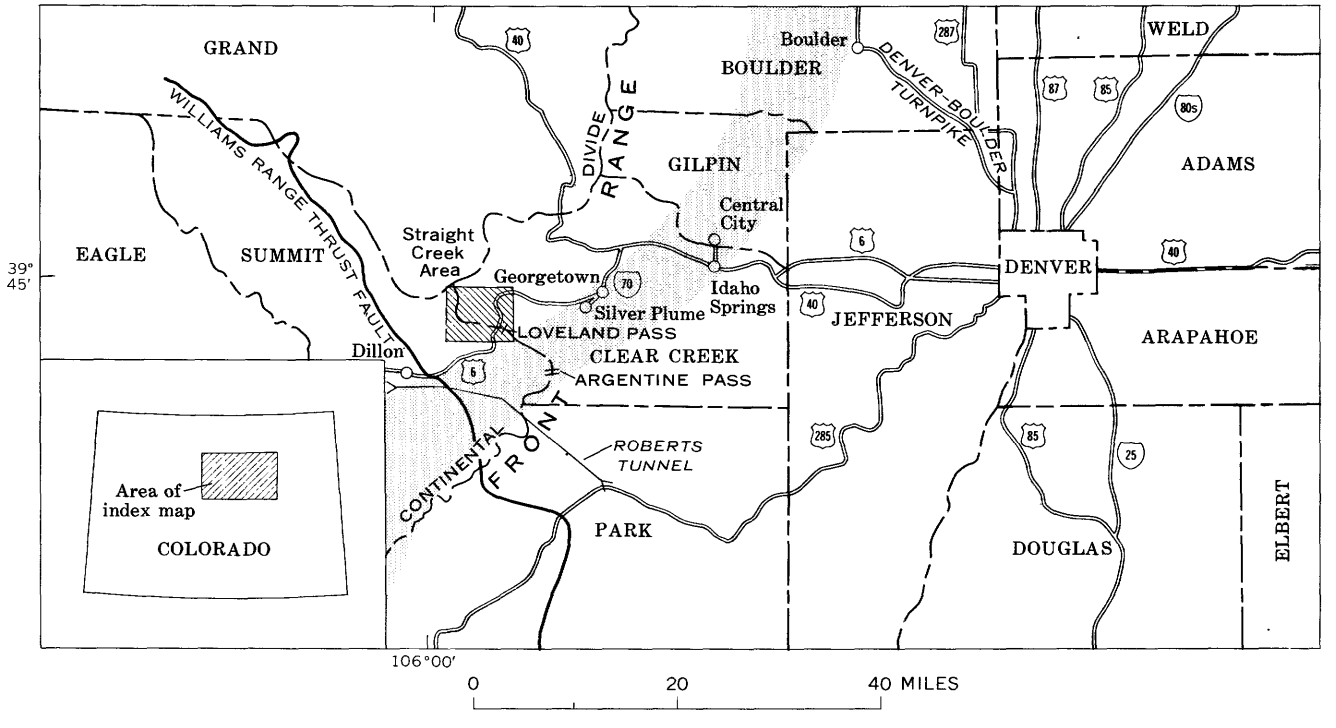

FIGURE 1. — Index map of part of Colorado, showing location of the Straight Creek Tunnel area. Shaded area indicates approximate location of Colorado mineral belt.

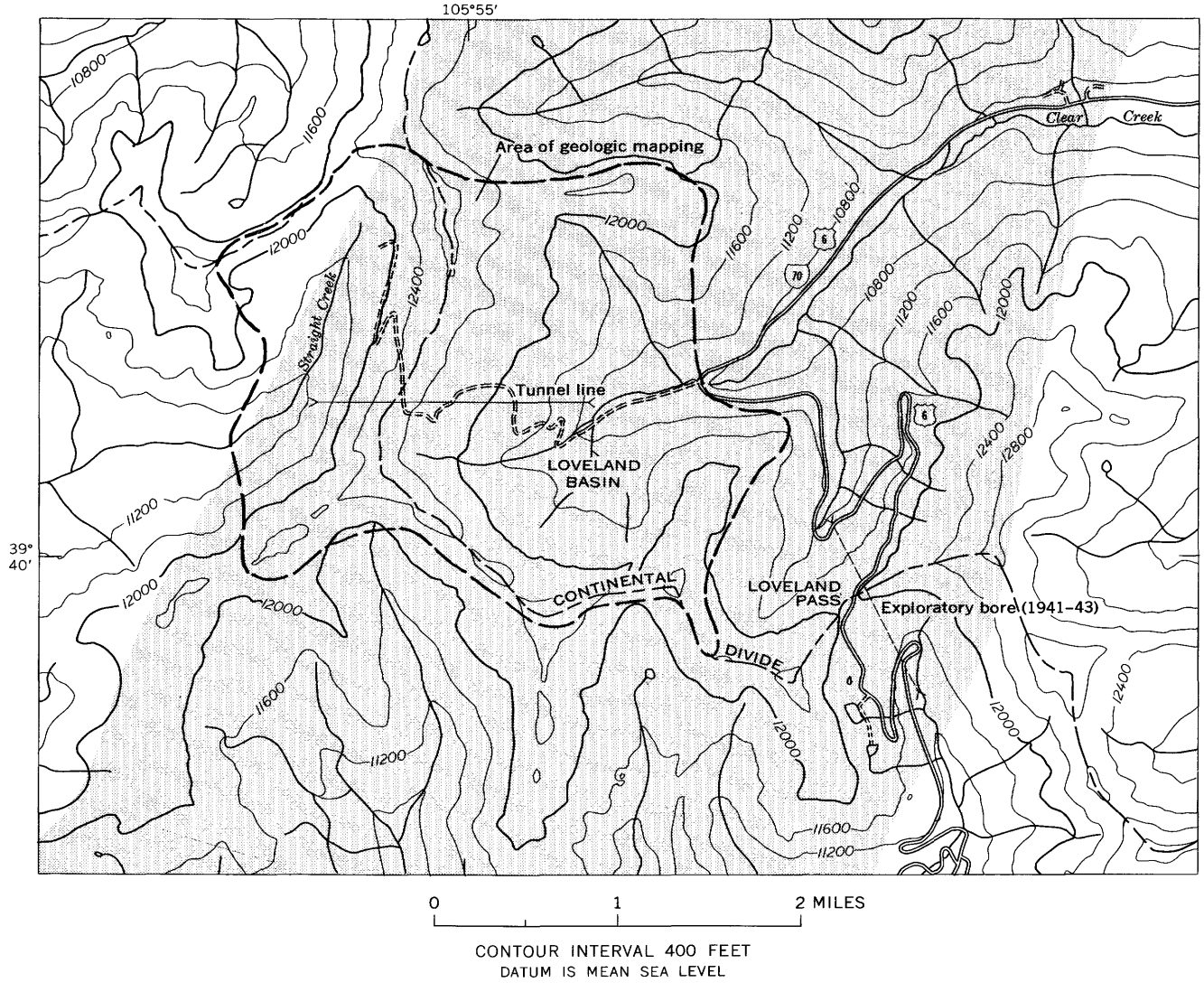

FIGURE 2. — Generalized topographic map of the Straight Creek Tunnel area. Base from U.S. Geological Survey Loveland Pass quadrangle, 1:24,000, 1958. Shaded area indicates approximate location of Loveland Pass-Berthoud Pass fault zone.

through the Sawatch Range between Buena Vista and Gunnison, Colo. The most famous of the railroad tunnels and the only one still in use through the Continental Divide in Colorado is the Moffat Tunnel (Lovering, 1928, p. 337–345), which was completed by the Moffat Tunnel Commission in 1928.

The first wagon road over Loveland Pass was completed about 1870. The road was abandoned in 1906 and was not restored until 1920. This wagon road was made a motor highway in 1931. A hard-surfaced highway was finally completed in 1950. To overcome the great differences in elevation between the head of Clear Creek valley and the summit of the Continental Divide, the highway is benched into the steep mountain slopes. This alinement requires many switchbacks that have small-radius curves, resulting in several miles of adverse travel at low operating speeds.

Highway travel over the Continental Divide is hazardous at best. Blizzards and avalanches are common during the winter, spring, and fall, and snow flurries can be expected even during the summer. The deep snow accumulation on Loveland Pass has presented a difficult and continuing maintenance problem. Snow usually begins falling and accumulating during late October or early November, with peak accumulations of as much as 250 inches occurring by late March or early April. There are several well-defined avalanche areas on the approach to Loveland Pass. Through continuing study and experience, the Colorado Department of Highways has developed techniques and procedures whereby roads can be maintained in passable condition throughout the snowfall season.

The first surveys for an automobile tunnel through the Continental Divide were started in 1932, and others were made in 1940 and 1941. An exploratory bore under Loveland Pass, about 1 mile south of the Straight Creek Tunnel site (figs. 1, 2), was started in 1941 and completed in 1943. This bore was about 7 feet in diameter and 5,500 feet

long. Because of adverse geologic conditions encountered and problems in financing, a full-diameter tunnel was never constructed. During 1943–60 the Colorado Department of Highways investigated several possible tunnel sites through the Continental Divide. One of these was the Straight Creek Tunnel site, where four diamond-drill holes were drilled and cored in 1955. The E. Lionel Pavlo Engineering Co. (1960) recommended the Straight Creek site for twin tunnels to carry Interstate Highway 70 through the Continental Divide. The contract for construction of a pilot bore at the Straight Creek Tunnel site was awarded to Mid-Valley, Inc., Houston, Tex., in October 1963. They started construction on October 21, 1963, and completed the pilot bore on December 8, 1964. The pilot bore was driven along the proposed centerline of the eastbound bore of the planned twin-bore highway tunnel.

The Straight Creek Tunnel will reduce the travel distance from Loveland basin to Dillon by 10 miles and will eliminate a climb of about 990 feet. Equally important, the route through the tunnel will bypass several avalanche areas that are on the present route. The Colorado Department of Highways estimated (1964) that the savings to motorists using the tunnel will be about $7 million per year.

PURPOSE OF GEOLOGIC INVESTIGATIONS

The cost of constructing underground openings in the Rocky Mountains — and in many other areas of the United States and the world — usually has exceeded, sometimes by a wide margin, the amount estimated. The increased cost can almost always be attributed to the presence of geologic conditions that, from an engineering point of view, either were not known or were not fully understood before the start of construction.

In 1960 the U.S. Geological Survey started a post-construction study of the geology of the Harold D. Roberts Tunnel and the relation of the geology to the construction of the tunnel. This tunnel, which was constructed by the Denver Board of Water Commissioners to bring water from the west side of the Continental Divide to the east side, is about 23 miles long and is located about 5 miles south of the proposed Straight Creek Tunnel. The study of the Roberts Tunnel was under the direction of E. E. Wahlstrom, who was assisted by L. A. Warner and by the senior author. Wahlstrom and Warner served as geologic consultants for the Denver Board of Water Commissioners during construction of the tunnel. The preliminary results of the Roberts Tunnel study showed that different types of geologic features — such as faults, veins, joints, and contacts between rock types — could be projected from the surface to tunnel level with varying degrees of accuracy, and that the accuracy depended on a thorough knowledge of both the regional geology — and therefore of the origin of these features — and on a detailed examination of the surface over the tunnel route. Rock type was found to be not as important in the construction of this tunnel as were other factors, such as the number of fractures per foot of tunnel, attitude of bedding, foliation, and fractures in relation to the trend of the tunnel, presence or absence of hydrothermal alteration, and the type of clay minerals, as the result of alteration, in fault gouge. Some of the results of the study of the Roberts Tunnel are published: Wahlstrom, Warner, and Robinson (1961), Wahlstrom (1962, 1964), Wahlstrom and Hornback (1962), Wahlstrom, Robinson, and Nichols (1968), and Warner and Robinson (1967). The study of the Roberts Tunnel led to the conclusion that a statistical compilation of geologic features — such as the distribution of rock types and the attitude of the bedding, foliation, faults, and joints — could be projected to a tunnel level more accurately than could individual features and would give a better basis for engineering design and construction. It also seemed possible that known geophysical techniques could be used to supplement the data obtained by surface examination and core drilling, particularly in areas of poor outcrop and poor core recovery. When the Colorado Department of Highways planned to start construction of a pilot bore for the Straight Creek Tunnel, an opportunity was afforded to test these ideas.

The purpose of the Straight Creek study was to conduct research in the prediction of the geology and its influence on construction at the depth of the pilot bore, to compare predictions with findings, and to evaluate the methods used after construction of the pilot bore. In addition, research on the use of geophysics for engineering geology purposes and on ground water in crystalline rocks was conducted in the pilot bore.

HISTORY AND SCOPE OF PROJECT

A geologic reconnaissance, of about 1 week's duration, was made of the Straight Creek Tunnel area in September 1961. Later that fall the U.S. Bureau of Public Roads and the Colorado Department of Highways agreed to allow the U.S. Geological Survey to conduct a research program on the Straight Creek Tunnel site and in the pilot bore. The Colorado Department of Highways also agreed to have four holes drilled along the proposed tunnel line (two to be cored) and to cooperate in any other way possible. The U.S. Geological Survey, in turn, agreed to furnish the Colorado Department of Highways a preconstruction report on the results of their geologic and geophysical research.

Field mapping and drilling were started in June 1962. The mapping and the drill-core logging were done by us. During the latter part of that summer a seismic survey, under the direction of R. A. Black and B. L. Tibbetts of the U.S. Geological Survey, was run on the surface. Resistivity logs of the drill holes were made by C. J. Zablocki and gamma-radiation and density logs were made by W. H. Bradley, both of the U.S. Geological Survey. R. M. Hazlewood and C. H. Miller, also of the U.S. Geological Survey (C. S. Robinson and R. M. Hazlewood, unpub. data, 1962), ran a

seismic survey in the vicinity of the east portal to determine the depth to bedrock. In December 1962 a preliminary report on the results of the surface investigations (Robinson and Lee, 1962) was furnished to the Colorado Department of Highways, who in turn furnished copies of the report to the firms bidding for the pilot-bore contract.

In the summer of 1963, during construction of a cut near the east portal of the pilot bore, a landslide developed at and upslope from the cut. The U.S. Geological Survey, in cooperation with the U.S. Bureau of Public Roads and the Colorado Department of Highways, conducted a brief geologic and geophysical investigation of this landslide (Robinson and others, 1964; Robinson, Lee, and others, 1972). As a result of the landslide, the east portal of the pilot bore was relocated about 150 feet to the south, and the grade was lowered 16 feet.

During construction, the tunnel walls were mapped at a scale of 1:600, and, with the assistance of engineers of the Colorado Department of Highways, at least one face section, at 1:24, was mapped per 8-hour shift. Terrametrics, Inc., was retained by the Colorado Department of Highways to install rock-mechanics instruments in the tunnel. The instrumentation was under the general supervision of B. E. Hartmann and the technical supervision of J. F. Abel, Jr., of Terrametrics, Inc. At each instrument station one or both walls of the tunnel were mapped, at a scale of 1:60, and the wooden blocking of the instrumented set, at 1:24. Water flows near the east portal were measured by a recorder on a Parshall flume. Water flows, and the decrease in water flows with time, from feeler holes and fractures were recorded by engineers of the Colorado Department of Highways. The ground-water investigations were under the supervision of R. T. Hurr and D. B. Richards of the U.S. Geological Survey. Wallrock temperatures were measured in the pilot bore in probe holes in the walls. The apparent resistivity of the wallrock was measured at most instrument stations, and seismic velocity was measured at five selected sites. The geophysical work was conducted under the supervision of J. H. Scott and R. D. Carroll of the U.S. Geological Survey. In support of the surface and underground work, extensive laboratory investigations were conducted, for the most part under the direction of T. C. Nichols, Jr., of the U.S. Geological Survey. These investigations consisted of the petrographic study of thin sections, determination of porosity, grain density, dry bulk density, saturated bulk density, elastic properties by static and dynamic methods, PVC (potential volume change) swell index of fault gouge and alteration products, size analysis of wallrock samples, and X-ray analysis of rock and clay samples. The pilot bore was holed through in December 1964. A preliminary report (Robinson and Lee, 1965) on the engineering geology of the pilot bore was transmitted to the Colorado Department of Highways in February 1965. Limited geologic, geophysical, ground-water, and laboratory investigations in connection with the pilot bore continued to 1967.

ACKNOWLEDGMENTS

Cooperation of the Colorado Department of Highways — in particular, Charles E. Shumate, Chief Engineer; Adolph Zulian, Engineer of Plans and Surveys; George N. Miles, District Engineer; Fred A. Mattei, Project Engineer; John D. Post, Engineer; and the associates of these men in the Department — is gratefully acknowledged. Terrametrics, Inc., made available all their records from the pilot-bore instrumentation. The contractor, Mid-Valley, Inc., cooperated fully; in particular, thanks are extended to Ted Adams, General Superintendent, and Frank Merrick, Project Superintendent.

Work on the project was encouraged by visits from, and by discussions with, many engineers of the U.S. Bureau of Public Roads — in particular, P. E. Warren, Assistant Division Engineer; J. S. Lacey, District Engineer; A. J. Siccardi, Regional Bridge Engineer; R. A. Bohman, Assistant Regional Materials Engineer; and J. I. Rooney, Tunnel Engineer.

J. E. Sharp and M. J. Cunningham, of the U.S. Geological Survey, assisted in the field. Many other members of the Survey assisted in geophysical and laboratory work and are acknowledged individually under the appropriate sections.

General Geology

By CHARLES S. ROBINSON *and* FITZHUGH T. LEE

ENGINEERING GEOLOGIC, GEOPHYSICAL, HYDROLOGIC, AND ROCK-MECHANICS INVESTIGATIONS OF THE STRAIGHT CREEK TUNNEL SITE AND PILOT BORE, COLORADO

GEOLOGICAL SURVEY PROFESSIONAL PAPER 815–B

ENGINEERING GEOLOGIC, GEOPHYSICAL, HYDROLOGIC, AND ROCK-MECHANICS INVESTIGATIONS OF THE STRAIGHT CREEK TUNNEL SITE AND PILOT BORE, COLORADO

GENERAL GEOLOGY

By CHARLES S. ROBINSON and FITZHUGH T. LEE

The Straight Creek Tunnel area is at the crest of the Front Range of the Colorado Rocky Mountains. The Front Range is a structurally complex area that consists predominantly of Precambrian metasedimentary and igneous rocks. The Colorado mineral belt, trending northeast across the Front Range, is a belt of Laramide intrusive rocks and ore deposits. The Straight Creek Tunnel area is near the northwest margin of the mineral belt (fig. 1).

The geology of the Colorado mineral belt has been studied extensively, the most comprehensive study being that of Lovering and Goddard (1950). Other reports which deal with specific areas or geologic problems, and which contribute to the understanding of the geology of the Straight Creek Tunnel site, are those by Harrison and Wells (1956, 1959), Harrison and Moench (1961), Moench, Harrison, and Sims (1962), Tweto and Sims (1963), Sims and Gable (1964), and Moench (1964).

REGIONAL GEOLOGY

The oldest rocks of the Front Range are chiefly of sedimentary origin and were metamorphosed, deformed, and intruded by igneous rocks in Precambrian time. These metasedimentary rocks were classified and mapped in the Colorado mineral belt by Lovering and Goddard (1950, p. 19–20) as the Idaho Springs Formation and the Swandyke Hornblende Gneiss. The Idaho Springs Formation consists of various biotite-quartz-microcline and plagioclase gneisses and lesser amounts of lime-silicate gneisses and amphibolites. The Swandyke Hornblende Gneiss consists of hornblende gneisses and biotite-quartz-plagioclase gneisses and amphibolites. More recently, Harrison and Wells (1956) and Moench (1964) recognized that the rock types do not constitute formations that can be correlated with complete accuracy from one area to another, and have used rock names, rather than formation names, to describe the units within each area of study. Lovering and Goddard (1950, pl. 2) included the metasedimentary rocks of most of the Straight Creek Tunnel area in their Idaho Springs Formation.

Radiometric dating showed that these metasedimentary rocks were metamorphosed about 1,700 to 1,750 m.y. (million years) ago (Peterman and others, 1968).

The major Precambrian igneous rock units in the Colorado mineral belt, from oldest to youngest, are the Boulder Creek Granite, 1,700 m.y.; the Silver Plume Granite, 1,440 m.y.; and the Pikes Peak Granite, 1,040 m.y. (Hedge, 1968, 1970; Peterman and others, 1968). These Precambrian igneous units range in composition from quartz diorite to granite; most of the Silver Plume Granite is equivalent in composition to a quartz monzonite. Of these units, only the Silver Plume Granite was recognized in the Straight Creek Tunnel area. The type locality of the Silver Plume Granite is in the quarry at the west side of the town of Silver Plume (fig. 1), about 9 miles east of the study area.

The Colorado mineral belt is characterized by Laramide and middle Tertiary igneous rocks that range in composition from basalts to granites (Lovering and Goddard, 1950, p. 42–49) and in habit from small dikes or sills to large stocks. These igneous rocks are represented in the Straight Creek Tunnel area by small dikes of augite diorite of the Tertiary age.

The regional structure of the Front Range is the result of deformation chiefly during Tertiary and Precambrian times. Tweto and Sims (1963) established that the Colorado mineral belt was a belt of Precambrian structures along which extensive faulting, intrusion of igneous rocks, and the formation of ore deposits occurred during Tertiary time.

The original Precambrian sedimentary rocks have had a long and complex history. The principal period of metamorphism, which formed the chief constituents of the mineral assemblages as exposed today, is believed to have been about contemporaneous with the first Precambrian period of deformation, 1,700 to 1,750 m.y. ago. The buried Precambrian sediments were metamorphosed, plastically deformed, and intruded by plutonic rocks. This deformation was followed at some time interval by a younger period of Precambrian deformation, 1,200 to 1,400 m.y. ago (Peter-

man and others, 1968), which was more limited in distribution and which was chiefly cataclastic (Moench, 1964, p. 66).

The Laramide orogeny started in Late Cretaceous time with the uplift of the area and the retreat of the Cretaceous sea. At some time after the uplift, major thrust faults, such as the Williams Range thrust fault about 8 miles west of the Straight Creek Tunnel area (Wahlstrom and Hornback, 1962, p. 1493–1497), developed along the west margin of the Front Range. The intrusion of the igneous rocks, some of which occurred after the development of the major thrust faults, was preceded, accompanied, and followed by faulting, mineralization, and hydrothermal alteration. In late Tertiary time the Front Range was vertically uplifted one or more times, the uplifts undoubtedly being accompanied by some faulting. Since this period of uplift and faulting, stream and glacial erosion and deposition have developed the present topography.

PHYSIOGRAPHY

The physiography of the Straight Creek Tunnel area is typical of the glaciated mountain regions of the Front Range. The valleys of Clear Creek and its tributaries, on the east side of the Continental Divide, and of Straight Creek, on the west side of the Continental Divide, were occupied by mountain glaciers, which had an average altitude of about 12,000 feet. Above this altitude the slopes are gentle and are covered by soil and rock debris as a result of frost action and solifluction. Locally, as a result of oversteepening of the slopes below the upper level of glaciation, this material has slumped to form landslides. At the heads of the glaciers, steep-walled cirques were formed, and, because of the incompetency of the bedrock, talus cones have accumulated in the cirques. Talus cones have also accumulated at the base of oversteepened valley walls. Locally, moraine and glacial-fluvial materials were deposited along the valley walls by the glaciers. After the retreat of the glaciers, some of these deposits slid, forming small landslides. Morainal deposits on the valley floors and sides have locally dammed the drainage and formed swampy areas and thin peat bogs. Erosion by present streams has only slightly modified the physiographic features resulting from the glaciation.

Altitudes within the Straight Creek Tunnel area range from about 10,820 feet at the entrance to the Loveland ski area to 13,010 feet at the crest of an unnamed peak along the Continental Divide about 1 mile northeast of the tunnel line. The slope of the surface along the tunnel line between the east portal and the Continental Divide is relatively gentle (fig. 3), whereas the slope between the west portal and the Continental Divide is steep (fig. 4). The altitude of the east portal of the pilot bore is about 11,000 feet, and that of the west portal is about 11,200 feet. The maximum thickness of the cover over the pilot bore at the Continental Divide is about 1,5000 feet.

ROCK UNITS

The rock units exposed at the surface and in the Straight Creek Tunnel pilot bore include a variety of biotite-rich gneisses and the Silver Plume Granite, with associated pegmatite and quartz dikes, of Precambrian age, and augite diorite dikes, of Tertiary age.

The gneisses occur as inclusions in the Silver Plume Granite and locally have been partly to completely assimilated by the granite. Thin dikes of Silver Plume Granite and pegmatite have commonly intruded the inclusions of gneiss parallel to the foliation or, through the mobilization and recrystallization of the constituents in the gneiss, thin layers of granitic material are interlayered with thin layers of gneiss forming a rock type commonly termed "migmatite." In mapping the rock types at the surface and in the pilot bore, the relative percentages of granitic material and gneiss were estimated. Those rocks that were more than 50 percent granitic material were mapped as granite, and those that were more than 50 percent gneiss were mapped as metasedimentary rocks.

The distribution of the rock types at the surface is shown on plate 1 and in the tunnel on plate 2.

METASEDIMENTARY ROCKS

The metasedimentary rocks include a wide variety of chiefly biotite-quartz-plagioclase gneisses and some hornblende-biotite-quartz plagioclase gneisses. The mineralogic varieties are interlayered and gradational, so a distinction was not attempted in geologic mapping. In general, the hornblende gneisses are restricted to the area west of the Continental Divide and are the most abundant on the east side of Coon Hill.

The metasedimentary rocks occur as inclusions in the granite. The inclusions range from schlieren of biotite gneiss a few millimeters wide and a few centimeters long to large bodies more than 2,500 feet in maximum dimension. The smaller inclusions are generally ellipsoids, with the major axis parallel to the foliation. The length of the major axis typically is twice to several times that of the minor axis. The larger inclusions — those measuring tens of feet in maximum dimension — are generally irregular in shape. Most of these inclusions are too small to be shown on the geologic maps (pls. 1, 2).

The contacts of the metasedimentary rock inclusions and the granite are typically gradational but are locally sharp. In walking from an area of predominantly metasedimentary rock to one of predominantly granite, it was noted that the percentage of biotite increases in the granite and that the mineral layering and the foliation of the granite become more distinct. This hybrid rock grades into a typical migmatite of interlayered gneiss and granite, and then grades into the typical gneiss. The contact between the metasedimentary rocks and granite, where it crosscuts the foliation of the metasedimentary rock, is generally sharp.

FIGURE 3. — Approach to east portal of the pilot bore, on east slope of the Continental Divide. View is to the west.

In outcrop the metasedimentary rocks are typically layered light to dark gray, depending on their mineral composition. Some hand specimens show a distinct greenish tinge from the partial alteration of biotite and hornblende to chlorite. The metasedimentary rocks are fine to medium grained, and their grain size differs from layer to layer in a single outcrop.

The minerals common to all the metasedimentary rocks are plagioclase, quartz, and biotite. Microcline is present in significant amounts in most samples, and muscovite is a conspicuous accessory mineral in many samples. Hornblende is abundant in some layers, and sillimanite is locally common. Accessory minerals are apatite, monazite, cordierite, and zircon, and the opaque minerals are magnetite and pyrite, which generally occur in euhedral or subeuhedral grains of <1 mm. Table 1 lists the mineral composition of typical samples from the surface, diamond-drill cores, and from the pilot bore.

The plagioclase grains typically are anhedral to subhedral and indistinctly polysynthetically twinned. They occur intergrown with the biotite and hornblende in the dark-colored layers but are more commonly intergrown with quartz or microcline in the light-colored layers. Mosaic boundaries with other minerals are common, and intergrowths of plagioclase and quartz and of plagioclase and microcline at the boundaries are typical. The grain size ranges from about 1 to 5 mm. Most plagioclase grains have been partially altered to sericite and clay minerals, and sericite is common along cleavage fractures. Cataclastic effects are common; crystals are veined with fractures filled with quartz or microcline. The anorthite content ranges from about An_{25} to An_{35}.

The quartz, whose average grain size is about 1 mm, is generally finer grained than the feldspar or biotite and hornblende and typically fills the interstices between the other grains. Veinlets containing quartz cut across grains of

FIGURE 4. — Approach to west portal of the pilot bore, on west slope of the Continental Divide. View is to the south.

all the other minerals. Intergrowths of quartz and feldspar occur at their mutual boundaries. The quartz has overgrowths of quartz around the larger grains. Most grains have been fractured, and the fractures have been healed with quartz. Cataclastic effects vary — in rocks that are moderately deformed, quartz shows undulatory extinction, whereas in severely deformed rocks, quartz is shattered to finely granulated.

The biotite occurs as individual grains, 1−5 mm in size, in the light-colored layers and as streaked aggregates in the dark layers. Cataclastic effects are common. Typically, the edges of the grains are shredded and streaked parallel to the foliation and show partial to complete alteration to chlorite. Some of the dark layers in the more schistose rocks consist almost entirely of biotite and contain only a few grains of quartz, plagioclase, and accessory minerals. In such layers, streaking of grains along the cleavage is most conspicuous.

Microcline is probably an original constituent of most of the metasedimentary rocks, but in some it may be the result of migmatization. It is most abundant in the metasedimentary units interlayered with granite and increases in percentage toward layers of granite. Grains average about 2 mm in maximum dimension. The microcline occurs as anhedral grains with quartz and plagioclase in the light-colored layers in the foliated rock and as cataclastic microveins in plagioclase grains. It is generally fresh and is altered only in those rocks in which the biotite and plagioclase have almost completely been destroyed.

The mineral assemblages of the metasedimentary rocks place the rocks in the almandine-amphibolite facies of Fyfe, Turner, and Verhoogen (1958, p. 228−232). The gradation between adjacent units suggests that the rocks were originally sedimentary rocks and that the differences in composition are mainly the result of differences in original

TABLE 1. — *Mineral composition, in volume percent, of metasedimentary rocks, Straight Creek Tunnel area*

[Leaders (---) indicate mineral was looked for but not found; Nd, not determined]

	Surface samples			Core samples					Pilot-bore samples[1]							
Sample No.	1	2	3	[2]4	[3]5	[3]6	[3]7	[3]8	9	10	11	12	13	14	15	16
Microcline	---	---	8.4	0.7	40.6	0.4	2.0	54.5	0.4	16.5	28.4	2.9	32.4	5.4	17.5	0.7
Plagioclase	30.1	36.8	39.6	---	10.0	41.9	37.0	3.8	40.5	6.1	30.4	36.2	11.1	23.8	24.6	74.5
Quartz	10.7	20.4	41.3	7.4	28.3	46.8	33.2	22.0	11.9	63.9	26.5	1.4	21.6	62.2	30.5	10.6
Biotite	.7	6.3	10.6	44.2	13.2	10.0	22.1	14.7	10.6	6.7	8.3	44.1	31.4	7.3	24.0	6.3
Muscovite	5.0	4.7	---	---	1.2	---	---	.9	4.5	1.2	5.9	1.4	3.0	.8	2.1	2.2
Hornblende	42.7	27.2	---	7.7	---	---	---	---	30.8	---	---	---	---	---	---	---
Sillimanite	---	.6	---	---	4.9	---	---	2.4	---	4.9	---	13.8	---	---	---	---
Cordierite	---	---	---	26.3	---	---	---	---	---	---	---	---	---	---	---	---
Chlorite	---	---	---	1.0	.2	---	---	---	---	.8	.1	---	.6	.2	1.2	.2
Calcite	---	---	---	9.9	---	---	---	1.2	.4	---	---	---	---	---	---	.2
Accessory[4]	.7	1.3	---	.9	---	.4	.6	Tr.	---	---	---	---	---	---	---	---
Opaque[5]	10.2	2.7	---	1.8	1.6	.4	5.0	.5	1.8	---	.2	.5	.3	---	.3	5.3
Composition of plagioclase	Nd	An_{37}	An_{26}	Nd	An_{25}	An_{35}	An_{32}	Nd	An_{26}	Nd	An_{26}	An_{25}	Nd	An_{25}	Nd	An_{25}

[1]Sample from pilot bore and station, south wall.
[2]Sample from diamond-drill-hole 2 (1962); footage shown as part of field number below.
[3]Sample from diamond-drill-hole 3 (1962); footage shown as part of field number below.
[4]Includes apatite, monazite, and zircon.
[5]Includes magnetite and pyrite.

SAMPLE DESCRIPTIONS

No.	*Field No.*	*Description*
1	SC−5	Fine-grained hornblende gneiss from outcrop, 500 ft east of Continental Divide and 2,800 ft north of pilot bore.
2	6CR−62	Fine-grained biotite-quartz-hornblende-plagioclase gneiss from talus slope, 2,000 ft west of Continental Divide and 3,000 ft north of pilot bore.
3	10CR−62	Fine-grained schist and gneiss from outcrop at road level, 2,500 ft east of east portal of pilot bore.
4	SC2−749.5−750.8	Fine- to medium-grained cordierite schist.
5	SC3−344−345	Fine-grained biotite-sillimanite schist and pegmatite (migmatite).
6	SC3−346−347	Fine-grained biotite schist.
7	SC3−429.5−431	Fine-grained biotite gneiss and schist with pegmatite stringers.
8	SC3−486−488	Fine-grained biotite schist and pegmatite (migmatite).
9	80+00S	Fine-grained chloritic gneiss with calcite veinlets.
10	90+00S	Fine-grained biotite-sillimanite schist and pegmatite (migmatite).
11	92+00S	Layered fine-grained biotite-muscovite schist and pegmatite (migmatite).
12	98+02S	Altered fine-grained biotite-sillimanite schist.
13	102+00S	Fine- to medium-grained biotite schist.
14	103+99.5S	Medium-grained quartzitic gneiss.
15	105+81S	Altered fine- to medium-grained biotite schist.
16	109+99.2S	Medium- to coarse-grained gneiss.

composition. The micaceous rocks represent a pelitic or quartz-feldspathic composition (Wahlstrom and Kim, 1959, p. 1223−1228) and the hornblendic rocks represent a calcareous or mafic composition.

GRANITIC ROCKS

Most rock in the Straight Creek Tunnel area is granitic — that is, it is medium-grained rock that consists of approximately equal amounts of quartz, potassium feldspar, and plagioclase feldspar. The granitic rock resembles in mineral composition and fabric the Silver Plume Granite throughout the Front Range, as described by Lovering and Goddard (1950, p. 28).

Many recent workers in the Front Range (Harrison and Wells, 1956, 1959; Sims and Gable, 1964; Moench, 1964) have used such mineralogic terms as "biotite-muscovite granite" for rocks of similar mineralogy, fabric, and age to the Silver Plume Granite. This was done chiefly because a direct correlation could not be established between the type locality of the Silver Plume Granite and the area being mapped. Lovering and Goddard (1950, pl. 2) showed that the Silver Plume Granite is continuous from the type locality near Silver Plume to the Straight Creek Tunnel area.

The granitic rocks are well exposed in the Straight Creek Tunnel area as scattered outcrops north and south of the tunnel line east of the Continental Divide (fig. 3) and in the cliffs above the west portal west of the Continental Divide (fig. 4). The rock is light gray and pinkish light gray in outcrop and light to medium gray on freshly exposed surfaces. In most exposures the rock is fine to medium grained, equigranular, and generally homogeneous in composition, and it contains megascopically recognizable microcline, plagioclase, quartz, and biotite. Most outcrops of granite are characterized by a subparallel orientation of the microcline grains, typical of the Silver Plume Granite, which gives the rock an indistinct foliation. The biotite grains, except those adjacent to inclusions of metasedimentary rocks, are not oriented parallel to the microcline grains.

Table 2 gives the mineral composition of samples of granitic rocks from the surface, from the cores of drill holes, and from the pilot bore. Most of the samples are muscovite-biotite quartz monzonite. Microscopically, the texture of

TABLE 2. — *Mineral composition in volume percent, of fine- and medium-grained granitic rocks (chiefly Silver Plume Granite), Straight Creek Tunnel area*

[Leaders (- - -) in figure columns indicate mineral was looked for but not found; Nd, not determined; Tr., trace]

	Surface samples					Core samples											
No	1	2	3	4	5	6	7	8	9	10	11	12	13	14	15	16	17
Microcline	32.6	27.7	29.2	27.8	33.6	27.8	40.0	42.0	36.4	34.1	30.2	33.8	33.9	34.4	54.8	36.2	48.0
Plagioclase	28.5	28.1	34.6	29.0	26.4	34.4	21.9	22.0	29.2	25.2	31.1	27.5	28.6	23.8	17.8	21.9	16.3
Quartz	30.3	31.7	28.0	26.2	25.2	26.5	29.1	25.7	26.2	28.3	27.8	27.9	25.5	30.1	17.0	33.0	30.0
Biotite	5.5	7.7	5.3	8.6	8.3	7.2	6.4	4.6	5.4	7.1	8.5	7.8	6.6	7.8	6.4	4.0	3.7
Muscovite	2.0	3.7	2.2	5.2	4.2	2.0	1.3	1.8	1.1	2.7	1.6	1.6	3.6	1.1	2.0	2.2	---
Sillimanite	---	---	---	---	---	---	.2	.6	.7	---	---	1.3	---	---	.1	1.4	---
Chlorite	---	---	---	---	---	---	.4	2.2	---	.4	Tr.	---	.8	---	1.1	---	.1
Calcite	---	---	---	---	---	.8	---	---	---	.6	.2	---	.7	2.1	.7	---	---
Opaque[1]	1.0	1.0	.8	2.3	2.0	.8	.7	.7	.9	.9	.4	---	.3	.3	.1	1.3	.4
Fine-grained gouge	---	---	---	---	---	---	---	---	---	---	---	---	---	---	---	---	---
Accessory[2]	.2	.1	---	1.1	.2	.5	---	.4	.2	---	Tr.	---	Tr.	.2	---	---	---
Composition of plagioclase	An_{17}	An_{26}	An_{23}	An_{24}	An_{28}	An_{25}	An_{27}	An_{24}	An_{25}	An_{24}	An_{24}	An_{28}	An_{25}	An_{26}	Nd	An_{24}	An_{28}
Average grain size (mm)	1.5	2.5	2.0	1.7	---	1.5	2.5	2.5	1.8	2.0	2.1	1.3	2.0	3.0	5.1	2.7	3.5

	Core samples — Continued										Pilot-bore samples						
No	18	19	20	21	22	23	24	25	26	27	28	29	30	31	32	33	34
Microline	37.1	28.3	22.6	41.1	27.6	35.6	17.6	16.6	16.8	25.9	32.2	22.3	15.2	41.4	61.1	34.2	29.0
Plagioclase	24.2	23.8	43.3	27.2	42.0	24.8	22.0	34.8	34.7	34.4	16.4	37.8	35.4	19.2	9.0	25.4	31.6
Quartz	27.6	42.8	28.9	24.9	22.3	32.9	29.0	26.0	35.0	26.1	37.2	26.7	27.6	31.5	14.5	35.7	26.6
Biotite	8.5	---	---	---	---	---	---	---	---	.5	10.6	4.6	18.4	6.5	Tr.	.2	11.1
Muscovite	2.0	1.6	1.8	.4	.4	---	1.3	---	---	---	.9	.2	.2	1.0	6.4	2.6	1.6
Sillimanite	Tr.	---	---	---	---	---	---	---	---	---	---	---	---	---	---	---	---
Chlorite	---	.2	2.6	2.9	5.4	4.8	9.5	1.5	1.9	4.7	Tr.	6.2	---	---	.4	.3	---
Calcite	Tr.	3.0	---	1.4	Tr.	1.0	17.0	18.6	6.4	3.2	---	---	---	---	7.6	1.1	---
Opaque[1]	.6	.3	.7	1.5	2.0	.4	1.8	2.2	4.7	4.1	1.7	2.4	3.6	---	.1	---	---
Fine-grained gouge	---	---	---	---	---	---	---	---	---	---	1.0	---	---	---	---	---	---
Accessory[2]	---	---	---	.6	.2	.4	1.0	.3	.4	1.0	---	---	---	---	1.0	---	---
Composition of plagioclase	An_{27}	An_{27}	An_{27}	An_{28}	An_{27}	Nd	An_{24}	An_{26}	An_{28}	An_{29}	An_{26}	An_{25}	An_{25}	An_{22}	Nd	An_{24}	Nd
Average grain size (mm)	1.8	2.0	1.9	2.3	1.5	1.5	1.2	1.0	1.2	---	2.2	1.8	1.8	3.0	1.8	1.2	1.1

	Pilot-bore samples — Continued															
No	35	36	37	38	39	40	41	42	43	44	45	46	47	48	49	50
Microcline	25.2	39.4	29.0	37.0	21.6	27.6	26.9	27.1	50.8	21.2	19.6	35.2	22.0	22.8	25.1	37.4
Plagioclase	35.0	26.8	31.3	25.1	34.6	27.0	39.1	15.3	8.0	32.7	34.6	25.7	27.6	38.4	33.0	28.0
Quartz	36.0	24.0	23.0	23.1	25.6	30.0	21.5	45.0	27.0	35.2	33.6	30.7	34.6	19.4	25.2	26.3
Biotite	Tr.	4.6	13.2	12.9	15.6	8.4	2.3	5.9	9.8	5.8	9.4	3.0	13.5	1.4	13.4	4.0
Muscovite	1.9	2.6	2.2	1.5	2.0	6.2	3.7	2.4	2.6	2.5	1.7	1.8	.8	2.4	1.8	1.8
Sillimanite	---	---	---	---	---	---	---	.5	---	---	---	---	---	---	---	---
Chlorite	.5	.6	.8	---	---	.1	---	---	---	.2	---	---	---	5.6	---	---
Calcite	1.3	1.5	---	---	---	---	5.6	---	.2	2.0	---	2.2	1.7	.2	---	.1
Opaque[1]	---	.4	.4	.4	.7	.8	.3	.5	1.7	.5	1.0	1.4	.3	---	.1	1.7
Fine-grained gouge	---	---	---	---	---	---	---	3.2	---	---	---	---	---	9.8	---	---
Accessory[2]	---	---	---	---	---	---	---	---	---	---	---	---	---	---	---	---
Composition of plagioclase	An_{25}	An_{25}	Nd	An_{25}	An_{26}	Nd	An_{26}	An_{25}	An_{25}	An_{25}	An_{25}	An_{25}	An_{25}	An_{25}	An_{26}	Nd
Average grain size (mm)	1.0	1.5	2.0	2.2	1.9	0.6	2.5	1.3	2.2	2.0	2.1	0.7	1.4	0.8	1.5	1.6

[1]Magnetite, hematite, and pyrite. [2]Apatite, monazite, zircon, and fluorite.

the fine- and medium-grained granitic rocks is hypidiomorphic granular. Microcline, plagioclase, and quartz are in about equal amounts and compose about 90 percent of most samples. Microcline grains are subhedral to anhedral and are <1–5 mm long. The grid-twinning characteristic of microcline is usually distinct. Most grains of microcline contain small rounded blebs or veins of quartz and small stringers or patches of perthitic intergrowths with albite. The plagioclase feldspar, which occurs in 1- to 3-mm anhedral grains, ranges in composition from An_{17} to An_{29}, and averages about An_{25}. Polysynthetic twinning is indistinct; a few grains show compositional zoning. Myrmekite is common at the mutual boundaries of the plagioclase and microcline grains. The plagioclase grains are characterized by partial alteration to sericite and clay minerals. The quartz grains are mostly <1 mm in diameter, and they occur generally as aggregates interstitial to the feldspar grains. Quartz also occurs as small distinct grains in the microcline and as microveinlets cutting all other minerals, including quartz. All the quartz grains show strain shadows and undulatory extinction.

The common minor minerals in the granitic rocks are biotite and muscovite. The biotite is moderate brown and occurs in ragged-edged grains that are <1–3 mm in diameter. Most biotite grains are partially altered to chlorite and magnetite grains and contain very fine grained subhedral to euhedral grains of zircon and monazite that are surrounded by pleochroic halos. The muscovite is unevenly distributed in most specimens. It typically occurs in fine-grained aggregates intergrown with biotite and plagioclase grains. In those specimens that contain sillimanite, muscovite is intergrown with, and contains needles of, sillimanite. The sillimanite, which occurs in bundles of fine-grained needles, was probably derived from the partial

TABLE 2 SAMPLE DESCRIPTIONS

No.	Field No.	Description
		Surface samples
1	5CR−62	Pinkish-gray medium-grained granitic rock from cliff 5,500 ft N. 25° E. of west portal at altitude of 12,000 ft.
2	7CR−62	Tannish-gray porphyritic granitic rock from knob 800 ft southwest of drill-hole 3 (1962).
3	8CR−62	Gray medium-grained granitic rock from roadcut.
4	11CR−62	Gray medium-grained to porphyritic granitic rock from type locality for Silver Plume Granite in quarry on north side of U.S. Highway
5	11CR−62−5C	6, on west edge of Silver Plume.
		Do.
		Core samples from diamond-drill-holes (1962) 2 and 3
		[Footage is shown as part of field number: 180−181, 260−261, and so forth]
6	SC2−180−181	Greenish-gray medium-grained moderately fractured and altered granitic rock.
7	SC2−260−261	Pinkish-gray medium-grained to porphyritic granitic rock; relatively fresh and unfractured.
8	SC2−264−265	Do.
9	SC2−387−388.5	Do.
10	SC2−392−393	Gray medium-grained granitic rock; relatively fresh and unfractured.
11	SC2−489−490	Light-pinkish-gray medium-grained granitic rock; little obvious fracturing.
12	SC2−532−534	Light-gray medium-grained unfractured granitic rock.
13	SC2−672−673	Pinkish-gray porphyritic granitic rock; very few fractures and little alteration.
14	SC2−673−675	Do.
15	SC3−378−379	Light-pinkish-gray medium-grained to porphyritic granitic rock; fractured; minor alteration.
16	SC3−429−430	Pinkish-gray medium-grained to porphyritic granitic rock. Similar to sample No. 15, but finer grained groundmass.
17	SC3−436−437	Pinkish-gray medium-grained granitic rock; minor fractures.
18	SC3−438−439	Do.
19	SC3−678−679	Pinkish-gray medium-grained granitic rock; moderately fractured and altered.
20	SC3−678−680	Gray-green medium-grained foliated granitic rock; highly sheared and altered.
21	SC3−849−856	Greenish-gray medium-grained conspicuously foliated granitic rock; fractures along and across foliation.
22	SC3−953−954.4	Pinkish-gray medium-grained foliated granitic rock; intensely sheared.
23	SC3−1034.3−1035.9	Greenish-pink medium-grained granitic rock; intensely sheared and altered.
24	SC3−1114−1119	Similar to sample No. 20; intensely sheared and altered.
25	SC3−1152−1154A	Light-pinkish-gray medium-grained granitic rock; intensely sheared and altered. Most fractures are tight and cemented.
26	SC3−1152−1154B	Do.
27	SC3−1152.6−1154	Greenish-pink to tan medium- to fine-grained franitic breccia. Most fractures are tight and cemented.
		Pilot-bore samples
		[N or S ending for field (station) number indicates north or south wall]
28	44+65S	Tannish-gray medium-grained granitic rock; minor fracturing and alteration.
29	57+57S	Pinkish-gray to greenish-gray medium-grained granitic rock; minor shearing and alteration.
30	69+25N	Dark-greenish gray medium-grained granitic rock; minor alteration.
31	75+20S	Pinkish-gray medium-grained to porphyritic granitic rock; minor fracturing and alteration.
32	82+00.6S	Pink to tan medium-grained granitic rock; moderately to intensely fractured and altered.
33	84+01.5N	Light-pinkish-tan medium-grained granitic rock; intensely sheared and altered; crumbles to sand.
34	84+65S	Light-pinkish gray medium-grained granitic rock; sheared and altered.
35	85+58S	Light-tannish-gray medium-grained granitic rock; sheared and altered; gouge on fracture surfaces.
36	87+99.1S	Gray porphyritic granitic rock; moderate fracturing and alteration.
37	94+02.8S	Light-grayish-green medium-grained to porphyritic granitic rock; intensely sheared; crumbly.
38	94+47N	Gray-green medium-grained granitic rock; minor alteration.
39	96+00S	Gray medium-grained to porphyritic granitic rock; relatively fresh and unaltered.
40	100+00S	Gray medium- to fine-grained granitic rock; minor gouge along joints.
41	104+06S	Tannish-gray medium-grained granitic rock; fractured and altered.
42	106+73S	Light-gray medium-grained granitic rock; prominent biotitic layers.
43	111+95N	Gray porphyritic gneissic granitic rock; few fractures; little alteration.
44	113+50S	Light-gray medium-grained to porphyritic granitic rock; minor fracturing; moderate alteration.
45	113+82S	Gray medium-grained granitic rock; minor shearing.
46	115+03.7S	Pinkish-gray medium-grained to porphyritic granitic rock; intensely sheared and altered; gouge along most fractures.
47	117+00S	Gray medium-grained granitic rock; minor fracturing and alteration.
48	118+15S	Dark-tannish-gray medium-grained granitic rock; minor fracturing and alteration.
49	118+84.3S	Medium- to dark-gray medium-grained biotite-rich granitic rock; gouge along fractures.
50	119+95.5S	Greenish-tan medium-grained granitic rock; intensely altered and crumbly.

assimilation of sillimanitic biotite-quartz-plagioclase gneiss.

The common accessory minerals — zircon, monazite, apatite, and opaque minerals of magnetite and pyrite — occur as very fine euhedral to subhedral grains as inclusions in the biotite. Chlorite and calcite, noted in table 2, are alteration products of the biotite and plagioclase feldspar.

Granitic rocks similar in mineral composition and grain size to the typical Silver Plume Granite are interlayered with the fine-grained gneiss. The layers range in width from <1 inch to 1 foot and constitute a rock type termed "migmatite." The migmatite occurs in the areas of contact between large bodies of typical Silver Plume Granite and large inclusions of metasedimentary rocks, or as inclusions in large bodies of Silver Plume Granite. The mineral composition and the grain size of the granitic layers resemble the Silver Plume Granite. This type of granitic material was probably derived in part by metasomatism as a result of the mobilization and recrystallization of the metasedimentary rocks.

PEGMATITE AND APLITIC ROCKS

Coarse- and fine-grained granitic rocks occur in the Straight Creek Tunnel area in association with the Silver Plume Granite. They constitute only a very small percentage of the total rock and were not differentiated in mapping from the other granitic rocks.

The coarse-grained rock, or pegmatites, are of two types — quartz-feldspar pegmatites and bull-quartz pegmatites. The quartz-feldspar pegmatites occur as dikes and as elliptical pods that range in width from <1 inch to >10 feet in the granitic and metasedimentary rocks. Most commonly,

the quartz-feldspar pegmatites occur along contacts between distinct intrusive bodies of Silver Plume Granite and large inclusions of metasedimentary rocks, and as dikes crosscutting migmatitic zones between bodies of Silver Plume Granite and inclusions of metasedimentary rocks. The composition of the quartz-feldspar pegmatites is similar to that of finer grained rocks, except that the quartz-feldspar pegmatites generally contain less biotite and less muscovite, as shown by the mineral analyses of six samples given in table 3.

TABLE 3. — *Mineral composition, in volume percent, of pegmatitic rocks, Straight Creek Tunnel area*

[Leaders (_ _ _) indicate mineral was looked for but not determined; Nd, not determined]

	Surface sample	Core samples			Pilot-bore samples[1]	
Sample No	1	[2]2	[3]3	[4]4	5	6
Microcline	64.7	18.4	59.3	38.2	23.5	2.0
Plagioclase	7.9	10.0	10.3	16.7	31.5	56.7
Quartz	26.8	40.1	26.0	43.6	38.3	39.0
Biotite	.2	_ _ _	_ _ _	.2	2.3	1.0
Muscovite	.5	.6	1.0	.1	1.6	.8
Sillimanite	_ _ _	.1	1.3	.2	_ _ _	_ _ _
Chlorite	_ _ _	1.1	.3	_ _ _	.1	.2
Calcite	_ _ _	29.3	1.2	.9	2.5	.1
Opaque[4]	_ _ _	.2	.1	_ _ _	2.0	.2
Composition of plagioclase	Nd	Nd	Nd	Nd	An_{25}	An_{25}
Average grain size (mm)	3.2	1.8	2.2	4.5	2.8	5.0

[1]Pilot-bore station, south wall.
[2]Sample from diamond-drill hole 2 (1962); footage shown as part of field number below.
[3]Sample from diamond-drill hole 3 (1962); footage shown as part of field number below.
[4]Magnetite, hematite, and pyrite.

SAMPLE DESCRIPTIONS

No.	*Field No.*	*Description*
1	9CR−62	Pinkish-tan pegmatitic rock; prominent fractures; 5,100 ft south-southeast from east portal at altitude of 12,400 ft.
2	SC2−853−854	Pinkish-gray coarse-grained to pegmatitic rock; fractured and weathered.
3	SC2−854−856	Light-tannish-gray coarse-grained to pegmatitic rock; strong hydrothermal alteration; some shearing.
4	SC3−377−378.1	Light-pinkish-gray pegmatitic rock. Fractures are cemented; minor shearing.
5	86+00S	Tan to light-gray pegmatitic granitic rock; fractured; gouge on most fracture surfaces.
6	107+99S	Light-gray coarse-grained to pegmatitic granitic rock; minor fracturing and alteration.

The bull-quartz pegmatites occur chiefly as dikes in the granitic rocks. They range in size from <1 inch wide and 1 foot long to 3 feet wide and 20 feet long. They occur most commonly parallel to and in the large northeast-trending shear zones (pl. 1). The bull-quartz pegmatites consist mostly of milk-white coarse-grained quartz. Some dikes contain vugs, 1−2 inches in diameter that are lined with quartz, calcite, or fluorite crystals or are filled with specular hematite and aggregates of euhedral crystals of magnetite as much as a quarter of an inch in diameter.

The aplitic rocks occur as small dikes (or as border zones of large dikes) that crosscut inclusions of metasedimentary rocks. The composition of the aplitic rocks is almost the same as that of the granitic rocks, the difference being that the average grain size of the aplitic rocks is <0.5 mm. In the larger dikes, the aplitic rock at the borders grades imperceptibly into the typical fine- or medium-grained granitic rock in the central part of the dike.

Most of the granitic rocks are believed to be Silver Plume Granite or are related to the intrusion of the Silver Plume Granite. The granitic material in migmatitic facies may have been derived from the Precambrian sediments at the time of their metamorphism. The aplitic rock is considered to be a fine-grained facies of the Silver Plume Granite that resulted from the more rapid cooling of thin dikes or the marginal areas of larger dikes. The quartz-feldspar pegmatites were probably generated as a late phase in the intrusion and crystallization of the Silver Plume Granite, as suggested by their spatial relationship and similarity in composition to the Silver Plume Granite. The origin of the bull-quartz pegmatites is not clear. Their coarse grain size, composition, and occurrence along shear zones, which were Precambrian shear zones, is indicative of a Precambrian age. The quartz veins of Tertiary age in the nearest mining district (Argentine district) are generally fine-grained quartz or cryptocrystalline silica, they contain sulfides of metallic elements or of their oxidation products, and they have associated hydrothermal alteration of the wallrock (Lovering and Goddard, 1950, p. 135−138).

DIKES

Augite diorite dikes of Tertiary age occur in the Straight Creek Tunnel area. At the surface they crop out along the Continental Divide for about 4,000 feet, starting about 1,000 feet north of the tunnel line (pl. 1). Underground, augite diorite dikes occur at about stations 76+00 and 78+00 (pl. 2). The dikes range in width from <1 to 200 feet and in length from about 10 to 1,200 feet. The dikes, in general, are parallel to the regional foliation (pl. 1), but in detail the contacts crosscut the foliation. The dikes themselves are not foliated.

The augite diorite is dark brown in outcrop and very dark brownish gray when fresh. The rock is porphyritic with a fine-grained to aphanitic groundmass. The grain size is proportional to the width of the dikes, the wider dikes being coarser grained. The wider dikes show a distinct chilled facies at their contacts. In hand specimens, euhedral to subhedral plagioclase and augite, with maximum dimensions of about 4 mm, can be identified.

Microscopically, it can be seen that samples of the augite diorite dikes consist of about equal parts of plagioclase feldspar and ferromagnesian minerals, and about 5−10 percent magnetite. Mineral composition analyses of three samples are given in table 4.

The plagioclase of the groundmass is subhedral to anhedral, twinned, and commonly altered, at least in part,

TABLE 4. — *Mineral composition, in volume percent, of augite diorite dike rocks, Straight Creek Tunnel area*

[Nd, not determined]

	Surface sample	Pilot-bore samples[1]	
	SC−4	75+59bS	76+00S
Microcline	---	---	1.0
Plagioclase	42.8	43.3	47.3
Quartz	3.7	7.1	4.3
Biotite	---	2.4	14.8
Calcite	---	6.1	1.1
Augite	42.9	30.2	25.6
Magnetite	10.6	11.2	6.2
Composition of plagioclase	An_{30}	Nd	An_{26}
Average grain size (mm)	.3	0.05	0.1

[1]Pilot-bore station, south wall.

SAMPLE DESCRIPTIONS

SC−4 Dark-gray fine-grained dike rock; no obvious alteration, and only minor fracturing; from 12-ft-wide dike 4,850 ft northeast of west portal at altitude of 12,420 ft.

75+59bS Dark-gray fine-grained dike rock; minor fracturing and alteration. Fractures are filled with calcite veins.

76+00S Dark-gray to black fine-grained dike rock; traces of gouge along some fractures.

to sericite. The composition of plagioclase in the groundmass averages about An_{30}. The phenocrysts of plagioclase are commonly zoned, and the cores have an anorthite content of as much as An_{45}. The augite is subhedral to anhedral, and the grains — particularly the phenocrysts — are rimmed with uralite. The biotite occurs as dark-olive-brown anhedral flakes generally smaller than the grains of plagioclase and augite. Magnetite occurs as a primary constituent in subhedral grains and as minute euhedral grains that resulted from alteration of the augite and biotite. Quartz occurs in scattered subhedral to anhedral corroded grains interstitial to the other minerals. Anhedral to subhedral apatite occurs in trace amounts.

The minerals in the main part of the augite diorite dikes show no tendency toward a preferred orientation, or foliation. Near the margins of the larger dikes, the phenocrysts of augite and plagioclase are locally subparallel to the margins of the dike. In section, most grains show no fracturing; therefore, the dikes are believed to be post-Precambrian in age. The subparallel orientation of the phenocrysts is probably the result of flow during intrusion of the dikes. Lovering (1935, pl. 3, p. 31) classified these dikes as Tertiary in age and Lovering and Goddard (1950, p. 44−47) assigned them to their group 2 of the intrusive rocks of the Front Range and concluded that these dikes were intruded during the early part of the Laramide orogeny.

SURFICIAL DEPOSITS

Only 4 percent of the Straight Creek Tunnel area mapped is outcrop; most of the area is covered by surficial material. The most common type of surficial material is mountaintop debris (not shown on the geologic map, pl. 1). This debris, which consists of soil mixed with pieces of country rock, developed in place as the result of weathering and of frost action on bedrock. On the steeper slopes some of this material has moved a little under the influence of gravity. The thickness of the mountaintop debris ranges from less than an inch to several feet. Thick deposits of moraines, swamps, talus, and landslide were mapped and are shown on plate 1.

MORAINE

The most extensive morainal deposits occur along Clear Creek northeast and south of the east portal of the pilot bore (pl. 1). Moraine underlies the swamp deposits east of the east portal and underlies the talus deposit at the west portal of the pilot bore. Other deposits of moraine, too small to be shown on the map (pl. 1), occur in patches above both the east and the west portals of the pilot bore. Seismic investigations near the east portal of the pilot bore, made prior to the start of construction of the pilot bore, showed that the morainal deposits ranged in thickness from 0 to 50 feet (C. S. Robinson and R. M. Hazlewood, unpub. data, 1962).

The morainal deposits consist mostly of unsorted boulders, gravel, sand, silt, and clay derived from the surrounding slopes and ridges. They were deposited by glaciers along the valley walls and in the bottoms of the valleys. The moraines along the steeper valley walls typically form narrow benches with relatively flat surfaces. Commonly, between a bench and the valley wall is a shallow swale. Excavations of these lateral moraines have shown that they contain lenses of sorted and stratified sand and gravel, which were probably deposited by melt water from the glacial ice.

Most of the morainal deposits are covered by boulders as a result of the removal of the finer material by glacial melting or by running water during spring runoff. Where the moraines have been deposited below cliffs or beneath slopes oversteepened by the glaciation, they are commonly covered by recent talus. Excavation of the talus deposit at the west portal showed that this talus had been deposited on the moraine.

SWAMP

The swamp deposits consist of fine sand, silt, and clay admixed with partly decayed organic material. They occur where surface drainage has been impeded, usually by the deposition of morainal material. The larger deposits were in the vicinity of the east portal of the pilot bore (pl. 1). Most of these deposits were removed during the construction of the highway and cut for the east portal. The deposits were less than 1 to about 5 feet thick. Several small deposits, too small to be shown on the map, occur in the morainal area along the two tributaries to Clear Creek from the south side of Loveland basin. In general, the deposits were not significant in the construction of the highways to the pilot bore or in the construction of the pilot bore.

TALUS

Talus deposits have accumulated at the base of the cliffs in the Straight Creek Tunnel area (pl. 1). Most of the cliffs are the result of glacial erosion and occur at the headwalls of the cirques and along the sides of the deeper valleys. Only the larger deposits are shown on plate 1. They occur around the head of Clear Creek and along Straight Creek.

Two types of talus deposits of different ages were mapped. One type consists of angular, partly weathered blocks of country rock, <0.1−3 feet in maximum dimension, that are mixed with soil, morainal material, and some glaciofluvial material. These deposits occur farther from the main source cliffs and typically form the outer slope and toe of the larger talus deposits. They are estimated to be as much as 50 feet thick. The best example of this type of talus deposit is the large deposit below the Continental Divide at the south edge of the mapped area. The second type of talus deposit consists of unweathered blocks of country rock that are <0.1−3 feet in maximum dimension. This second type of talus does not include any fine material. It occurs at the base of the cliffs and, in most places, overlies the weathered talus or moraines.

LANDSLIDE

Landslides, shown on plate 1, are areas where surficial material and weathered bedrock have moved downslope. The moraines were probably deposited by the last ice that occupied the valley. Downslope movement occurred as the ice melted. For example, the large landslide northwest of the head of Straight Creek is composed of a mixture of talus and morainal material. The landslide on the west side of the Continental Divide, north of the tunnel line, is composed of morainal material in its lower part and of mountaintop debris and bedrock in its upper part. The failure of the moraine probably removed the support from the material accumulated above the moraine, which then moved downslope behind the moraine. When a mass of surficial material fails along high mountain valleys, some of the bedrock below the surficial material also fails and becomes part of the landslide mass — particularly in those areas where the surficial material has been deposited on sheared and altered bedrock.

A major landslide (pl. 1) occurred during excavation for the approach road to the east portal of the pilot bore. The landslide occurred north-northwest of the east portal and prompted the relocation of that portal. This landslide was about 1,500 feet long and 800 feet wide, and its maximum thickness was about 70 feet. It was estimated to contain about 1,700,000 cubic yards of material — mostly altered bedrock, lying in the large shear zone at the east portal. A detailed report of an investigation of this landslide has been published (Robinson, Lee, and others, 1972.)

STRUCTURE

The Straight Creek Tunnel area is near the northwest margin of the Colorado mineral belt. Tweto and Sims (1963) summarized the structure and the origin of the Colorado mineral belt. They concluded that the mineral belt — characterized chiefly by intrusive rocks and ore deposits of Laramide and Tertiary age — coincides with a zone of deformation of Precambrian age. Crustal movement occurred within this zone throughout much of Precambrian time and was accompanied at different times by igneous activity. The environment of the deformation changed with time from relatively deep seated deformation, which resulted in folding and plastic flow, to relatively shallow deformation, which resulted chiefly in fracturing and retrograde metamorphism. During Tertiary time this zone was invaded by magma and ore-forming fluids. Faulting took place along old faults and formed new faults within the mineral belt, but the Laramide and Tertiary faulting was on a minor scale compared with that of the Precambrian faulting.

Many geologists (Lovering and Goddard, 1950; Harrison and Wells, 1956, 1959; Harrison and Moench, 1961; Sims and others, 1963; Moench, 1964; Wells and others, 1964) have recognized one or more periods of Precambrian and Tertiary deformation in the Front Range. The small area mapped during this investigation can contribute little to the regional structural geology of the Front Range, and the structures cannot be directly correlated with known periods of deformation or with known structures at other places in the Front Range. Precambrian folding was recognized by the foliation of the metasedimentary rocks, Precambrian faulting was recognized by the cataclasis of the Precambrian rocks, and Precambrian faulting and jointing were recognized by the offset of Precambrian structures. The entire Straight Creek Tunnel area is considered to be within a wide zone of Precambrian and Tertiary faulting related to the Loveland Pass fault zone (Lovering and Goddard, 1950, pl. 2).

Mineralized rock in the Straight Creek Tunnel area and possible associated hydrothermally altered rock were considered as a potential problem in construction of the pilot bore. It was determined, however, that the only mineralization was probably of Precambrian age, inasmuch as it is associated with Precambrian structures, and the alteration was the result of ground water and was controlled by Laramide structures. The mineralization and alteration are therefore discussed under this section on structure.

FOLIATION

Two types of primary foliation were recognized in the Straight Creek Tunnel area — the foliation of the metasedimentary rocks resulting from metamorphism of compositional layers and the foliation of the granite resulting from flow. A third type of foliation, the result of cataclasis, is conspicuous locally in the granite.

METASEDIMENTARY ROCKS

The metasedimentary rocks exhibit a compositional layering and, in those layers that contain planar minerals, a

preferred orientation of the minerals. In the study area the compositional layering and the preferred orientation of the planar minerals were parallel. The compositional layering is attributed to original differences in composition of the parent sedimentary rock before metamorphism, which is considered to have been parallel to the original bedding (Lovering and Goddard, 1950, p. 52). The attitude of the foliation is the result of an early period of plastic deformation modified by rotation of the inclusions of metasedimentary rocks during Precambrian emplacement of the Silver Plume Granite.

The attitudes of the folation are shown in the equal-area diagrams (fig. 5). The foliation of the metasedimentary rocks at the surface within a 1-mile-wide strip, with the original proposed pilot-bore line at the center, strikes generally about N. to N. 30° E. and dips 60°−90° NW. or SE. (fig. 5*A*). The foliation in the metasedimentary rocks exposed at the level of the pilot bore strikes generally about N. 10°−60° E. and dips 10°−50° NW. or SE. (fig. 5*B*). The compilation from the underground mapping also shows a secondary pair of maximums that represent foliations that strike about N. 60° W. and dip about 30° NE. or SW.

GRANITE

Foliation in the Silver Plume Granite is of two types — flow foliation, which is predominant, and cataclastic foliation.

The flow foliation, the result of the subparallel orientation of microcline feldspar crystals, formed at the time of intrusion of the granite (Lovering and Goddard, 1950, p. 28). In outcrops of uncontaminated granite this foliation is difficult to recognize, particularly so in the pilot bore, where only a two-dimensional exposure of the granite could be observed. In the uncontaminated granite the micaceous minerals (chiefly biotite) are not normally parallel to the feldspar laths. Most outcrops of the Silver Plume Granite, however, contain different amounts of partially assimilated metasedimentary rocks. The Silver Plume ranges in composition from almost pure granite, containing only a few schlieren of biotite-rich rock, to a migmatite. In these rocks, where the biotite and other micaceous or mafic minerals are generally oriented parallel to the feldspar crystals, the foliation is distinct.

The cataclastic foliation was noted in many outcrops of Silver Plume Granite. Where outcrops of granite are within or adjacent to a shear zone, the mineral grains may have been fractured and offset along numerous microshears and then recrystallized. The micaceous minerals are typically rotated and streaked out parallel to the shear direction. This cataclastic foliation is difficult to distinguish from the flow foliation without microscopic examination.

The foliation of the Silver Plume Granite at the surface within a 1-mile-wide strip, with the original proposed tunnel line at the center (fig. 5*C*), strikes generally N. to N. 30° E. and dips about 70° NW. or SE. The foliation of the granite in the pilot bore (fig. 5*D*) is represented by two maximums — attitudes of about N. 45° E., 30° SE. and about N. 60° W., 15° NE. Less than half as many observations were made in the pilot bore as were made on the surface because of the difficulty in observing the foliation on a planar surface in the pilot bore.

The attitudes of foliation of the metasedimentary and granitic rocks at the surface are similar, and for purposes of projecting the attitudes to the depth of the pilot bore, diagrams in figure 5*A* and 5*C* were combined, which gives an average strike of N. to N. 30° E. and dips of 60°−90° NW. or SE. The attitudes of foliation of the metasedimentary and granitic rocks in the pilot bore are also similar. A combination of diagrams in figure 5*B* and 5*D* gives an attitude for the folaition of N. 10°−60° E., 10°−50° SE. At the surface, about four times as many observations were made in the granite as were made in the metasedimentary rocks, but in the pilot bore, about twice as many observations were made in metasedimentary rocks as in the granite. This imbalance illustrates the relative lack of good exposures of metasedimentary rocks at the surface and the difficulty in measuring the foliation of the granite exposed in the pilot bore.

The lack of agreement between the attitude of the foliation at the surface, in the drill holes, and in the pilot bore is the result of the origin of the attitude of the foliation. The foliation of the metasedimentary rocks was measured on inclusions ranging in size from<1 foot to several hundred feet. These inclusions were undoubtedly rotated to some degree by the intrusion of the granite. The foliation of the granite is considered to be the result of flow. The direction of flow was controlled in part by the attitude of the foliation of the metasedimentary rocks, as indicated by their general parallelism in this area and in other areas in the Front Range (Warner and Robinson, 1967), but local deviation from the regional foliation is typical in the granite. The strike of the foliation at the surface is more closely parallel to that in the pilot bore than is the dip. The difference in dip is related to the fact that low angles of dip, not only of foliation but also of joints and faults, are not so well exposed in surface outcrops as are higher angles of dip. The opposite is true in diamond-drill cores. The conclusion reached from this investigation is that the foliation measured on the surface in this type of geologic environment can be projected to a tunnel level with only limited accuracy. To accurately project the foliation to depth, the dip of the foliation in any core from diamond-drill holes must be considered.

FAULTS AND SHEAR ZONES

The Straight Creek Tunnel area is within a wide zone of Precambrian and Tertiary faulting that is related to the Loveland Pass fault (Lovering and Goddard, 1950, pl. 2). The Loveland Pass fault and its northern extension, the Berthoud Pass fault, can be traced for almost 30 miles northeastward from the Straight Creek Tunnel area. The

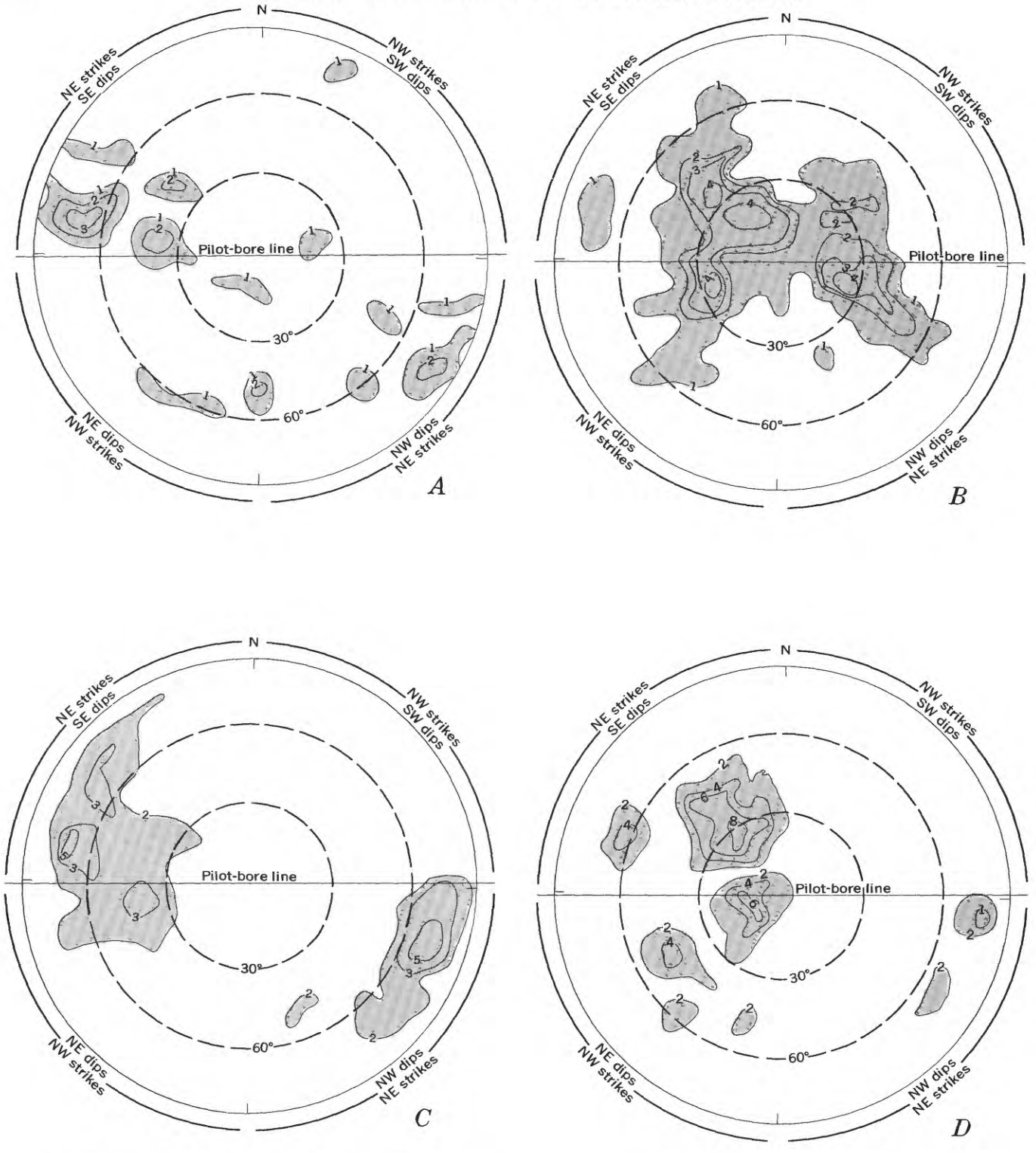

FIGURE 5. — Contoured equal-area diagrams (lower hemisphere) showing attitudes of the foliation of rocks in the Straight Creek Tunnel area. *A*, Metasedimentary rocks at the surface (1-mile-wide strip; 28 poles; contoured on 1, 2, and 3 percent of poles per 1 percent of area). *B*, Metasedimentary rocks in the pilot bore (140 poles; contoured on 1, 2, 3, and 4 percent of poles per 1 percent of area). *C*, Granitic rocks at the surface (1-mile-wide strip; 161 poles; contoured on 2, 3, and 5 percent of poles per 1 percent of area). *D*, Granitic rocks in the pilot bore (66 poles; contoured on 2, 4, 6, and 8 percent of poles per 1 percent of area).

Loveland Pass fault is a zone of Precambrian faulting along which later movements occurred during the Tertiary time.

The age of the faults can only be inferred from indirect evidence. In the granitic and metasedimentary rocks, faults considered to be of Precambrian age are characterized by cataclastic structures and by zones of mylonite or cataclastic gneiss. Commonly, dikes of Silver Plume Granite, pegmatite, or bull quartz are parallel to and in the cataclastic zones in the larger areas of metasedimentary rocks, and dikes of pegmatite and bull quartz occur in the cataclastic zones in the granite. Associated with the dikes are veins containing fluorite and specular hematite. Later faults, considered to be of Tertiary age, are characterized by sheeting, granulation, and gouge. The Tertiary faults have been superimposed on the earlier faults, and, therefore, the attitude of the earlier faults is difficult to determine. In general, the Precambrian and Tertiary faults are considered to be parallel, as they are in other places along the Colorado mineral belt (Tweto and Sims, 1963).

The distinction between a fault and a shear zone is one of width. Faults, as shown on plate 1, are areas of crushed rock 5−50 feet wide, and shear zones are areas of crushed rock 50 feet or more wide. Zones <5 feet wide were too numerous to be shown at the map scale. On the plan of the pilot bore (pl. 2), faults are classified and shown by different patterns as zones 1−2 feet wide, 2−5 feet wide, and >5 feet wide. Shear zones, shown on the section by an overpattern, represent zones >5 feet wide where the average spacing between fractures is <0.1−0.5 foot and the visual estimate of the alteration is 25 percent or greater. Only faults and shear zones with sheeting, granulation, and gouge are shown on plates 1 and 2.

PRECAMBRIAN FAULTS AND SHEAR ZONES

Precambrian faults and shear zones are not well exposed on the surface. As previously stated, the later faulting took place along the Precambrian faults and shear zones and destroyed much of the evidence of Precambrian faulting. These zones weather more easily, and outcrops within the fault or shear zones are rare. The best exposures of shear zones at the surface are north of the tunnel line a few hundred feet east of the Continental Divide, south of the west portal on the southeast side of Straight Creek, and in the south headwall of the cirque at the head of Loveland basin.

East of the Continental Divide and north of the tunnel line, granite, with inclusions of metasedimentary rock, is exposed along a faultline scarp of a later fault. This granite shows a strong cataclastic structure. Each mineral grain has been sheared and stretched along the shears, and the shears have been healed by recrystallization of the minerals or by cementing with microcline or quartz. The inclusions of metasedimentary rock in the granite have been stretched by shearing parallel to the cataclastic direction in the granite. West of the faultline scarp, lenticular bull-quartz bodies are exposed locally. The long dimension of these bodies, which ranges from a few inches to several feet, is parallel to the cataclastic direction in the granite. The bull-quartz bodies are also sheared parallel to the cataclastic direction. The strike of the cataclastic direction in this area is between N. 10° W. and N. 15° E., which is subparallel to the strike of the later fault.

About 2,500 feet south of the west portal of the pilot bore, at an altitude of about 11,800 feet, on the southeast side of Straight Creek are several small outcrops of granite containing inclusions of metasedimentary rock. The foliation of the rocks in this area strikes N. to N. 30° W. Careful examination of these outcrops shows a strong cataclastic direction of N. 70°−90° E. The mineral grains in these outcrops have been sheared parallel to the cataclasis, the shears healed by recrystallization of the minerals or by quartz, and the area resheared by later faulting.

In the headwall of the cirque on the south side of Loveland basin are several outcrops of mixed granitic and metasedimentary rocks whose foliation shows a strong cataclastic direction of N. 70°−90° E. The cataclastic shears have been healed. Between the outcrops are later faults and shear zones that strike N. 5° E. to N. 10° W. and N. 80°−90° E.

Evidence of Precambrian faulting was observed at several places in the pilot bore. The most striking example was noted between stations 62+10 and 62+85 in the south wall. The rock, which is fairly competent, is a fine-grained mylonite gneiss. Microscopic examination showed that the rock consists of crushed grains of feldspar and quartz <1 mm in size, and streaks of biotite, all recemented with quartz. Veins of bull quartz <1−6 inches wide cut the mylonite. The veins contained specular hematite. A 1.5-foot-wide Tertiary shear zone containing 0.2 foot of gouge cuts the mylonite. West of the mylonite gneiss, between stations 59+35 and 62+10, a Precambrian shear zone parallels the tunnel. The wallrocks consist of cataclastic granite and sheared metasedimentary rock that have been recrystallized and cemented with quartz. A vein consisting of quartz and calcite parallels the cataclastic directions and contains stringers and small vugs lined with fluorite. Veinlets of fluorite, generally <0.1 inch wide, also occur in the wallrock of the vein. The rock of the Precambrian shear zone and vein is relatively competent, except where intersected by later Tertiary faults and shear zones.

TERTIARY FAULTS AND SHEAR ZONES

The geologic structural features that most influenced the construction of the pilot bore were the faults and shear zones of Tertiary age. These faults and shear zones consist of rock that shows varying degrees of shearing, crushing, and alteration and that lacks evidence of recrystallization.

The contact of the zones is typically gradational. Near the margins the rock consists of slivers, <0.1−1 inch wide, bounded by slickensided shear planes parallel to the strike of the fault or shear zone. Where the shearing has been more intense, some of the rock has been ground to a coarse to fine sand, and the shear planes are <0.01−0.5 inch apart and strike in all directions. Where the shearing has been most intense — accompanied by some alteration — the material is clay (fault gouge) containing various amounts of quartz and feldspar sand. The gouge usually does not occur near the center of a sheared zone, but nearer one margin or the other; most commonly, it is nearer the footwall of the zone. The gouge occurs in discontinuous streaks, a few inches to several hundred feet long and <0.1 inch to 200 feet wide, elongated parallel to the trend of the shear zone.

The effect of shearing is different on the different rock types. The typical granite when sheared produces sharp unaltered, or only partly altered, rock fragments and sand. Gouge, if present, has a low proportion of clay and is mostly sand. The metasedimentary rocks that contain a high percentage of plagioclase and biotite are sheared and extensively altered where they are intersected by a shear zone. Regardless of the relation of the original attitude of the foliation and direction of shearing, the foliation layers are resheared parallel to the foliation, and each foliation lamina is paralleled by shear planes. The gouge, where present, consists chiefly of clay and of lesser amounts of quartz and feldspar sand. Under the most adverse conditions, metasedimentary rocks in a shear zone become completely sheared and altered to a plastic sandy clay; yet the foliation and layering, though commonly contorted in many minor folds, remain recognizable.

The faults and shear zones change width and length within short distances. The individual faults or shear zones pinch and swell and may end abruptly against relatively unbroken rock. Some of the larger shear zones contain blocks of country rock, as much as 100 feet in maximum dimension, that are relatively unsheared despite being surrounded by intensely sheared rock. In mapping the surface we did not project the shear zones and faults through covered areas — because of their general discontinuity — unless there was good evidence that they continued. For this reason the abrupt ending of most of the shear zones (pl. 1) is so shown because of cover, not because of an observed ending.

The trends of the faults and shears at the surface, as determined on the basis of mapping and measuring in the field, are shown in figure 6*A*. The attitude of a fault or shear zone is difficult to measure in the field because each zone is made up of many small shear planes at many attitudes. Along a few faults one of the walls was sharply defined, and the attitude of this wall was taken as the attitude of the fault. In some shear zones, seams of gouge were exposed. The attitude of a gouge seam whose width was greater than 1 inch was assumed to represent the attitude of a shear zone.

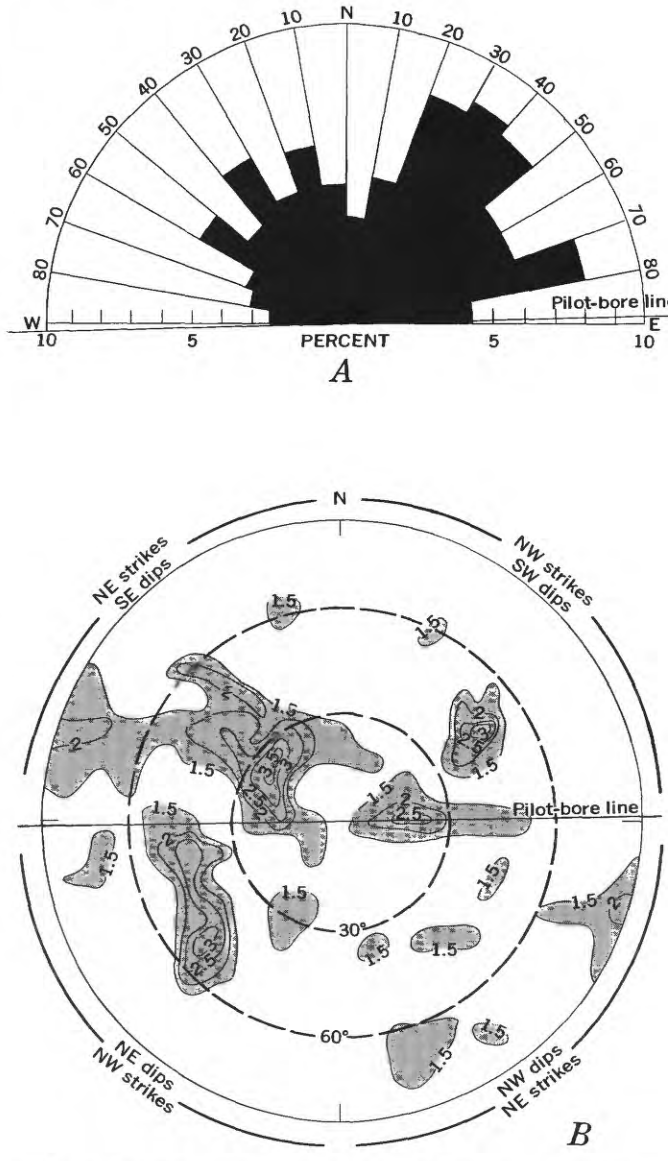

FIGURE 6. — Strike-frequency diagram (*A*) and contoured equal-area diagram (*B*) of faults and shear zones of the Straight Creek tunnel area. *A*, 284 faults and shear zones at the surface. *B*, Lower hemisphere; faults and shear zones in the pilot bore (244 poles; contoured on 1.5, 2, 2.5, 3, and 3.5 percent of poles per 1 percent of area).

The average dip of 74 faults or shear zones measured at the surface was 75°. With a dip of 75°, the difference between the trend and the true strike would be only about 268 feet horizontally for each 1,000 feet of relief, or a difference of 15° from the true strike for 1,000 feet along the strike for a relief of 1,000 feet. It can therefore be assumed that the strike-frequency diagram (fig. 6*A*) represents the strike of the faults and shear zones observed at the surface in the Straight Creek Tunnel area. Most faults strike N. 20°−50° E.; in the second most abundant set, the faults strike N. 70°−80° E.

Many faults and shear zones were mapped in the pilot bore, but their true attitudes were difficult to determine

because, as at the surface, they consist of many small shear planes at many attitudes and because the underground observations were limited to the diameter of the bore, about 13 feet. From surface mapping it was known that minor changes in the attitude of a fault or shear zone were common locally within short distances along the strike of a fault or shear zone. The attitudes of the Tertiary faults and of shear zones >1 foot wide observed in the pilot bore are shown in figure 6*B*. The maximums represent faults that strike N. 45° E. and dip 30° or 70° SE. and those that strike N. 10°–20° E. and dip 70°–90° SE. or 85°–90° NW. The maximums represented by an attitude of about N. 45° E., 30° SE. correspond to the maximums for the foliation of the metasedimentary rocks in the pilot bore (fig. 5*B*), which illustrates the influence that the foliation of the metasedimentary rocks had on the attitude of the faulting and shearing.

The strike of the faults and shear zones in the pilot bore corresponds, in general, to that determined at the surface; however, the average dip in the pilot bore is considerably less than that at the surface. This again illustrates that structures of low dip probably are not as conspicuous at the surface as those of higher dip.

JOINTS

Joints are considered to be fractures along which little or no significant movement has occurred. Attitudes were measured of only those individual joints that could be traced for at least 10 feet or of zones of short joints that could be traced for 10 feet. The attitudes of joints are not shown on the geologic maps (pls. 1, 2) but have been compiled on a series of equal-area diagrams (figs. 7, 8).

During the early stages of the surface mapping, an attempt was made to distinguish between possible shear and tension joints, on the basis of the presence or absence of slickensides on the joint surfaces and whether the joints were tight or open. It soon became obvious that many of the joint surfaces which were not extensively weathered or altered showed slickensides; therefore, distinguishing the types of joints no longer seemed valid. The bearing and plunge of slickensides and of other linear features on joint surfaces, such as streaked mineral aggregates, were recorded during the early part of the surface mapping. It was noted however that there was a wide range in bearing and plunge of the slickensides on a single joint surface and between adjacent parallel joint surfaces, and that the equal-area plots of these linear elements gave a completely random pattern, so the observations were discontinued. It was concluded that the surfaces of fractures that were recorded as joints — at the surface, in the drill hole core, and underground — were chiefly microfaults and shears. In addition to the attitude of joints, the rock type in which the joints occurred and the spacing between joints in a set were recorded.

JOINTS AT THE SURFACE

The surface joint measurements were restricted to a 1-mile-wide strip, with the proposed tunnel line at the center.

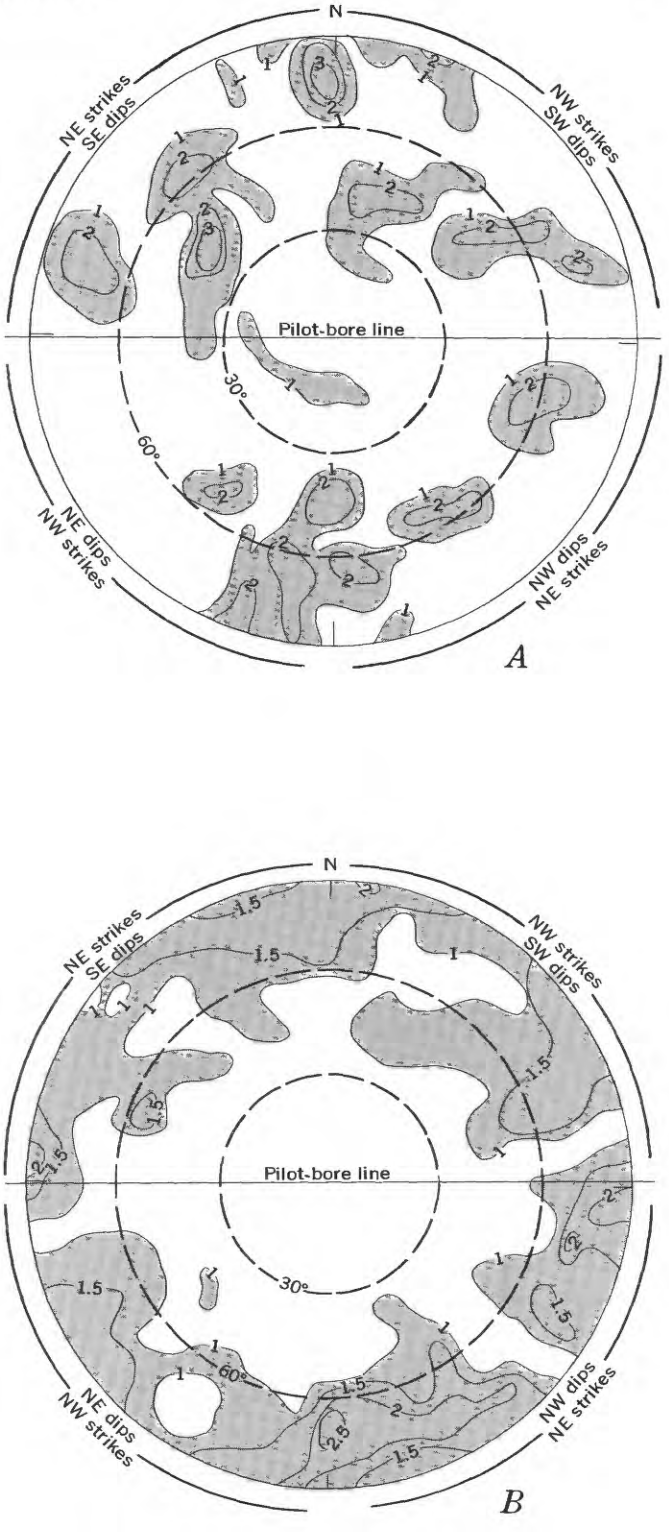

FIGURE 7. — Contoured equal-area diagrams (lower hemisphere) of joints at the surface (1-mile-wide strip), Straight Creek Tunnel area. *A*, Metasedimentary rocks (77 poles; contoured in 1, 2, and 3 percent of poles per 1 percent of area). *B*, Granitic rocks (838 poles; contoured in 1, 1.5, 2, and 2.5 percent of poles per 1 percent of area).

The joints in the metasedimentary rocks and the Silver Plume Granite along this strip are shown in figure 7.

In the metasedimentary rocks two maximums were obtained. One represents joints that strike about N. 35° E. and dip 45° SE. and the other represents joints that strike about N. 85° E. and dip 85° SE. Some of the joint attitudes are represented by foliation attitudes (figs. 5*A*, 7*A*). The exceptions are joints that strike nearly east-west and dip 70°–90° N. or S. and joints that strike northwest and dip southwest. These probably represent joints that strike at about right angles to the strike of the foliation. Joints in layered rock commonly strike parallel to the strike of the rock and have dips of 90° to the dip of the layering. Also common are joints that strike at 90° to the strike of the layered rocks and have near-vertical dips in either direction.

In the granite at the surface, the joints having dips of greater than 45° are randomly distributed. Most of the joints strike north to east and dip east to south. The average dip for all joints is about 70°. The foliation direction in the granite is not as strong as the joint direction in the metasedimentary rocks. (Compare figs. 5*C* and 7*B*.) The attitudes of the faults and joints have a similar distribution, as shown by comparing figures 6*A* and 7*B*. Most of the faults and joints strike north to east, although they are well distributed in all directions. The average dip of the faults was determined to be 75° in either direction, and that of the joints, 70°. These facts are the basis for concluding that most of the fractures recorded as joints were microfaults or shears.

JOINTS IN THE DRILL-HOLE CORE

In logging the cores from diamond-drill holes 2 and 3, the authors recorded the attitude of the joints in relation to the foliation by assuming that foliation would strike north, the strike of a joint was measured as a compass bearing from this line of reference. The dip was measured as the angle between a horizontal plane through the core and the joint. It was assumed that the strike of the folation in the area would be relatively constant and that a contour diagram of the attitude of the joints could be rotated so that the north pole of the joint diagram corresponded to the strike of the maximum for the foliation. The attitudes of the joints in the cores were plotted, and the plots showed that the joints in the cores had strikes in all directions. The average dip of the joints was about 50° in the cores, however, as compared with about 70° for the joints measured at the surface. It was recognized that near-vertical joints would not be accurately represented in a vertical drill hole and that near-horizontal joints would be overemphasized. The average dip of all joints in the area was therefore assumed to be about 60°.

JOINTS IN THE PILOT BORE

The recognition of a significant joint in underground mapping depended in part upon the direction in which the opening was driven and in part upon the surface along which the joint occurred in relation to the axis of the opening. The pilot bore was driven nearly due west from the east portal. The measurements of the attitudes of the joints in the pilot bore, therefore, were compiled on separate diagrams for the walls and for the faces of the bore. These data were further subdivided according to rock type. The attitudes of the joints in the metasedimentary rocks and granite, as measured on the walls and on the faces of the pilot bore as the bore was advanced, are shown in figure 8. The pilot-bore walls were mapped at 1:600 and the faces at 1:24. At least one face map was prepared per 8-hour work shift and, because of the larger scale, more than three times as many poles were plotted for the face mapping as for the wall mapping. In addition to recording the attitude of the joints underground, the joints at each point of measurement were classified from 1 to 3, depending upon their relative abundance, with No. 1 joints being the most abundant; and the average spacing between joints in a set was recorded.

In the metasedimentary rocks the joints measured in the walls (fig. 8*A*) and in the faces (fig. 8*B*) give different diagrams. In the walls the joints give poles equally distributed in the quadrants of the net, except for poles representing joints that strike north to east and dip northwest. Three maximums are defined, representing joints that strike and dip about east to west (parallel to the trend of the pilot bore) — 65° N.; N. 30° E., 65° SE.; and N. 70° W., 65° SW. In the faces the joints give poles concentrated in the east half of the net, representing joints that strike north to east and dip northwest and that strike north to west and dip southwest. Four maximums are defined that represent joints that strike and dip about N. 55° W., 45° SW.; N. 45° W., 25° SW.; N. 70° E., 65° NW.; and N. 50° E., 75° NW. The two diagrams do not contain a common maximum.

In the granite the joints measured in the walls (fig. 8*C*) and in the faces (fig. 8*D*) also give different diagrams. The maximum on the diagram representing joints in the walls corresponds to joints that strike east to west (parallel to the trend of the pilot bore) and dip 85°–90° N. or S. Minor maximums represent joints that strike and dip N. 50° W., 55° SW.; E.–W. 10° S.; N. 70° E., 25° SE.; and N. 80° E., 70° NW. In the faces the joints are concentrated in the east half of the net and strike north to east and dip northwest and strike north to west and dip southwest. Three maximums are defined, representing joints that strike and dip N. 40° W., 45° SW.; N. 75° E., 70° NW.; and N. 85° E., 80° NW. The two diagrams do not contain a major common maximum.

TABLE 5. — *Joint maximums in metasedimentary rocks and granite in the pilot bore (from figure 8)*

[Attitudes which are similar are printed in italic type]

Walls		Faces	
Metasedimentary rocks	Granite	Metasedimentary rocks	Granite
N. 30° E., 65° SE.	N. 70° E., 25° SE. N. 80° E., 70° NW.	N. 50° E., 75° NW. *N. 70° E., 65° NW.*	*N. 75° E., 70° NW.* N. 85° E., 80° NW.
N. 70° W., 65° SW.	*N. 50° W., 55° SW.*	*N. 55° W., 45° SW.* *N. 45° W., 25° SW.*	*N. 40° W., 45° SW.*
E.–W., 65° N.	*E.–W., 85°–90° N. or S.* E.–W., 10°–10° S.		

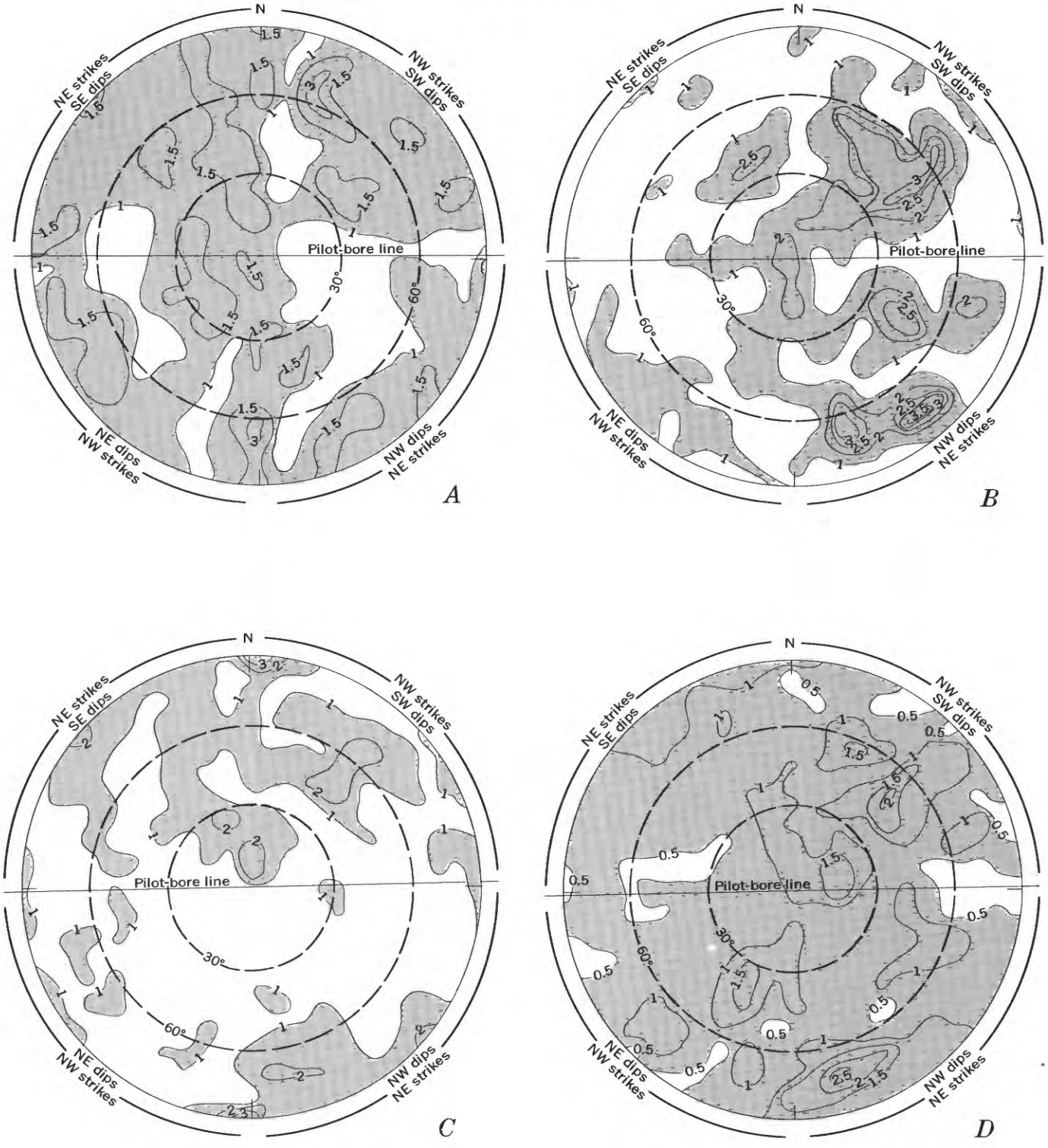

FIGURE 8. — Contoured equal-area diagrams (lower hemisphere) of joints in the pilot bore. *A*, Metasedimentary rocks in the walls (128 poles; contoured on 1, 1.5, and 3 percent of poles per 1 percent of area). *B*, Metasedimentary rocks in face sections (446 poles; contoured on 1, 2, 2.5, 3, and 3.5 percent of poles per 1 percent of area). *C*, Granitic rocks in walls (400 poles; contoured on 1 and 2 percent of poles per 1 percent of area). *D*, Granitic rocks in face sections (1,506 poles; contoured on 0.5, 1, 1.5, and 2 percent of poles per 1 percent of area).

Table 5 shows that joints similar in strike (within 10°) and dip (within 20°) were measured in the metasedimentary rocks and the granite in the walls and in the faces, and that one joint set was common to the granite in the walls and to

the metasedimentary rocks in the faces. It was concluded from this analysis that the attitude of joints measured only on the walls or only on the faces of a tunnel as the tunnel is advanced would not be representative. As a result, the attitudes of the joints measured on the walls were plotted (fig. 9) with the attitudes of the most conspicuous joints measured on each face. This diagram shows four maximums: a 3-percent maximum, which represents joints that strike about N. 75° E., and dip 75° NW. (about parallel to one of the major directions of faulting); a 2.5-percent maximum, which represents joints that strike about N. 45° W. and dip 45° SW.; and two 2-percent maximums, one of which represents joints that strike about N. 75° W., and dip about 65° SW. These maximums are probably not very significant, inasmuch as the largest one represents the attitudes of only 35 joints out of a total of 1,179 plotted. It was concluded that, in general, the joints in the pilot bore strike in all directions. The average dip for the joints was calculated as about 45°.

ORIGIN OF STRUCTURAL FEATURES

The structural features in the Straight Creek Tunnel area can be classified simply as foliation and fractures. The foliation of the metasedimentary rocks is the result of metamorphism of the compositional layering of the original sedimentary rocks. The attitude of the foliation is the result of plastic folding and of rotation of the inclusions of metasedimentary rocks by the intrusion of the granite. In the metasedimentary rocks the foliation is a surface of weakness, as the rocks have been fractured parallel to the foliation. In the Silver Plume Granite, where the foliation is not a principal direction of weakness, the main foliation is the result of flow, and a secondary foliation is the result of Precambrian shearing.

Fractures consist of faults, shear zones, and joints. The faults and shear zones that influenced the construction of the pilot bore are the result of Tertiary fracturing and brecciation. Tweto and Sims (1963, p. 1009–1012) determined that faults of different ages have different attitudes. In the limited area of the Straight Creek Tunnel site the ages of Tertiary faulting could not be distinguished. Locally, Precambrian faults that were healed were recognized, and Tertiary faults, which contain breccia and gouge. Joints were probably developed during periods of Precambrian folding and faulting, periods of Tertiary faulting, and possibly other periods, such as during the uplift of the ancestral Rocky Mountains in Pennsylvanian and Permian time. The joints in the Straight Creek Tunnel area could not be related to any period of crustal disturbance as was done by Harrison and Moench (1961) for the Central City–Idaho Springs area of the Front Range to the east. There probably was some movement along older joints, and new shear joints were developed during Tertiary faulting and uplift of the Front Range.

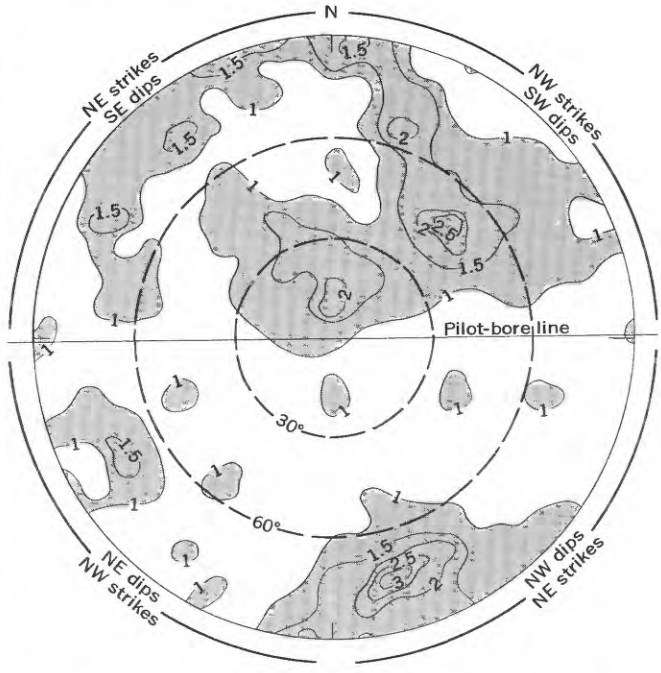

FIGURE 9. — Composite contoured equal-area diagram (lower hemisphere) of joints in pilot bore measured on walls and face sections (1,179 poles; contoured on 1, 1.5, 2, 2.5, and 3 percent of poles per 1 percent of area).

ALTERATION AND MINERALIZATION

Rock alteration in the Straight Creek Tunnel area is believed to be related to metamorphism, weathering, and ground water, rather than to hydrothermal alteration, which is common in other areas of the Front Range and is related to the formation of the Tertiary ore deposits.

Retrograde metamorphism occurred during the period of cataclastic deformation of rocks in Precambrian time. The cataclastic deformation reduced the grain size and produced a change in texture. Some of the minerals were recrystallized after deformation; an extreme example was the formation of mylonite gneiss. In most of the Precambrian rocks, chlorite has replaced some of the biotite and hornblende, muscovite has replaced sillimanite, and microfractures are filled with microcline or quartz. Twinning of feldspars has become less distinct, and overgrowths on mineral grains are common. All these changes are attributed to mechanical and chemical alteration during Precambrian time.

Chlorite, talc, calcite, dolomite, selenite, silica, epidote, and clay occur on many joint and fault surfaces, and the country rock adjacent to these structures may be partially altered for a considerable distance from the structure. These minerals are believed to be the result of alteration by weathering and ground water. Alteration products commonly coat the surfaces, and fill some joints. The typical joint surface in the granite is coated with chlorite or silica, on which slickensides have developed. The typical joint sur-

face in the metasedimentary rocks is coated with chlorite or epidote, and shows slickensides. At the surface few such joints were noted, but in the west half of the pilot bore, joints filled with clay, calcite, dolomite, selenite, and talc are common. In most of the country rock, the feldspar grains are dusted with clay, but the most extensively altered country rock is adjacent to joints and faults and in fault and shear zones. The width of the altered zones, which ranges from <0.1 foot to about 600 feet, depends largely on the amount of fracturing. The widest zones are associated with and include bands of fault gouge, which resulted from the mechanical grinding of the rock and the chemical alteration of the grains. The widest altered zone at the surface is along the shear zone east of drill hole 3 (1962). A bulldozer trench north of the tunnel line exposed 150−200 feet of gouge. The widest altered zone underground was exposed between stations 80+85 and 86+95. X-ray mineralogic analyses of samples of altered rock are given in table 9 (chapter C) of this report.

Ground water is considered to be the chief agent of the alteration adjacent to the joints and in the faults and shear zones. Although this alteration is spatially related to Tertiary structures, no evidence of Tertiary ore deposition, such as the deposition of sulfide minerals, other than pyrite, was observed. The alteration products — chiefly clay minerals, chlorite, and silica — can be derived by ground-water action on the granite and the metasedimentary rocks. The chemical composition of the ground water is given, and the origin of the elements in the ground water is discussed by Hurr and Richards in chapter E of this report. They concluded that the elements in the ground water were derived from the granite and metasedimentary rocks in the vicinity of the pilot bore.

Minerals typical of ore deposits — pyrite, chrysocolla, fluorite, and hematite — were noted in drill core and in the pilot bore. Pyrite is sparsely disseminated in all the rock and is considered to be syngenetic. In the pilot bore and in drill-hole 3 (1962) below a depth of 800 feet, pyrite occurs in gouge, along joints, and in sheared and altered country rock. This pyrite is believed to have been deposited by ground water. Chrysocolla, probably from the oxidation of chalcopyrite, in association with some fluorite was noted at a depth of 250 feet in drill-hole 3 (1962). In the pilot bore, fluorite in thin veins is common between stations 50+00 and 70+00. Specular hematite occurs in the pilot bore in bull-quartz veins and in mylonite near stations 62+10 to 62+80 and on the surface in bull-quartz veins in the north-trending shear zone east of the Continental Divide. The fluorite and hematite occur in Precambrian shear zones and are believed to be related to that period of faulting and mineralization.

Engineering Geology

By CHARLES S. ROBINSON *and* FITZHUGH T. LEE

ENGINEERING GEOLOGIC, GEOPHYSICAL, HYDROLOGIC, AND ROCK-MECHANICS INVESTIGATIONS OF THE STRAIGHT CREEK TUNNEL SITE AND PILOT BORE, COLORADO

GEOLOGICAL SURVEY PROFESSIONAL PAPER 815–C

ENGINEERING GEOLOGIC, GEOPHYSICAL, HYDROLOGIC, AND ROCK-MECHANICS INVESTIGATIONS OF THE STRAIGHT CREEK TUNNEL SITE AND PILOT BORE, COLORADO

ENGINEERING GEOLOGY

By CHARLES S. ROBINSON and FITZHUGH T. LEE

INTRODUCTION

The objectives of this project were to evaluate known methods and develop new methods of predicting geology at the depth of an underground opening ahead of construction, and to make measurements and observations during the construction period to determine the relative importance of the geologic factors that influence engineering design, construction practices, and economic aspects of construction of an underground opening. Various investigations were made; some were successful, and some were not. The purpose of this chapter is to describe the methods and results of investigation, the methods used to compile the data and predict the conditions at tunnel level prior to construction, and the engineering operations and construction practices used in the construction of the pilot bore.

METHODS AND RESULTS OF INVESTIGATION

The methods of investigation can be divided into surface and underground geologic studies, drill-core logging, laboratory sample testing, hydrologic studies, and rock-mechanics measurements. Some of these investigations were made only prior to construction of the pilot bore, some were both prior to and during construction, and others were only during construction. Three special studies — geophysical, ground water, and rock mechanics — developed from these investigations; these are only summarized in this chapter, inasmuch as each is the subject of a separate chapter.

SURFACE AND UNDERGROUND GEOLOGIC STUDIES

In the surface and underground geologic investigations, emphasis was placed on studying three geologic factors that were believed would influence the design and construction of the pilot bore and the final tunnel — rock structure, rock composition, and rock alteration. These factors are indirectly related to two major problems in tunneling — ground water and rock loads.

Engineering geologic studies of the Roberts Tunnel (Wahlstrom and Hornback, 1962; Warner and Robinson, 1967; Wahlstrom, Warner, and Robinson, unpub. data) have shown that rock fractures, regardless of origin, are probably the most important geologic influence on the driving and support of tunnels in the Front Range area of Colorado. Different types of fractures are separations along planes of weakness in a rock, such as bedding planes, foliation planes, joints, and faults. In mapping the surface and the pilot bore and in logging the core from the drill holes, both the range in distance and the average distance between fractures were recorded for each exposure. The average distance between fractures is defined as the fracture spacing. The distance between fractures determines the size of pieces of unfractured rock in an exposure, so fracture spacing may also be defined as the average size of pieces of unfractured rock in an exposure. In part, fractures control the size of the rock pieces produced in mining operations, particularly where the distance between fractures is less than 0.5 foot, and can be considered as about equivalent to the breakage of a rock due to the mining process.

The fracture spacing was the basic unit in classifying the rock structure for engineering purposes. On the surface, all outcrops were classified as having a fracture spacing of $<0.1-0.5$, $0.5-1$, $1-3$, and >3 feet. In the pilot bore the ground was classified as having a fracture spacing of <0.1, $0.1-0.5$, $0.5-1$, >1 feet. The classifications were changed during the underground mapping because it became apparent from the mapping and instrumentation that (1) when the average spacing between fractures exceeds 1 foot, the support requirements are determined more by the nature of the fracture surface than by the distance between fractures, and (2) the largest loads developed on the support when the average fracture spacing was <0.1 foot.

Rock composition and the degree of alteration determine the behavior of the rock under stress. In the metasedimentary rocks and strongly foliated granitic rocks, the principal planes of weakness (and fracturing) are parallel to the foliation. Those layers with the highest concentration of biotite are the most fractured. In the Silver Plume Granite the composition is relatively uniform, and laboratory experiments (Nichols and Lee, 1966) did not show clearly the relation of composition to strength.

The amount of alteration is determined partly by the amount of fracturing and partly by the composition of the

rock. The highly fractured rocks were more highly altered because of greater exposure to ground water. Under ground-water conditions, alteration first affects the ferromagnesium minerals, then affects the plagioclase and the microcline and, finally, the quartz. Those rocks with the highest percentage of ferromagnesium minerals and plagioclase and the greatest degree of fracturing were altered the most. For surface mapping the rocks were classified as unaltered, slightly altered, or highly altered. For underground mapping the relative percentages of the altered minerals of a rock were noted.

SURFACE GEOLOGIC MAPPING

A surface area of about 6 square miles was mapped geologically at a scale of 1:12,000 on a topographic base enlarged from the 1:24,000, 7½-minute Loveland Pass quadrangle (pl. 3). Every accessible outcrop within this area was examined, and the rock composition (or type), fracture spacing, attitudes of fractures, characteristics of fracture surfaces, and degree of alteration were recorded. Representative samples of rock types and fault gouge were collected for laboratory analysis. It was calculated that only 4 percent of the area was outcrop. The surface mapping was done by the authors and, including logging of drill-hole core, required about 4 man-months. This includes about 2 man-weeks spent by Robinson in preliminary mapping during the year preceding the geologic mapping.

UNDERGROUND GEOLOGICAL MAPPING

Underground geologic investigations were conducted to evaluate the geologic and engineering predictions based on the surface investigations and drill-hole logging, and in support of the geophysical, ground-water, and rock-mechanics instrumentation programs. As construction of the pilot bore advanced, the walls of the tunnel were mapped geologically at 1 inch to 50 feet (1:600), as shown on plate 2 at a reduced scale. Rock type, fracture spacing, attitudes of foliation and fractures, percentage alteration, characteristics of fracture surfaces, ground-water conditions, spacing and types of support, lagging and blocking as a percentage of the circumferential area above the invert, progress, and location and length of feeler holes were recorded. Representative samples of wallrock were collected for laboratory analysis. In support of the tunnel-wall mapping, the face was mapped at 1 inch to 2 feet (1:24) by the authors or by engineers of the Colorado Department of Highways at least once per 8-hour shift. The mapping was done on a preprinted sheet that showed the payline of the tunnel section. Figure 10 is a typical example of the more than 800 face maps that were prepared.

In support of the rock-mechanics instrumentation and geophysical investigations, at least one wall and in some places both walls were mapped at 1 inch to 5 feet (1:60) for at least 50 feet on each side of an instrument station. An example of these maps is shown in figure 11. The maps were made at the level where the geophysical measurements were taken, or about 4 feet above the invert. In most places only the south wall was mapped, inasmuch as it was relatively free of cable and pipelines. Every 50 feet, however, a careful survey was made of rock type, fracture spacing, degree of alteration, and other rock features on the north wall and in the roof. This information was used in all the statistical correlations made on the basis of pilot-bore geologic mapping, thereby reducing the potential bias inherent in data obtained from mapping only one wall. Mapping the face added another mapping dimension that provided a valuable comparison with the structural information gained from the wall mapping. The results of both types of mapping are discussed in the section on structure in chapter B. In conjunction with the detailed mapping at the instrument and geophysical stations, chip samples for laboratory analysis were taken along the line of mapping for 5 feet on each side of each station.

As the measurement results from the instrumented sets were obtained, it became apparent that the loads that developed depended on the manner in which the supports were installed, as well as on the geologic conditions. The blocking and lagging around each instrumented set, therefore, was mapped at a scale of 1 inch to 2 feet (1:24). Figure 12 shows examples of the mapping of the blocking of the sets.

The underground geologic investigations required an average of about 4 man-days per week for the 13-month period of pilot-bore construction.

DRILL-CORE LOGGING

Prior to the start of the present project, the Colorado Department of Highways had holes drilled for core in two separate preliminary investigations. In November 1953 Minerals Engineering, Inc., drilled two core holes, which had a combined total length of 240 feet, in the eastern part of the area. In the summer of 1955 Sprague and Henwood, Inc., drilled four core holes (pl. 1), which had a combined total length of 1,848 feet, along a proposed tunnel line. The core from these holes was logged by R. H. Carpenter. Graphic logs of these core holes were made available. In the summer of 1962, while the surface geologic mapping was being done, the Colorado Department of Highways supervised the drilling of four holes (pl. 1). Holes 1 and 4 were drilled near the east and west portals for use as seismic shotholes. These holes were not core drilled and only drillers' logs were made. Holes 2 and 3 were cored, and the core logged. These holes were also logged geophysically and were used for emplacement of geophones during the surface seismic investigations.

The Colorado Department of Highways had originally considered drilling several additional core holes but decided against the drilling because it was recommended that

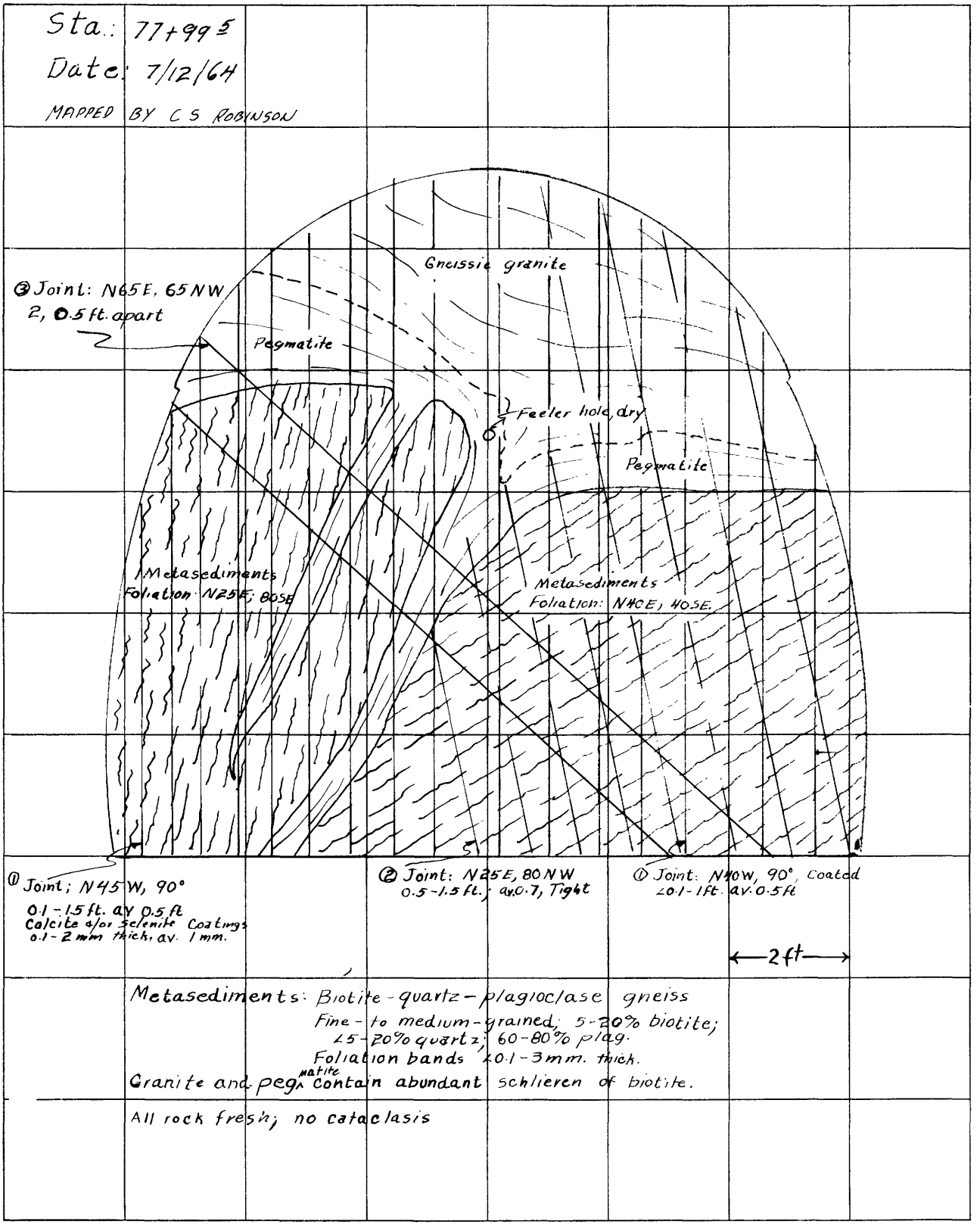

FIGURE 10. — Example of a geologic map of a tunnel face. The circled numbers adjacent to the attitudes of fractures indicate the relative abundance of the fractures. The numbers following the attitude show the range in spacing of the fractures and the average spacing.

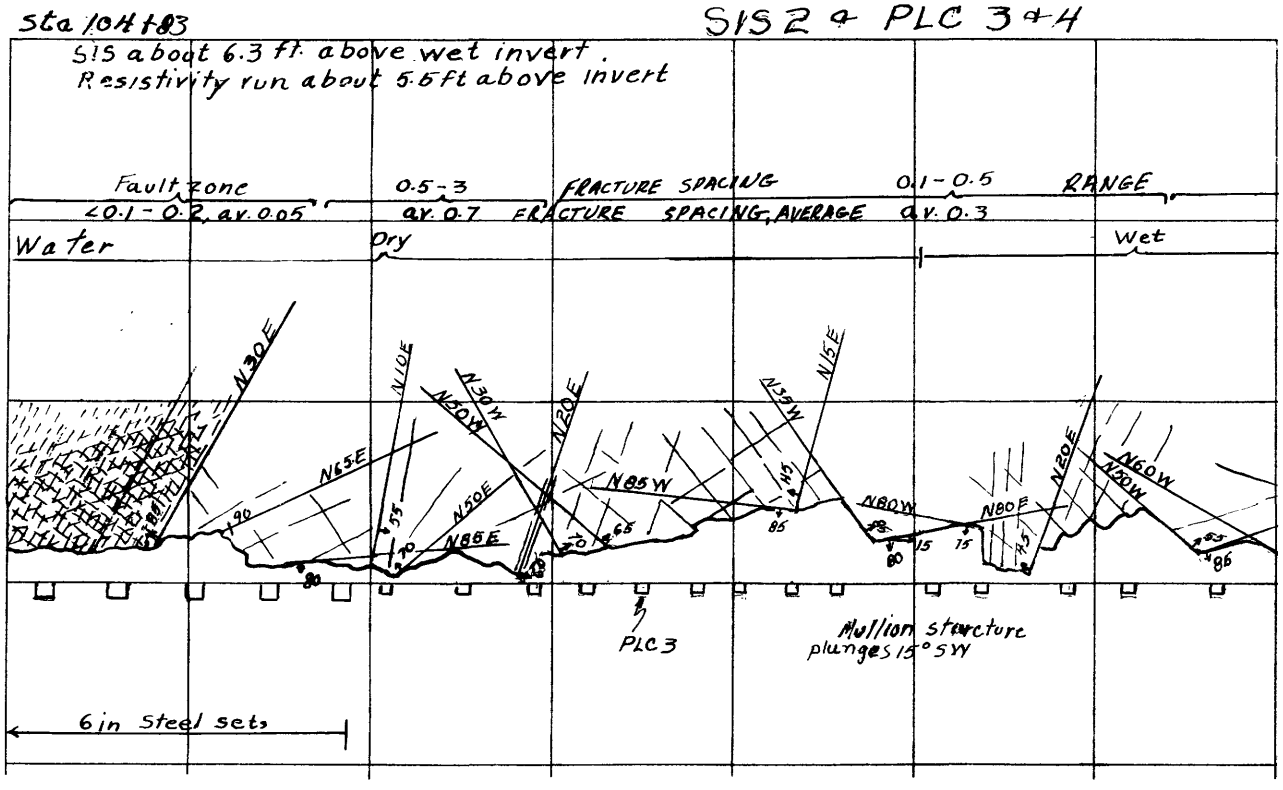

detailed surface mapping in this type of sheared and altered geologic environment would be more valuable, and much less expensive, than additional core holes. A piece of core represents only about a 2-inch-diameter sample for the length of the hole. The significance of such a sample can be evaluated and the drilling data extrapolated only on the basis of detailed geologic mapping and a thorough knowledge of the regional geology.

The geologic log of the core from these holes was originally plotted on a scale of 1 inch to 10 feet. Plate 3 shows the logs at a reduced scale of 1 inch to 20 feet. This type of log attempts to give a maximum amount of geologic information for engineering interpretation. It differs from standard logs primarily in that the size, range in length of pieces of core, and the average length of pieces of core were recorded. The size of the pieces of core was thought to be indicative of the competency of the rock and of the way the rock would break during mining operations. Because much of the rock has a distinct foliation, the attitude of the joints could be measured in relation to the strike of the foliation.

Structural data can be summarized in terms of the average distance between fractures. From the logging it was determined that the average minimum distance between fractures, regardless of rock type, was 0.11 foot; the average maximum distance was 0.68 foot; and the average distance was 0.25 foot. This means that the average piece of rock, as determined from the drilling, had an unfractured length of 0.25 foot. The geophysical logs of the core holes are described in the D chapter of this report.

LABORATORY INVESTIGATIONS

Laboratory studies were conducted throughout the period of surface and subsurface investigations. Physical properties were determined from a representative variety of surface and subsurface samples. The purpose of these studies was not only to furnish the necessary data for the interpretation of field geologic and geophysical information for engineering purposes, but also to attempt to correlate physical properties as determined in the laboratory with those determined in situ, and to conduct research on new techniques and instruments for determining physical properties in the laboratory and field.

Although laboratory test results were valuable, and many represented the best information available, some values — particularly rock-strength determinations — are maximum values that were measured on the more competent rocks; therefore, they are not representative of the rock mass. Likewise, other laboratory test results cannot be expected to represent field conditions of fractured and altered rock masses. Many of these same test results, however, when properly interpreted with reference to known field conditions, yielded information that could be extrapolated to field-engineering use.

We gratefully acknowledge the assistance of T. C. Nichols, Jr., of the U.S. Geological Survey, for his overall guidance and many valuable suggestions throughout the testing program. E. F. Monk, also of the U.S. Geological Survey, supervised and performed many of the dynamic tests, as well as the porosity and density determinations.

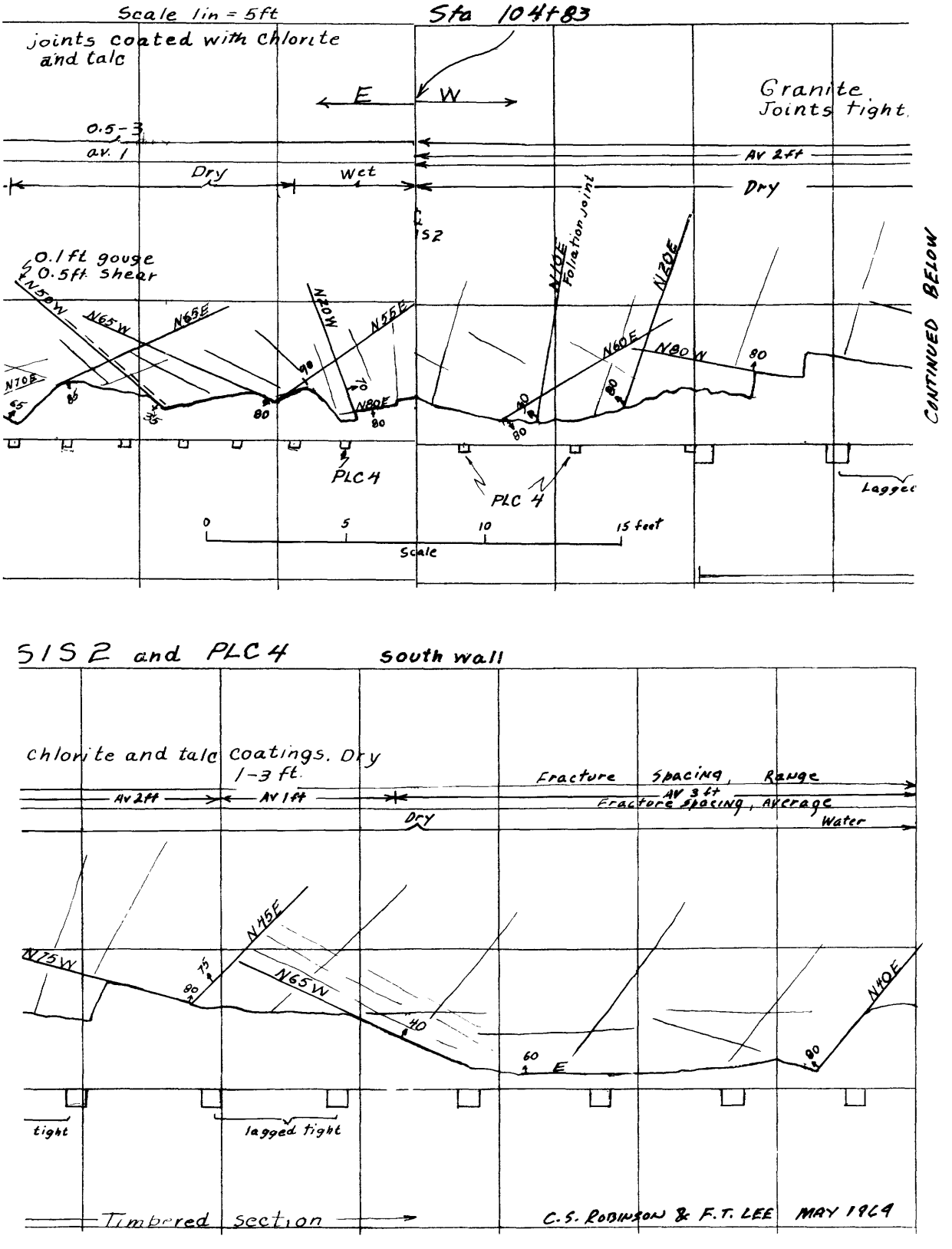

FIGURE 11. — Example of a geologic map of a tunnel wall at an instrument station.

The work of individual analysts is acknowledged in the appropriate tables.

The following information was determined from laboratory tests:

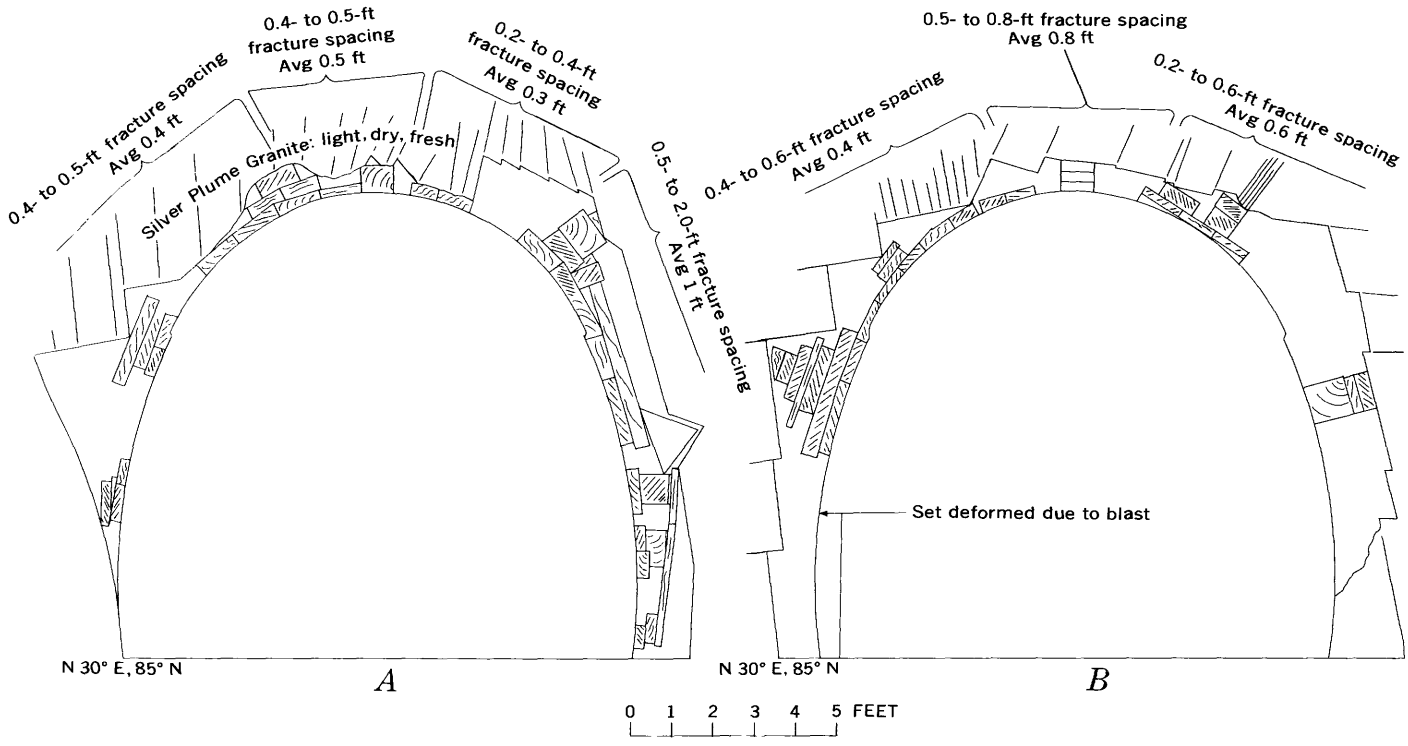

FIGURE 12. — Example of sections showing mapping of wood blocking for instrumented sets. *A*, Set 411, instrument station PLC4; *B*, set 412, instrument station PLC4.

Porosity
Grain density (calculated and powdered in kerosene)
Dry bulk density
Saturated bulk density (kerosene and water)
Powder grain density (in water)
Static tests; confined and unconfined
- E, Secant Young's modulus
- μ, Poisson's ratio
- K, Bulk modulus
- G, Shear modulus
- Compressive strength
- Tensile strength

Dynamic tests (sonic-pulse and bar-resonance methods)
- V_P, Longitudinal (compressional) velocity
- V_S, Transverse (shear) velocity
- σ, Poisson's ratio
- E, Young's modulus
- G, Modulus of rigidity (shear modulus)
- K, Bulk modulus
- N, Modulus of rigidity

Swelling characteristics and mineralogy of fault gouge
Size analyses of wallrock chip samples

Many of these tests involve generally accepted standard procedures that have been well documented by previous investigators; therefore, the procedures are not discussed in detail in this report. Rather, the specific application of tests to the present investigation is emphasized. Test methods that are new or relatively unpublicized are discussed in some detail.

The sample numbers in tables 6–9 indicate where the samples were collected. Core-sample numbers indicate the drill hole from which the sample was taken — SC2, drill-hole 2, or SC3, drill-hole 3 (pl. 1) — and the footage interval, as 678.8–680. Surface samples are designated by number, initials of collector, and year collected, as 5CR62. Samples from the pilot bore are identified by station number (pl. 2) and north or south wall, as 39+18N and 44+65S. The samples from the surface and pilot bore used in the physical and elastic property tests (tables 6, 7, 8) were obtained from large blocks specifically collected to be representative of the rocks in the Straight Creek Tunnel area. One sample, 11CR62, was collected from the quarry at Silver Plume and is representative of typical Silver Plume Granite.

POROSITY AND DENSITY

Porosity and density determinations of surface, drill-hole, and pilot-bore samples are shown in table 6. Slightly higher porosities occurred in the schistose or gneissis samples, probably the result of fracturing parallel to the foliation, whereas the more massive granite samples have fewer planar discontinuities. Petrographic examination revealed that most of the fractures in the granite were bordered by thin selvages of gouge or alteration products. This material also fills many fractures, and, because of its fine grain size, it reduces the porosity of the rock. The average porosity of the 18 samples of granitic rock from the surface and drill holes was 1.2 percent, and of eight samples of metasedimentary rock from the surface and drill holes, 1.4 percent.

TABLE 6. — *Porosity and density determinations of surface, drill-hole, and pilot-bore samples*

[Analysts: John Moreland, Jr., E. F. Monk, and E. D. Seals]

Sample No.	Description	Porosity[1] (percent)	Density (g cm^{-3})			
			Grain	Dry bulk	Saturated bulk	Powder-grain in water
Surface samples						
5CR–62	Medium-grained Silver Plume Granite	0.8	2.65	2.63	2.64	2.67
6CR–62	Fine-grained biotite-plagioclase gneiss	.6	2.80	2.78	2.79	2.87
7CR–62	Porphyritic Silver Plume Granite	1.2	2.65	2.62	2.63	2.63
8CR–62	Medium-grained Silver Plume Granite	.9	2.65	2.62	2.63	2.65
9CR–62	Pegmatitic Silver Plume Granite	1.2	2.60	2.57	2.59	2.63
10CR–62	Fine-grained schist and gneiss (migmatite)	1.1	2.69	2.66	2.67	2.70
11CR–62	Silver Plume Granite from type locality	1.0	2.70	2.68	2.69	2.71
Drill-hole samples (footage shown as part of sample number)						
SC2–180–181	Fine- to medium-grained foliated Silver Plume Granite	1.2	2.66	2.63	2.64	2.68
SC2–264–265	Medium-grained chloritic Silver Plume Granite; iron and calcite along joints.	.5	2.66	2.65	2.65	2.66
SC2–392–393.2	Medium-grained chloritic Silver Plume Granite	1.2	2.66	2.63	2.64	2.62
SC2–489–490.2	do	.8	2.65	2.63	2.64	2.65
SC2–532.2–534	do	.5	2.68	2.66	2.67	2.69
SC2–673.5–675.3	Massive gneissic Silver Plume Granite	.7	2.66	2.64	2.64	2.67
SC2–749.5–750.8	Medium- to fine-grained banded schist and gneiss	3.7	2.77	2.67	2.70	2.81
SC2–853–854.8	Medium- to coarse-grained altered chloritic Silver Plume Granite	2.0	2.70	2.65	2.67	2.73
SC3–346–346.8	Fine-grained biotite-sillimanite schist	1.4	2.76	2.72	2.74	2.72
SC3–377–378.1	Pink pegmatite; grains intensely fractured	.7	2.63	2.61	2.62	2.62
SC3–429.5–431	Fine-grained biotite gneiss and schist with pegmatite stringers	.8	2.85	2.83	2.84	2.84
SC3–436.6–437.8	Coarse-grained massive chloritic Silver Plume Granite	.6	2.64	2.63	2.63	2.67
SC3–486.5–488.5	Fine-grained biotite schist and pegmatite (migmatite)	2.1	2.63	2.57	2.59	2.67
SC3–678.8–680	Chloritic gnessic granite	3.3	2.65	2.56	2.60	2.66
SC3–849–856.8	Rather massive medium-grained Silver Plume Granite; hematite-cemented fractures.	.3	2.67	2.66	2.66	2.68
SC3–953.5–955.4	Gneissic Silver Plume Granite	.7	2.64	2.62	2.63	2.67
SC3–1034.3–1035.9	Chloritic gneissic granite; coarser grained than 953.5	.6	2.66	2.64	2.65	2.67
SC3–1114–1119	Medium-grained chloritic gneissic granite. Many cemented joints and fractures.	1.8	2.73	2.68	2.70	2.73
SC3–1152.6–1154	Granite, as at 1114, but with prominent fluorite veins	2.6	2.69	2.62	2.64	2.71
Pilot-bore samples						
39+18N	Intensely altered medium-grained Silver Plume Granite	[2]1.9	2.62	2.57	---	---
44+65S	Gneissic Silver Plume Granite	[2].7	2.70	2.68	---	---
57+51S	Medium-grained Silver Plume Granite; calcite-cemented fractures	[2]1.1	2.75	2.72	---	---
69+25.4N	Medium-grained biotite gneiss	[2]2.2	2.77	2.71	---	---
75+20S	Medium- to coarse-grained Silver Plume Granite	[2]1.9	2.68	2.63	---	---
84+64S	Moderately altered gneissic Silver Plume Granite	[2]2.2	2.70	2.64	---	---
94+47N	Moderately altered Silver Plume Granite	[2]2.2	2.70	2.64	---	---
106+73S	Medium-grained altered biotite gneiss	[2]4.1	2.69	2.58	---	---
113+82S	Medium-grained Silver Plume Granite	[2].7	2.70	2.68	---	---
118+15S	Moderately altered gneissic Silver Plume Granite	[2]3.0	2.69	2.61	---	---

[1]Water saturation.
[2]Calculated total.

The metasedimentary rocks, in general, have higher densities than the granitic rocks. The average grain density of 18 samples of granitic rock from the surface and drill holes is 2.66, and of eight samples from the pilot bore, 2.69. The average grain density of eight samples of metasedimentary rock from the surface and drill holes was 2.73 and was the same for two samples from the pilot bore.

STATIC TESTS

Compressive and tensile tests were run on representative surface, drill-hole, and pilot-bore samples. Static constants were determined by loading core samples axially in compression and measuring the longitudinal and lateral strain. The results of these tests are given in table 7. Stress-strain diagrams were plotted from the load and deformation measurements made for each specimen. The unconfined compressive strength ranged from 1,400 to 33,300 psi (pounds per square inch). Confined compressive strength ranged from 8,600 psi at 1,500 psi confining pressure to 65,000 psi at 4,000 psi confining pressure.

All samples were prepared in the following manner, described in part by Nichols and Lee (1966):

1. Samples not already existing as cores were cored with a 2⅛-inch core barrel.
2. Cores were trimmed and planed so that the length-to-

TABLE 7. — *Confined tests of surface, drill-hole, and pilot-bore samples, and unconfined and tensile tests of drill-core samples*

[Analysts: T. C. Nichols, Jr., R. A. Farrow, J. C. Thomas, R. A. Speirer, B. K. Barnes, and M. P. Lane]

Sample No.	Rock type, generalized	Core size (in.) Diameter	Core size (in.) Length	Confined compressive strength[1] (psi)	Secant Young's modulus[2] (psi × 10^6 (E))	Poisson's ratio[3] (μ)	Secant range[4] (psi)	Confining pressure[5] (psi)	Remarks[6]
CONFINED TESTS OF SURFACE, DRILL-HOLE, AND PILOT-BORE SAMPLES									
Surface samples									
5CR-62	Granite	2 7/64	4 5/32	60,300	10.5	0.20	2,000-18,700	1,500	Core good. Biotite foliation 15° to horizontal. Failure planes 90° and 75° to horizontal.
6CR-62	Gneiss	2 7/64	4 11/64	46,500	11.8	.19	1,500-18,400	1,500	Core good. Foliation 35°-40° to horizontal. Shear failure started in same direction as foliation, but deviated to 60° from horizontal.
7CR-62	Porphyritic granite	2 7/64	4 7/32	28,900	7.89	.19	200-16,000	200	Core good. Shear fractures 60°-70° to horizontal.
8CR-62	Granite	2 7/64	4 1/4	44,900	9.20	.25	1,500-18,000	1,500	Microbrecciated granite. Core bulged, many small fractures, major shear fracture at 60° to horizontal.
9CR-62	Pegmatitic granite	2 7/64	4 11/64	32,400	5.67	.11	1,500- 9,500	1,500	Well-developed fracture 65° with horizontal, partly cemented with iron oxide. Shear failure partly followed old fracture.
10CR-62	Migmatite	2 7/64	4 11/64	17,000	4.15	.18	3,800- 9,500	200	Core good. Foliation parallel to horizontal. Failure occurred along planes about 80° to horizontal.
11CR-62-1	Silver Plume granite	2 7/64	4 1/4	59,300	8.56	.20	4,000-23,300	4,000	Core good. Shear failure at 71° to horizontal.
2	do	2 7/64	4 1/4	38,000	8.61	.24	7,600-13,300	1,000	Core good. Shear failure at 62° to horizontal.
3	do	2 7/64	4 1/4	31,400	6.97	.16	4,800-10,500	200	Core good. Shear failure at 67° to horizontal.
4	do	2 7/64	4 1/4	46,400	8.77	.18	9,200-26,300	4,000	Core good. Shear failure at 65° to horizontal.
5	do	2 7/64	4 1/4	44,000	8.89	.27	14,700-26,200	4,000	Core good. Core loaded to near failure, but not allowed to fail. Thin section cut to determine possible structural changes
6	do	2 7/64	4 1/4	65,000	8.29	.13	4,000-21,200	4,000	Core good. Shear failure at 66° to horizontal.
7	do	2 7/64	4 5/16	64,300	8.78	.28	9,000-26,200	4,000	Core good. Shear failure at 72° to horizontal.
Drill-hole samples (footage shown as part of sample number)									
SC2-180-181	Granite	2 9/64	4 5/32	38,700	8.41	---	1,500-26,700	1,500	Core good. No lateral strain recorded, gage broken, shear failure 62° to horizontal.
SC2-264-265	do	2 1/16	4 1/4	43,200	11.3	0.35	1,500-31,200	1,500	Only one lateral gage. Shear failure.
SC2-392-393.2	do	2 1/16	4 1/8	43,100	9.94	.16	1,500-16,200	1,500	Core good. Shear failure at 63° to horizontal.
SC2-489-490.2	do	2 1/16	4 1/8	31,700	8.63	---	1,500-22,200	1,500	Core good. Old fracture cemented with calcite. No lateral strain; gage broken. Shear failure along old plane, and fresh one at 70° to horizontal.
SC2-532.2-534	do	2 7/64	4 1/4	43,500	9.48	.21	1,500-18,100	1,500	Core good. Shear failure at 64° to horizontal.
SC2-673.5-675.3	do	2 1/16	4 15/64	47,000	10.7	.20	1,500-22,800	1,500	Core good. Shear failure at 67° to horizontal.
SC2-749.5-750.8	Schist	2 1/16	4 1/4	19,400	2.88	.12	1,500- 7,200	1,500	Core good. Foliation 30° to horizontal. Shear failure 66° to horizontal.
SC2-853-859.8	Granite	2 1/8	4 1/4	25,000	6.81	.09	1,500-13,000	1,500	Core good. Preexisting microbrecciation and weak zones filled with calcite. Failed partially along old failure zone, 58° to horizontal. Many small shear zones within zone of failure.
SC3-346-346.8	Migmatite	1 55/64	3 13/16	25,800	8.84	.27	1,500-14,700	1,500	Core good. Foliation about 40° to horizontal. Shear failure at 67° to horizontal.
SC3-377-378.1	Pegmatite	1 55/64	3 3/4	38,100	9.00	.22	1,500-15,300	1,500	Core good. Shear failure 67° to horizontal.
SC3-429.5-431	Schist	1 55/64	3 5/8	30,000	10.38	.21	1,500-15,300	1,500	Core good. Foliation 65° to horizontal. Shear failure along foliation, 66° to horizontal.
SC3-436.6-437.8	Granite	1 55/64	3 3/4	30,700	8.20	.14	1,500-16,000	1,500	Core good. Preexisting fracture zone cemented with calcite. Failed along old fracture zone, 71° to horizontal.
SC3-486.5-488.5A	Migmatite	1 55/64	3 3/4	11,800	2.34	.13	1,500-8,500	1,500	Core good. Foliation 56° to horizontal. Failure along foliation, 62° from horizontal
SC3-486.5-488.5B	do	1 55/64	3 3/4	15,700	4.28	.11	1,500	1,500	Do.
SC3-678.8-680	Granite gneiss	1 55/64	3 5/8	13,300	4.45	.43	1,500- 4,100	1,500	Old fractures, gages across fractures, failure along old fractures.
SC3-849-856.8B	Granite	1 55/64	3 3/4	52,600	11.3	.17	1,500-23,100	1,500	Core good. Preexisting fractures with chlorite and calcite. Shear failure at 66° to horizontal. Partial failure along fracture.
SC3-849-856.8A	do	1 55/64	3 3/4	43,800	10.7	.20	1,500-22,800	1,500	Core good. Preexisting fractures with chlorite and calcite. Shear failure at 71° to horizontal along weak zone.
SC3-953.5-955.4	do	1 55/64	3 31/32	47,800	12.4	.17	1,500-18,300	1,500	Core good. Preexisting fractures containing chlorite and some calcite. Shear failure 72° to horizontal, partly along old fracture plane.
SC3-1034.3-1035.9A	do	1 55/64	3 11/16	41,900	10.9	.23	1,500-15,500	1,500	Core good. Preexisting fractures filled with chlorite. Shear failure along chlorite-filled fracture, 74° to horizontal.
SC3-1034.3-1035.9B	do	1 55/64	3 3/4	41,700	10.5	.17	1,500-26,900	1,500	Core good. Preexisting chlorite-filled fractures. Shear failure, 72° to horizontal, along old fracture plane.
SC3-1114-1119A	do	1 25/64	2 3/4	31,100	8.40	.18	1,500-16,900	1,500	Core good. Preexisting fractures filled with calcite. Failed along old fracture plane at 69° to horizontal.
SC3-1114-1119B	do	1 27/64	2 5/8	33,300	7.19	.13	1,500-13,100	1,500	Core good. Preexisting fractures filled with calcite. Failed along existing fracture plane at 70° to horizontal.
SC3-1152.6-1154	do	1 27/64	2 27/64	41,000	8.86	.17	1,500-16,600	1,500	Core good.

TABLE 7. — *Confined tests of surface, drill-hole, and pilot-bore samples, and unconfined and tensile tests of drill-core samples* — Continued

Sample No.	Rock type, generalized	Core size (in.) Diameter	Core size (in.) Length	Confined compressive strength[1] (psi)	Secant Young's modulus[2] (psi × 10^6 (E))	Poisson's ratio[3] (μ)	Secant range[4] (psi)	Confining pressure[5] (psi)	Remarks[6]
CONFINED TESTS OF SURFACE, DRILL-HOLE, AND PILOT-BORE SAMPLES — Continued									
Pilot-bore samples									
39+18 N	Granite	2 1/8	4 5/8	8,600	7.69	0.08	2,900– 8,600	1,500	Open fractures. Failed along preexisting fractures.
44+65S	do	2 1/8	4 5/8	44,200	8.90	.21	11,400–25,500	1,500	No obvious fractures.
57+51S	do	2 1/8	4 21/64	38,500	10.6	.21	11,400–25,500	1,500	Do.
69+25.4N	Biotite gneiss	2 1/4	4 3/8	32,700	10.4	.19	7,800–15,400	1,500	Do.
75+20S	Granite	2 1/8	4 11/32	35,100	10.4	.33	11,400–22,700	1,500	Do.
84+64S	do	2 1/4	4 1/16	27,900	7.16	.26	11,300–22,900	1,500	A few small fractures 60°–70° to horizontal; failed mainly along preexisting fractures. Core partly oil saturated during test; results questionable.
94+47N	do	2 1/4	4 11/32	32,600	8.06	.20	10,300–20,400	1,500	Vertical open fracture, two fractures at 60° to horizontal. Failed partially along preexisting fractures.
113+82S	Granite	2 1/8	4 3/8	35,600	6.65	.37	8,600–24,100	1,500	No obvious fractures.

Sample No.	Rock type generalized	Core size (in.) Diameter	Core size (in.) Length	Confined compressive strength[1] (psi)	Secant Young's modulus[2] (psi × 10^6 (E))	Poisson's ratio[3] (μ)	Secant range[4] (psi)	Tensile strength[7] (psi)	Remarks[8] (x = number of loading cycles)
UNCONFINED AND TENSILE TESTS OF DRILL-HOLE SAMPLES (footage shown as part of sample number)									
SC2–260–261	Granite	2 1/8	4 3/4	30,000	6.65	0.15	1,400–12,700	1,900	Core good. x = 3.
SC2–387–388.5	do	2 1/16	4 1/8	24,600	8.44	.24	1,500–15,000	800	Core good. x = 4.
SC2–672–673	do	2 1/16	4 1/8	29,000	8.13	.19	1,500–15,000	1,260	Core good. x = 4.
SC2–854–856	do	2 1/16	4 1/8	15,000	5.40	.20	600– 6,000	210	Preexisting chlorite-filled fractures 80° to horizontal. x = 4. Shear failure intersected, but did not follow, old fracture.
SC3–344–345	Migmatite	1 7/8	3 3/4	17,400	7.10	.16	700– 9,000	890	Core good. Foliation 42° to horizontal. x = 4. Major failure 84° to horizontal. Failed in part along foliation.
SC3–378.8–379	Pegmatite	1 7/8	3 3/4	1,400	---	---	---	---	Preexisting failure plane filled with iron oxide and calcite, 67° to horizontal. Core failed along preexisting fracture plane.
SC3–438–439	Granite	1 7/8	3 3/4	33,300	9.20	.18	1,800–18,000	2,280	Core good. x = 4.
SC3–429.5–431	do	1 7/8	3 3/4	21,700	7.58	.39	1,800– 9,000	---	Core good. x =4. Vertical extension fractures.
SC3–678–679	Granite gneiss	1 7/8	3	9,800	6.43	.28	700– 7,000	510	Preexisting fracture (chlorite), 63° to horizontal. Foliation 62° to horizontal. x = 3. Failed along preexisting fracture cemented with chlorite.
SC3–1152–1154	do	1 37/64	2 1/8	20,300	8.47	.22	1,300–13,000	910	Preexisting fracture filled with calcite 65°–80° to horizontal. x = 4. Failed along preexisting fracture 72° to horizontal.

[1]Maximum stress supported by core; usually the stress at failure.
[2]Obtained from stress-strain diagrams of rocks which can be of the straight-line, S-shaped, and steady curving type (Wuerker, 1956, p. 4). Most of the tested specimens from the Straight Creek area display a modified S-shaped curve. The secant modulus given here generally has the proportional elastic limit as its upper stress bound.
[3]Ratio of the lateral (or radial) strain $\Delta C/C$ to the longitudinal (or axial) strain $\Delta L/L$.
[4]Range of applied stress over which secant line is drawn on stress-strain curve.
[5]Lateral (radial) stress maintained on core during triaxial testing.
[6]All cores oven dried. End parallelism <0.001 inch. "Core good" indicates that there were no major megascopic gouge seams or weak zones in core prior to testing unless specifically noted.
[7]Measure of the ability of the sample to resist a stress tending to pull it apart, as determined by the Reichmuth point-loading method. Some of the tensile values are extremely low because the cores failed along planes of foliation and fracture zones. Especially susceptible to tensile failure were planes of foliation in which biotite was the main mineral.
[8]All cores oven dried. End parallelism <0.0001 inch.

diameter ratio was 2:1 or greater. The end parallelism was held to a tolerance of 0.001 inch or less. Foliation and weakness planes were recorded and are described in the "Remarks" column in table 7. Cores used for tensile testing were trimmed to fit the size of the test apparatus. Parallelism of the ends of these samples is unimportant.

3. For triaxial confined compression tests, strain gages were applied to the surface of each core midway between the top and bottom. Two rosette gages, each with two 90° gages, were applied, with one gage parallel and the other perpendicular to the long axis. The gages were mounted on opposite sides of the core with the parallel components connected in series to obtain average strain measurements. Radial strain was determined by comparing the ratio of the change in circumference (ΔC) to the original circumference (C), or conversely the ratio of the change in radius (ΔR) to the original radius. It can be shown that $\Delta C/C = \Delta R/R$ or that circumferential strain is elastically equal to radial strain. Thus, radial strain was measured directly by circumferentially mounted strain gages. Axial strain was measured by gages mounted parallel to the long axis.

The cores used in triaxial tests were covered with a tough membrane of polyvinyl chloride and placed between loading platens in a triaxial chamber capable of transmitting axial loads of 400,000 pounds and holding fluid pressures of 8,000 psi. The chamber, after being filled with hydraulic fluid and sealed, was placed in a hydraulic press capable of exerting

TABLE 8. — *Dynamic test results, surface, drill-hole and pilot-bore samples*

[Analysts: D. R. Cunningham, John Moreland, Jr., E. F. Monk, and E. D. Seals]

Sample No.	Rock type	Longitudinal velocity (V_p) (ft/sec)	Shear velocity (V_s) (ft/sec)	Young's modulus (E) (psi × 10^6)	Shear modulus (G) (psi × 10^6)	Poisson's ratio (σ)
BAR RESONANCE METHOD						
Surface samples						
5CR–62	Granite	21,600	9,900	9.1	3.3	0.37
6CR–62	Gneiss	20,100	11,200	12.5	4.9	.28
7CR–62	Porphyritic granite	16,400	8,600	7.2	2.8	.31
8CR–62	Granite	15,800	9,200	7.8	3.2	.24
9CR–62	Pegmatitic granite	13,000	7,700	5.3	2.2	.23
10CR–62	Migmatite	15,400	7,100	5.1	1.9	.37
11CR–62	Silver Plume Granite	12,700	8,200	5.8	2.5	.15
Drill-hole samples (footage shown as part of sample number)						
SC2–180–181	Granite	16,900	9,800	8.2	3.3	0.24
SC2–264–265	do	18,800	10,200	9.3	3.6	.30
SC2–392–393.2	do	16,400	9,800	8.0	3.3	.23
SC2–489–490.2	do	14,900	9,800	7.4	3.3	.12
SC2–532.2–534	do	17,000	10,200	8.8	3.6	.21
SC2–673.5–675.3	do	14,600	9,400	6.9	3.0	.14
SC2–749.5–750.8	Schist	11,400	7,000	4.1	1.7	.20
SC2–853–854.8	Granite	[1]	[1]	[1]	[1]	[1]
SC3–346–346.8	Migmatite	13,100	7,350	5.4	2.1	.27
SC3–377–378.1	Pegmatite	16,300	9,400	8.3	3.3	.25
SC3–429.5–431	Schist	21,100	10,000	11.2	4.1	.36
SC3–436.6–437.8	Granite	17,400	10,100	9.4	3.8	.25
SC3–486.5–488.5	Migmatite	11,800	7,000	4.4	1.8	.23
SC3–678.8–680	Granite gneiss	17,100	9,700	8.6	3.3	.26
SC3–849–856.8	Granite	21,800	10,650	11.4	4.2	.34
SC3–953.5–955.4	do	18,200	11,200	11.2	4.7	.20
SC3–1034.3–1035.9	do	19,500	11,200	11.7	4.7	.25
SC3–1114–1119	do	17,500	9,500	8.1	3.1	.29
SC3–1152.6–1154	do	16,600	9,700	8.0	3.2	.24
SONIC-PULSE METHOD						
Pilot-bore samples						
39+18N	Granite	14,550	8,700	6.4	2.6	0.22
44+65S	do	14,450	9,550	7.3	3.3	.11
57+51S	do	17,700	10,400	9.8	4.0	.24
69+25.4N	Biotite gneiss	17,500	10,650	10.0	4.1	.21
75+20S	Granite	15,550	10,400	8.4	3.8	.10
84+64S	do	14,700	9,900	7.6	3.5	.09
94+47N	do	16,000	9,950	8.3	3.5	.19
106+73S	Biotite gneiss	18,100	10,500	8.9	3.8	.16
113+82S	Granite	16,050	10,400	8.8	3.9	.14
118+15S	do	17,900	9,950	8.9	3.5	.28

[1] No core.

loads up to 400,000 pounds at uniform loading rates. Electrical connections necessary for monitoring changes of strain were then completed. Figure 13 illustrates a core after failure in the triaxial chamber and shows the method of preparation of the cores.

Triaxial loading tests were performed to investigate:

1. The effect of different confining pressures on the elastic and other physical properties of the samples.
2. The range in physical measurements that could be expected for the rock types tested.
3. The applicability of Mohr's failure envelope in predicting strength and internal friction for different confining stress.
4. The likelihood of, and amount of, creep under different confining pressures.
5. Modes of failure, fabric changes, and behavior as a result of stress applications.
6. Whether modes of failure and fabric changes can be related to geologic phenomena, such as faults, shear zones, slickensides, and possible rock stiffening (hardening).

In general, the confined and unconfined tests were performed by loading cores axially until t ıey failed. Preliminary cyclic loading was used on many unconfined cores to induce permanent set. Strain measurements in unconfined tests were made with calibrated mechanical extensometers.

FIGURE 13. — Core after failure, showing method of preparation for triaxial compression testing.

The results of these tests are given in Nichols and Lee (1966). In summary, the strength of migmatite and gneiss associated with the Silver Plume Granite, although high, was found to vary with the orientation of well-developed foliation, lineation, and joints and with the differences in mineralogy and grain size. Cores of metamorphic rock with foliation oriented subparallel to the maximum shear stress failed along the foliation at relatively low compressive-stress values. Also, the compressive strengths of these rocks changed with differences in mineralogy — as the biotite or quartz content increased, the strength decreased. In such rocks, Mohr's failure envelope could not be used successfully to predict ultimate strengths of the rocks or the angles of internal friction. For the granite samples, however, most of the strengths and internal angles of friction under different confining pressures and core orientations could be predicted by using Mohr's failure envelope plots. The poorly developed foliation in these cores had little effect on the strength. Similarly, the slight differences in mineral composition of the granite samples have only a minor influence on rock strength. Creep tests showed that if a granite sample is loaded to 5,000 psi confining pressure and 51,000 psi axial stress for 3 days, the creep rate will slow to a negligible amount after 3 days, after which small strain caused by temperature fluctuations will be dominant. Energy release, recorded as the granite specimens were loaded, indicated that small local failures along fractures occurred at a uniform rate for the duration of the test until complete failure occurred. Complete failure released a large amount of energy, indicating that the number of fractures probably increased along planes of high shearing stress, possibly accompanied by movement along the fractures throughout the test. The failure surfaces had slickensides and gouge similar to that observed along faults and joints in the Straight Creek Tunnel area. Results of the triaxial loading tests are somewhat limited in their direct application to actual rock behavior in the field, inasmuch as the strength of small samples of the different rocks is high, whereas engineering problems are most commonly related to faults, gouge zones, joints, strong lineations, and foliations, rather than to the inherent strength of the rocks themselves.

The tensile tests on the core samples were made by using the apparatus designed by Reichmuth (1968) utilizing a point-loading method. Strain was not measured in these tests.

DYNAMIC TESTS

Dynamic elastic moduli were determined by bar-resonance and sonic-pulse methods for surface outcrop, drill-hole core, and pilot-bore samples from the Straight Creek Tunnel area (table 8).

The following description of the two test methods is taken largely from the work of E. F. Monk (written commun., 1967), who conducted many of the tests.

SONIC-PULSE METHOD

In the sonic-pulse method, P-wave pulses were generated by a ceramic barium titanate transducer that was pressure-coupled to one end of a cylindrical rock sample. The

ceramic transducer was driven by an electronic pulse generator. An identical transducer was pressure-coupled to the other end of the sample and served as a receiver. Silicone grease was used to aid the transmission of sonic energy across the sample-transducer interface. Output of the receiver was displayed on an oscilloscope. The sweep of the oscilloscope was triggered by the driving pulse. Traveltime of the pulse through the sample was determined by observing the time of the first-arrival energy on the oscilloscope. S-waves were generated and detected by coupling the same transducers to two triangular Pyrex glass prisms that were attached to each end of the sample with phenyl salicylate. The first prism converted the P-waves to S-waves by reflection at the glass-air interface. The S-waves traveled through the sample and were reconverted to P-waves by the second prism. Traveltime through the sample was determined by correcting the total time observed on the oscilloscope for delay caused by the glass prisms. This technique has been described more fully by Jamieson and Hoskins (1963).

Results of the sonic-pulse measurements were used to compute P- and S-wave velocities and elastic moduli by use of the following formulas (Howell, 1959; Jaeger, 1962):

$$V_p = \frac{L}{t_p},$$

$$V_s = \frac{L}{t_s},$$

$$E = \frac{\rho V_s^2 (1+\sigma)}{72g},$$

$$G = \frac{E}{2(1+\sigma)}, \text{ and}$$

$$\sigma = \frac{0.5\left(\frac{V_p}{V_s}\right)^2 - 1}{\left(\frac{V_p}{V_s}\right)^2 - 1},$$

where

V_p = longitudinal-wave velocity, in feet per second;
V_s = shear-wave velocity, in feet per second;
σ = Poisson's ratio;
E = Young's modulus, in pounds per square inch;
G = shear modulus, in pounds per square inch;
L = length, in feet;
t_p = longitudinal-wave traveltime, in seconds;
t_s = shear-wave traveltime, in seconds;
ρ = density, in pounds per cubic foot; and
g = acceleration due to gravity, 32.2 feet per second^2.

BAR-RESONANCE METHOD

P- and S-wave velocities and elastic moduli were also determined by the bar-resonance method, in which a core with a length at least four times its diameter was used. To make the measurement, the core was placed on a piece of foam rubber so that it could vibrate freely. Vibration was induced by resting one end of the core on a rod that was mechanically coupled to a loudspeaker driver. An audio-oscillator was used to drive the system through a range of frequencies. Flexural and torsional resonant frequencies were determined by probing the core with an accelerometer and finding the two frequencies at which maximum amplitudes occurred. The output of the accelerometer was amplified and then monitored on an oscilloscope. The flexural resonant frequency was distinguished from the torsional resonant frequency by finding the nodal points of standing waves that were set up in the sample. A more complete treatment of this method has been given by Mitchell (1954) and by American Society for Testing and Materials (1952).

P- and S-wave velocities and elastic moduli were calculated from the following formulas:

$$E = CWF_f^2,$$

$$\sigma = \frac{E}{2G} - 1,$$

$$V_p = \sqrt{\frac{Eg\,(1-\sigma)}{12M\,(1+\sigma)\,(1-2\sigma)}},$$

$$V_s = \sqrt{\frac{Eg\,1}{12M\,2(1+\sigma)}}, \text{ and}$$

$$G = BWF_t^2$$

where

V_p = longitudinal-wave velocity, in feet per second;
V_s = shear-wave velocity; in feet per second;
E = Young's modulus, in pounds per square inch;
G = shear modulus, in pounds per square inch;
σ = Poisson's ratio;
M = density, in pounds per cubic inch;
C = 0.00416 (L^3T/d^4) for a cylinder, in seconds^2 per inch^2, where d is the diameter;
g = acceleration due to gravity, 32.2 feet per second^2, or 386.4 inches per second^2;
W = weight of sample, in pounds;
B = $4LR/gA$, in seconds^2 per inch^2;
L = length of sample, in inches;
R = shape factor (one for a cylinder);
T = correction factor for Poisson's ratio (Goen's equation);
A = cross-sectional area of sample, in square inches;
F_f = fundamental flexural resonant frequency, in cycles per second; and
F_t = fundamental torsional resonant frequency, in cycles per second.

SWELLING CHARACTERISTICS AND MINERALOGY OF FAULT GOUGE

Table 9 gives the results of PVC (potential volume change) swell capacity, swell index, and estimated final swell pressure of samples of fault gouge collected from the

TABLE 9. — *Swelling characteristics and mineralogy of fault gouge, surface, drill-hole, and pilot-bore samples*

[Analysts: T. C. Nichols, Jr., G. S. Erickson, J. C. Thomas, R. A. Speirer, and E. E. McGregor. Tr., trace; leaders (---), looked for but not found]

Sample No.	Predominant associated rock type	PVC swell capacity (ml)	PVC swell index (psf)	Estimated final swell pressure (psf)	Mineralogy (to nearest 5 percent)							
					Clay	Quartz	Microcline	Plagioclase	Calcite and dolomite	Amorphous iron and siderite	Biotite	Relative abundance of clay minerals[1]
Surface samples												
SC-6	Granite	---	2,130	2,900	20	55	25	---	---	---	---	K>M = ML>I
2CR-62	---do	2.0	1,300	1,700	---	---	---	---	---	---	---	---
3AFL-62	---do	2.0	1,600	2,130	---	---	---	---	---	---	---	---
3BFL-62	Schist(?)	2.0	2,000	2,700	---	---	---	---	---	---	---	---
Drill-hole samples (footage shown as part of sample number)												
SC3-112-112.5	Schist and gneiss	2.4	2,000	2,700	---	---	---	---	---	---	---	---
SC3-273-275	---do	2.0	1,200	1,600	---	---	---	---	---	---	---	---
Pilot-bore samples												
44+71	Granite	3.0	2,100	2,850	45	25	10	5	15	---	---	Mb>K>I
72+13	---do	3.0	1,300	1,700	35	35	5	15	10	---	---	K>I = ML =M
81+00	---do	2.9	2,350	3,270	50	25	5	5	10	5	---	I>K>ML
83+27	Schist and gneiss	2.7	1,700	2,280	50	15	---	10	5	10	10	K≥I>ML>M
83+32S	---do	2.5	1,000	1,300	35	30	10	5	5	5	10	K>I>ML>M
83+49S	Granite	2.5	600	750	5	35	35	20	5	---	---	K>ML
83+86.5S	---do	3.0	1,500	2,000	15	35	30	15	5	---	Tr.	K≥I =Mb
83+93S	---do	2.5	600	750	15	45	30	10	---	Tr.	---	I≥K>M≥ML
83+97.3S	Schist and gneiss	4.5	2,480	3,380	45	30	10	---	5	5	---	I>K>ML
84+10.5S	Granite	2.5	700	890	30	25	20	10	10	---	5	I>K>ML≥M
85+82S	---do	3.0	1,100	1,440	45	30	5	---	15	---	5	I>K>ML
85+98N	---do	2.5	1,100	1,440	45	30	5	---	15	5	---	I>K
89+92a	---do	2.5	1,400	1,850	35	35	10	5	5	Tr.	10	I>K>M = ML
89+92b	Schist	2.3	1,100	1,440	45	25	10	---	---	---	15	I>K>ML>M
93+84	Granite	2.5	1,350	1,780	50	15	10	Tr.	15	10	---	K>M>D
94+10	---do	2.5	1,000	1,300	30	15	15	5	10	10	10	M>K>I>ML
97+20	Schist and gneiss	2.5	400	500	40	35	Tr.	5	---	5	15	K>ML>I>M
106+05	Schist	3.5	1,900	2,550	35	20	5	5	5	20	10	M>K>I
106+17	Granite	2.5	500	625	45	15	15	10	5	10	---	ML>K>M
106+20	---do	2.5	500	625	50	10	15	10	---	15	---	ML>I = M>K
107+35	---do	4.2	1,700	2,280	40	20	15	---	10	---	10	M>K>I
108+73	---do	3.0	1,100	1,475	50	10	20	5	10	5	---	M>I>K
114+11	Schist	2.5	500	625	60	15	5	5	---	10	---	ML>I>K>M
116+05	Granite	2.7	1,400	1,850	60	15	15	10	---	---	---	ML = M>K>I
118+15	Gneiss	2.1	200	230	40	10	10	15	---	15	---	C>ML>I>M>K
118+26	---do	4.4	4,800	≈9,000	65	15	5	Tr.	---	10	---	M>C = K
118+66	Granitic gneiss	2.4	400	500	40	40	5	5	5	5	---	I>K>M>ML>C
118+91	Schist and gneiss	2.3	650	820	40	15	25	10	5	5	---	M≥K>I>ML
119+92	Granite	2.6	500	625	40	15	20	5	5	5	---	M>K>I

[1]Clay minerals: K, kaolinite; M, montmorillonite; Mb, montmorillonite with brucite layer; ML, mixed layer; I, illite; C, chlorite. Mixed layer composed of various proportions of montmorillonite and illite.

surface, drill holes, and the pilot bore. X-ray mineralogic analyses were performed on most of the samples, and these results are also shown in table 9.

The PVC test and instrument were devised to determine swelling characteristics of soils in foundations. The procedures and instrumentation are described by Lambe (1960), who developed the method for the Federal Housing Administration. Basically, the instrument makes possible the rapid measurement of the partially confined pressure exerted by a water-saturated sample and indicates semiquantitatively the anticipated reaction of the material under conditions encountered in excavation. The meter measures pressure in only one direction, and, inasmuch as in underground openings the movement of material at any point into the opening can be considered as unidirectional, this test is considered to be valid for estimating the behavior of fault gouge in tunneling operations. The original purposes and procedures of this test as described by Lambe (1960) have been somewhat modified for application of the test to tunnel geologic research. The test as currently used has been described by Wahlstrom, Robinson, and Nichols (1968).

Because some samples of fault gouge contained numerous hard-rock fragments, it was necessary to crush the samples so all the material would pass a 20-mesh screen before placing them in the PVC sample holder. The test samples were wetted (equivalent to "moist classification" of Lambe, 1960, p. 20) and compacted in the consolidation ring of the test device, using seven blows of the standard compacting

TABLE 10. — *Size analyses of wallrock chip samples, Straight Creek Tunnel pilot bore*

[Analyst, G. S. Erickson. Leaders (- - -) indicate not determined]

Screen mesh size	>2 in.	2 in.	1½ in.	1 in.	¾ in.	½ in.	0.371 in.	4	10	18	35	60	120	230
Diameter of particles (mm)	>50.80	50.80	38.10	25.40	19.10	12.7	9.423	4.76	1.98	0.991	0.495	0.246	0.124	0.061
Sample No.[1]	Percent of total weight passing through screen (cumulative weight percent)													
PIS1-NW (118+19-24)	100	42.0	15.7	9.8	9.1	7.9	7.8	6.5	5.1	4.2	3.2	1.9	1.1	0.5
PIS1-NE (118+24-29)	100	14.9	12.9	10.6	8.4	6.6	6.0	4.8	3.5	2.6	1.8	1.2	.8	.4
PIS2-SW (117+16-21)	100	23.0	15.8	10.4	9.0	7.2	6.6	5.0	3.6	2.7	1.9	1.3	.9	.6
PIS2-SE (117+21-26)	100	7.0	6.0	3.6	3.4	2.4	2.1	1.6	1.2	1.0	.7	.6	.4	.2
SIS1-SW (114+48-53)	100	14.1	3.4	2.3	1.6	.9	.7	.5	.3	.2	.2	.1	.1	.02
SIS1-SE (114+53-58	100	5.6	3.8	.8	.7	.6	.5	.5	.4	.3	.3	.2	.2	.1
PIS3-SW (111+43-48)	100	12.0	8.4	6.3	5.5	4.4	3.9	3.1	2.4	1.7	1.2	.7	.4	.2
PIS3-SE (111+48-53)	100	18.5	9.0	6.3	4.7	3.8	3.4	2.7	2.1	1.6	1.2	.9	.6	.5
PIS4-SW (109+61-66)	100	8.5	.95	.9	.75	.43	.37	.25	.17	.13	.10	.06	.03	.005
PIS4-SE (109+66-71)	100	3.9	2.4	.8	.7	.6	.6	.5	.5	.4	.4	.4	.3	.3
PIS5-SW (107+60-65)	100	12.3	5.8	2.7	1.9	1.5	1.4	1.0	.8	.6	.4	.3	.1	.1
PIS5-SE (107+65-70)	100	17.3	6.9	3.0	2.6	2.0	1.8	1.3	.9	.7	.6	.4	.3	.1
PLC2A-NW (105+76-81)	100	77.5	62.9	52.3	43.5	35.5	31.8	23.8	16.0	11.1	7.2	4.2	2.2	1.3
PLC2A-NE (105+81-86)	100	65.6	55.5	44.8	39.6	34.1	31.4	23.7	15.8	11.0	6.9	3.8	1.8	1.0
PLC3-SW (105+13-18)	100	47.2	30.0	19.8	15.8	12.6	11.2	8.9	6.8	5.0	3.3	2.0	1.1	.6
PLC3-SE (105+18-23)	100	58.1	46.9	29.9	24.9	19.9	17.6	13.7	10.1	7.3	4.8	2.0	1.4	.8
SIS2-SW (104+78-83)	100	72.6	57.6	38.3	23.9	17.6	14.9	10.7	7.4	5.1	3.3	1.9	1.0	.6
SIS2-SE (104+83-88)	100	56.3	37.2	17.7	11.5	8.8	7.7	5.8	4.3	3.2	2.2	1.4	.8	.4
PIS6-SW (101+52-57)	100	9.5	3.4	1.1	1.1	1.1	.9	.6	.5	.4	.3	.2	.1	.01
PIS6-SE (101+57-62)	100	14.0	12.0	4.4	4.0	2.6	2.3	1.6	1.2	.9	.7	.5	.3	.2
PIS7-SW (98+53-58)	100	22.3	16.4	11.7	9.0	7.4	6.4	5.1	3.9	2.7	1.6	.9	.5	.2
PIS7-SE (98+58-63)	100	36.7	22.2	15.3	10.9	8.5	7.6	5.8	4.2	2.9	1.9	1.2	.7	.4
PLC5-SW (97+00-05)	100	34.9	25.9	12.7	9.4	6.5	5.8	4.1	2.9	2.1	1.4	.9	.5	.3
PLC5-SE (97+05-10)	100	45.2	27.0	12.8	9.5	7.4	6.6	5.3	3.9	2.9	1.9	1.1	.6	.4
PIS8-SW (95+89-94)	100	26.4	14.5	7.9	6.7	5.1	4.8	4.1	3.3	2.5	1.8	1.2	.8	.4
PIS8-SE (95+94-99)	100	13.5	3.8	2.4	2.1	1.6	1.5	1.3	1.1	1.0	.8	.5	.4	.2
SIS3-SW (93+85-90)	100	79.1	72.2	56.6	51.8	46.0	43.0	35.0	26.7	19.7	13.7	8.9	5.2	3.1
SIS3-SE (93+90-95)	100	66.6	43.8	28.7	23.0	19.3	17.6	14.1	10.8	8.2	5.8	3.7	2.1	1.2
PIS9M-SW (92+15-20)	100	73.9	62.0	38.2	29.4	22.7	19.5	13.5	8.6	5.9	3.9	2.4	1.3	.7
PIS9M-SE (92+20-25)	100	58.1	38.7	25.6	21.9	17.8	16.0	12.7	8.9	6.5	4.8	3.4	1.0	.6
PLC8-SW (90+45-50)	100	51.5	39.9	27.1	22.1	16.0	13.6	9.0	5.9	4.2	2.9	1.8	.9	.5
PLC8-SE (90+50-55)	100	69.6	59.0	43.6	33.6	24.2	20.7	14.5	9.9	6.9	4.3	2.4	1.2	.6
PIS10-SW (89+93-98)	100	55.4	49.9	28.0	23.5	18.0	15.3	11.2	7.7	5.6	3.9	2.5	1.4	.8
PIS10-SE (89+98-90+03)	100	66.9	56.4	38.8	31.1	23.8	21.5	15.8	10.9	7.9	5.4	3.4	1.8	1.0
PIS11-SW (87+14-19)	100	59.0	46.3	32.5	25.4	18.2	13.9	8.9	5.7	4.1	2.8	1.8	1.1	.6
PIS11-SE (87+19-24)	100	72.4	47.5	31.1	23.2	17.8	16.0	12.0	8.5	6.2	4.2	2.7	1.5	.8
PLC9-SW (85+61-66)	100	71.7	46.1	27.8	22.2	14.8	12.4	8.3	5.4	3.7	2.4	1.4	.7	.5
PLC9-SE (85+66-71)	100	66.5	58.6	39.6	29.0	21.3	17.9	11.9	7.8	5.3	3.7	2.4	1.5	.7
SIS4-NW (83+88-93)	100	95.8	92.7	83.2	79.0	70.1	67.0	53.9	41.2	30.7	20.7	12.8	6.7	3.8
SIS4-NE (83+93-98)	100	87.0	82.2	67.1	58.1	45.6	41.4	30.3	22.1	16.5	11.4	7.2	3.9	2.1
PIS12M-SW (81+37-41)	100	28.1	24.5	16.7	12.1	9.6	8.6	7.0	5.0	3.6	2.4	1.5	.8	.4
PIS12M-SE (81+41-47)	100	57.8	35.2	25.5	19.2	15.6	14.2	10.8	7.6	5.3	3.5	2.2	1.2	.7
PLC10-SW (79+87-92)	100	35.4	26.4	14.8	11.7	8.6	7.5	5.5	4.0	3.1	2.3	1.6	1.1	.7
PLC10-SE (79+92-97)	100	27.1	15.3	7.9	5.9	4.3	3.7	2.6	2.0	1.5	1.2	.9	.6	.3
PIS13-SW (78+07-12)	100	20.0	13.9	6.3	3.9	2.3	2.1	1.3	.8	.6	.4	.3	.2	.07
PIS13-SE (78+12-17)	100	11.4	6.9	5.3	3.8	2.9	2.5	1.7	1.1	.8	.6	.4	.2	.1
PIS14-SW (73+52-57)	100	39.1	23.4	13.3	9.9	7.4	6.2	4.1	2.9	2.2	1.6	1.1	.7	.4
PIS14-SE (73+57-62)	100	39.0	22.9	11.2	8.3	5.5	4.4	3.0	2.1	1.6	1.2	.9	.6	.4
PLC11-SW (71+78-83)	100	54.7	39.2	23.8	17.8	12.4	10.4	6.8	4.6	3.2	2.2	1.5	1.0	.7
PLC11-SE (71+83-88)	100	63.1	34.8	21.8	15.1	9.6	7.2	4.6	3.1	2.2	1.6	1.1	.7	.3
SIS5-SW (69+76-81)	100	44.0	30.5	14.2	10.0	6.9	5.9	4.1	2.6	1.7	1.1	.7	.4	.2
SIS5-SE (69+81-86)	100	15.8	9.7	5.6	4.1	3.1	2.8	2.0	1.3	.9	.6	.4	.2	.1
PIS15-SW (65+89-94)	100	14.6	5.4	1.3	.8	.3	.2	.1	.1	<.1	<.1	<.1	<.1	<.1
PIS15-SE (65+94-99)	100	11.7	7.2	2.0	1.7	1.2	1.0	.6	.5	.4	.3	.2	.1	.1
PLC12-SW (62+54-59)	100	56.5	43.5	26.0	19.8	13.7	11.1	7.4	5.3	4.2	3.2	2.5	1.8	1.1
PLC12-SE (62+59-64)	100	20.7	16.9	12.8	8.8	6.3	5.5	3.9	2.9	2.2	1.6	1.1	.7	.9
SIS6-SW (59+30-35)	100	5.7	3.4	1.5	1.4	1.2	1.0	.7	.6	.5	.4	.3	.2	.1
SIS6-SE (59+35-40)	100	20.5	10.9	3.4	1.7	1.1	1.0	.5	.5	.4	.3	.2	.1	.02

TABLE 10. — *Size analyses of wallrock chip samples, Straight Creek Tunnel pilot bore* — Continued

Screen mesh size	>2 in.	2 in.	1½ in.	1 in.	¾ in.	½ in.	0.371 in.	4	10	18	35	60	120	230
Diameter of particles (mm)	>50.80	50.80	38.10	25.40	19.10	12.7	9.423	4.76	1.98	0.991	0.495	0.246	0.124	0.061
Sample No.[1]	Percent of total weight passing through screen (cumulative weight percent)													
PIS16–SW (54+55–60)	100	20.0	11.0	6.5	3.6	2.8	2.1	1.4	1.0	.8	.6	.4	.3	.2
PIS16–SE (54+60–65)	100	37.7	29.8	11.9	8.2	5.6	4.5	3.1	2.1	1.5	1.1	.8	.5	.2
SIS7–NW (49+22–27)	100	31.3	15.9	11.2	9.0	7.1	6.0	4.8	2.6	1.9	1.2	.7	.4	.2
SIS7–NE (49+27–32)	100	33.3	18.6	8.2	6.3	3.8	---	---	---	---	---	---	---	---
SIS8–SW (43+83–88)	100	53.1	31.0	14.6	9.6	6.4	5.6	4.1	3.1	2.5	1.9	1.5	1.0	.6
SIS8–SE (43+88–93)	100	29.5	18.2	10.1	6.5	3.7	3.2	2.1	1.5	1.2	.9	.7	.5	.2

[1]Sample numbers refer to the Terrametrics, Inc., instrument stations, as PIS1; to the sample locality in relation to the station, as NW, NE, SW, or SE (which, respectively, indicate north wall, west of the station; north wall, east of the station; south wall, west of the station; and south wall, east of the station) and to the 5-foot tunnel-station interval from which the sample was taken, as (118+19–24).

hammer for each of three layers of sample material. Other parts of the test procedure were the same as those described by Lambe. The compacted sample material was placed between two porous disks, a cover added, and zero adjustments were made in the proving ring and dial. Water was added to cover the sample and the porous disks. The pressure, due to the expansion of the sample material, that had developed after 2 hours was recorded as the swell-index pressure.

The potential volume change (PVC) was read from a chart prepared by Lambe (1960, fig. 20), who defined PVC (p. 4) as "the maximum possible volume change that the soil could undergo from water content changes." Final swell pressure, obtained when constant volume in the wetted sample is maintained, can also be estimated from the swell-index pressure. Swell pressures above 3,000 psf (pounds per square foot) are of only limited value, as discussed by Lambe (1960, p. 36); however, they do indicate that the pressure increases in confined samples.

Swell capacity was determined by following the procedure outlined by Knechtel and Patterson (1952, p. 5). A 2-gram sample of air-dried minus-40-mesh material was added slowly to 100 milliliters of distilled water, and after 1 hour the resulting volume increase, in milliliters, was recorded as the swell capacity.

The mineralogy of most of the fault-gouge samples was determined by means of an X-ray diffractometer. The composition percentages are expressed to the nearest 5 percent, and values are probably accurate to ±5 percent. Relative abundance of clay minerals, as interpreted from the X-ray record, is shown in the right-hand column of table 9. This method of representation does not provide a basis of comparison of clay-mineral abundance among samples.

SIZE ANALYSES AND MINERALOGY OF WALLROCK CHIP SAMPLES

Size analyses were performed on linear chip samples (McKinstry, 1948, p. 45) of wallrock from the pilot bore. The samples were collected from the 5-foot interval on each side of each rock-mechanics instrumentation station. Table 10 gives the results of these size analyses, in cumulative weight percent. Each sample represented the aggregate rock condition and approximate size range of the fractured rock at each sample location. Only sieve analyses were performed because the 0.074-mm fractions constituted less than 5 percent of the total material, thereby eliminating the need for hydrometer analysis. Most samples contained a few pieces larger than 2 inches in smallest dimension, which are not shown in table 10.

Representative fractions of the wallrock samples were prepared for X-ray analysis by crushing each sample and obtaining a split. All the sample material used for X-ray identification was 230-mesh size or smaller. X-ray-diffraction traces of all samples were used for both quantitative and qualitative analyses of the mineral constituents. On the basis of petrographic examination of samples, modifications of accepted X-ray techniques were developed for quantitative analyses of minerals. Samples that were difficult to interpret quantitatively by these modified techniques were then checked petrographically for comparison. These results are given in table 11. Relative quantities of the minerals, determined both by X-ray methods and by petrographic analyses, are stated to the nearest part in 20 parts, 20 parts being 100 percent. Because of this order of precision and, also, because of the presence of small amounts of unidentified minerals, the total identified constituents of each sample may not equal 100 percent. Types of feldspar were not differentiated in the petrographic analyses.

STATISTICAL ANALYSIS OF LABORATORY TEST RESULTS

A complete set of 16 laboratory tests was performed on each of 41 rock samples from surface drill holes and from the pilot bore (tables 6, 7). The results were analyzed by means of stepwise multiple regression to see whether cheaper and more rapid laboratory testing procedures could be substituted for the more expensive and time-consuming static-compression tests without losing the ability to describe the essential physical properties of the rock. The analysis indicated that the compressive strength and static-elastic modulus could be predicted for these rocks within a known degree of accuracy, provided that the porosity, shear velocity, and longitudinal velocity were first measured, and that a biaxial confining stress was selected — for testing

TABLE 11. — *Mineralogy of wallrock chip samples, Straight Creek Tunnel pilot bore*

[Analysts, R. A. Speirer, G. S. Erickson, E. E. McGregor, and T. C. Nichols, Jr. Tr., trace. Leaders (---) indicate mineral looked for but not found]

Sample[1] No	Abundance ratio of minerals in parts per 20 parts																	Relative abundance of clay minerals[2]	Remarks[3]
	Clay		Quartz		Feldspar						Biotite		Calcite		Siderite		Other		
					Microcline		Plagioclase		Total										
	X-ray	Petrography	X-ray	Petrography	X-ray	Petrography	X-ray	Petrography	X-ray	Petrography	X-ray	Petrography	X-ray	Petrography	X-ray	Petrography			
PIS1-NW	5	---	5	---	5	---	3	---	8	---	2	---	---	---	---	---	---	I>C≥ML≥K	Siderate includes some hornblende. Mixed layer predominantly montmorillonite.
PIS1-NE	5	5	5	4	4	---	3	---	7	8	1	2	---	---	2	2	---	ML≥I>C≥K	Do.
PIS2-SW	3	---	5	---	3	---	4	---	7	---	5	---	---	---	---	---	---	K>I>ML	Mixed layer predominantly montmorillonite.
PIS2-SE	3	---	5	---	3	---	4	---	7	---	3	---	---	---	1	---	---	K≥ML>I	Do.
SIS1-SW	3	---	5	---	4	---	2	---	6	---	5	---	---	---	1	---	---	K>I>C	
SIS1-SE	3	---	5	---	5	---	3	---	8	---	4	---	---	---	Tr.	---	---	K>I	
PIS3-SW	4	2	6	6	3	---	3	---	6	8	5	4	---	---	Tr.	---	Tr. magnetite	C>I>ML	Mixed layer predominantly montmorillonite.
PIS3-SE	6	6	4	4	2	---	2	---	4	6	6	4	---	---	---	---	---	C≥I>ML	Do.
PIS4-SW	2	---	2	---	1	---	5	---	6	---	8	---	---	---	---	---	2 opaque ---	K>C>I	Very minor chlorite and illite.
PIS4-SE	2	---	2	---	1	---	6	---	7	---	8	---	---	---	---	---	1 opaque ---	K≥I>ML	Mixed layer predominantly montmorillonite.
PIS5-SW	2	---	4	---	4	---	6	---	10	---	4	---	---	---	---	---	---	K>ML	Do.
PIS5-SE	2	---	6	---	4	---	3	---	7	---	4	---	---	---	---	---	1 opaque ---	K>C≥I	Very minor chlorite and illite.
PLC2A-NW	6	---	4	---	2	---	1	---	3	---	7	---	1	---	---	---	---	M+ML>K+I	Mixed layer predominantly illite.
PLC2A-NE	6	4	4	---	3	3	1	---	4	3	6	7	1	1	---	---	Tr. opaque	K>I>ML	Mixed layer predominantly montmorillonite.
PLC3-SW	2	5	6	3	5	---	3	---	8	8	4	3	---	---	1	1	---	ML>K>I	Do.
PLC3-SE	5	4	2	2	6	---	2	---	8	9	4	3	1	1	---	---	---	K>++ML>I	Do.
SIS2-SW	3	3	4	4	4	---	4	---	8	8	4	4	---	---	1	1	---	K>ML≥I	Do.
SIS2-SE	3	4	3	4	6	---	3	---	9	6	3	3	---	---	2	1	1 opaque, 1 dolomite.	K≥ML>I+M	Do.
PIS6-SW	2	2	5	4	4	---	3	---	7	6	6	8	---	---	---	---	1 opaque ---	K>I	Trace of illite.
PIS6-SE	2	2	6	4	3	---	4	---	7	8	5	4	---	---	---	---	<1 opaque --	K>ML	Trace of illite.
PIS7-SW	4	---	5	---	1	---	4	---	5	---	6	---	---	---	---	---	<1 opaque --	K>ML	Mixed layer predominantly montmorillonite.
PIS7-SE	4	---	6	---	---	---	3	---	3	---	7	---	---	---	---	---	---	I>ML>K	Do.
PLC5-SW	3	3	4	4	6	---	3	---	9	8	4	3	---	Tr.	1	1	---	K>I>ML	Do.
PLC5-SE	4	---	4	---	5	---	3	---	8	---	4	---	Tr.	---	1	---	Tr. dolomite -	K>ML>I	Do.
PIS8-SW	3	---	5	---	4	---	2	---	6	---	6	---	---	---	---	---	---	K>ML=I	Do.
PIS8-SE	3	---	2	---	4	---	2	---	6	---	7	---	---	---	---	---	---	K>ML	Do.
SIS3-SW	6	8	3	2	5	---	2	---	7	6	2	---	---	---	---	---	1 opaque	K>ML+M>I	Do.
SIS3-SE	4	---	4	---	4	---	4	---	8	---	4	---	---	---	---	---	---	K>ML>I	Do.
PIS9M-SW	8	---	3	---	1	---	1	---	2	---	8	---	---	---	---	---	---	ML+M>K>I	Do.
PIS9M-SE	6	5	3	4	3	---	2	---	5	4	7	5	---	1	---	---	1 opaque	K>ML=I>M	Do.
PLC8-SW	3	---	2	---	7	---	Tr.	---	7	---	8	---	Tr.	---	---	---	---	K>I>ML	Mixed layer equal amounts of montmorillonite and illite.

PLC8–SE	4	4	4	4	3		1		4	3	7	7		1				K=ML>I	Mixed layer predominantly montmorillonite.
PIS10–SW	5	4	4	3	3				3	3	7	8		1			1 opaque	K>ML>I	Do.
PIS10–SE	4	2	4	4	2		1		3	4	9	10		1				K>ML>I	Do.
PIS11–SW	6		6		2		1		3		4		Tr.					I>K>ML	Mixed layer predominantly illite.
PIS11–SE	5		4		6		3		9		1				1			K>ML>I	Mixed layer predominantly montmorillonite.
PLC9–SW	7		6		1		6		7						Tr.		K>ML>I		Do.
PLC9–SE	7		4		6		3		9									K>I>ML	Mixed layer equal amounts of montmorillonite and illite.
SIS4–NW	5		3		6		2		8		3				1			K>ML>I	Mixed layer predominantly montmorillonite.
SIS4–NE	7		5		5		1		6		2							K>ML;M>I	Do.
PIS12M–SW	4	5	5	4	4		2		6	7	4	2			1		1 opaque	I>K>ML	Mixed layer predominantly illite(?).
PIS12M–SE	4	3	4	4	1		2		3	3	10	10			Tr.		Tr. opaque	I>K>ML	Do.
PLC10–SW	4	3	3	3	1		3		4	5	4	4	1	1			4 hornblende	C>ML	
PLC10–SE	7	6	3	2	2		4		6	8	1	2	1	1			2 rhodochrosite	C>I	
PIS13–SW	2		4		6		5		11		2		1					K≥C>ML	Mixed layer predominantly illite.
PIS13–SE	4		4		5		5		10		2							K≥C>ML	Do.
PIS14–SW	5	4	3	3			2		2	3	6	7	3	3				K>ML	Mixed layer predominantly montmorillonite. Some chlorite included under calcite.
PIS14–SE	6		3		1		2		3		3		1				4 dolomite	K>I>ML	Mixed layer predominantly illite.
PLC11–SW	5		2		1		1		2		4		1				1 hornblende, 4 dolomite.	I>ML>K	Do.
PLC11–SE	3	2	5	5	6		4		10	12	3	2	Tr.				Tr. dolomite	K>ML	Mixed layer predominantly montmorillonite.
SIS5–SW	3		5		6		5		11		2							K>I>ML	Mixed layer predominantly illite.
SIS5–SE	3		5		6		4		10		2		Tr.					K>I	
PIS15–SW	4		5		4		4		8		3		Tr.					C≥K>I>ML	Mixed layer predominantly illite.
PIS15–SE	3		4		5		5		10		3							K>C>ML	Do.
PLC12–SW	3	2	1	2	1		15		16	14	Tr.	1		1				K>ML=I	Do.
PLC12–SE	3	3	2	2	5		9		14	15	1	1		Tr.				K=I	
SIS6–SW	3	2	4	4	5		5		10	12	3	2						C>I	Possibly minor kaolinite and mixed layer.
SIS6–SE	4	5	4	3	4		3		7	8	5	3		Tr.			1 chlorite	C>I	Do.
PIS16–SW	4	4	4	3	4		2		6	6	6	6		Tr.			Tr. opaque	K>I	
PIS16–SE	4		4		4		4		8		4							I≥K≥ML	Mixed layer predominantly montmorillonite.
SIS7–NW	5	5	3	4	2		1		3	3	10	8						K>ML>I	Mixed layer predominantly montmorillonite.

See footnotes at end of table.

TABLE 11. — *Mineralogy of wallrock chip samples, Straight Creek Tunnel pilot bore* — Continued

Sample[1] No.	Abundance ratio of minerals in parts per 20 parts																Relative abundance of clay minerals[2]	Remarks[3]
	Clay		Quartz		Feldspar						Biotite		Calcite		Siderite			
					Microcline		Plagioclase		Total									
	X-ray	Petrography	X-ray	Petrography	X-ray	Petrography	X-ray	Petrography	X-ray	Petrography	X-ray	Petrography	X-ray	Petrography	X-ray	Petrography	Other	
SIS7–NE	3	2	4	4	3	---	4	---	7	6	7	8	---	---	---	---	Tr. opaque	I>K>ML	Mixed layer predominantly illite.
SIS8–SW	2	---	4	---	4	---	5	---	9	---	5	---	---	---	---	---	---	K>ML	Mixed layer predominantly montmorillonite.
SIS8–SE	2	---	4	---	6	---	4	---	10	---	4	---	---	---	---	---	---	K present	

[1]Sample numbers refer to the Terrametrics, Inc., instrument stations, as PIS1; and to the locality in relation to the station, as NW, NE, SW, or SE (which, respectively, indicate north wall, west of the station; north wall, east of the station; south wall, west of the station; and south wall, east of the station).

[2]K, kaolinite; I, illite; ML, mixed layer; C, chlorite; M, montmorillonite.

[3]Most mixed-layer clays are illite and montmorillonite, and in many clays montmorillonite is predominant. When the mixed-layer clay was less than 5 percent, by volume, of the total sample, the clay minerals were not differentiated.

TABLE 12. — *Dependence of compressive strength of Straight Creek Tunnel area rocks on other physical properties*

Variable	Maximum effect on compressive strength (psi) (+ = increase) (− = decrease)	Variation	
		Range	Type
Shear-wave velocity (*Vs*).	+19,200	7,100–11,200 fps	Continuous nonlinear increase.
Confining pressure	+15,900	0–1,500 psi	One maximum increase.
Logitudinal-wave velocity (*Vp*).	−8,350	11,400–21,800 fps	One maximum decrease.
Porosity	−15,200	0.6–3.3 percent	One minor maximum and one minor minimum superimposed on nonlinear decrease.

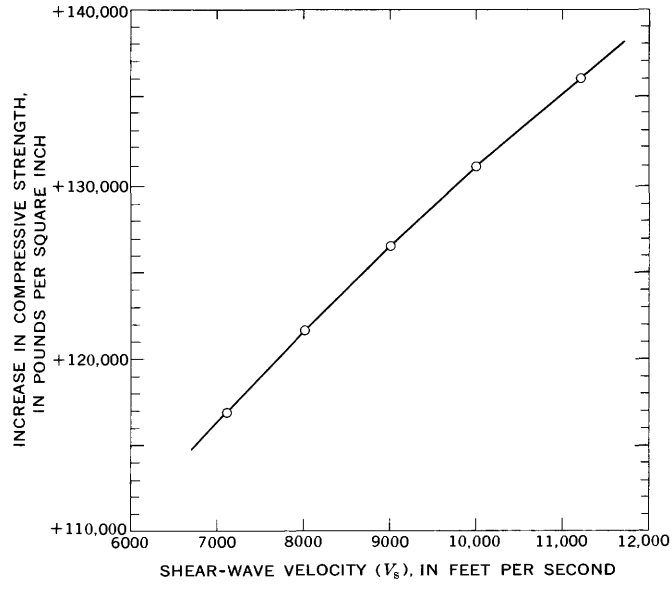

FIGURE 14. — Relation of shear-wave velocity to compressive strength.

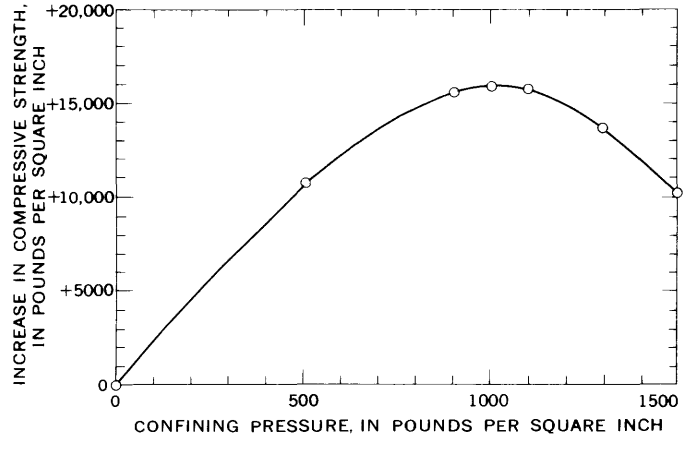

FIGURE 15. — Relation of confining pressure to compressive strength.

compressive strength — and that the stress level be chosen at which the static modulus was desired.

Whether the equations developed for the rocks tested will be applicable for other rocks in other areas is not known. Because the rocks tested represent a broad range of crystalline rocks (granites, pegmatites, gneisses, and schists) with different degrees of alteration, however, the equations developed here could be applicable to similar crustal environments. The interdependent nature of some tests may be the result of a common physical property of the rock substance, but more likely it is the result of several factors, possibly including fracturing, alteration, mineral composition, and various types of layering. The approach indicates that some expensive and time-consuming physical tests can be replaced by other cheaper laboratory tests with minimal loss in understanding of the physical characteristics of these rocks.

The regression equation for estimating compressive strength on the basis of the 41 samples follows:

$$\text{Compressive strength} = -62{,}700 + 131{,}000\,(V_s/10{,}000)^{1/3} + 23{,}200\,(C_p/1{,}000) + 11{,}050\,(V_p/10{,}000)^3 - 29{,}100\,(V_p/10{,}000)^2 - 7{,}300\,(C_p/1{,}000)^3 - 750\,p^2 - 11{,}250\,p^{1/3},$$

where,

C_p = confining pressure;
V_s = shear wave velocity, in feet per second;
V_p = Longitudinal wave velocity, in feet per second; and
p = porosity.

The assumptions made are that the variables are continuous in their influence on compressive strength and that the possible modes of interaction are limited to: (1) Linear, (2) continuously increasing or decreasing nonlinear, (3) one maximum or one minimum, (4) one maximum and one minimum, and (5) combinations of the above.

The equation estimates compressive strength to one standard error of approximately 9,000 psi and has a multiple correlation coefficient squared greater than 0.5.

The effect of the several variables on the prediction of compressive strength is shown in figures 14–17 and table 12. To employ the curves presented in figures 14–17, the increase or decrease in compressive strength from each variable was added, and then the intercept value, 62,700 psi, was subtracted.

For example, for a known set of sample conditions, as follows:

Shear-wave velocity	7,350 fps,
Confining pressure	1,500 psi,
Longitudinal-wave velocity	13,100 fps,
Porosity	1.4 percent,

the estimated values, in pounds per square inch, are

Shear-wave velocity (fig. 14)	+118,000
Confining pressure (fig. 15)	+10,300
Longitudinal-wave velocity (fig. 16)	−24,500
Effect of porosity (fig. 17)	−14,000
Sum	+89,800
Less intercept value	−62,700
Estimated compressive strength	+27,100
Less measured compressive strength	−25,800
Error	1,300

The regression equation for estimating the static Young's modulus (E_s) on the basis of the 41 samples follows:

$$E_s = 101.96 + 3.16\,(V_s/10{,}000)^3 - 484.84\,(\text{MPS}/10{,}000)^{1/3} + 9.95\,(\text{MPS}/10{,}000)^3 + 424.00\,(\text{MPS}/10{,}000)^{1/2} - 39.47\,(\text{MPS}/10{,}000)^2 + 2.25\,(V_p/10{,}000)^3 - 5.69\,(V_p/10{,}000)^2,$$

where

E_s = static Young's modulus (psi/$\frac{\mu\text{-in.}}{\text{in.}}$);
MPS = midpoint of stress range at which the secant modulus is desired, in pounds per square inch;
V_p = longitudinal-wave velocity, in feet per second; and
V_s = shear-wave velocity, in feet per second.

The same variation assumptions were made as previously for compressive strength. This equation has a standard error of about 1.4 psi/$\frac{\mu\text{-in.}}{\text{in}}$ and a multiple-correlation coefficient squared of about 0.70.

The effect of the variables is presented on figures 18, 19, and 20 and table 13. To employ the curves presented, add the increase or decrease in static modulus for each variable and then add the intercept value of 101.96.

For the example conditions presented previously and for a selected stress level of 8,100 psi, the following graphical determination can be made:

Shear-wave velocity (fig. 18)	+1.24
Selected stress level (fig. 19)	−90.89
Longitudinal-wave velocity (fig. 20)	−4.70
Sum	−94.35
Intercept value	+101.96
Estimated static Young's modulus	+7.61
Measured static Young's modulus	−8.10
Error	−0.49

GEOPHYSICAL INVESTIGATIONS

In the past geophysical investigations have been conducted in support of geologic and engineering investigations

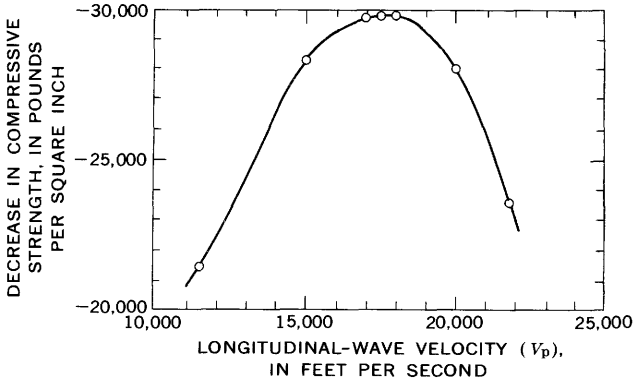

FIGURE 16. — Relation of longitudinal wave velocity to compressive strength.

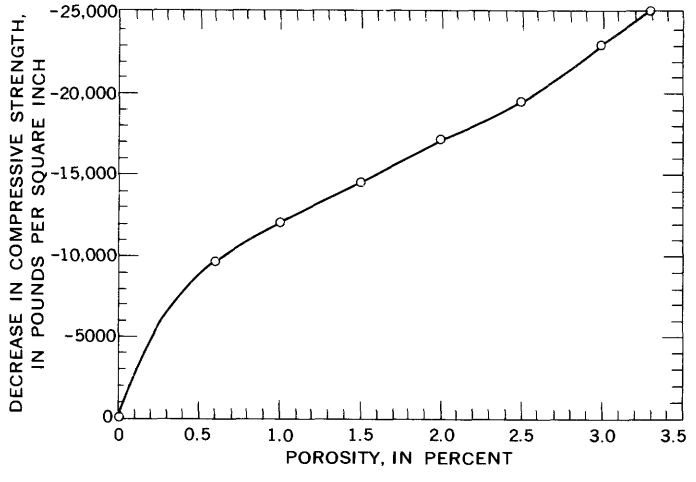

FIGURE 17. — Relation of porosity to compressive strength.

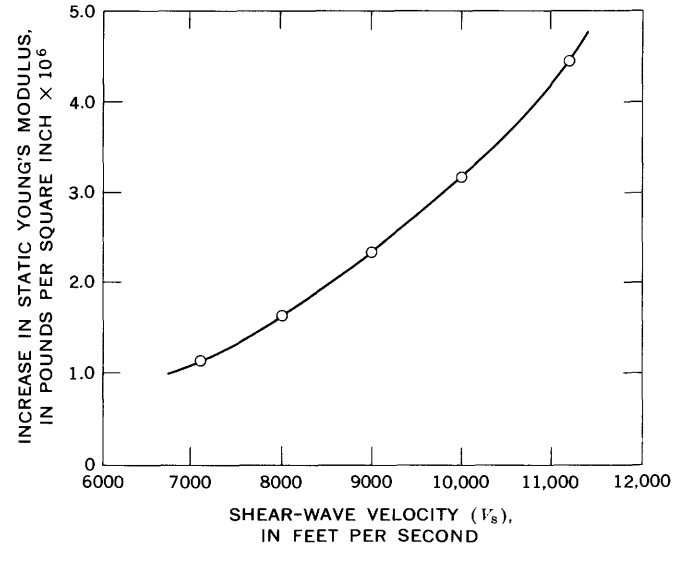

FIGURE 18. — Relation of shear-wave velocity to static Young's modulus (*E*s).

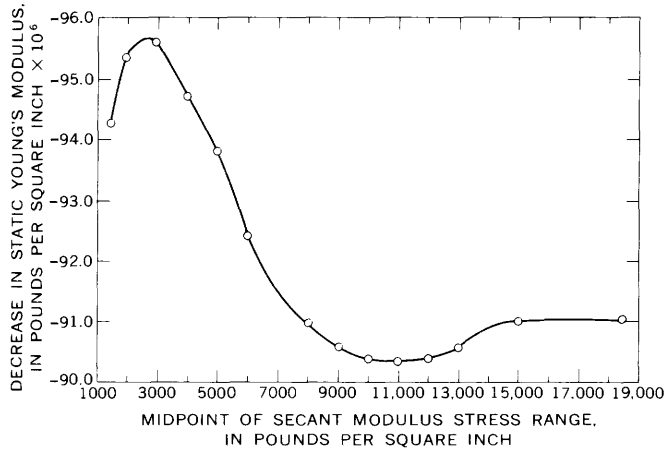

FIGURE 19. — Relation of selected stress level to static Young's modulus (*E*s).

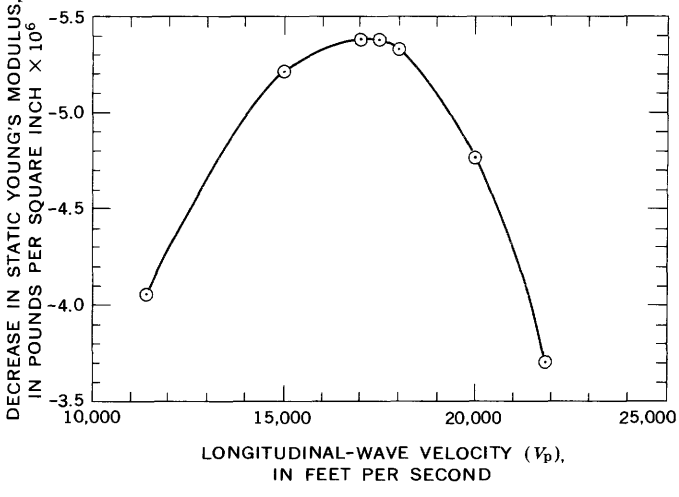

FIGURE 20. — Relation of longitudinal-wave velocity to static Young's modulus (*E*s).

TABLE 13. — *Dependence of static Young's modulus (Es) of Straight Creek Tunnel area rocks on other physical properties*

Variable	Maximum effect on *Es* (+ = increase) (− = decrease)	Variation	
		Range	Type
Shear-wave velocity (*Vs*)	+3.32	7,100–11,200 fps	Continuous nonlinear increase.
Stress level selected (MPS)	−5.42	1,500–18,450 psi	One maximum and one minimum superimposed on continuous nonlinear decrease.
Longitudinal-wave velocity (*Vp*)	−1.67	11,400–21,800 fps	One maximum decrease.

for the construction of underground openings. Most geophysical investigations have been restricted to gravity measurements, such as those by Wilson and Boyd (1932) and by Plouff (1961) for the Roberts Tunnel for surveying purposes, and to wallrock-temperature measurements. More recently, research has been conducted in the use of

seismic methods to determine the effect of an opening on rock properties and the thickness of the affected zone (Wantland, 1964; Kujundžić and Čolić, 1959). One of the objectives of the Straight Creek Tunnel project was to experimentally apply geophysical techniques to predict geologic conditions at the depth of the proposed pilot bore, and to help define the relations of geology to both the engineering and the construction of the pilot bore.

The geophysical objectives of the project were restricted by the availability of geophysicists and equipment. Prior to construction of the pilot bore, the available geophysical data were from a seismic survey of the depth to bedrock in the area around the east portal of the pilot bore and from geophysical logs of drill holes. During construction of the pilot bore, wallrock temperatures and electrical resistivity measurements were made at selected localities along the walls of the pilot bore. After construction of the pilot bore, seismic data obtained at the surface prior to the construction of the pilot bore were analyzed and plotted, seismic measurements were made in the pilot bore, and electrical-resistivity measurements were made at the surface. The results of the electrical-resistivity and seismic studies are given in chapter D of the present report.

HYDROLOGIC INVESTIGATIONS

Ground water is always a major concern in the construction of an underground opening. In the Roberts Tunnel, a few miles south of the Straight Creek Tunnel site, large water flows were encountered that materially slowed construction and increased cost. In collecting data for estimating the ground water that might be anticipated in the construction of the Straight Creek pilot bore, very little reliable data were found on the occurrence of ground water in crystalline rocks; therefore, it was proposed that the U.S. Geological Survey make a study of the occurrence of ground water during construction of the pilot bore. R. T. Hurr and D. B. Richards made this study.

The hydrologic investigations included the installation of a Parshall flume and recorder in the drainage ditch at station 117+70 of the pilot bore to determine the flow of water from the pilot bore. Initial water flows, and the decrease in water flows with time, from feeler holes and fractures were recorded. The results of these observations are shown graphically on plate 4. The water level in drill-hole 2 (1962) was recorded from the surface periodically during construction of the pilot bore and for a period after completion of the pilot bore. Rates of ground-water flow at different points in the drainage ditch of the pilot bore were recorded periodically, and samples of water from feeler holes and fractures and from the drainage ditch were collected for analyses.

Summaries of these data and an analysis of the data and their significance to the construction of underground openings are given in chapter E of this report.

ROCK-MECHANICS INSTRUMENTATION

During the original planning for the engineering geologic investigations of the Straight Creek Tunnel site, a limited rock-mechanics instrumentation program for the pilot bore was proposed. Prior to the start of construction of the pilot bore, Terrametrics, Inc., a rock-mechanics instrumentation firm of Golden, Colo., contracted with the Colorado Department of Highways for an extensive instrumentation program. The rock-mechanics program is summarized from chapter F of the present report, which describes the methods of construction and installation of the instruments used, the locations of the instrument stations, and the measurements obtained.

Three types of rock-mechanics instruments were used in the pilot bore — load cells, borehole extensometers, and bar extensometers. Where possible, all three types were installed at the same tunnel station. For example, in supported sections, load cells were placed under the supports, borehole extensometers were placed in the roof and walls, and pins for the bar extensometer were placed in the roof, floor, and walls. In the unsupported sections, borehole extensometers and pins for the bar extensometers were installed.

Terrametrics, Inc., prepared monthly progress reports and a final report for Colorado Department of Highways, giving the results of the instrumentation program. Copies of these reports were made available to the authors.

GEOLOGIC, ENGINEERING, AND CONSTRUCTION PREDICTIONS

A primary purpose of the Straight Creek tunnel project was the prediction, before construction, of geologic conditions at the depth of the pilot bore. The data compiled from the geologic, geophysical, and laboratory investigations were used to construct a predicted geologic section along the proposed pilot-bore line. Plate 2 shows this geologic section, together with the engineering and construction predictions, all of which were compiled prior to underground excavation.

Experience has shown that individual geologic features observed in surface mapping and drilling cannot be projected accurately to tunnel level. Statistical analysis of the geologic data, however, can give estimates of the type and magnitude of geologic features to be encountered in driving a tunnel. For example, in an area such as the Straight Creek Tunnel site, it is not possible to show exactly where the pilot bore will intersect granite and metasedimentary rock, but it is possible to estimate approximately what percentage of the bore will be in granite and what percentage will be in metasedimentary rock. It would likewise be impracticable to project each fault or shear zone to pilot-bore level and expect to intercept that fault or shear zone at that point. It is possible, however, from surface mapping, drilling, geophysical measurements, and experience in other tunnels, to predict the number, attitude, size, and general area in

which faults and shear zones can be expected. From this type of geologic information, it is then feasible to calculate the amount of ground water, the rock load per foot of tunnel (and therefore the amount of support required), the areas that should be investigated by feeler holes, and the probable amount of grout required.

GEOLOGIC PREDICTIONS

In constructing the predicted geologic section, no effort was made to project individual rock units, faults, or shear zones to the pilot-bore level. To predict the position of the metasedimentary rock inclusions by projection from the surface exposures and drill holes was impracticable because their maximum dimension averages only about 20 feet. However, on the basis of surface and drill-hole information, a prediction was made that 75 percent of the pilot bore would be in granite and 25 percent would be in metasedimentary rocks (Robinson and Lee, 1962).

Geologic mapping before and after the construction of other tunnels in Colorado has shown that only about 10 percent of the faults and shear zones which are >5 and <50 feet in width and which are intersected by a tunnel can be mapped on the surface, and that only about 1 to 5 percent of those faults <5 feet wide have been noted. These percentages vary somewhat, partly depending upon the percentage of outcrop. The resultant plots of the trends of the faults and shear zones and the attitudes of joints, however, agree well with similar plots made after the mapping of the tunnels. This knowledge was the basis for the interpretation of the structure to be expected in driving the pilot bore.

Rather than project the individual faults and shear zones from surface to pilot-bore level, therefore, the different zones of the average spacing between fractures, as determined at the surface, were projected to pilot-bore level on the basis of the average dip of faults and shear zones, as calculated from surface and drilling data.

The strike-frequency diagram (fig. 6*A*) illustrates the relation of the trend of the observed faults and shear zones to the trend of the pilot bore. The diagram shows that only about 4 percent of the faults and shear zones trend parallel to the trend of the pilot bore. No fault or shear zone more than 5 feet wide, however, was noted at the surface that would be expected to follow the trend of the pilot bore at depth.

The structure map of the surface (pl. 1) showed that the pilot bore should cross the major shear zones at angles of about 25°−75°. The angle at which a tunnel intersects a fault or shear zone determines the length of that fault or shear zone within a tunnel. The dip for 74 of these faults or shear zones on the surface ranged from 35° to 90° and averaged 75°. The amount of dip also determines the amount of fault exposed in a tunnel.

The contour diagram of joints observed at the surface (fig. 7) showed that there was no principal joint direction, or directions, and that the joints could be expected to intersect the pilot bore at any angle.

ENGINEERING AND CONSTRUCTION PREDICTIONS

The engineering and construction data calculated for estimating the cost of construction of the pilot bore were the rock loads, spacing of support sets, amount of lagging, the need for feeler holes and grouting, and the amount of ground water. These calculations were based on the predicted geologic section (pl. 2) and the laboratory data, and the results are shown on figure 32 as a series of graphs below the geologic section.

ROCK LOADS

The calculations for rock load were based on the assumptions that the pilot bore, outside the supports, would be about 10.5 feet wide and 11.5 feet high and that the rates of driving the pilot bore and installing the supports — both factors affect the rock load — would be as efficient as possible. The rock load, then, was predicted primarily on the basis of geologic conditions.

From the information on the geologic section, the rock mass at tunnel level was classified into one of three categories depending upon the fracture spacing and number of faults and shear zones — each category is shown by a different pattern along the tunnel line on plate 2.

The boundaries between each section of the pilot bore in different categories were predicted to be gradational and indefinite with a 25-percent error in length expected. The location of each category was also determined statistically, and it was anticipated that each section could be shifted in either direction a distance probably equivalent to about half its length.

The average distance between fractures ranged in the first category from less than 0.1 to 0.5 foot, in the second category from 0.5 to 1 foot, and in the third category from 1 to 3 feet. In category 1 the rock was considered to be that which occurs in faults and shear zones, and it was expected to account for the maximum rock loads. In categories 2 and 3 it was estimated that 20 and 10 percent, respectively, of the length would be represented by faults and shear zones.

To calculate the rock load, the density was determined for 20 samples of granite and six samples of metasedimentary rocks (table 6). For the purpose of the rock-load calculations, the average saturated bulk density was determined to be 2.67. The average weight of 1 cubic foot of rock in the Straight Creek Tunnel area, then, would be 166.88 pounds.

Another factor that would affect the rock load would be the swelling of the clay of the fault gouge or of the clay produced as an alteration product. Experience in mining and tunneling in other areas in the Front Range had shown that maintaining an opening through swelling clays could be difficult. To calculate the potential volume change, swell capacity, and swell index for clay material for the pilot bore,

those factors were determined (table 9) for four gouge samples collected at the surface and for two samples from drill hole 3 (1962).

SUPPORT

Rock loads, fracture spacing, and the amount of fault gouge or clay-alteration products were expected to vary from place to place. Although these factors are interrelated, different values for fracture spacing and amount of swelling clay could produce similar rock loads. The total effect of these geologic factors on the construction of the pilot bore was expressed, more or less quantitatively, by the amount of support that could be required. Therefore, the estimates of support requirements were a relative measure of the severity of geologic conditions, rather than an attempt to formulate definitive engineering-design requirements. For the purpose of the support calculations, it was assumed that the sets would be designed to carry a maximum load of 10,000 psf and that the pilot bore would be driven on a three-shifts-a-day basis. The results of these calculations are shown on a graph below the geologic section on plate 2. Note that for some sections, where wide zones of fault gouge were anticipated, invert struts were indicated.

The calculations for the predicted rock loads were made using the following formula, which is modified from Terzaghi (1946, p. 61):

$$P = C\,(b + h)\,(W),$$

where,

P = rock load, in pounds per square foot;
C = a constant depending upon rock conditions;
b = width of tunnel;
h = height of tunnel; and
W = weight per cubic foot of rock.

The results of the calculations of rock load are given in a graph below the geologic section on plate 2. The values for b, h, and W were assumed to be constant for the entire length of the pilot bore. The values for C ranged from 0.35 to 1.60, depending on the interpretation of fracture spacing expected and on predictions of the presence of swelling clay in fault gouge.

The prediction of the spacing of sets and the amount of lagging was empirical. It was stated (Robinson and Lee, 1962) that locally, in practice, sets and lagging might need to be added or omitted. It was realized that the actual spacing of sets and the amount of blocking and lagging required would be determined only during pilot-bore excavation. The purpose of the graph was only to estimate the probable total amount of support material that would be required and the approximate location where support problems might exist.

FEELER HOLES AND GROUT

The geologic conditions ahead of some sections of a tunnel should be determined by drill holes in advance of the face. The predicted location of those sections in the Straight Creek Tunnel pilot bore is shown on plate 2. Many zones of badly broken and crushed rock were noted on the surface. It was anticipated that these zones might contain large volumes of water at the depth of the pilot bore. By locating these zones in advance of the face, it should be possible to seal off the water and consolidate the broken rock in advance of the pilot bore. It was recommended that feeler holes be kept at least 50 feet in advance of the face for those sections of the pilot bore where water-saturated crushed rock might be expected. The number of holes would depend upon conditions encountered and the number necessary for estimating grouting requirements.

The amount of grout that might be required would also depend upon the conditions encountered. The sections in which the geologic conditions indicated that grouting might be required are shown on plate 2. The predicted grout requirement was based on the amount used in the nearby Roberts Tunnel, which averaged about 10 cubic feet (sacks) per foot of grouted section.

The sections indicated to be tested by feeler holes and the sections to be grouted were estimates only. During tunneling, rock conditions at the face should be continually and carefully observed, and if there is any indication of a possible water-bearing section ahead of the face, that section should be tested by feeler holes. The cost of feeler holes is small in comparison with the cost of recovering a caved face.

GROUND WATER

The amount of ground water that was expected to be encountered depended upon the porosity and permeability of the rock mass and the height of the water table above the pilot-bore level. It was thought that the porosity of the rock would be controlled largely by the fracture spacing, as calculated for each interval of the pilot bore. The permeability would depend primarily on the size and interconnection of the fractures. These factors were determined from field and laboratory investigations and equated with records of water flows in other tunnels and with test data from wells in similar rocks. In making these calculations the authors were assisted by G. H. Chase of the U.S. Geological Survey.

The average amount of ground water that was expected to flow from the pilot-bore portal is shown by a graph on plate 2. This graph was based on an estimated rate of advance of the heading of 1,000 feet per month. An increase in the rate of advance would increase the amount of flow, and, conversely, a slower rate would decrease the amount of flow. By projecting this rate beyond the time of driving the pilot bore, it was predicted that the average flow at the east portal should decrease to about 300 gpm (gallons per minute) in 2 weeks and to about 100 gpm within 1 year.

The maximum amount of flow that was expected from the various fracture-spacing intervals in the pilot bore is shown by a histogram on plate 2. This amount was the maximum initial flow that was anticipated from a fault or shear

zone within the interval. These initial flows were expected to decrease rapidly within 5 to 10 days. According to these calculations the maximum average flow from the portal was estimated to be about 500 gpm; the maximum initial flow from any section of the pilot bore was estimated to be about 1,000 gpm.

An important point is that these figures were based on averages that were obtained by comparing the predicted geologic conditions with well data for similar rocks and with records of flows from other tunnels. Within any section of the pilot bore, the water was not expected to issue at a uniform rate but was expected to flow primarily from faults and shear zones and the more closely jointed rock within that section.

Geophysical Investigations

By JAMES H. SCOTT, RODERICK D. CARROLL, CHARLES S. ROBINSON, *and* FITZHUGH T. LEE

ENGINEERING GEOLOGIC, GEOPHYSICAL, HYDROLOGIC, AND ROCK-MECHANICS INVESTIGATIONS OF THE STRAIGHT CREEK TUNNEL SITE AND PILOT BORE, COLORADO

GEOLOGICAL SURVEY PROFESSIONAL PAPER 815-D

ENGINEERING GEOLOGIC, GEOPHYSICAL, HYDROLOGIC, AND ROCK-MECHANICS INVESTIGATIONS OF THE STRAIGHT CREEK TUNNEL SITE AND PILOT BORE, COLORADO

GEOPHYSICAL INVESTIGATIONS

By JAMES H. SCOTT, RODERICK D. CARROLL, CHARLES S. ROBINSON, *and* FITZHUGH T. LEE

INTRODUCTION

In the past, geophysical investigations have been made in support of geologic and engineering investigations for construction of underground openings. Most geophysical investigations have been restricted to gravity measurements, such as those by Wilson and Boyd (1932) and Plouff (1961) for surveying purposes for the Roberts Tunnel, and wallrock-temperature measurements, such as those in the Roberts Tunnel by E. E. Wahlstrom (unpub. data). More recently, studies have been made in the use of seismic methods to determine the effect of an opening on rock properties and the thickness of the affected zone (Wantland, 1964; Kujundžić and Cǒlić, 1959). One objective of the Straight Creek Tunnel project was to experiment with applying geophysical techniques to predict geologic conditions at the depth of the proposed pilot bore and to help define the relations of geology to the engineering and the construction of the pilot bore.

Geophysical surveys were made in the Straight Creek Tunnel area at the surface and in the pilot bore. The work was part of the general program of research at the tunnel site and was done before, during, and immediately after pilot-bore construction. Surface geophysical measurements were made on the ground surface and in holes drilled from the surface along the line of the pilot bore. Underground geophysical measurements were obtained from detector arrays placed along the walls of the pilot bore.

SURFACE AND BOREHOLE GEOPHYSICAL MEASUREMENTS

The following geophysical surveys were made along the surface above the pilot bore and in core holes drilled from the surface:

1. Surface seismic survey to determine depth to bedrock in the vicinity of the east portal.
2. Seismic survey to determine velocity layering and velocity of rock from the surface to the depth of the tunnel.
3. Electrical-resistivity depth soundings made to detect differences in physical characteristics of rock along the tunnel route.
4. Geophysical logging of holes drilled along the tunnel line.

The location of these surface geophysical measurements is shown in figure 21.

EAST PORTAL SEISMIC-REFRACTION SURVEY

Prior to construction of the approach road and the cut for the pilot bore for the east portal of the Straight Creek Tunnel, a surficial geologic map and a seismic survey were made. The geologic mapping was done by C. S. Robinson. The seismic survey was made by R. M. Hazlewood and C. H. Miller. The result of this work was made available to the Colorado Department of Highways in October 1962 (C. S. Robinson and R. M. Hazlewood, unpub. data, 1962). Figure 22 is modified from the map submitted to the Colorado Department of Highways.

The surficial geology was mapped and the seismic shot holes were located by tape and compass and plotted on a topographic base, at a scale of 1:1,200, prepared for the Colorado Department of Highways by Continental Engineers, Inc. The depth to bedrock was determined from records of a portable seismograph. Generally, eight geophones about 50 feet apart were spread at approximately right angles to the topographic slope. Dynamite charges were detonated in holes, driven into the ground with a steel rod, at each end of the geophone spread. The time interval between the detonation of the explosive charge and the arrival of seismic energy at each geophone was determined from the seismograph records, and these times were plotted on graph paper as a function of the distance between each geophone and shotpoint. Standard delay-time interpretation techniques were used to determine depths to the refracting horizon (bedrock), as illustrated on figures 23 and 24.

The altitude of bedrock surface (fig. 22) was determined by subtracting the calculated thickness of the surficial material from the altitude of the ground surface at the shot-

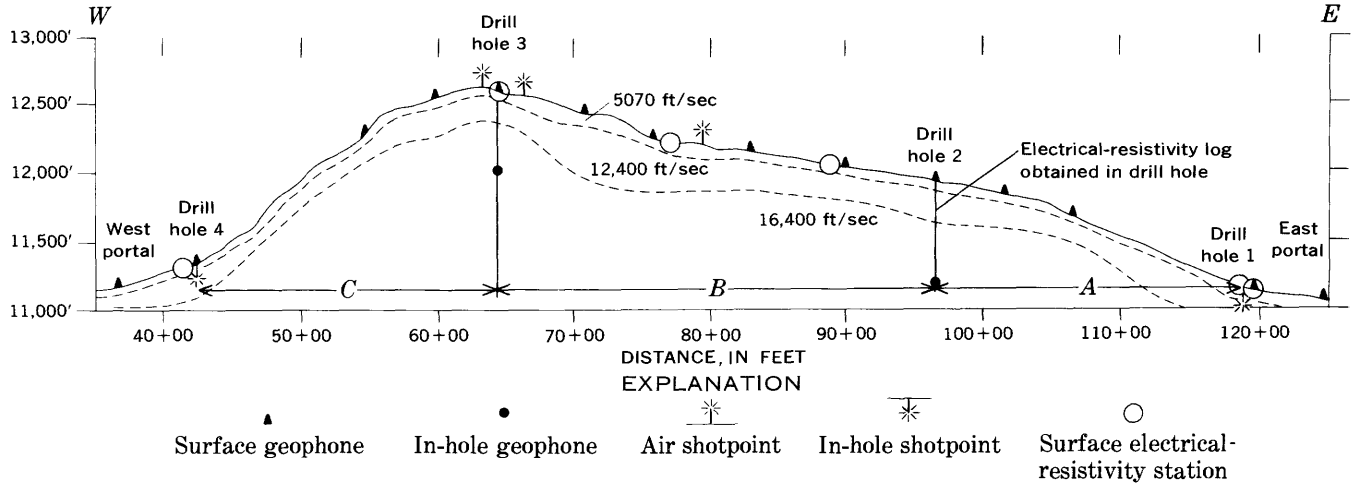

FIGURE 21. — Cross section of Straight Creek Tunnel pilot bore, showing locations of surface and in-hole geophysical measurements and interpretation of seismic-refraction survey. A, B, and C indicate intervals discussed in text.

point. The topography of the bedrock surface was then contoured on the basis of these points. The approximate thickness of the surficial material of any point may be obtained by subtracting the altitude of the bedrock from the altitude of the ground surface.

PORTAL-TO-PORTAL SEISMIC-REFRACTION SURVEY

Surface seismic measurements were made by use of five mobile seismic-refraction units of the U.S. Geological Survey under the direction of R. L. Black and B. L. Tibbetts. These units have been described in detail (Warrick and others, 1961). Geophones were placed on the ground surface along, and at right angles to, the line of the proposed pilot bore; in addition, probes containing triaxial geophones were lowered into and fastened to the walls of drill-holes 2 (1962) and 3 (1962) (pl. 1) at depths of 712 and 526 feet, respectively. Velocity-layering interpretations were made by plotting the refraction traveltimes obtained from the seismic records against the distance between shotholes and surface geophones and computing the thickness of the layers represented by the plotted points by standard delay-time-interpretation techniques. Direct-transmission seismic velocities were obtained from the traveltime records of the in-hole phones for the in-hole charges.

Results of the interpretation indicated that three distinct layers of rock occur approximately parallel to the ground surface (fig. 21). The upper layer has an average velocity of 5,070 fps (feet per second) and extends to depths ranging from 35 to 90 feet. This layer probably represents rock that is weathered, fractured, and undersaturated. The middle layer has an average velocity of 12,400 fps, and extends to depths ranging from 180 to 465 feet. The third layer has an average velocity of 16,400 fps and extends to an unknown depth. The underground seismic measurements, described later in this chapter, indicated that the apparent velocity of the third layer detected by these surface refraction measurements is somewhat higher than the average velocity of rock measured in the pilot bore. Because first-arrival refraction energy was carried by this high-velocity layer, it was not possible to determine the velocity of rock beneath it at the depth of the pilot bore. Fortunately, data for the direct-transmission seismic travel paths between the in-hole shotpoints and the in-hole geophones (fig. 21, intervals A, B, and C) provided velocities that were more representative of rock at the level of the pilot bore and more useful in assessing rock character at tunnel depth. Tests of predictability of construction parameters from these measurements are also presented in this chapter.

PORTAL-TO-PORTAL ELECTRICAL-RESISTIVITY SURVEY

Electrical-resistivity measurements were made along the surface over the pilot bore in 1966, about 2 years after the completion of the pilot bore, by J. H. Scott and R. D. Carroll, to obtain a better understanding of the electrical resistivity measured in the pilot bore and to compare electrical-resistivity results with seismic results at the surface.

The electrical-resistivity measurements were made with the Schlumberger array at six stations at the surface over the pilot bore. The equipment used (fig. 25) was a high-sensitivity, high-impedance, low-voltage recorder and portable battery pack, with current meter and control, and electrodes placed in the Schlumberger configuration.

The resistivity measurements were made by placing the electrodes along the projection of the centerline of the pilot bore at the surface. The two current electrodes (fig. 25, A and B) were made of 2- to 3-foot-square sheets of aluminum foil placed in holes dug in the ground, to which salt and water were added. The two potential electrodes (fig. 25, M and N) were made of 4-inch-square ⅛-inch-thick pieces of lead sheeting buried about 0.5 foot below the ground surface. The current electrode spacing AB/2 was expanded in increments of 10 to 2,000 feet from the center of the spread to obtain a depth sounding. Potential electrode spacings

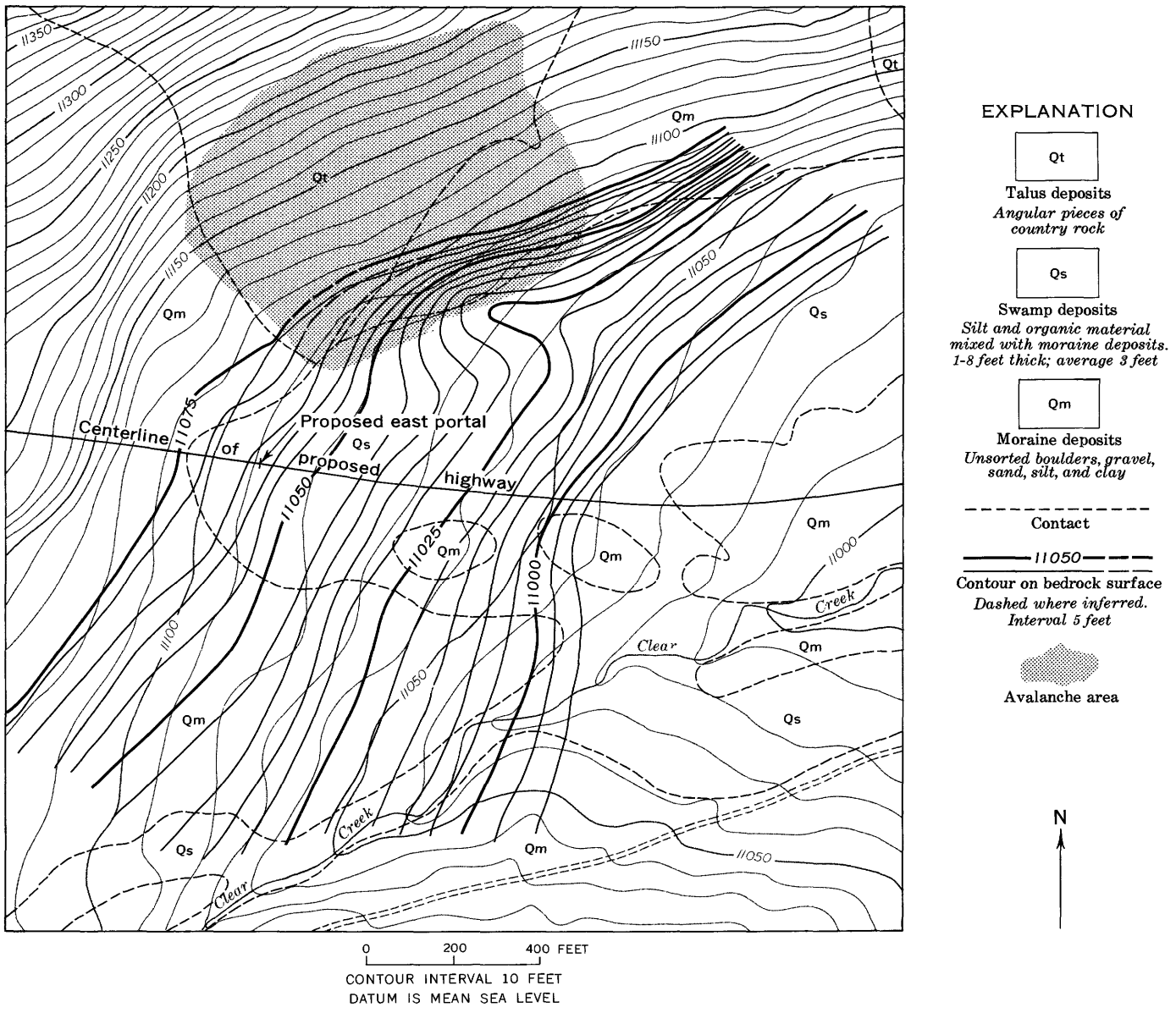

FIGURE 22. — Surficial deposits and bedrock topography, east portal area, Straight Creek Tunnel. Thickness of surficial deposits can be determined from bedrock contours and topography. Seismic data by R. M. Hazlewood and C. H. Miller, 1962. Geology by C. S. Robinson, 1962. Topography by Continental Engineers, Inc., 1961, from Colorado Department of Highways Project I-70-3(13)212.

were also expanded with the ratio AB/2:MN, maintained at 3:1 or larger. To make a measurement at any given electrode spacing, the electrodes were placed in the ground, and the time-drive recorder was started, with no current being supplied to the current electrodes. This gave a measure of the natural potential between the potential electrodes. Current was then supplied to the current electrodes, and a constant current was maintained by manually controlling a variable resistance between the batteries and the current electrodes. The potential was recorded for about 30 seconds, and then the current was shut off. The recorder was run for another 30 seconds to record the natural potential. The procedure was then repeated with the current direction reversed, to minimize polarization errors. The true potential difference was calculated by subtracting the average of the natural potential, which was measured before and after the application of current, from the average potential, which was recorded during the application of current for both directions of current flow.

The following formula was used to compute the apparent resistivity from measurements made at each electrode spacing:

$$\rho_a = \frac{2\pi V}{I}\left[\frac{a^2}{b} - \frac{b}{4}\right], \quad \rho_a = \frac{2\pi V}{I}\left[\frac{(AB/2)^2}{MN} - \frac{MN}{4}\right],$$

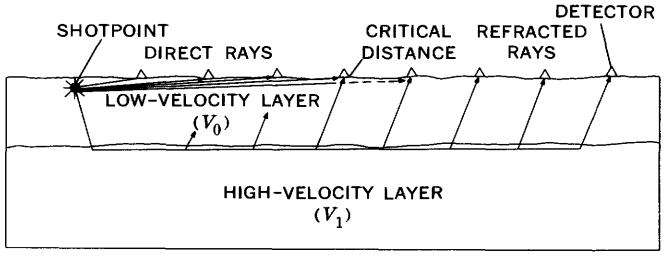

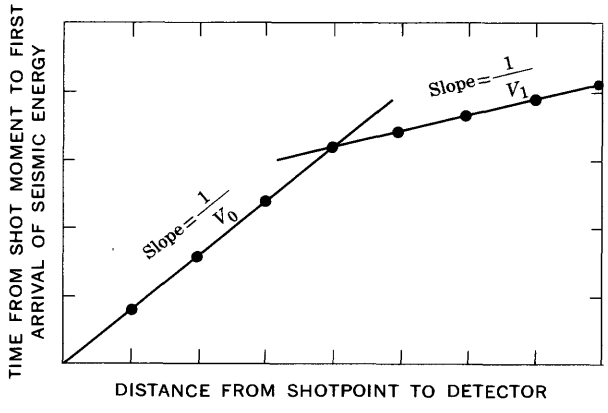

FIGURE 23. — Cross section showing direct- and refracted-ray paths and graph showing traveltime for a two-layer seismic model.

where

ρ_a = apparent resistivity,
AB/2 = spacing between a current electrode and the center of the spread,
MN = spacing between the two potential electrodes,
V = average recorded potential difference between electrodes M and N minus average natural potential, and
I = current measured between electrodes A and B.

The apparent-resistivity values were plotted as a function of current-electrode spacing AB/2 on log-log graph paper similar to the plots shown for apparent resistivity in the pilot bore (fig. 37). Interpretations were made by the curve-matching techniques in which two-layer Schlumberger curves and auxiliary curves (Zohdy, 1965) were used.

GEOPHYSICAL LOGGING OF DRILL HOLES

On the completion of the core drilling in 1962, geophysical logs were run of the accessible parts of drill-holes 2 (1962) and 3 (1962) (pl. 3) — 752 feet of a total depth of 872 feet and 950 feet of a total depth of 1,258 feet, respectively. The geophysical logs were made to supplement the geological logs and were used primarily to determine or confirm zones of shearing, particularly where core recovery had been poor. All the logging had one difficulty in common: those sections of the holes in badly broken ground caved (many within a few hours of drilling); as a result, the probes could not reach the bottom, or the holes required cementing

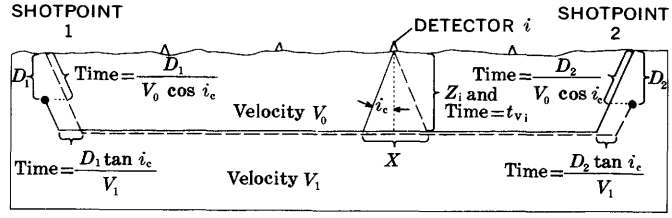

FIGURE 24. — Cross section illustrating method used to determine thickness of low-velocity layer beneath each detector beyond the critical distance.

or casing, which prevented the effective operation of one method or the other. Resistivity logs were made by C. J. Zablocki, and gamma-radiation and density logs by W. A. Bradley, both of the U.S. Geological Survey.

Figure 26 shows part of the geophysical log of drill-hole 2 (1962). To aid interpretation of the geophysical logs, a general description and graphic representation was made of the core and of the intervals cemented and cased. This information is plotted with the geophysical logs shown in figure 26.

RESISTIVITY LOGGING

Resistivity values are largely dependent on the amount and chemical composition of the water within the rock mass (Pirson, 1963, p. 21–26). In crystalline rocks, such as those of the Straight Creek Tunnel site, the porosity (table 6, chap. C) and permeability of the unfractured rocks is small, and the resistivity values reflect secondary porosity and permeability as a result of fracturing.

The resistivity logs were obtained by lowering three electrodes, arranged in the "normal" configuration, into water-filled drill holes and attaching a fourth electrode to the hole casing, or grounding it near the surface. Figure 27 is a schematic diagram showing a typical arrangement of electrodes for resistivity measurements in drill holes (Pirson, 1963, p. 82).

The resistivity curve shown in figure 26 illustrates the use of such logs in crystalline rocks: Shear zones, such as the one between about 555 and 578 feet, have a low resistivity, whereas the relatively unfractured rock, as between 542 and 555 feet, has a high resistivity. In the sheared interval, core recovery was only about 20 percent, and it was not possible to determine where the core came from within this interval. The resistivity log indicates that the entire interval is highly fractured.

GAMMA-RADIATION LOGGING

A gamma-ray log indicates the relative amounts of gamma radiation in the rock surrounding the drill holes. The gamma radiation is emitted by natural radioisotopes in the decay of uranium, thorium, and potassium. The amount of natural radioisotopes in a rock is related to the origin and the geologic history of the minerals in the rock. Gamma-ray logs have been used very successfully in the petroleum industry to correlate sedimentary rock units between drill

FIGURE 25. — Schlumberger electrical-resistivity equipment and cross section of electrode configuration. A, B, current electrodes; M, N, potential electrodes.

holes. In areas of igneous and metamorphic rocks, the rock type may be identified by its characteristic level of radiation. In the Straight Creek Tunnel area, for example, the Silver Plume Granite contains monazite — a thorium mineral — and a higher percentage of potassium feldspar than the metasedimentary rocks, and, therefore, in unaltered sections it emits more gamma radiation than the metasedimentary rocks.

Figure 26 illustrates the relation of gamma radiation to rock type and alteration. In the interval from 520 to 527 feet is unaltered gneiss and schist with a relatively low level of gamma radiation. In the interval from 527 to 543 feet is unaltered granite with a relatively high level of gamma radiation. In the interval from 586 to 613 feet is sheared and altered granite with a relatively low level of gamma radiation. The lower level of radiation in the sheared and altered granite as compared with the fresh granite is the result of the removal of radioisotopes because of alteration. The gamma-radiation logging has the advantage that the relative gamma radiation is not appreciably affected by cementing or casing of a hole, and, in cemented or cased sections of poor core recovery, an interpretation can be made from the logs as to the rock type and relative degree of alteration.

RELATIVE-DENSITY LOGGING

Rocks of different composition, origin, and geologic history have different densities. As shown in table 6 (chap. C), the density of the metasedimentary rocks is, in general, greater than the density of the granitic rocks in the Straight Creek Tunnel area. The density of the original rock is changed by shearing and alteration. A log of the density of the rocks around a drill hole may be interpreted in conjunc-

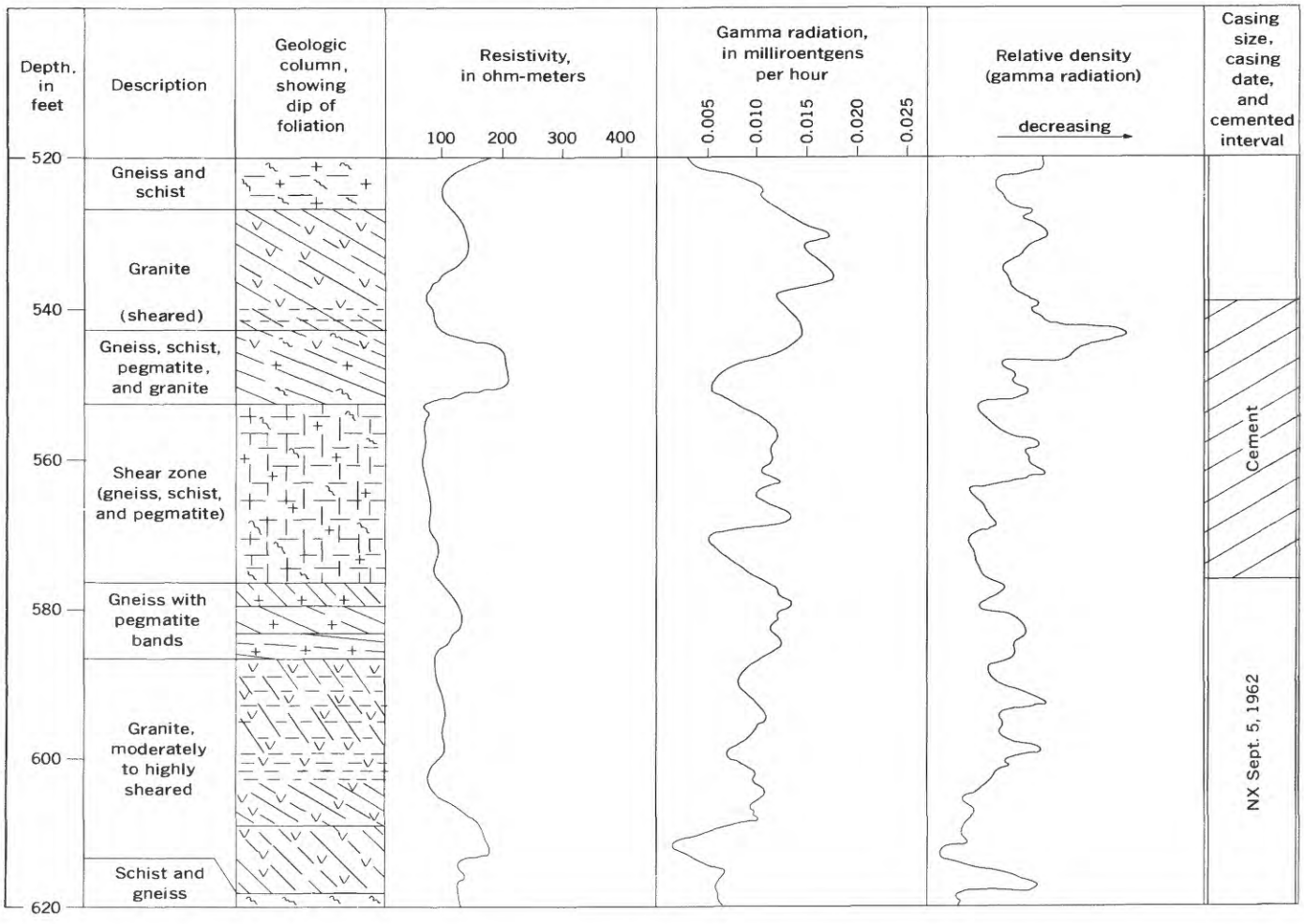

FIGURE 26. — Lithologic correlation with geophysical logs, drill-hole 2 (1962), Straight Creek Tunnel project.

tion with partial lithologic logs to determine rock types and relative amounts of shearing and alteration.

The density of the rock around a drill hole is measured by detecting the backward scatter of gamma rays from a gamma-ray source. A shielded collimated source of gamma rays and a gamma-ray detector above the source (shielded to record only the back-scattered rays) are mounted in a probe. In the U.S. Geological Survey equipment used, the gamma-ray source was radium and the detector was a Geiger-Müller tube. The intensity of the back-scattered gamma rays varies according to the electron density of the matter penetrated by the gamma rays. The back-scattered rays penetrate about 3 inches into the walls of the drill hole. The Geiger-Müller tube is connected to a calibrated recorder, which records the relative density of the rock while the probe is being lowered into or withdrawn from the drill hole.

The density logs of the drill holes in the Straight Creek Tunnel area were not very effective in determining rock composition, structure, or alteration because of the high background of natural gamma radiation. In future logging in this environment, this problem could probably be avoided by using a higher intensity gamma-ray source.

UNDERGROUND GEOPHYSICAL MEASUREMENTS

The following geophysical surveys were made at selected locations along the walls of the pilot bore: (1) Seismic-refraction surveys, (2) electrical-resistivity surveys, and (3) wallrock-temperature measurements. The purpose of the underground geophysical studies was to search for relationships between geophysical measurements, geological conditions, and tunnel-construction parameters.

The localities of these measurements (fig. 28) were selected so that the measurements sampled the full range of rock conditions existing in the pilot bore. Poor conditions were characterized by intense fracturing and extensive mineral alteration of the rock, whereas good conditions were characterized by few fractures and little mineral alteration of the rock.

SEISMIC-REFRACTION SURVEYS

Seismic-refraction measurements were made with 10 accelerometers positioned along the tunnel walls in linear

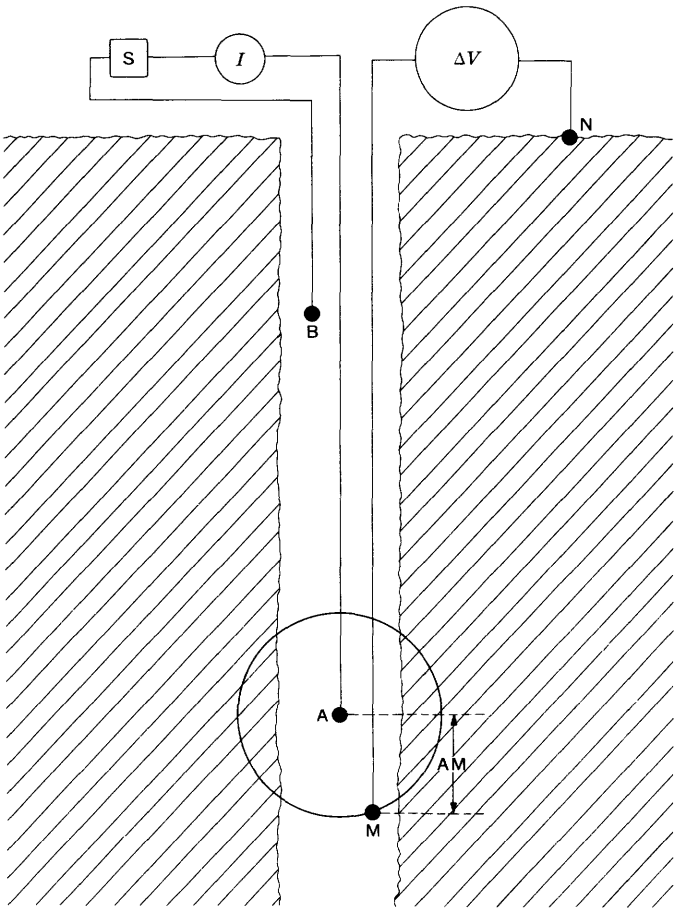

FIGURE 27. — Electrode arrangement for normal-resistivity measurements in drill holes (from Pirson, 1963, fig. 7–1, p. 82). A and B, current electrodes; M and N, potential electrodes; S, power source; I, meter — current to electrodes A and B; ΔV, meter — potential between electrodes M and N.

arrays about 200 feet long. Spacing between adjacent accelerometers ranged from 5 to 25 feet. Small explosive charges were detonated in shallow drill holes in the tunnel walls near the ends and near the midpoint of each accelerometer array. Energy from each of the three successive seismic shots was picked up by the accelerometers and converted to electric-analog signals. These signals were amplified and recorded photographically by a high-resolution 10-channel system especially designed for tunnel seismic studies. The recorded data were analyzed to obtain the velocity and the thickness of the low-velocity layer surrounding the pilot bore, the velocity of rock behind that layer, and the amplitude of energy arriving at the accelerometers.

Instrumentation is shown schematically in figure 29. The accelerometers contained barium-titanate ceramic piezoelectric elements and had a sensitivity of 40 to 50 millivolts per gravitational acceleration unit, with virtually flat response over the frequency range of 10 to 10,000 Hz (hertz). Because of their high electrical impedance, the accelerometers were connected by short cable to transistorized preamplifiers. The preamplifiers, with gains set at 20 decibels; were coupled to 4-kHz (kilohertz) low-pass filters to eliminate high-frequency noise. Outputs of the preamplifier-filter pairs were fed to low-output impedance transistorized line drivers; this permitted the signals to be transmitted through long cables to the recording station located at a safe distance from the seismic shot points. At the recording station, the signals were fed to amplifiers with gains variable from 0 to 1,000 decibels. Amplifier outputs were connected to galvanometers in a high-speed-recording oscillograph. The oscillograph provided a paper speed of about 250 inches per second and timing lines at 1-millisecond intervals; this permitted seismic-arrival times to be picked with a precision of ±0.0001 second. Explosive charges were detonated by a blaster that also switched on the drive motor feeding the paper in the oscillograph approximately 300 milliseconds prior to detonation of the explosive charge, thereby allowing the paper to reach full speed in the oscillograph before seismic energy was recorded.

The accelerometers were emplaced along the tunnel walls about 4 feet above the invert. They were mounted by their base studs being screwed into fiber-epoxy (Micarta) wedges grouted into shallow holes drilled in the walls. Spacing between accelerometers was generally 20–25 feet except near the shotpoints, where the spacing was reduced to 5–10 feet to obtain accurate velocity measurements within the near-surface layer.

Shotpoints were located in line with the accelerometers at both ends and at the middle of the accelerometer spreads. Explosive charges, consisting of about 45 grams (0.1 lb) of dynamite (45-percent gel), were detonated at the bottom of shotholes drilled to a depth of about 1 foot. The charges were stemmed with water or mud.

The seismic-refraction measurements were analyzed to determine (1) the velocity of the rock within the low-velocity layer surrounding the pilot bore, (2) the velocity of rock outside this layer, (3) the thickness of the low-velocity layer, and (4) the relative amplitude of the seismic energy arriving at the detectors. The first three determinations were made from the oscillograph records by using the procedures described by Scott, Lee, Carroll, and Robinson (1968). The relative amplitude of the seismic energy arriving at detectors beyond the critical distance was determined in the following manner: The maximum peak-to-peak deflection of the first three cycles of incoming energy was measured on the seismic records. The acceleration amplitude was computed at each detector by using the following formula:

$$A = \frac{D/2\,(S_g)}{G\,(S_a)},$$

where

A = acceleration, in gravitational acceleration units;
D = maximum peak-to-peak displacement, in inches;

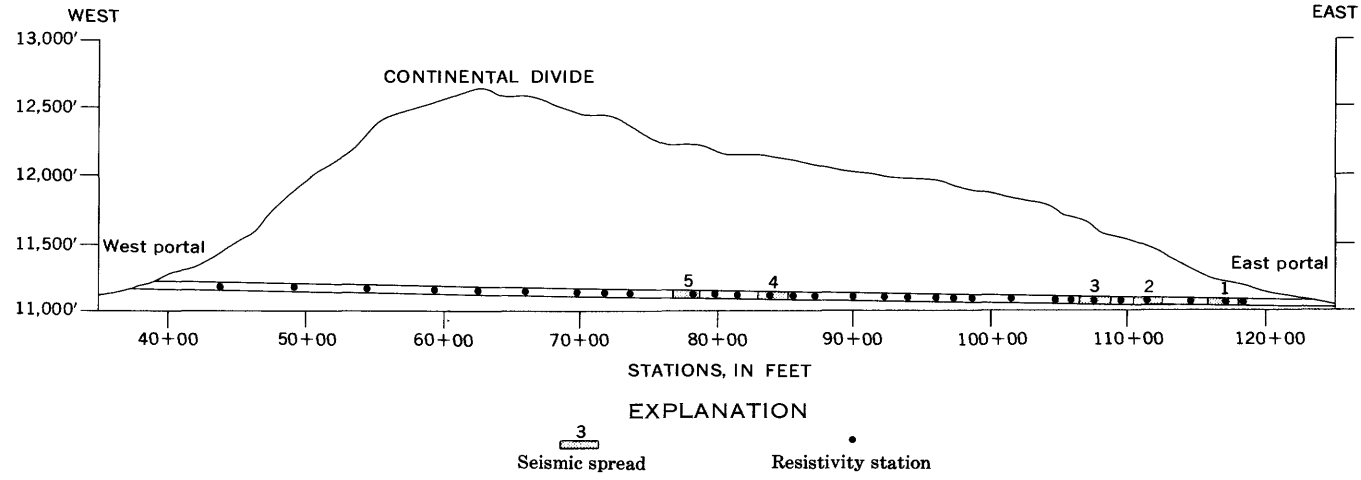

FIGURE 28. — Cross section of Straight Creek Tunnel pilot bore, showing location of geophysical measurement stations.

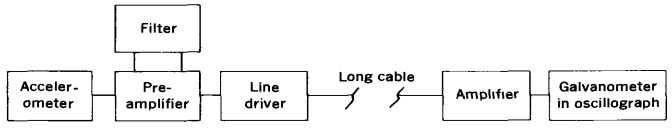

Oscillograph records were obtained with up to 10 channels identical to this one

FIGURE 29. — Schematic diagram of seismic instrumentation.

S_g = sensitivity of the recording galvanometer, in volts per inch;
G = overall gain of the amplifier system; and
S_a = sensitivity of the accelerometer, in volts per gravitational acceleration unit.

The logarithms of computed accelerations were plotted as a function of the logarithms of shotpoint-to-accelerometer distances for all seismic measurements made in the pilot bore, and a straight line was fitted to the data by regression (fig. 30). The residuals between the data points and the fitted line were obtained, and an average residual value for each accelerometer was calculated from the two residuals obtained from shotpoints at opposite ends of the accelerometer spread. At a few of the accelerometer locations, no information was obtained because amplitudes of recorded energy were too large (traces went off the paper or were distorted) or were too small to make reliable measurements.

Analyses of relative amplitude, thickness of the low-velocity layer, and velocity are presented in figures 31–35 for the five selected test sections in the pilot bore, together with the rock type and fracture spacing mapped along the spreads. The figures indicate that correlations exist between increasing fracture spacing and the following parameters: Increasing seismic amplitude, increasing seismic velocity of rock at depth, and decreasing thickness of the shallow low-velocity layer.

The development of the low-velocity layer in the rock around the pilot bore is attributed to two mechanisms — blast damage and the adjustment of rock in response to stress associated with the presence of the opening. The layer

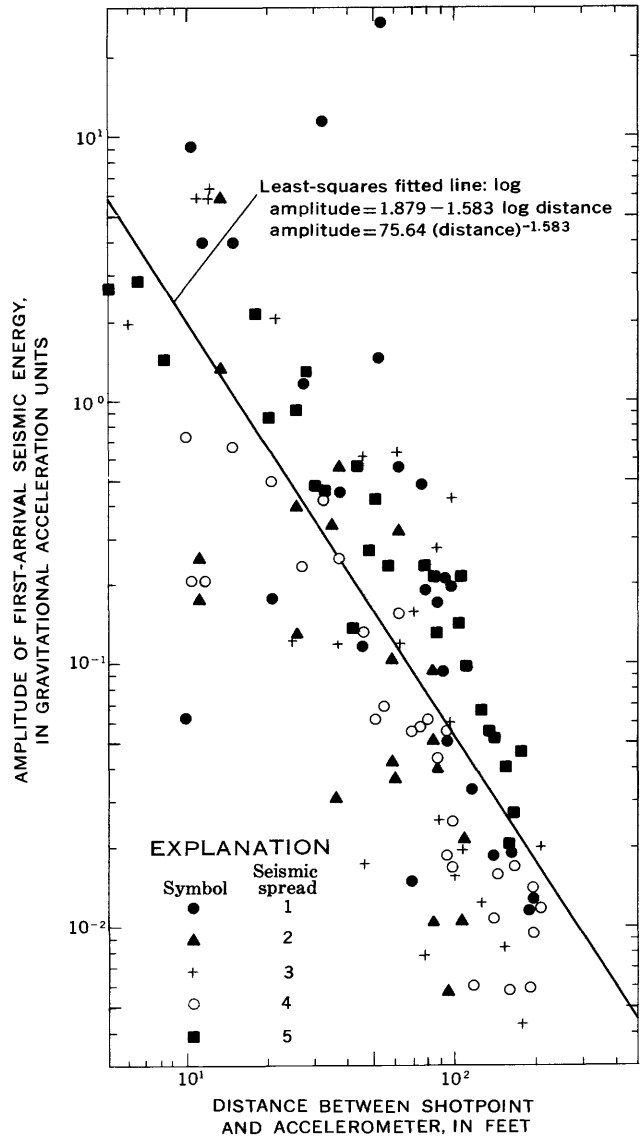

FIGURE 30. — Amplitude of first-arrival seismic energy from 45-gram explosive charges plotted versus distance between shotpoint and accelerometer.

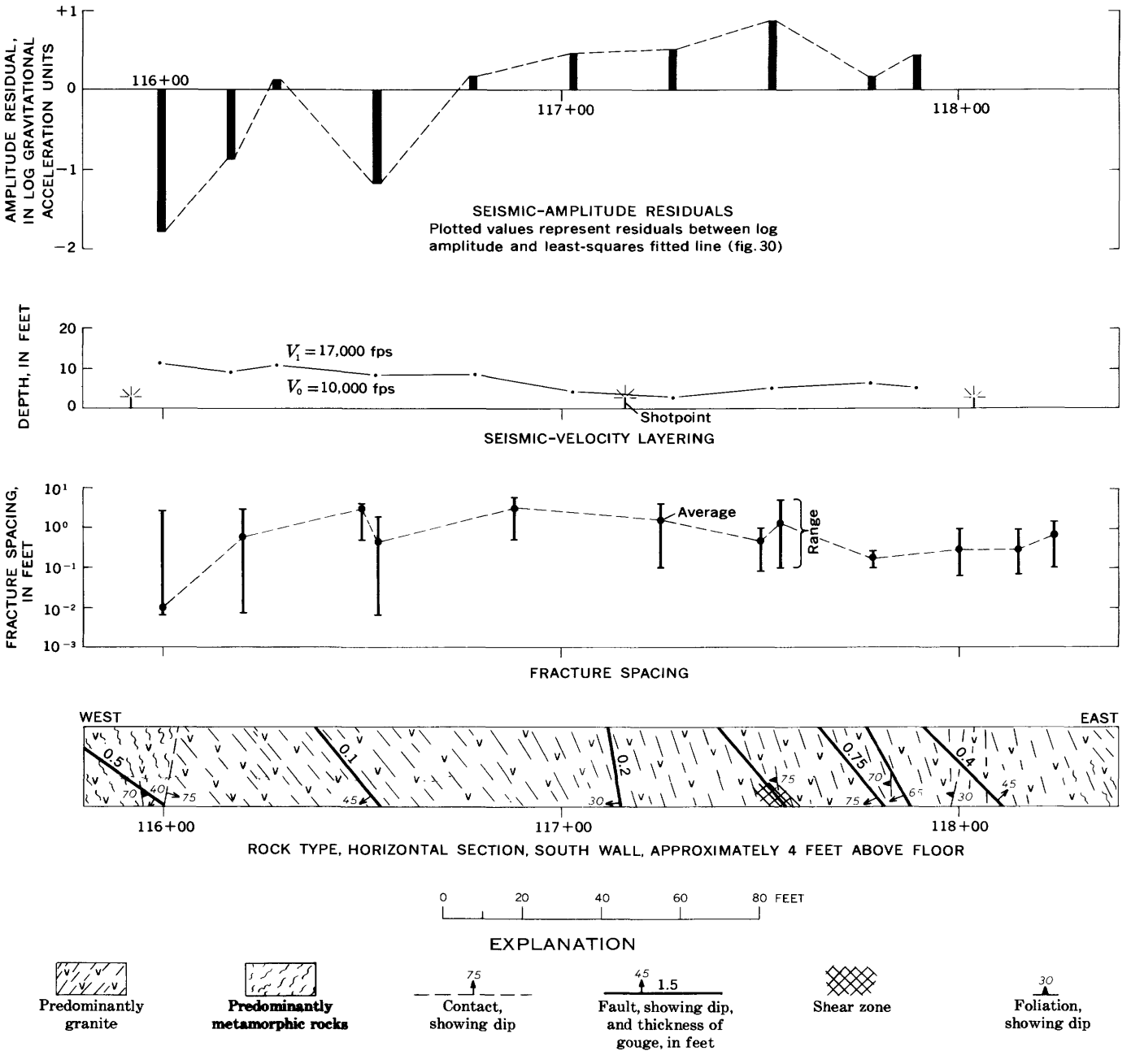

FIGURE 31. — Seismic and rock-type information for seismic-spread 1, Straight Creek Tunnel pilot bore.

of rock affected by blast damage is probably at most only a few feet thick. The thickness of the low-velocity layer, however, commonly exceeds 10 feet and reaches a maximum of nearly 17 feet on seismic-spread 4 (fig. 34). At these locations, where rock is moderately to severely fractured, the stress caused by the presence of the pilot bore probably exceeded the natural strength of the rock mass, resulting in movement of rock toward the center of the opening. Movement probably proceeded along existing fractures and joint planes until equilibrium was reached between stress and rock strength. Extensometer measurements substantiate this explanation of the formation of the low-velocity layer in poor-quality rock. In high-quality rock (fig. 35, seismic-spread 5) the low-velocity layer had an average thickness of only 2.5 feet and a maximum thickness of 5 feet.

ELECTRICAL-RESISTIVITY SURVEYS

Electrical-resistivity measurements were made on one wall, and in a few places on both walls, of the pilot bore at each of the rock-mechanics instrument stations (31 locations, fig. 28). The purpose of these measurements was to determine whether a correlation exists between the detailed geologic mapping at the instrument stations, the results of the instrumentation, and the resistivity of the

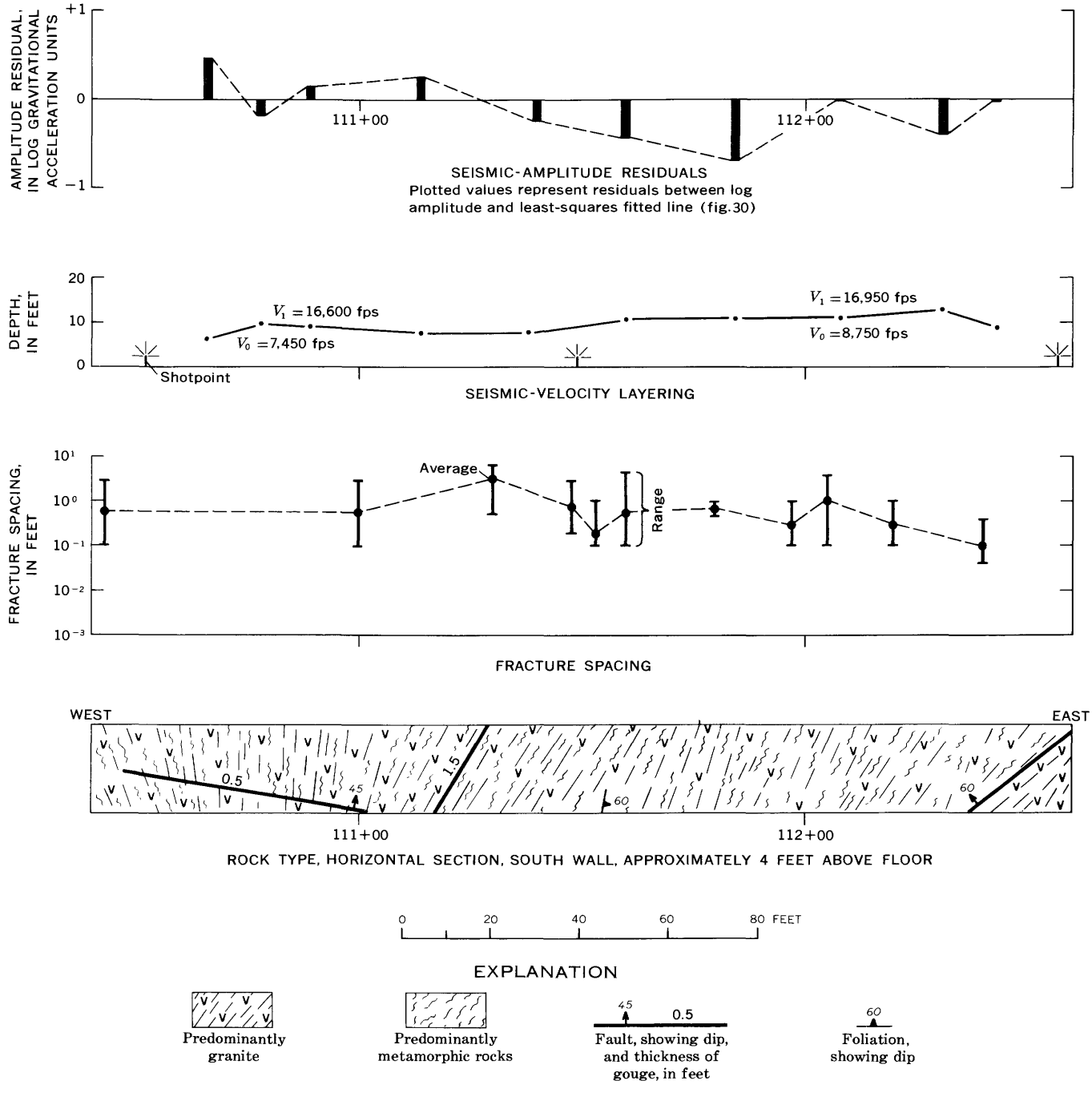

FIGURE 32. — Seismic and rock-type information for seismic-spread 2, Straight Creek Tunnel pilot bore.

wallrock. The authors, assisted by J. E. Sharp and M. J. Cunningham, made most of the resistivity measurements.

The electrical-resistivity measurements were made using Gish-Rooney equipment. Specially designed electrodes with contact pads made from sponge rubber and saturated with a mixture of brine and powdered bentonite were used to make electrical contact with the rock along the walls of the pilot bore. Figure 36 is a schematic illustration of the resistivity equipment and the circuit used.

Electrical-resistivity measurements were made by using the Wenner electrode configuration, with four equidistant electrodes placed in a horizontal line about 4 to 6 feet above the invert (fig. 36*B*). Spring-loaded electrodes were hand held or were placed against lagging or wood planks propped

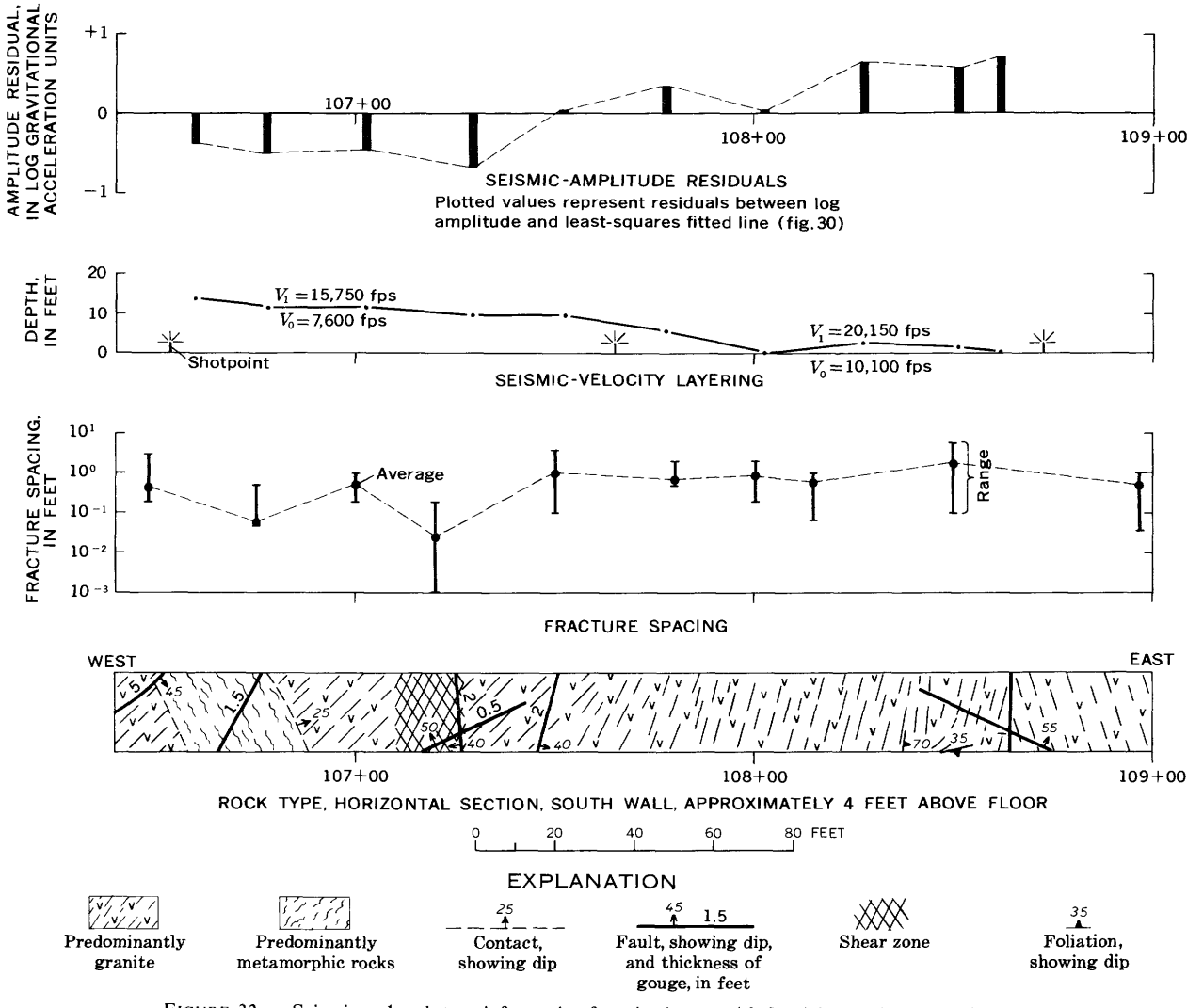

FIGURE 33. — Seismic and rock-type information for seismic-spread 3, Straight Creek Tunnel pilot bore.

against the side of the tunnel. Electrical depth soundings were made at each station by expanding the electrode array from an initial spacing of 0.5 foot to a maximum spacing of 30 feet.

The following formula was used to compute apparent resistivity from measurements made at each electrode spacing:

$$\rho_a = \frac{KaV}{I},$$

where

ρ_a = apparent resistivity,
K = geometric factor ($2\pi < K < 4\pi$),
a = spacing between adjacent electrodes,
V = potential difference measured between electrodes M and N (fig. 36), and
I = current measured between electrodes A and B (fig. 36).

The geometric factor (K) approaches a value of 2π for electrode spacings that are very small compared with the tunnel diameter and approaches a value of 4π for electrode spacings that are very large compared with the tunnel diameter. The value of K for a given ratio between electrode spacing and tunnel diameter (a/D) was evaluated from the graph shown in figure 37, which is based on laboratory model studies (Scott and others, 1968). Apparent-resistivity values were plotted against electrode spacing (a) on log-log paper, as illustrated in figure 38. The sounding curves indicated that at every station a thin high-resistivity layer occurred near the surface of the pilot bore and that the resistivity of rock at depth was significantly lower. The true resistivities of the two layers and the depth of the interface may be determined by the matching of theoretically derived curves to the plotted field data. The derivation of the theoretical curves and the principles of the curve-matching method of resistivity-data analysis have been described by Roman (1960). Horizontally layered earth analyses were made for each sounding curve to obtain (1) the true

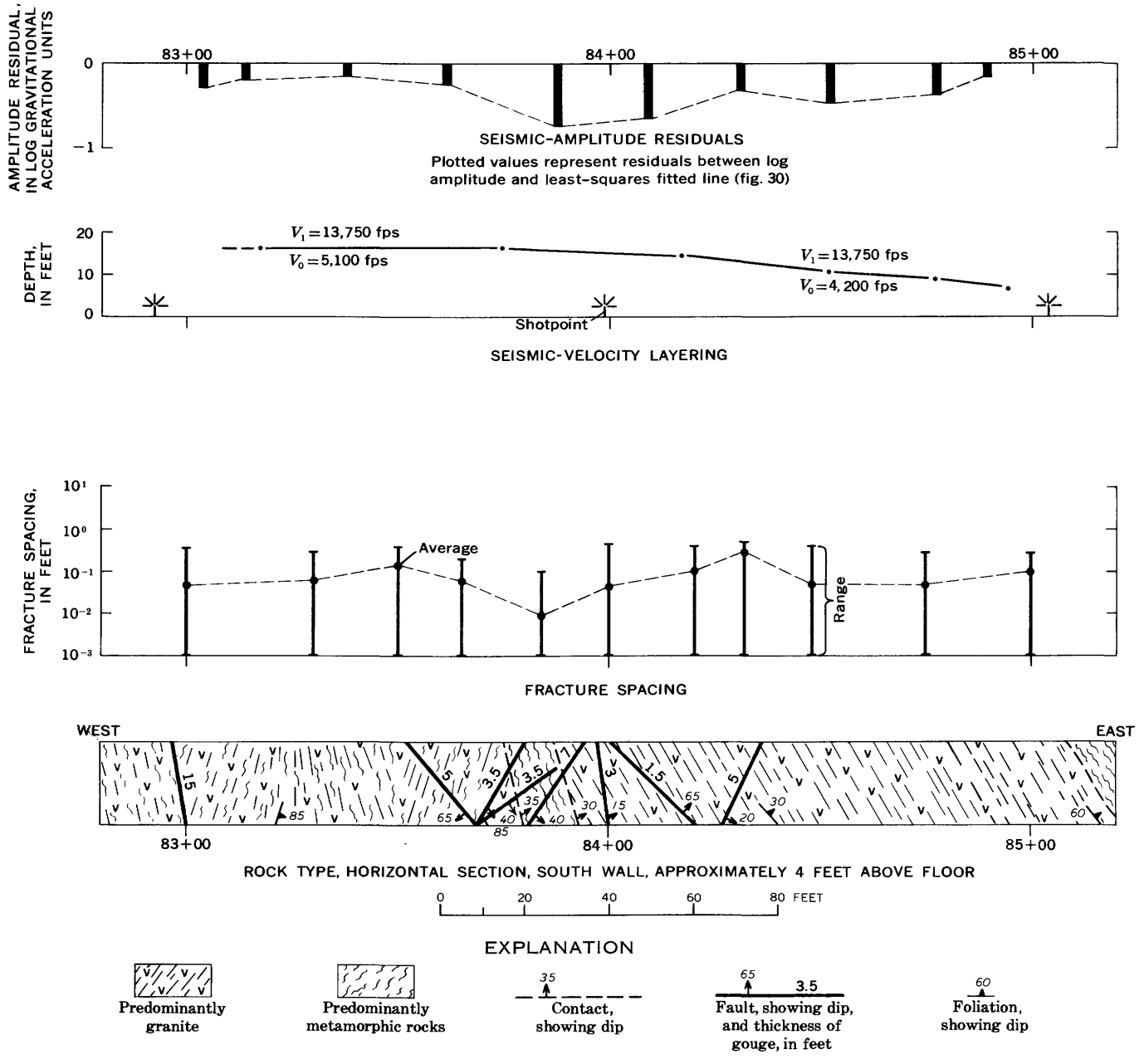

FIGURE 34. — Seismic and rock-type information for seismic-spread 4, Straight Creek Tunnel pilot bore.

resistivity of the shallow high-resistivity layer surrounding the pilot bore, (2) the true resistivity of the rock behind the shallow layer, and (3) the thickness of the shallow layer.

The results of analyses of the resistivity measurements, the rock type, and the average fracture spacing are shown in figure 39. A good correlation exists between increasing fracture spacing and increasing resistivity of rock at depth (solid bars in fig. 39). A similar but less obvious relationship exists between fracture spacing and resistivity of the rock near the surface (designated by open bars, fig. 39). Blast damage probably increases both the thickness of the surface layer and the variability of its resistivity, as the fracturing caused by blasting enhances drainage and evaporation, causing the resistivity to be increased. Thus, the depth to the base of the shallow layer probably represents an upper limit on the depth to which blast damage occurs. The thickness of the shallow layer ranged from 1 to 10 feet, and its resistivity ranged from 60 to 5,300 Ω-m (ohm-meters), whereas the resistivity of rock behind the layer was somewhat lower, ranging from 36 to 2,200 Ω-m.

WALLROCK-TEMPERATURE MEASUREMENTS

The temperature of the wallrock was measured at approximately 500-foot intervals in the holes drilled for rock-mechanics instrumentation. The holes were 2¼-inch air-drilled holes, 15–30 feet deep, located 10–30 feet behind

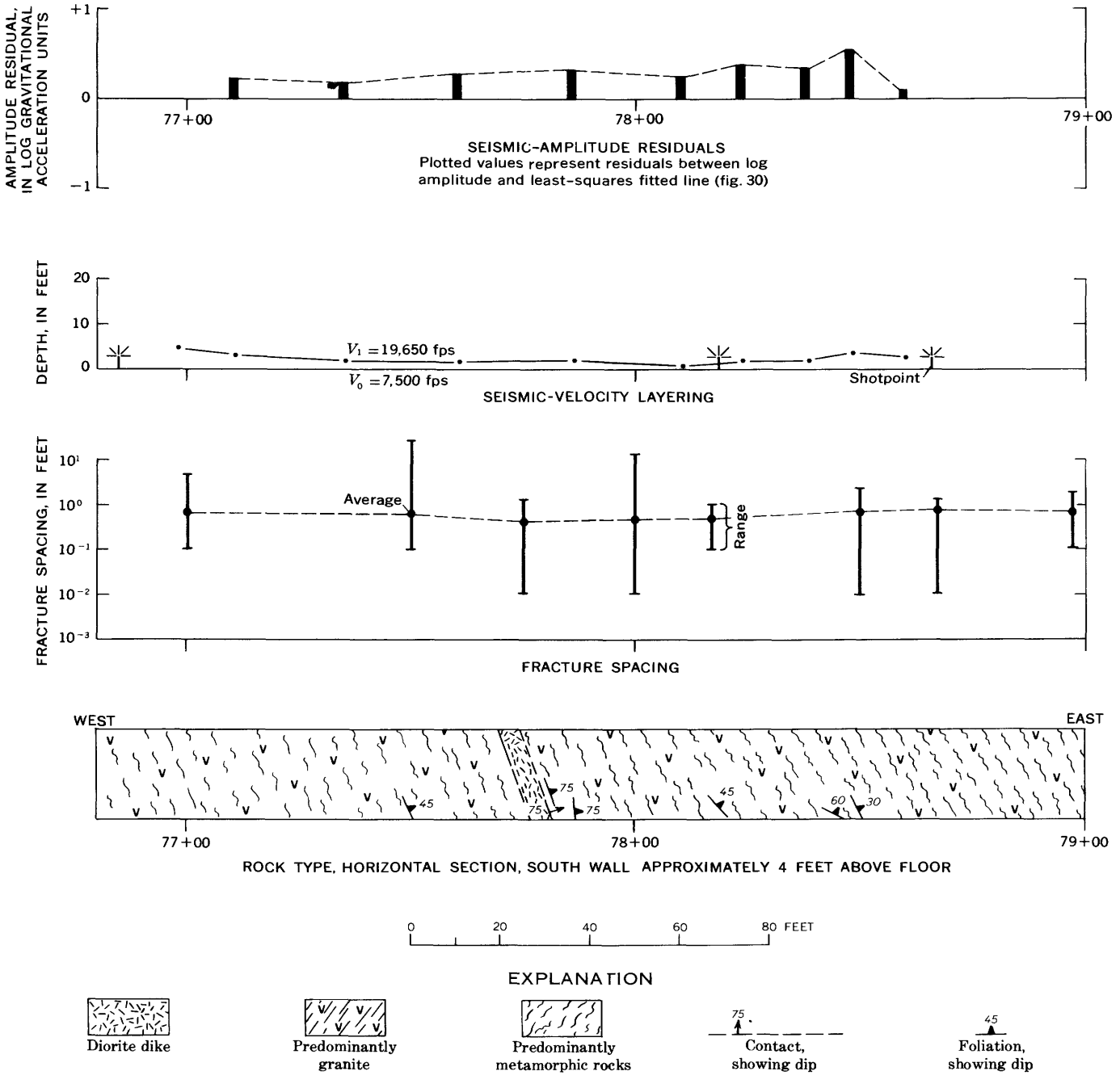

FIGURE 35. — Seismic and rock-type information for seismic-spread 5, Straight Creek Tunnel pilot bore.

the advancing face. Holes were generally drilled in both walls about 6 feet above the invert and were sloped downward at 1°−10°, so they could be filled with water to within a foot of the collar. Temperature was measured 1 to 6 hours after the holes were drilled, and it was assumed that the temperature of the water in the holes had reached equilibrium with the temperature of the wallrock. East of station 66+50 the temperatures were measured by thermistors, which have an available precision of ±0.001°C. West of station 66+50 the temperatures were measured by mercury thermometer, which had an accuracy of 0.01°C.

The thermistor temperature equipment consisted of two thermistors wired to read-out equipment, consisting of a Wheatstone-bridge circuit mounted in a suitcase. To measure the temperature in a hole, the two thermistors were taped about 2 feet apart to jointed wooden dowels. The thermistors were inserted to the bottom of the hole, and, after reaching equilibrium, the resistance was balanced by the Wheatstone bridge. The temperature was determined from a calibration chart for the Wheatstone-bridge circuit. The thermistors were then withdrawn from the hole, and the temperature was determined for about each 2-foot interval.

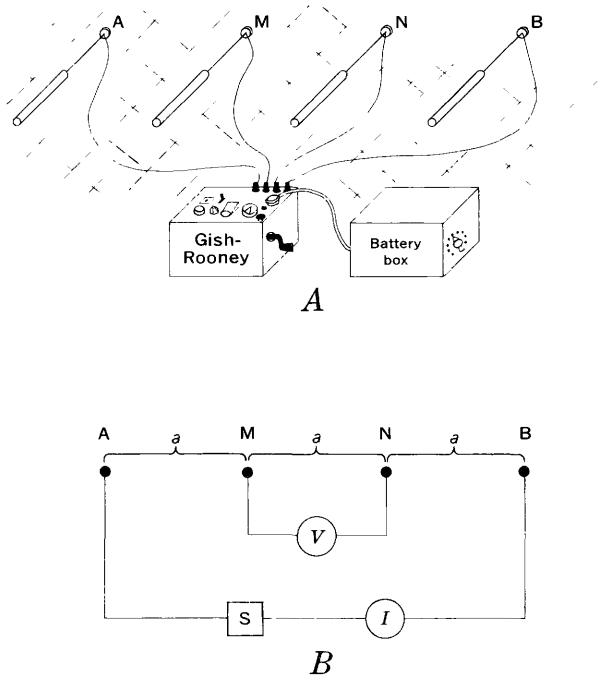

FIGURE 36. — Electrical-resistivity measurements. *A*, Sketch showing Gish-Rooney equipment; *B*, circuit diagram for resistivity measurements made with electrodes positioned in Wenner configuration. A and B, current electrodes; M and N, potential electrodes; V, voltmeter; I, ammeter; S, square-wave power source.

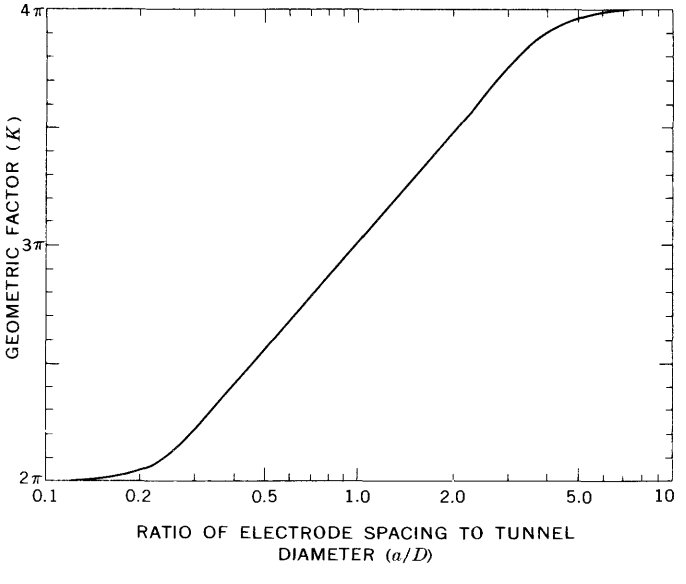

FIGURE 37. — Graph showing the geometric factor (K) as a function of the ratio of electrode spacing to tunnel diameter (a/D) for Wenner-configuration electrical-resistivity measurements (from Scott and others, 1968).

The Wheatstone-bridge circuit first incorporated a light-beam galvanometer, which proved to be very sensitive to being level, to shock, and to the normal moisture in the air in the tunnel. Later, a null detector was substituted for the galvanometer and proved to be less sensitive to external influences. Even with the most careful handling, however, the read-out equipment gave questionable results in some cases because of moisture affecting the circuits, so a mercury thermometer was used for the temperature measurements west of station 66+50.

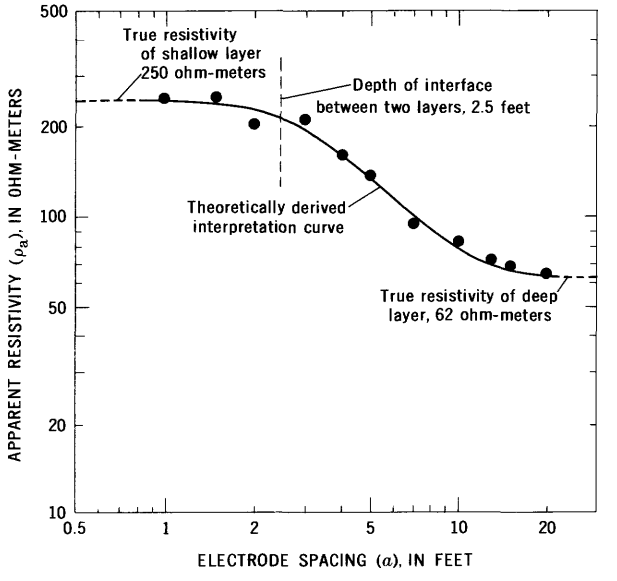

FIGURE 38. — Example of electrical-resistivity field data, showing theoretically derived curve matched to field data for determination of true resistivity (from Scott and others, 1968).

The mercury thermometer measured the temperatures only in the first 1−2 feet of the holes. More measurements could be made at a single station, however, because thermometer equilibrium was reached more rapidly than was thermistor equilibrium, and the temperature of ground water draining from the fractures, as well as that in the drill holes, could be measured. The temperature of the ground water in the drill holes and of that draining from the fractures at a station generally corresponded within a few hundreths of a degree. The average of these measurements was considered to represent the wallrock temperature.

The average wallrock temperatures measured at a station are plotted on plate 2. In general, the wallrock temperature increases with the height of the rock column above the pilot bore.

CORRELATION OF RESULTS OF UNDERGROUND GEOPHYSICAL STUDIES WITH GEOLOGIC, ROCK-MECHANICS, AND CONSTRUCTION DATA

The seismic-refraction and electrical-resistivity measurements show the presence and thickness of both low-velocity and high-resistivity layers adjacent to the pilot bore. The characteristics of these layers can be correlated to rock quality, height of tension arch, stable vertical rock load on supports, and rate and cost of construction.

A numerical scale was devised for quantitatively describing the quality of the rock in the pilot bore. The scale is

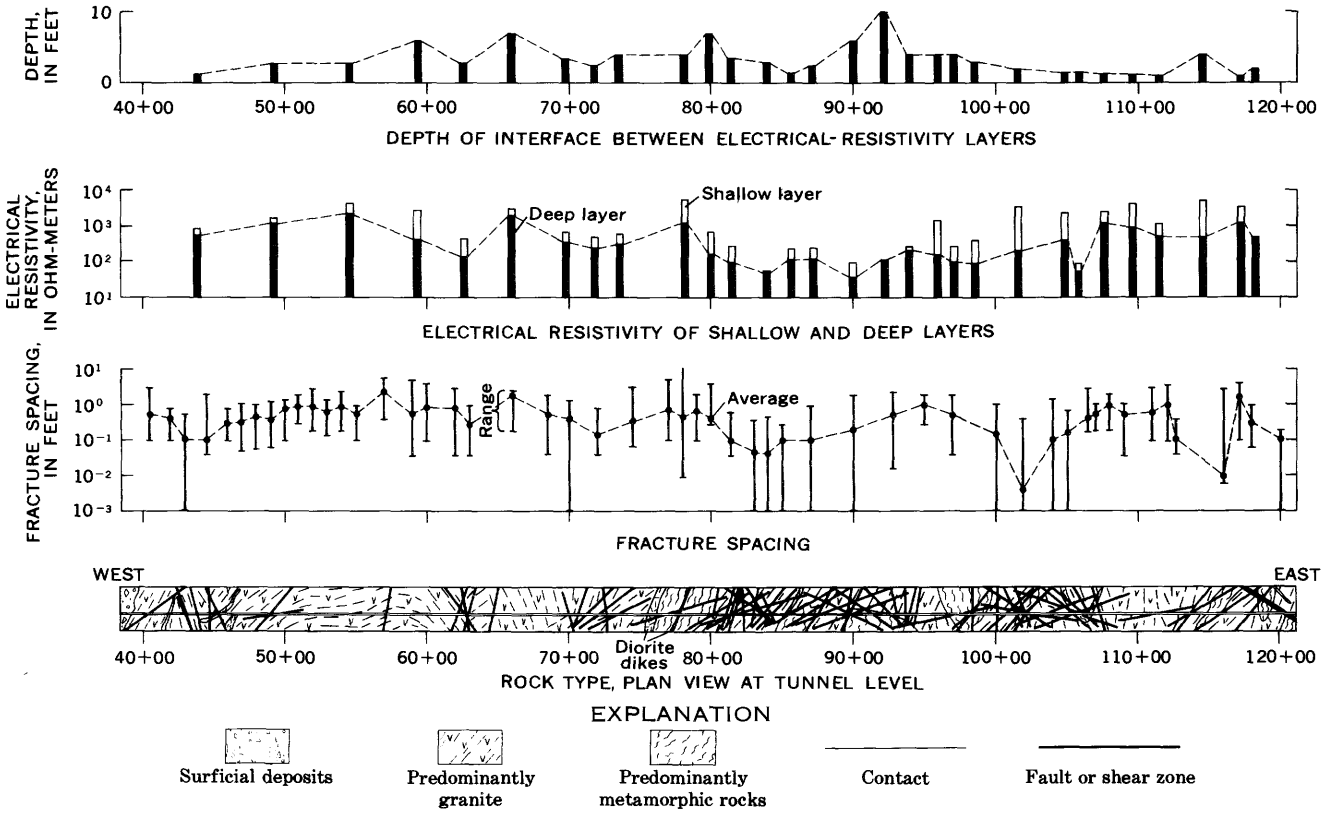

FIGURE 39. — Electrical-resistivity and rock-type information, Straight Creek Tunnel pilot bore.

TABLE 14. — *Rock quality, based on geologic characteristics, observed in the Straight Creek Tunnel pilot bore*

Rock quality (1 = best)	Fracture spacing (ft)	Mineral alteration (percent of rock)	Faulting	Foliation	Rock type
1	>3	<5	None	None; prominent banding in migmatite.	Predominantly granite or diorite dikes; sparse migmatite.
2	1–3	5–10	Minor; a few slicks and minor gouge.	Poorly defined; prominent banding in migmatite.	Commonly granite; sparse gneiss and migmatite.
3	0.3–1	10–15	Moderate; slicks common, minor gouge.	Poorly to well defined; may be absent in granite.	Granite and metasedimentary rocks; occurrence about equal.
4	0.1–0.3	15–20	Moderate to severe; slicks and gouge on most surfaces.	Well defined in metasedimentary rocks; may be absent in granite	Commonly gneiss or migmatite; sparse granite.
5	<0.1	>20	Intense; frequency of gouge seams may be greater than fracture spacing.	Very well defined; may be absent in granite.	Predominantly gneiss; sparse granite.

based on geologic parameters — fracture spacing, degree of mineral alteration, faulting, foliation, and rock type — obtained by direct observation of the rock exposed in the pilot bore. Fracture spacing and mineral alteration were found to be the predominant factors influencing rock quality. On the basis of these parameters and, to a lesser extent, on the extent of faulting and foliation, the rock-quality scale was assigned an arbitrary numerical range of 1 to 5 in which 1 represented the best and 5 the poorest rock exposed in the pilot bore. Rock quality was found to be generally related to rock type in the pilot bore. The rock-quality scale and the geologic parameters to which it is related are shown in table 14.

The height of the tension arch was determined from extensometer measurements made by Terrametrics, Inc. These measurements indicated that rock near the periphery of the pilot bore moved inward, toward the opening, in response to tensional stress and that at greater depths rock

moved outward, away from the opening, because of compressional stress. The height of the tension arch was taken as the point of no movement, which separates the zones of tension and compression. Because extensometer measurements indicated that rock movement was erratic for a few days after mining operations, the height of the tension arch was obtained from measurements made after rock motion had stabilized. At locations where extensometer measurements were not available, load-cell measurements were used to estimate the height of the tension arch. This procedure is justified because the load on tunnel supports is largely determined by the height of the column of rock in the tension arch above the tunnel. Estimates of tension-arch height, made on the basis of load information, were calculated by use of the following formula:

$$H = L/D, \quad (1)$$

where

H = height of tension arch, in feet;
L = stable vertical rock load, in pounds per square foot; and
D = rock density, in pounds per cubic foot.

Stable vertical rock load is defined, for the purposes of this paper, as the vertical load that exists after the period of erratic rock movement and stress adjustment which occurs with the advance of the working face. Load-cell measurements were made at many locations along the pilot bore. The stable vertical rock load was calculated from these measurements by use of the following formula:

$$L = W/A, \quad (2)$$

where

L = stable vertical rock load, in pounds per square foot;
W = weight measured by load cell, in pounds;
A = area of influence in square feet = tunnel width $\times$ set spacing.

At locations where load-cell measurements were not available, loads were estimated from extensometer measurements by use of formula 1 solved for L.

Data on the time-rate of construction and total cost of construction were obtained from G. N. Miles, District Engineer, Colorado Department of Highways (oral commun., March 1965). Construction cost per foot in various sections of the pilot bore was computed by dividing the average cost per day, in dollars, by the rate of construction, in feet per day. This method of obtaining cost per foot is not completely valid because the cost per day fluctuated from day to day during construction. The cost data were included to demonstrate that first-approximation estimated of cost can be obtained from estimates of the rate of construction.

The geologic, rock-mechanics, and construction parameters — rock quality, height of tension arch, load, rate of construction, and cost of construction per foot — were correlated with (1) seismic velocity of undisturbed rock behind the shallow low-velocity layer, (2) thickness of the shallow low-velocity layer, (3) relative amplitude of seismic energy, and (4) electrical resistivity of rock in the deep layer behind the shallow high-resistivity layer. Regression analyses were made of some of the data by use of logarithmic and reciprocal transformations. The following data sets were transformed logarithmically: Electrical resistivity, seismic amplitude, height of tension arch, and stable vertical load. Reciprocal transformations were applied to data on cost of construction and on set spacing. All other data sets were analyzed without transformation.

First, correlations exist between the seismic velocity and the other three geophysical parameters (fig. 40). In figure 40*A* the position of the regression line is strongly influenced by the position of the point in the lower left corner. This point is a significant one because it represents a large volume of rock of extremely low quality.

Second, correlations exist between the four geophysical parameters and the height of the tension arch (fig. 41) and between those same parameters and the stable vertical rock load (fig. 42).

Third, because one would expect the height of the tension arch and the stable vertical rock load to depend on rock quality, the correlation between these parameters was examined (fig. 43). Fourth, correlations between rock quality and the geophysical parameters were examined (fig. 44). Fifth, because one would expect rock quality to influence economic and construction aspects of tunneling, correlations between rock quality and the following parameters were examined: (1) Rate and cost of construction, (2) percentage of lagging and blocking, and (3) set spacing (fig. 45). For figure 45, data from the first 500 feet of construction were omitted from the regression analysis because, in the early stages of pilot-bore excavation, the rate of construction was abnormally low.

Because geophysical parameters, as well as economic and construction parameters, were correlated with rock quality, one would expect correlations to exist between the four geophysical parameters and the economic and construction parameters. These correlations are illustrated in figures 46–48. Figure 46 shows a regression of geophysical parameters against rate of construction and cost of construction per foot. Data for the first 500 feet of construction were omitted from the regression analysis of data in figure 46 because the rate of construction was abnormally low in that interval. Figure 47 shows a regression of geophysical parameters versus the percentage of lagging and blocking, and figure 48 shows geophysical parameters versus the set spacing. The data shown in figures 46–48 indicate that the economic and construction aspects of tunneling can be predicted with reasonable accuracy from the geophysical measurements obtained in feeler holes drilled ahead of the working face, if such relationships as those shown are established beforehand.

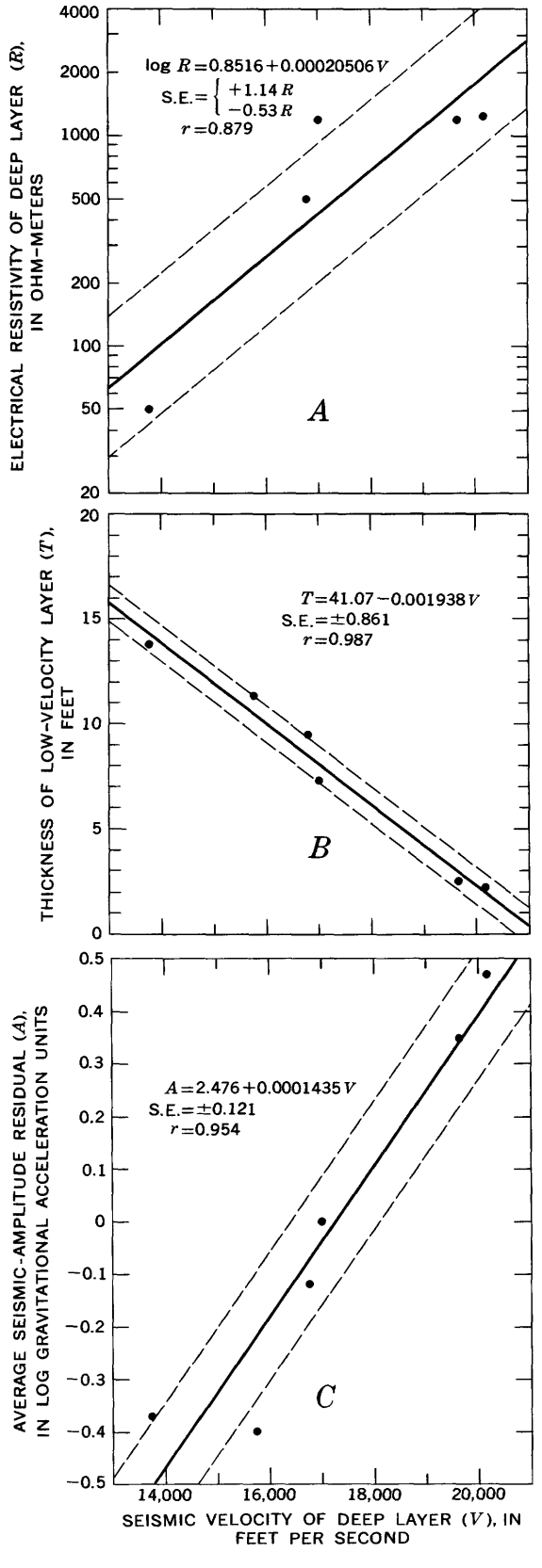

FIGURE 40. — Seismic velocity of deep layer plotted against: *A*, Electrical resistivity of deep layer; *B*, thickness of low-velocity layer; and *C*, average seismic-amplitude residual. Solid line represents regression line, and upper and lower dashed lines represent plus or minus one standard error, respectively. S.E., standard error; *r*, linear correlation coefficient. For those data sets to which logarithmic or reciprocal transformations were applied, *r* represents the correlation coefficient of the transformed values.

Because numerous electrical-resistivity measurements were available, a statistical study was made to determine whether the type and amount of steel support used in construction were related to variations in electrical resistivity of the rock along the walls of the pilot bore. Figure 49 shows that no support was used where the rock had resistivity values greater than about 1,000 Ω-m and that maximum support, consisting of 6-inch steel arches with invert struts, was used where rock resistivity was less than about 60 Ω-m. The type and amount of steel support used were gradational between the two extremes, indicating that support requirements could be predicted from resistivity measurements. Had more seismic measurements been available, a similar relationship probably could have been established between the seismic data and the type and amount of support used.

TESTS OF PREDICTABILITY OF TUNNEL-CONSTRUCTION PARAMETERS FROM SURFACE GEOPHYSICAL MEASUREMENTS

After the correlations were established between tunnel-construction parameters and underground geophysical measurements, the use of the correlations were tested with surface geophysical measurements obtained previously. The purpose of the tests was to determine how accurately the tunneling parameters could be predicted from surface geophysical measurements that could be made prior to tunnel construction. Although this exercise was of no practical benefit to the Straight Creek Tunnel pilot-bore construction, it served to indicate the potential value, in future similar tunnel projects, of making predictions on the basis of surface geophysical measurements.

The results of the predictions of tunneling parameters based on seismic surface and in-hole measurements are shown in table 15.

Resistivity values interpreted from the surface measurements, together with those obtained from an electric log in drill-hole 2, were used to estimate the average resistivity of rock in intervals A, B, and C (fig. 21) in the pilot bore. Results of engineering and economic estimates based on these average values are given in table 16. These estimates are less accurate than those that were based on seismic velocity (table 15). One possible cause for the difference in accuracy is that seismic velocity from surface measurements was determined along straight-line segments near the line of the pilot bore, whereas surface resistivity measurements represented a large volume of rock surrounding the bore. The discrepancies between actual values and estimates based on interpretation of resistivity data indicate

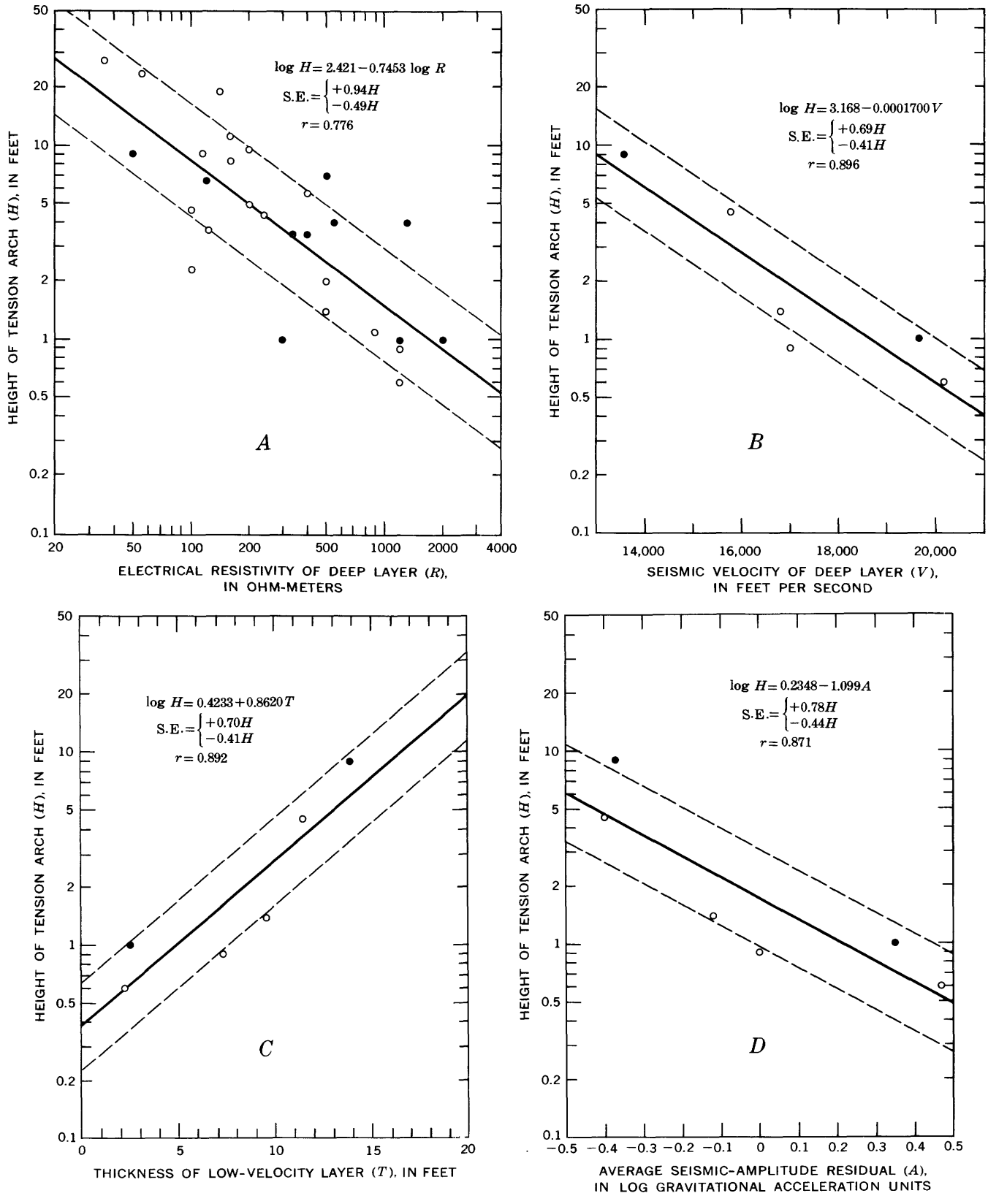

FIGURE 41. — Height of tension arch determined from extensometer measurements (black dots) or estimated from load-cell data (open circles) plotted against: *A*, Electrical resistivity of deep layer; *B*, seismic velocity of deep layer; *C*, thickness of low-velocity of deep layer; and *D*, average seismic-amplitude residual. Solid line represents regression line, and upper and lower dashed lines represent plus or minus one standard error, respectively. S.E., standard error; *r*, linear correlation coefficient. For those data sets to which logarithmic or reciprocal transformations were applied, *r* represents the correlation coefficient of the transformed values.

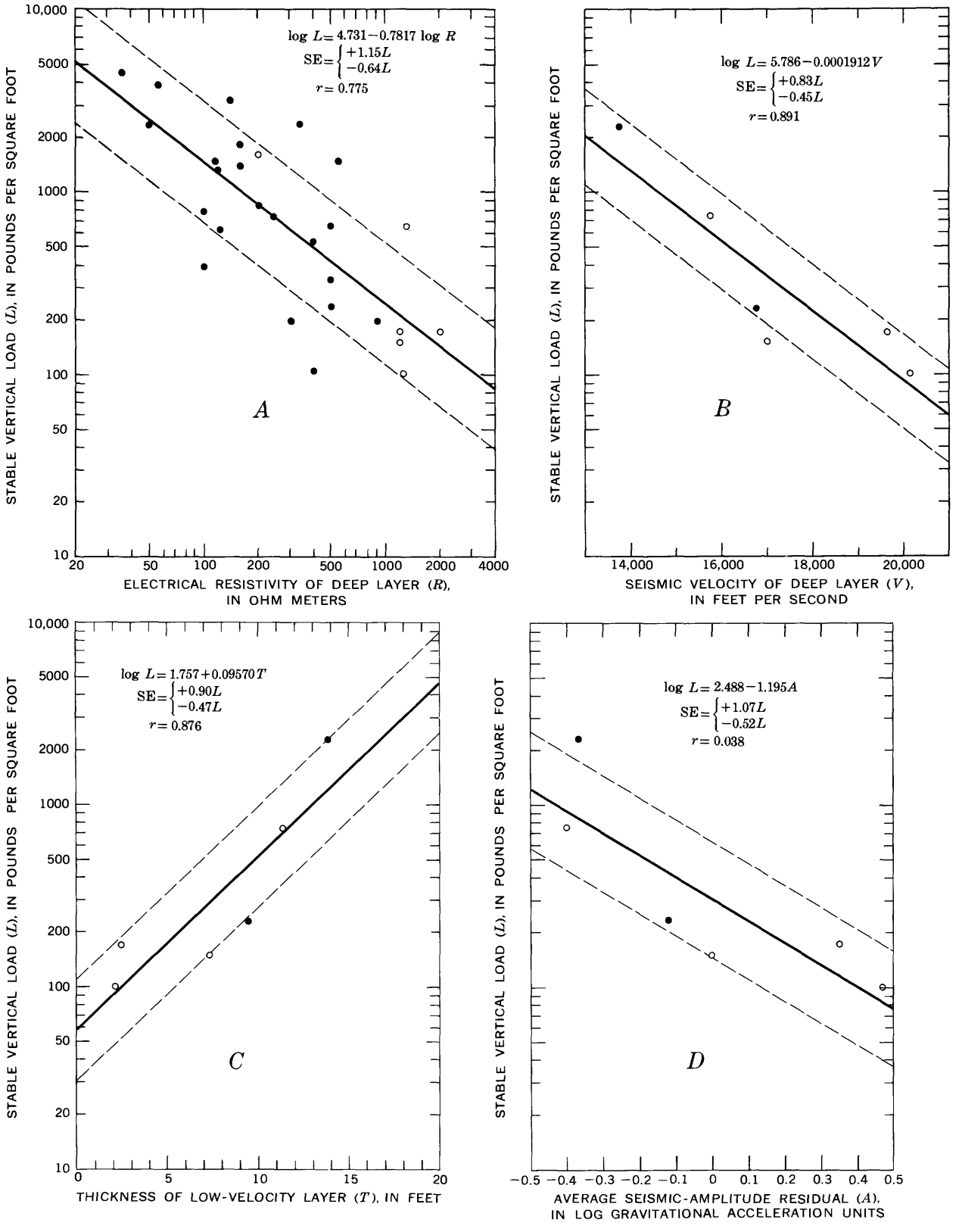

FIGURE 42. — Stable vertical rock load determined from load-cell measurements (black dots) or estimated from extensometer data (open circles) plotted against: *A*, Electrical resistivity of deep layer; *B*, seismic velocity of deep layer; *C*, thickness of low-velocity layer; and *D*, average seismic-amplitude residual. Solid line represents regression line, and upper and lower dashed lines represent plus or minus one standard error, respectively. S.E., standard error; *r*, linear correlation coefficient. For those data sets to which logarithmic or reciprocal transformations were applied, *r* represents the correlation coefficient of the transformed values.

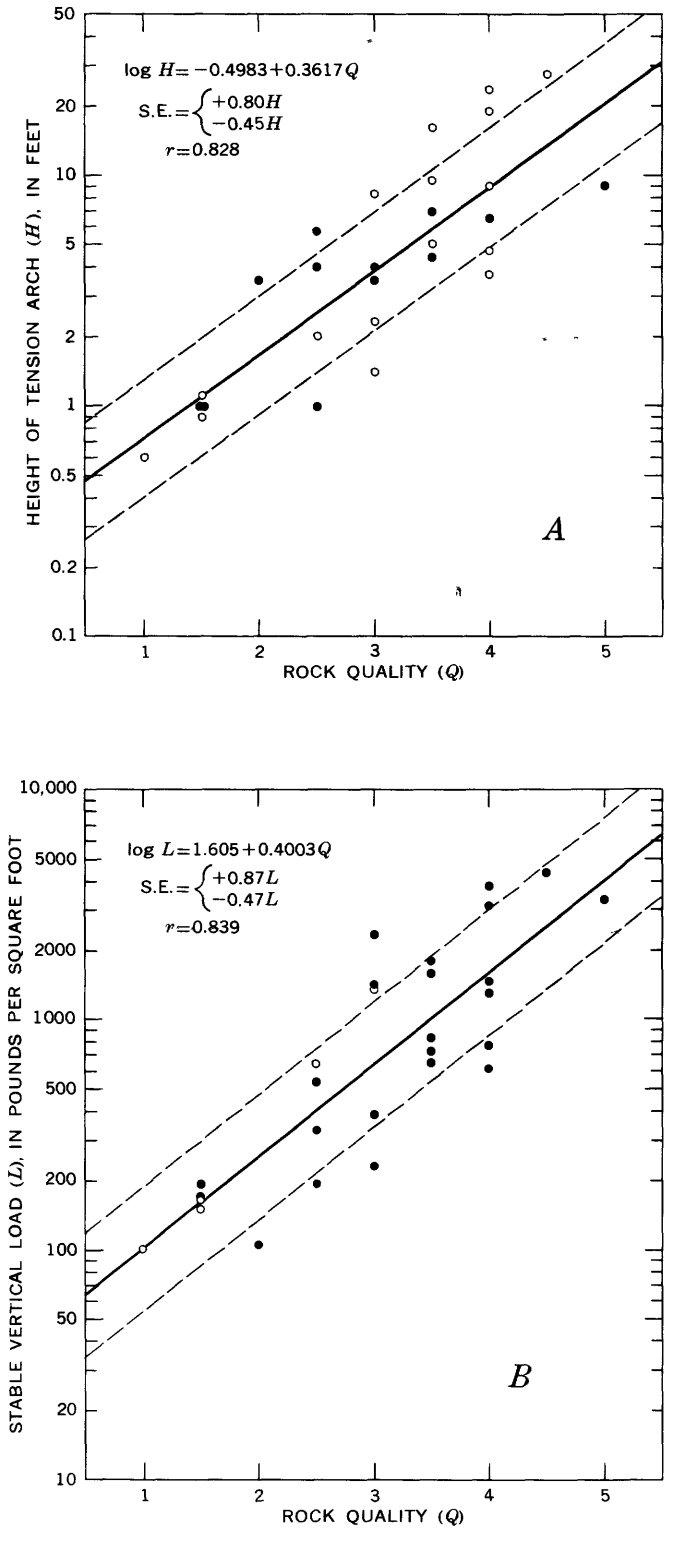

FIGURE 43. — Rock quality plotted versus: *A*, Height of tension arch, determined from extensometer measurements (black dots) or estimated from load-cell measurements (open circles); and *B*, stable vertical rock load, determined from load-cell measurements (black dots) or estimated from extensometer data (open circles). (See table 14 for rock-quality characteristics.) Rock quality: 1 = best. Solid line represents regression line, and upper and lower dashed lines represent plus or minus one standard error, respectively. S.E., standard error; *r*, linear correlation coefficient. For those data sets to which logarithmic or reciprocal transformations were applied, *r* represents the correlation coefficient of the transformed values.

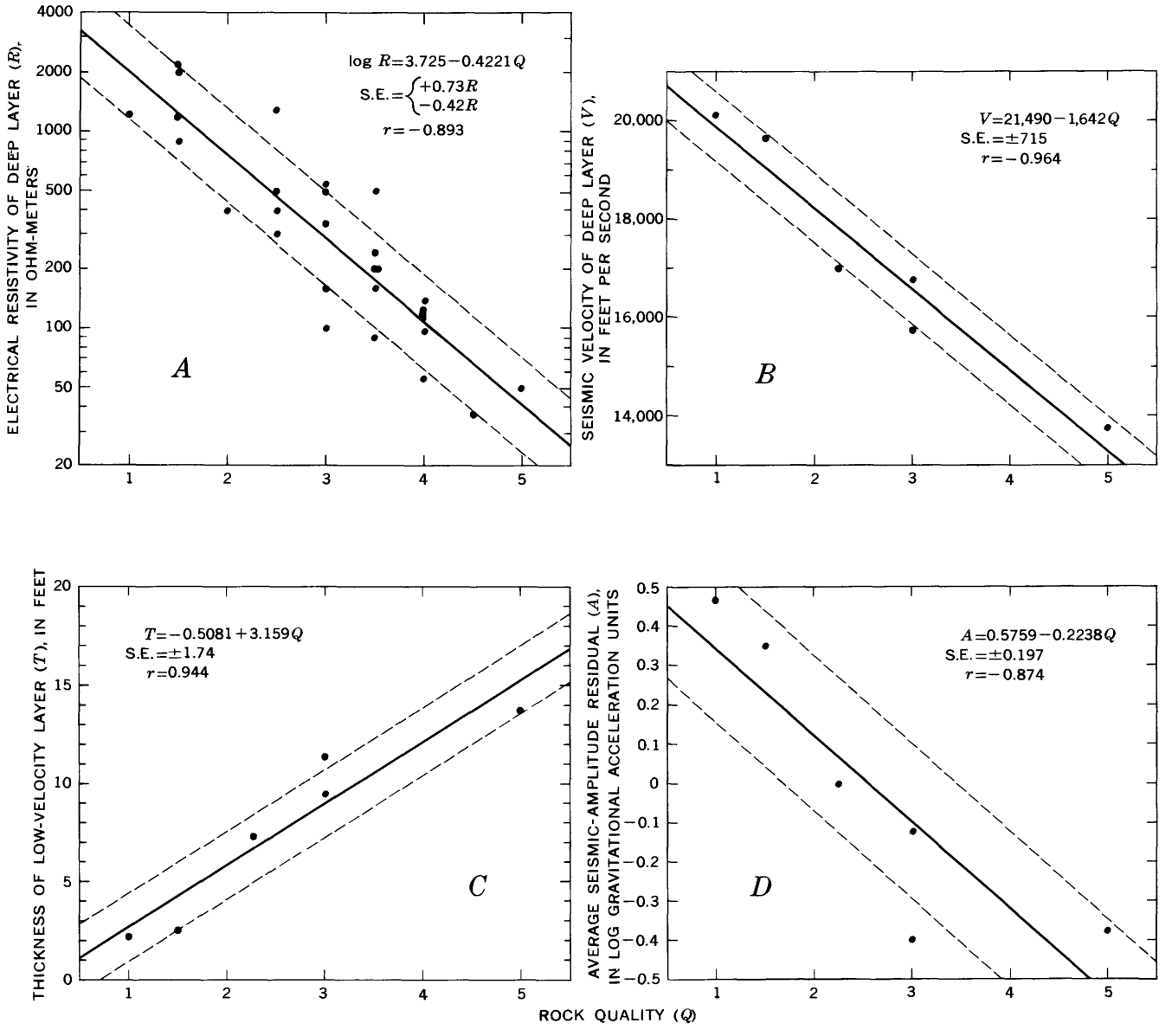

FIGURE 44. — Rock quality plotted versus: *A*, Electrical resistivity of deep layer; *B*, seismic velocity of deep layer; *C*, thickness of low-velocity layer; and *D*, average seismic-amplitude residual. (See table 14 for rock-quality characteristics.) Rock quality: 1= best. Solid line represents regression line, and upper and lower dashed lines represent plus or minus one standard error, respectively. S.E., standard error; *r*, linear correlation coefficient. For those data sets to which logarithmic or reciprocal transformations were applied, *r* represents the correlation coefficient of the transformed values.

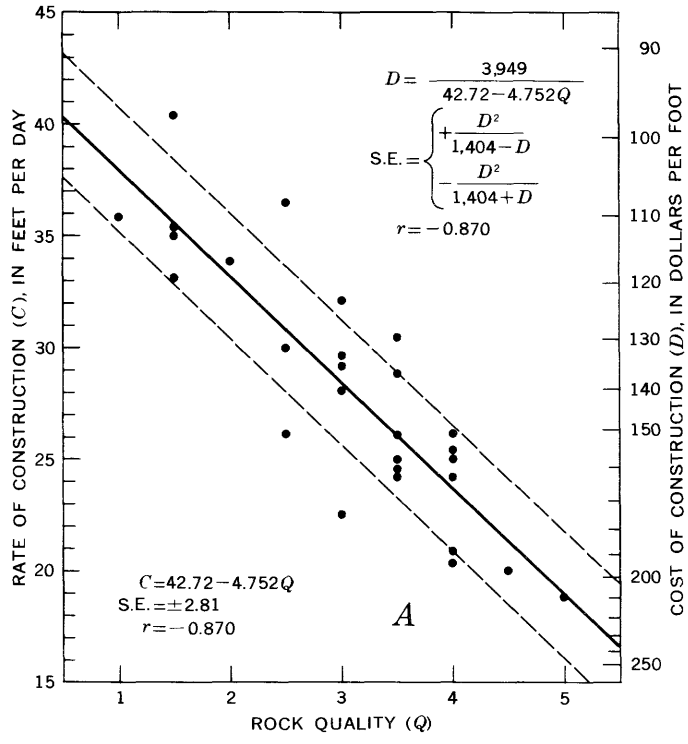

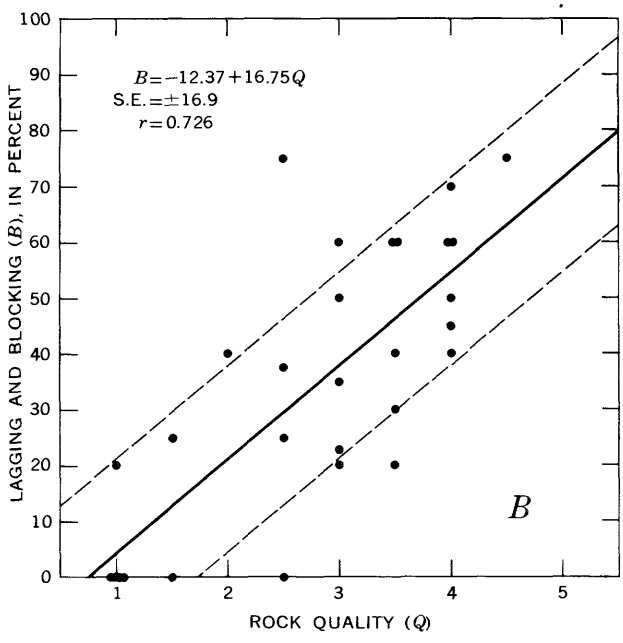

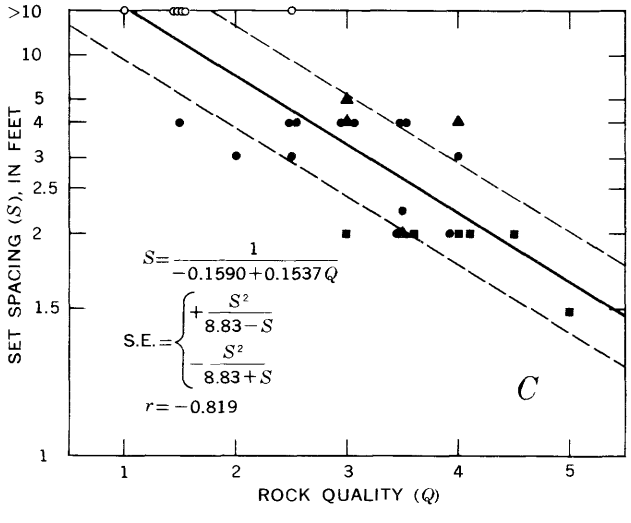

EXPLANATION

6-inch steel with invert struts

6-inch steel without invert struts

4-inch steel without invert struts

No support

FIGURE 45. — Rock quality plotted versus: *A*, Rate of construction and cost of construction; *B*, lagging and blocking; and *C*, set spacing. (See table 14 for rock-quality characteristics.) Rock quality: 1 = best. Cost and rate of construction information from G. N. Miles, District Engineer, Colorado Department of Highways (oral commun., March 1965). Solid line represents regression line, and upper and lower dashed lines represent plus or minus one standard error, respectively. S.E., standard error; *r*, linear correlation coefficient. For those data sets to which logarithmic or reciprocal transformations were applied, *r* represents the correlation coefficient of the transformed values.

FIGURE 46. — Rate of construction and cost of construction plotted versus: *A*, Electrical resistivity of deep layer; *B*, seismic velocity of deep layer; *C*, thickness of low-velocity layer; and *D*, average seismic-amplitude residual. Cost and rate of construction information from G. N. Miles, District Engineer, Colorado Department of Highways (oral commun., March 1965). Solid line represents regression line, and upper and lower dashed lines represent plus or minus one standard error, respectively. S.E., standard error; *r*, linear correlation coefficient. For those data sets to which logarithmic or reciprocal transformations were applied, *r* represents the correlation coefficient of the transformed values.

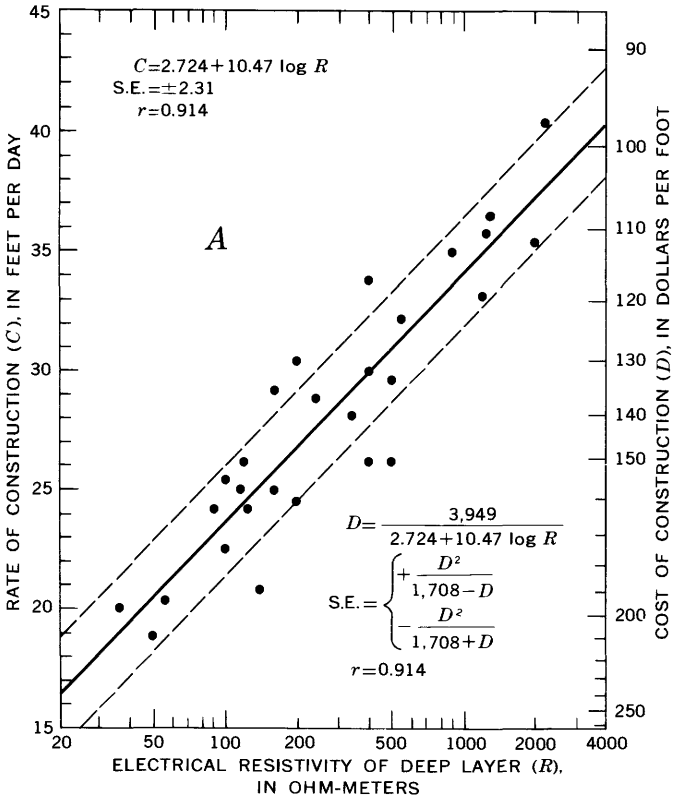
C=2.724+10.47 log R
S.E.=±2.31
r=0.914
A
D=3,949/(2.724+10.47 log R)
S.E.=+D²/(1,708−D), −D²/(1,708+D)
r=0.914
RATE OF CONSTRUCTION (C), IN FEET PER DAY
COST OF CONSTRUCTION (D), IN DOLLARS PER FOOT
ELECTRICAL RESISTIVITY OF DEEP LAYER (R), IN OHM-METERS

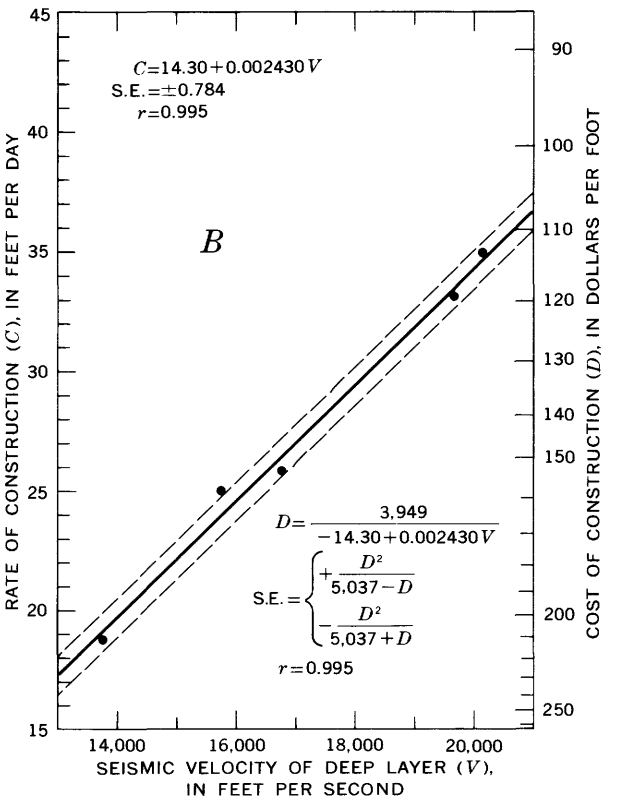
C=14.30+0.002430V
S.E.=±0.784
r=0.995
B
D=3,949/(−14.30+0.002430V)
S.E.=+D²/(5,037−D), −D²/(5,037+D)
r=0.995
RATE OF CONSTRUCTION (C), IN FEET PER DAY
COST OF CONSTRUCTION (D), IN DOLLARS PER FOOT
SEISMIC VELOCITY OF DEEP LAYER (V), IN FEET PER SECOND

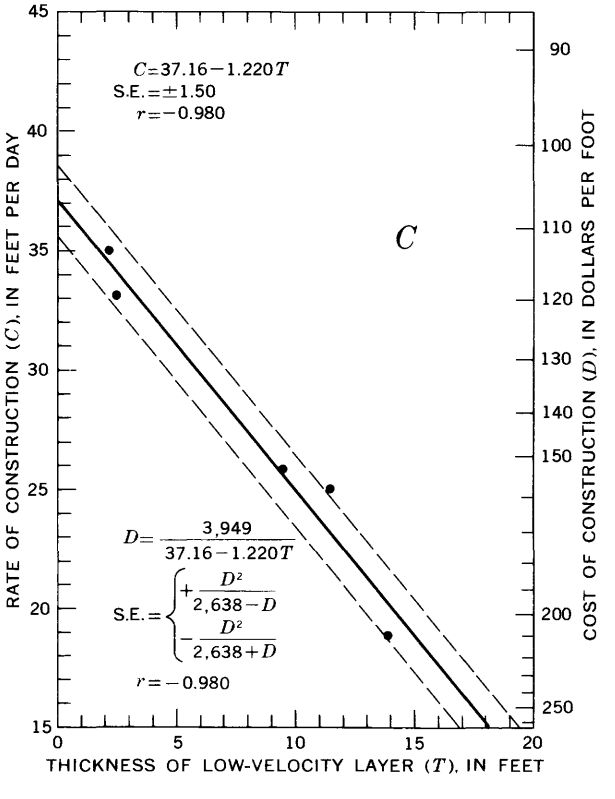
C=37.16−1.220T
S.E.=±1.50
r=−0.980
C
D=3,949/(37.16−1.220T)
S.E.=+D²/(2,638−D), −D²/(2,638+D)
r=−0.980
RATE OF CONSTRUCTION (C), IN FEET PER DAY
COST OF CONSTRUCTION (D), IN DOLLARS PER FOOT
THICKNESS OF LOW-VELOCITY LAYER (T), IN FEET

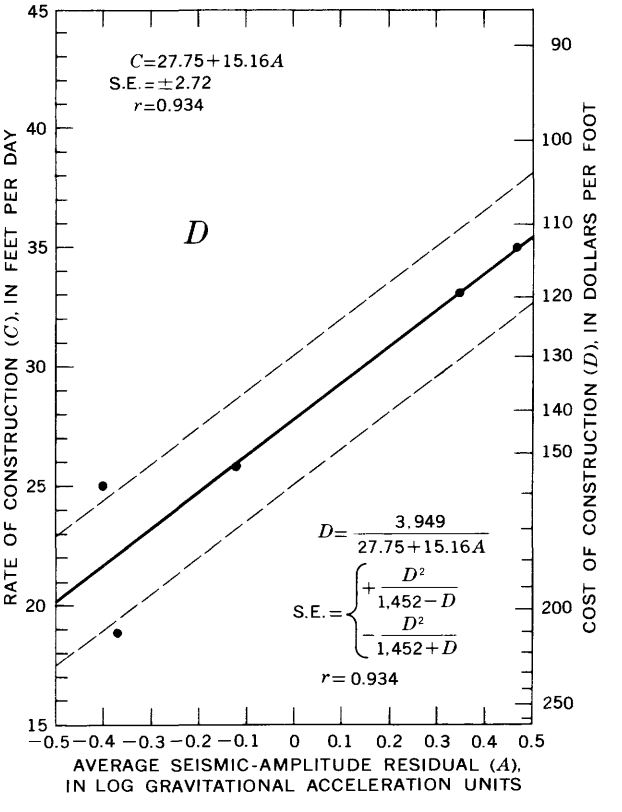
C=27.75+15.16A
S.E.=±2.72
r=0.934
D
D=3,949/(27.75+15.16A)
S.E.=+D²/(1,452−D), −D²/(1,452+D)
r=0.934
RATE OF CONSTRUCTION (C), IN FEET PER DAY
COST OF CONSTRUCTION (D), IN DOLLARS PER FOOT
AVERAGE SEISMIC-AMPLITUDE RESIDUAL (A), IN LOG GRAVITATIONAL ACCELERATION UNITS

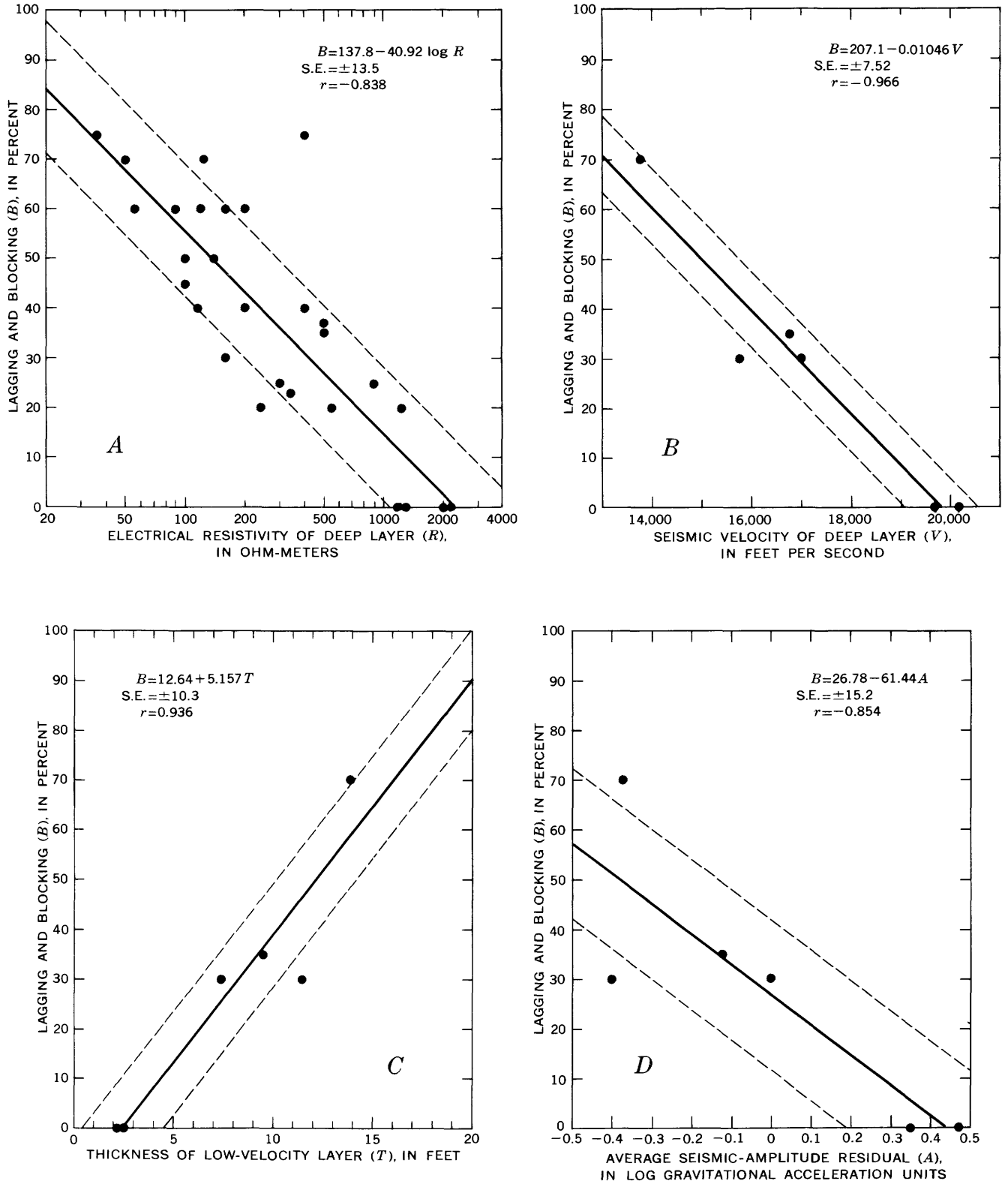

FIGURE 47. — Lagging and blocking plotted versus: *A*, Electrical resistivity of deep layer; *B*, seismic velocity of deep layer; *C*, thickness of low-velocity layer; and *D*, average seismic-amplitude residual. Solid line represents regression line, and upper and lower dashed lines represent plus or minus one standard error, respectively. S.E., standard error; *r*, linear correlation coefficient. For those data sets to which logarithmic or reciprocal transformations were applied, *r* represents the correlation coefficient of the transformed values.

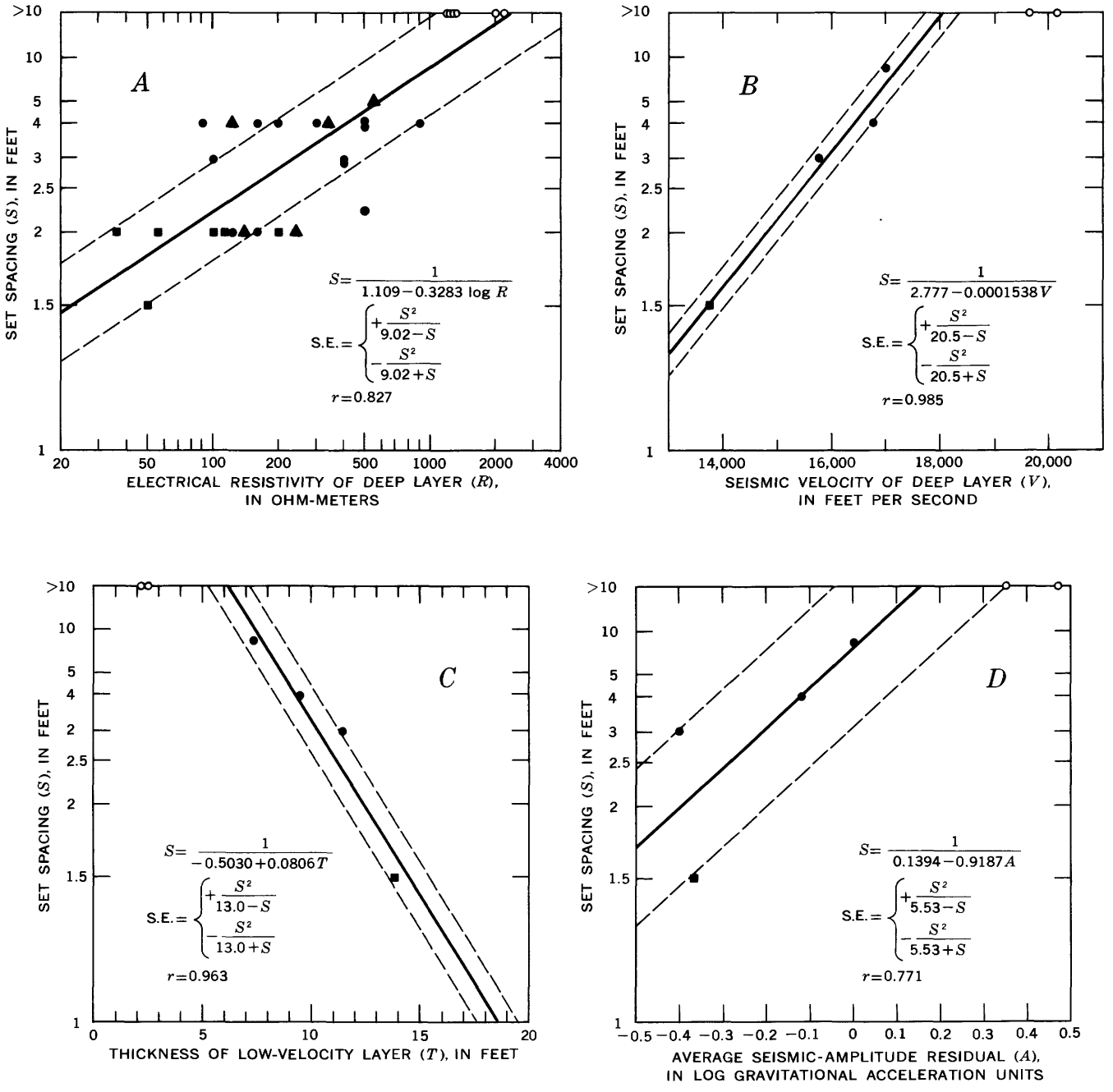

FIGURE 48. — Set spacing plotted versus: *A*, Electrical resistivity of deep layer; *B*, seismic velocity of deep layer; *C*, thickness of low-velocity layer; and *D*, average seismic-amplitude residual. In graphs *B*, *C*, and *D*, data points for no support (open circles) were omitted in calculating the equations of the regression lines because the data suggest an abrupt change of slope. Solid line represents regression line, and upper and lower dashed lines represent plus or minus one standard error, respectively. S.E., standard error; *r*, linear correlation coefficient. For those data sets to which logarithmic or reciprocal transformations were applied, *r* represents the correlation coefficient of the transformed values.

TABLE 15. — *Estimated versus actual values of engineering and economic parameters, with estimates based on direct-travel-path seismic velocities[1] and statistical correlations[2], Straight Creek Tunnel pilot bore*

Section	Seismic velocity (ft per sec.)	Parameter: Average set spacing (ft)		Average lagging and blocking (percent)		Average rate of construction (ft per day)		Cost of construction	
		Estimated	Actual	Estimated	Actual	Estimated	Actual	Estimated	Actual
Interval A	15,400	2.4	3.7	46	51	23	17	$420,000	$420,000
Interval B	15,300	2.3	2.9	48	35	23	26	560,000	540,000
Interval C	17,400	9.4	7.3	26	13	28	29	370,000	440,000
East portal to west portal	15,700	4.5	4.6	40	33	24	23	1,350,000	1,400,000

[1]Velocities measured between in-hole shotpoints and in-hole geophones (intervals A, B, and C, fig. 21).
[2]Established from underground geophysical measurements.

TABLE 16. — *Estimated versus actual values of engineering and economic parameters, with estimates based on surface electrical-resistivity measurements, electric-log measurements[1], and statistical correlations[2], Straight Creek Tunnel pilot bore*

Section	Electrical resistivity (Ω-m)	Parameter: Average set spacing (ft)		Average lagging and blocking (percent)		Average rate of construction (ft per day)		Cost of construction	
		Estimated	Actual	Estimated	Actual	Estimated	Actual	Estimated	Actual
Interval A	180	2.7	3.7	46	51	26	17	$380,000	$420,000
Interval B	230	3.0	2.9	41	35	28	26	460,000	540,000
Interval C	600	5.1	7.3	24	13	32	29	320,000	440,000
East portal to west portal	330	3.6	4.6	37	33	29	33	1,160,000	1,400,000

[1]Drill-hole 2.
[2]Established from underground geophysical measurements.

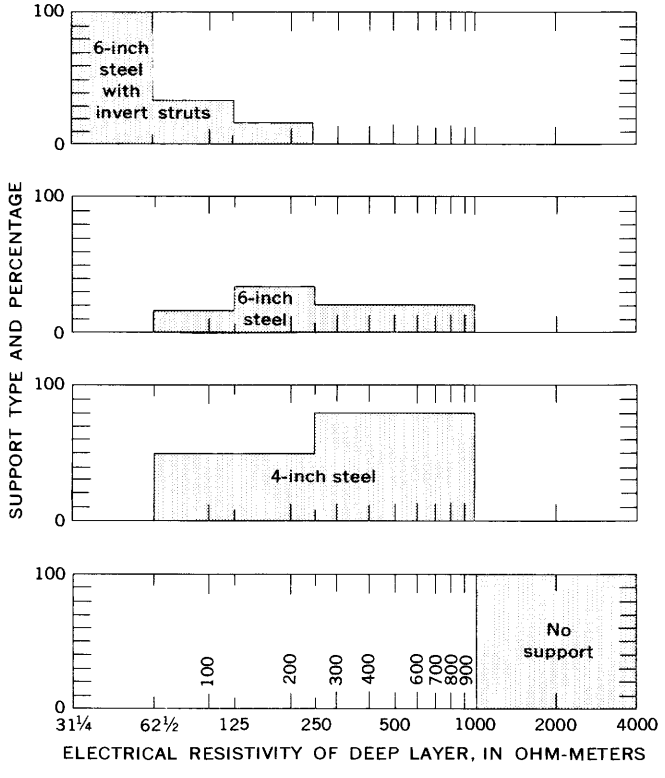

FIGURE 49. — Support type and percentage of support type used in rock classified on the basis of electrical resistivity of deep layer. Resistivity class intervals are logarithmic.

that the resistivity of rock in the immediate vicinity of the pilot bore was generally lower than the average resistivity of the large volumes of rock that influenced the surface resistivity measurements.

SUMMARY AND CONCLUSIONS

Seismic-refraction and electrical-resistivity measurements in the Straight Creek tunnel pilot bore indicated the presence of both low-velocity layers and high-resistivity layers adjacent to the pilot bore. The seismic measurements were used to determine the thickness and velocity of rock in the low-velocity layer, the velocity of rock behind this layer, and the relative amplitude of seismic energy arriving at the detectors. Electrical-resistivity measurements were used to determine the thickness and resistivity of the high-resistivity layer surrounding the pilot bore and the resistivity of the rock behind this layer.

Regression studies were made to test the existence of correlations between the following geophysical parameters:

1. Electrical resistivity of the deep layer
2. Seismic velocity of deep layer
3. Thickness of the low-velocity layer
4. Average relative seismic amplitude

and the following geologic, rock-mechanics, and construction parameters:

1. Rock quality

2. Height of tension arch
3. Stable vertical rock load
4. Rate of construction
5. Cost of construction
6. Lagging and blocking
7. Set spacing
8. Type and amount of support (steel sets and invert struts).

Correlation coefficients ranged in absolute value from about 0.7 to nearly 1.0, indicating that the parameters were correlated.

The importance of the statistical results presented here is that the correlations indicate the possibility of predicting economic and engineering aspects of tunnel construction from geophysical measurements. Preconstruction geophysical measurements on the surface or in holes drilled from the surface would be useful for selecting a site if several alternative tunnel routes were under consideration. Although the correlations described here would not be directly applicable to a tunnel driven in a different geologic environment, or to a tunnel of a different size driven in the same environment, the correlations do indicate that certain basic relationships exist between the measurable properties of rock and the economic and engineering aspects of tunneling. More specifically, in any given geologic environment, rock having high seismic velocity and high electrical resistivity is generally stronger and easier to excavate than rock having a low seismic velocity and low electrical resistivity. Therefore, even if appropriate correlations are not available, geophysical measurements would be useful for estimating the relative cost and the degree of difficulty of construction along each of several possible routes. If correlations are available from measurements made in a similar tunnel in the same environment, then quantitative estimates can also be made.

After a tunnel site is selected, geophysical measurements made during the early stages of construction in long feeler holes drilled ahead of the working face could be used to establish correlations or to improve existing ones. Then, when statistical tests indicate that sufficient data have been obtained to make the correlations valid, the geophysical measurements could be used to predict engineering and economic parameters ahead of construction. New data points could be added to the correlations as construction progressed, so that the percentage of accurate predictions would continue to improve throughout the period of construction. Further development of the surface and underground geophysical predictive capabilities described here would undoubtedly increase the efficiency of tunneling and would probably eliminate the need for costly and time-consuming pilot-bore construction.

Hydrologic Investigations

By R. THEODORE HURR *and* DAVID B. RICHARDS

ENGINEERING GEOLOGIC, GEOPHYSICAL, HYDROLOGIC, AND ROCK-MECHANICS INVESTIGATIONS OF THE STRAIGHT CREEK TUNNEL SITE AND PILOT BORE, COLORADO

GEOLOGICAL SURVEY PROFESSIONAL PAPER 815–E

ENGINEERING GEOLOGIC, GEOPHYSICAL, HYDROLOGIC, AND ROCK-MECHANICS INVESTIGATIONS OF THE STRAIGHT CREEK TUNNEL SITE AND PILOT BORE, COLORADO

HYDROLOGIC INVESTIGATIONS

By R. THEODORE HURR and DAVID B. RICHARDS

A chief purpose for driving the pilot bore was to determine engineering criteria for the design of the twin bores for Interstate Highway 70. These criteria include the definition and functioning of the ground-water system. This chapter presents the basic ground-water data collected during and after construction of the pilot bore. On the basis of interpretation of these data, the relationship between geologic conditions and the flow and occurrence of ground water is described.

The ground-water part of the Straight Creek Tunnel pilot bore investigation was done by the U.S. Geological Survey as part of a statewide program in cooperation with the Colorado Water Conservation Board.

BASIC GROUND-WATER DATA

Ground-water flow rates (tables 17, 18) were measured with flumes installed in the drainage ditch of the pilot bore. The main flow, at station 117+70, was measured with a 6-inch Parshall flume equipped with a recording gage. Flows at other stations were measured with portable 3-inch modified Parshall flumes.

The water pressure (table 19) was measured in a feeler hole in the pilot-bore heading at station 62+91. Temperature and specific conductance of the water in the drainage ditch are given in table 20. The temperature, specific conductance, and pH of the water flowing from rock fractures along the tunnel bore are given in tables 21 and 22. Water flowing from rock fractures was also sampled for chemical analysis (table 26).

GENERAL HYDROLOGY

Structures in crystalline rocks control the occurrence and movement of ground water and are therefore pertinent when evaluating subsurface hydrology in relation to tunnel construction. These geologic structures include joints and faults, which are collectively referred to as fractures. The amount of fracturing is expressed as the fracture spacing, which is one of the criteria used to evaluate the occurrence and movement of ground water.

Open-fracture widths and the interconnection between fractures is variable, and, as a result, there can be a marked difference in the hydraulic conductivity in different directions. Also, hydraulic conductivity generally decreases with depth, as has been well substantiated by Davis and Turk (1963). The variation in hydraulic conductivity with depth can be attributed largely to weathering processes that make the near-surface rock more permeable than the rock at depth. This generalized relationship can be highly variable, depending upon the intensity of fracturing. The Straight Creek Tunnel site is structurally complex, both in plan (pl. 1) and with depth (pl. 2); therefore, some deviation from the relationship between depth and hydraulic conductivity is to be expected.

The study of structural features, weathering or alteration of the rock, variations in chemical quality of ground water, and discharge characteristics of the rock led to the definition of two water-bearing zones penetrated by the pilot bore — an active zone and a passive zone. The active zone is defined as that permeable rock underlying the topographic surface which is subject to seasonal fluctuations in recharge, discharge, and ground-water level. The passive zone is defined as that rock underlying the active zone in which water is stored for long periods of time (from tens of years to thousands of years). The passive zone is generally less permeable than the active zone, although in some places it contains pockets or zones of highly permeable rock. These highly permeable pockets or zones are surrounded by less permeable rock which isolates them from each other and from the active zone. These pockets are 10^x (where $x = <10$, probably about 5 or 6) cubic feet in size and may yield water at a rate of several hundred gallons per minute when penetrated by a tunnel. The contact between the active and passive zones is gradational and can have a considerable range in depth below the land surface, depending on local geology. The transition from one zone to the other depends chiefly upon the structure of the rock and the associated alteration or weathering.

The active zone is mainly recharged each spring by snowmelt, generally between the middle of May and the first part of July. The amount of recharge to the active zone depends on the amount of snow accumulated during the preceding winter, on the moisture content and melt rate of

TABLE 17. — *Average weekly rate of ground-water flow at station 117+70*
[Dates shown are midweek; rates are in gallons per minute]

Date	Rate	Date	Rate	Date	Rate	Date	Rate	Date	Rate
1964		*1964—Con.*		*1965*		*1965—Con.*		*1966*	
Jan. 15	245	July 1	350	Jan. 6	103	July 7	552	Jan. 5	64
22	175	8	360	13	99	14	494	12	63
29	112	15	319	20	95	21	413	19	59
		22	267	27	90	28	346	26	59
Feb. 5	59	29	184						
12	59			Feb. 3	85	Aug. 4	301	Feb. 2	59
19	59	Aug. 5	180	10	83	11	251	9	54
26	47	12	457	17	81	18	213	16	51
		19	413	24	77	25	188	23	51
Mar. 4	45	26	467						
11	49			Mar. 3	72	Sept. 1	171	Mar. 2	49
18	45	Sept. 2	588	10	72	8	153	9	49
25	49	9	516	17	72	15	135	16	49
		16	413	24	72	22	122	23	48
Apr. 1	45	23	324	31	67	28	112	30	47
8	45	30	279						
15	48			Apr. 7	66	Oct. 6	102	Apr. 6	45
22	49	Oct. 7	251	14	65	13	99	13	45
29	47	14	242	21	65	20	90	20	46
		21	215	28	65	27	85	27	47
May 6	47	28	310						
13	45			May 5	66	Nov. 3	83	May 4	49
20	54	Nov. 4	215	12	67	10	81		
27	128	11	188	19	67	17	72		
		18	175	26	85	24	69		
June 3	174	25	153						
10	211			June 2	117	Dec. 1	67		
17	296	Dec. 2	149	9	130	8	67		
24	350	9	131	16	233	15	67		
		16	128	23	440	22	65		
		23	116	30	552	29	64		
		30	112						

the snow, and on the infiltration potential of the surface material. As the downward-percolating melt water reaches the water table, the water table rises. Because the rate of discharge from the active zone is proportional to the height of the water table, the rise in water table increases the rate of discharge from the active zone to surface drainage. When recharge stops, the water table declines, and discharge from the active zone diminishes at a decreasing rate. The active zone can also be recharged by summer rain or by fall snowstorms that are followed by warm weather if (1) the storms produce more water than is needed to replenish soil moisture and if (2) the excess moisture is not evaporated or transpired before it can percolate down to the water table. Data indicate, however, that recharge from summer and fall precipitation accounts for less than 10 percent of the total annual ground-water recharge.

Some water obviously must also recharge the passive zone. However, because of the low permeability and the small area of discharge, water movement through the passive zone is slower than that through the active zone, and rises in the water table are reflected only slightly by increased rates of discharge from the passive zone.

The concept of an active zone overlying a passive zone is in agreement with the geomorphologic principles which influence the occurrence of ground water in fractured crystalline rocks. Weathering forms a zone of relatively high permeability in the rock near the surface that grades downward into an unweathered zone of lower permeability. The active and passive zones can be defined by seismic surveys; a low seismic velocity is indicative of porous low-density material, and a high seismic velocity is indicative of a dense material. Such seismic data were obtained by J. D. Scott and R. D. Carroll (chap. D) for the rock overlying the Straight Creek Tunnel site. Their data delimit three major seismic-velocity layers: 5,070 fps (feet per second), 12,400 fps, and 16,400 fps (pl. 4). The seismic velocity of unfractured granite is approximately 20,000 fps, and the velocities of 5,070 and 12,400 fps indicate substantial increases in pore space and (or) alteration. The rock overlying the 16,400-fps seismic-velocity layer was interpreted to constitute the active zone. The position, or depth, of the velocity change from 12,400 fps to 16,400 fps approximately delineates the contact between the active and passive zones.

FACTORS AFFECTING GROUND-WATER YIELD

The flow of ground water to a tunnel is affected by both geologic and construction factors. The geologic factors, such as rock type, amount of fracturing, and effect of alteration and (or) weathering, are more significant than the construction factors, such as tunnel cross section and rate of advance. When the geologic factors were evaluated, the construction factors were assumed to be relatively constant.

A statistical analysis of the frequency of various rates of ground-water discharge and of the occurrence of various rock types indicated a small but definite tendency for the granite to yield more water (fig. 50) than the metasedimentary rock, probably because the granite is more competent under tectonic stress. At moderate pressures the granite is more brittle, and its fractures have a greater tendency to remain open, whereas metasedimentary rocks tend to deform plastically. A sample of granite gouge also showed a much higher hydraulic conductivity than a sample of metasedimentary gouge (table 23), owing mainly to a larger percentage of clay-size material in the metasedimentary gouge.

The most significant factors affecting ground-water yield are the fracture spacing (table 24) and the degree of rock alteration. On the basis of the fracture-spacing classification discussed previously (chap. C, p. 27), the occurrence of ground water in the pilot bore has the following relation to fractures:

1. Rock in shear zones, where fractures are less than 0.1 foot apart, is relatively impermeable, owing to extensive chemical and mechanical alteration.
2. Rock whose fractures are 0.1—0.5 foot apart is the most porous and has the greatest hydraulic continuity.
3. Rock whose fractures are 0.5—1 foot apart is less porous and has less hydraulic continuity.
4. Rock whose fractures are more than 1 foot apart is relatively impermeable and generally yields little water.

The attitudes of fractures do not seem to affect water yield. A plot of fracture attitudes on a Schmidt equal-area net showed that the attitudes of wet and dry fractures are about the same.

Chemical and mechanical alteration affect both the hydraulic conductivity and the hydraulic continuity of rock

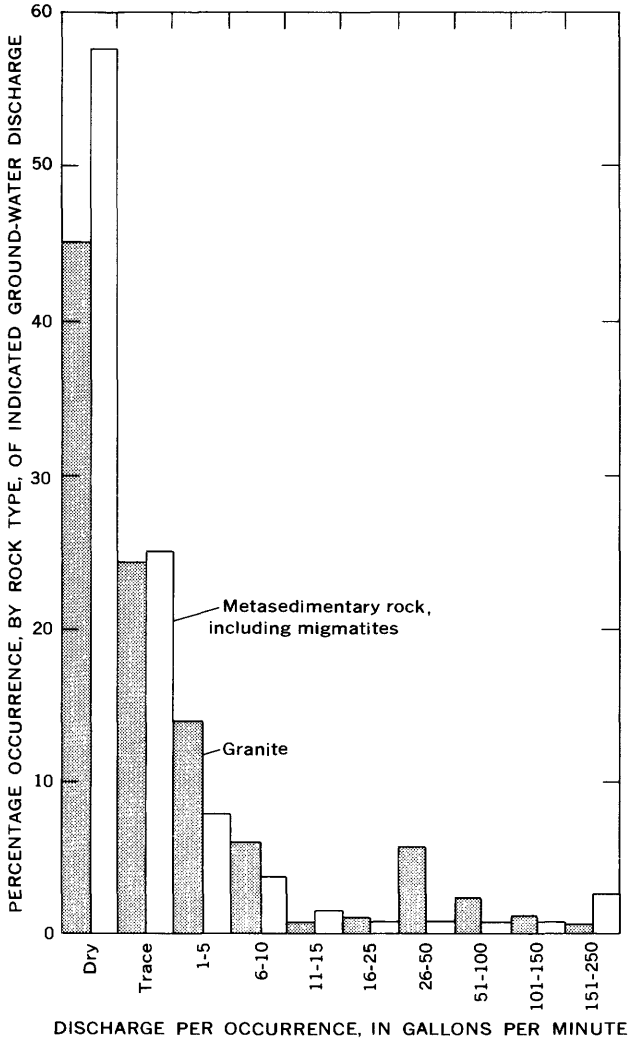

FIGURE 50. — Percentage occurrence, by rock type, of indicated ground-water discharge at the pilot-bore face. Based on 261 granite and 133 metasedimentary-rock faces.

by forming alteration products that seal fractures and retard water movement. Chemical alteration includes the retrograde metamorphism of biotite and hornblende to chlorite and the action of ground water on minerals to form clay — principally kaolinite and montmorillonite. Mechanical alteration results in the formation of gouge and clastic fragments in and along faults and shears, due to grinding action. The degree of alteration is a function of fracture spacing and of ground-water action. The rock adjacent to fractures is altered, the intensity of alteration decreasing with distance from the fracture surface. The more fractures, therefore, the more alteration. Ground water contributes to retrograde metamorphism by supplying the water necessary for the conversion of anhydrous minerals to hydrous minerals. Circulating ground water can increase rock permeability by dissolving minerals along fractures, or it can decrease permeability by filling fractures with chemical precipitates.

TUNNEL HYDROLOGY

The hydrologic characteristics of the pilot bore can be divided into two parts according to the hydraulic characteristics of the two water-bearing zones: the active zone, near the portals, and the passive zone, in the central part of the bore. (See pl. 4.)

Water drained from the active zone into the advancing pilot bore from the east portal (station 121+15) to station 110+00. In this section of the bore, the greatest ground-water discharge occurred between stations 112+00 and 115+50. The largest initial flow from the face was 225 gpm (gallons per minute). Initial flows were derived from ground-water storage above and around the bore. The rate of flow past the main flume decreased progressively with the advance of the bore as the active zone near the portal became drained and the water was transmitted through an increasingly greater thickness of rock to reach the level of the bore.

As the bore advanced, the cumulative record of flows was recorded at the 6-inch Parshall flume installed at station 117+70. This station, 425 feet into the bore from the east portal, was selected because it was far enough into the bore to prevent ice from forming at the flume. Consequently, most, but not all, of the flow from the eastern part of the active zone was measured. The average weekly flow rates at the 6-inch flume, the water levels in diamond-drill-hole 2 (1962), and the streamflow at Clear Creek near Lawson, Colo., are shown in figure 51.

At several stations along the length of the bore, supplemental measurements of the ditch flow were made with a 3-inch portable flume to determine both the rate at which water seeped into the bore in a given reach and the variation in that rate with time (fig. 52). The limit of the active zone at each end of the bore was determined from these measurements and from differences in chemical quality of the ground water along the reaches.

The measurements indicated a significant rate of ground-water seepage into the tunnel west of station 52+30 and between station 104+83 and the Parshall flume at station 117+70. The greatest seepage occurred east of station 109+74; therefore, station 110+00 was selected as the approximate active-passive zone contact. The reach between stations 105+17 and 106+44 is probably an irregular downward extension of the active zone because ground-water flow continued at an increasing rate. The gradual increase in flow from this reach of the bore was probably caused by the fractures being cleansed as a result of gradual physical removal or chemical solution by ground water of fine particles that were in the fractures.

Location of the active-passive zone contact at the west end of the tunnel was estimated to be at station 44+00 on the basis of the seepage into the bore west of station 52+30 and the sharp contrast between the water quality of samples collected at stations 43+24 and 49+30 (fig. 53) — the sam-

TABLE 18. — *Ground-water flow at various*

[Data are in gallons per minute.

Tunnel Station	117+70	116+25	115+95	115+48	115+00	114+35	113+92	113+60	112+43	112+30	112+10	112+05	111+51	110+38	109+74	109+43	106+44	105+17	104+83
1964																			
Jan. 15	---	425	---	---	---	---	246	---	---	---	---	---	---	---	---	---	---	---	---
Apr. 2	43	---	---	---	---	---	---	---	---	---	---	---	---	---	---	---	8	2	---
May 10	45	---	44	---	41	41	---	34	31	---	---	---	---	---	11	7	9	6	---
13	45	---	---	---	---	---	---	---	28	---	---	16	14	12	6	---	---	4	---
24	85	---	---	---	---	---	---	---	44	---	---	---	22	---	13	---	11	5	---
31	171	---	---	---	---	---	---	---	---	---	---	---	---	---	11	---	---	5	---
June 3	173	---	180	---	159	---	---	120	89	---	55	---	52	31	14	---	12	7	---
7	175	---	---	---	172	---	---	124	---	---	---	---	---	---	11	---	---	---	---
10	211	---	---	---	205	---	---	125	---	---	---	---	---	---	16	---	---	---	---
21	350	---	---	---	---	---	---	---	---	---	---	---	---	---	12	---	---	---	---
24	350	---	---	---	---	---	---	---	---	---	---	---	---	---	23	---	---	---	---
28	350	---	---	---	---	---	---	---	---	---	---	---	---	---	18	---	---	---	---
July 1	375	---	---	---	---	---	---	---	---	---	---	---	---	---	24	---	---	---	---
5	368	---	---	---	---	---	---	---	---	---	---	---	---	---	22	---	---	---	---
8	360	---	---	---	---	---	---	---	---	---	---	---	---	---	19	---	---	---	---
12	341	---	---	---	---	---	---	---	---	---	---	---	---	---	28	---	---	---	---
15	321	---	---	210	---	---	---	185	---	150	---	---	---	---	29	---	---	---	---
19	283	---	---	---	---	---	---	---	---	---	---	---	---	---	27	---	---	---	---
23	256	---	---	---	---	---	---	---	---	---	---	---	---	---	45	---	---	---	---
Aug. 2	183	---	---	---	---	---	---	---	---	---	---	---	---	---	23	---	---	---	---
9	415	---	---	---	---	---	---	---	---	---	---	---	---	---	300	---	---	---	---
23	393	---	---	---	---	---	---	---	---	---	---	---	---	---	---	---	---	---	---
Dec. 29	112	---	---	---	---	---	---	---	---	---	---	---	---	---	---	---	---	---	---
1965																			
Jan. 1	---	---	---	---	---	---	---	---	---	---	---	---	---	---	---	---	---	---	82
11	99	---	---	---	---	---	---	---	---	---	---	---	---	---	---	---	---	---	78
13	99	---	---	---	---	---	---	---	---	---	---	---	---	---	---	---	---	---	73
21	90	---	---	---	---	---	---	---	---	---	---	---	---	---	---	---	---	---	87
Feb. 3	85	---	---	---	---	---	---	---	---	---	---	---	---	---	---	---	---	---	59
10	72	---	---	---	---	---	---	---	---	---	---	---	---	---	---	---	---	---	63
17	72	---	---	---	---	---	---	---	---	---	---	---	---	---	---	---	---	---	59
Mar. 4	72	---	---	---	---	---	---	---	---	---	---	---	---	---	---	---	---	---	52
17	67	---	---	---	---	---	---	---	---	---	---	---	---	---	---	---	---	---	52
Apr. 1	67	---	---	---	---	---	---	---	---	---	---	---	---	---	---	---	---	---	39
12	59	---	---	---	---	---	---	---	---	---	---	---	---	---	---	---	---	---	44
29	67	---	---	---	---	---	---	---	---	---	---	---	---	---	---	---	---	---	39
May 11	67	---	---	---	---	---	---	---	---	---	---	---	---	---	---	---	---	---	39
24	81	---	---	---	---	---	---	---	---	---	---	---	---	---	---	---	---	---	39
June 19	242	---	---	---	---	---	---	---	---	---	---	---	---	---	---	---	---	---	104
July 13	503	---	---	---	---	---	---	---	---	---	---	---	---	---	---	---	---	---	95
Aug. 6	291	---	---	---	---	---	---	---	---	---	---	---	---	---	---	---	---	---	89
Sept. 15	130	---	---	---	---	---	---	---	---	---	---	---	---	---	---	---	---	---	57
Dec. 9	67	---	---	---	---	---	---	---	---	---	---	---	---	---	---	---	---	---	35
1966																			
Jan. 4	64	---	---	---	---	---	---	---	---	---	---	---	---	---	---	---	---	---	31
26	63	---	---	---	---	---	---	---	---	---	---	---	---	---	---	---	---	---	28
Mar. 6	49	---	---	---	---	---	---	---	---	---	---	---	---	---	---	---	---	---	26
May 9	112	---	---	---	---	---	---	---	---	---	---	---	---	---	---	---	---	---	25
June 13	283	---	---	---	---	---	---	---	---	---	---	---	---	---	---	---	---	---	65

ple with the higher content of dissolved solids represented water from the passive zone. The active zone at the west end of the bore is thinner than the active zone at the east end and does not yield as much water (fig. 54). The difference in thickness of the active zone at the two ends of the tunnel results from the rock at the west end being less fractured.

The passive zone extends from station 44+00 to station 110+00, a distance of about 6,600 feet. Within this zone, most of the bore yielded only small quantities of water continuously (less than 10 gpm) from any associated groups of fractures (pl. 4). However, the three major pockets that yielded large quantities of water from the passive zone were penetrated between stations 69+30 and 70+50, stations 62+60 and 66+40, and stations 45+90 and 47+40. These three pockets yielded 40, 7, and 1.5 million gallons of water, respectively. These pockets are in fractured granitic rock, where the fracture spacing is 0.1 to 1 foot, adjacent to intensely sheared areas. Initial rate of discharge from any pocket did not exceed 350 gpm; however, because discharge from each pocket was added to the declining flow from the previous pocket, which in turn was added to the declining flow of the 1964 spring melt water, the cumulative flow at the main flume was approximately 675 gpm.

TABLE 19. — *Water pressure in feeler hole at station 62+91*

Date	Time (hr)[1]	Pressure (psia)[2]
Sept. 6, 1964	1000	20.0
Sept. 7, 1964	1700	19.8

[1]Astronomical time.
[2]Pounds per square inch absolute.

The gain in rate of flow between each of the 3-inch portable flumes is shown in figure 55. Measurements made between stations 52+30 and 74+09 (fig. 55) show the effect of the draining of the two larger pockets in the passive zone.

stations in the Straight Creek Tunnel pilot bore

Leaders (- - -) indicate no data collected]

104+72	103+98	103+47	99+15	96+47	92+20	86+46	86+14	81+17	80+66	74+08	72+09	71+00	70+08	68+92	52+30	Face position	Remarks
---	---	---	---	---	---	---	---	---	---	---	---	---	---	---	---	113+90	
---	---	---	---	---	---	---	---	---	---	---	---	---	---	---	---	97+74	Face dry; feeler-hole flow 46 gpm.
---	5	---	4	3	---	---	---	---	---	---	---	---	---	---	---	89+92	Face damp; feeler hole dry.
---	---	---	---	---	---	---	---	---	---	---	---	---	---	---	---	89+82	Do.
---	---	---	---	4	---	---	---	---	---	---	---	---	---	---	---	89+00	Face dry.
---	---	---	---	---	---	---	---	---	---	---	---	---	---	---	---	87+14	Do.
---	---	---	---	---	---	---	---	---	---	---	---	---	---	---	---	86+37	Do.
---	---	---	---	---	---	---	---	---	---	---	---	---	---	---	---	85+58	Do.
---	---	---	---	---	---	---	---	---	---	---	---	---	---	---	---	84+85	Do.
3	---	---	---	---	---	---	---	---	---	---	---	---	---	---	---	83+20	Do.
4	---	4	---	---	---	---	---	---	---	---	---	---	---	---	---	82+27	Do.
5	---	3	---	---	---	---	---	---	---	---	---	---	---	---	---	81+28	Do.
16	---	11	---	---	---	---	---	---	---	---	---	---	---	---	---	80+55	Face flow 5 gpm.
12	---	10	---	---	---	---	---	---	---	---	---	---	---	---	---	79+87	Face damp.
30	---	39	---	---	---	---	---	---	---	---	---	---	---	---	---	79+11	Face dry.
21	---	16	---	---	---	---	---	---	9	---	---	---	---	---	---	78+00	Feeler hole dry.
---	---	21	---	---	---	---	---	---	16	---	---	---	---	---	---	76+91	Feeler-hole flow 2–4 gpm.
---	---	18	---	---	---	---	---	---	9	---	---	---	---	---	---	75+59	Face damp; feeler hole dry.
---	---	23	---	---	---	---	---	23	---	---	---	---	---	---	---	74+16	Feeler-hole flow 5 gpm.
---	---	27	---	---	---	---	---	16	---	---	---	---	---	---	---	71+39	Face damp.
---	---	---	---	---	---	---	---	---	---	---	---	---	---	---	---	69+75	Face flow 100 gpm.
---	---	---	---	---	---	---	---	---	---	---	---	272	---	81	---	65+74	Face damp.
---	---	---	---	---	---	---	---	---	---	---	---	---	70	---	14	---	Tunnel holed through.
---	---	---	---	---	82	---	80	---	---	---	---	---	---	---	---	---	
---	---	---	---	---	69	---	73	---	---	---	76	---	---	---	11	---	
---	---	---	---	---	70	---	69	---	---	58	---	---	---	---	---	---	
---	---	---	---	---	69	---	---	---	---	---	61	---	---	---	11	---	
---	---	---	---	---	54	---	---	---	---	---	54	---	---	---	8	---	
---	---	---	---	---	56	---	---	---	---	---	50	---	---	---	9	---	
---	---	---	---	---	50	---	---	---	---	---	47	---	---	---	8	---	
---	---	---	---	---	46	---	---	---	---	---	44	---	---	---	8	---	
---	---	---	---	---	43	---	---	---	---	---	44	---	---	---	8	---	
---	---	---	---	---	36	---	---	---	---	---	44	---	---	---	8	---	
---	---	---	---	---	39	30	---	---	---	---	31	---	---	---	7	---	
---	---	---	---	---	33	31	---	---	---	---	31	---	---	---	6	---	
---	---	---	---	---	33	31	---	---	---	---	31	---	---	---	5	---	
---	---	---	---	---	33	30	---	---	---	---	28	---	---	---	6	---	
---	---	---	---	---	99	98	---	---	---	---	98	---	---	---	69	---	
---	---	---	---	---	87	84	---	---	---	---	73	---	---	---	57	---	
---	---	---	---	---	80	69	---	---	---	---	65	---	---	---	57	---	
---	---	---	---	---	50	44	---	---	---	---	44	---	---	---	31	---	
---	---	---	---	---	37	23	---	---	---	---	22	---	---	---	14	---	
---	---	---	---	---	30	23	---	---	---	---	20	---	---	---	8	---	
---	---	---	---	---	27	20	---	---	---	---	19	---	---	---	8	---	
---	---	---	---	---	24	19	---	---	---	---	16	---	---	---	6	---	
---	---	---	---	---	24	20	---	---	---	---	16	---	---	---	5	---	
---	---	---	---	---	23	61	---	---	---	---	54	---	---	---	46	---	

TABLE 20. — *Temperature and specific conductance of drainage-ditch water, Straight Creek Tunnel pilot bore*

[Dash leaders (- - -) indicate no data collected]

Station	May 13, 1964		May 24, 1964		May 24, 1965	
	Temperature (°C)	Specific conductance (μmhos/cm) at 25°C	Temperature (°C)	Specific conductance (μmhos/cm) at 25°C	Temperature (°C)	Specific conductance (μmhos/cm) at 25°C
117+80	4.50	---	---	---	---	---
117+70	4.50	255	4.83	---	5.81	400
115+95	4.60	275	4.90	---	---	---
115+00	4.65	280	---	---	---	---
114+35	4.75	280	4.58	---	---	---
113+59	4.82	275	5.14	---	---	---
112+43	5.00	300	5.35	---	---	---
112+19	5.07	---	---	---	---	---
112+10	5.25	325	---	---	---	---
112+00	---	---	---	---	7.17	500
111+51	5.48	340	5.90	---	---	---
110+40	5.85	340	6.55	---	---	---
109+76	6.02	350	6.70	---	---	---
107+00	---	---	---	---	8.16	580
106+45	6.42	345	6.93	---	---	---
105+18	6.90	350	7.54	---	---	---
104+83	---	---	---	---	8.78	640
103+98	7.07	---	7.65	---	---	---
99+15	7.49	---	7.93	---	---	---
96+47	7.76	---	8.06	---	---	---
94+50	---	---	8.08	---	---	---
92+50	---	---	8.08	---	---	---
92+20	---	---	---	---	9.32	650
89+50	---	---	8.10	---	---	---
86+46	---	---	---	---	9.32	650
79+00	---	---	---	---	9.26	670
74+09	---	---	---	---	9.28	700
71+50	---	---	---	---	9.26	700
63+30	---	---	---	---	8.14	640
61+60	---	---	---	---	7.34	580
57+10	---	---	---	---	6.43	550
54+60	---	---	---	---	5.89	540
54+50	---	---	---	---	5.82	550
52+30	---	---	---	---	5.43	490
49+30	---	---	---	---	4.81	480
46+70	---	---	---	---	4.32	370
45+00	---	---	---	---	3.78	350
42+80	---	---	---	---	3.40	330
41+75	---	---	---	---	3.15	280
40+20	---	---	---	---	2.51	300

TABLE 21. — *Temperature and specific conductance of water flowing from rock fractures, Straight Creek Tunnel pilot bore*

[Leaders (- - -) indicate no measurement made on that date]

Station	Temperature (°C)	Specific conductance (μmhos/cm at 25°C)	Date
42+00	5.0	250	5- 9-66
42+60	4.0	300	5- 9-66
43+05	4.0	320	5- 9-66
43+24	3.5	- - -	11-22-64
45+40	4.5	420	5- 9-66
46+57	4.5	380	5- 9-66
47+44	5.0	770	5- 9-66
48+15	5.5	840	5- 9-66
49+30	5.5	1,160	5-24-65
	7.0	860	5-9-66
52+12	6.0	890	5- 9-66
58+50	8.0	580	5- 9-66
62+89	9.0	850	9- 6-64
	9.0	460	5- 9-66
63+30	9.0	800	5-24-65
73+80	10.0	380	5- 9-66
75+60	10.0	360	5-24-65
77+85	10.0	410	5- 9-66
91+20	10.0	225	5- 9-66
106+20	7.0	270	5- 9-66
107+85	7.0	240	5- 9-66
111+90	5.0	250	5- 9-66
112+19	4.5	- - -	5-13-64
113+92	4.0	250	1-13-64
114+05	4.0	- - -	5-24-64
	4.0	100	5- 9-66
116+10	5.0	190	5- 9-66

TABLE 22. — *The pH of water flowing from rock fractures, June 13, 1966, Straight Creek Tunnel pilot bore*

Station	pH	Station	pH
41+50	7.5	58+50	7.6
42+00	7.4	62+90	8.1
42+60	7.9	73+80	8.1
43+05	7.7	77+85	8.1
45+40	7.6	91+20	7.9
46+57	7.7	106+20	7.6
47+44	7.4	107+85	7.5
48+15	7.4	111+90	7.3
49+30	7.8	114+05	7.0
52+12	7.5	117+70	7.4

TABLE 23. — *Summary of physical and hydrologic properties of fault-gouge samples from the pilot bore*

Parent material	Field No.	Specific gravity of solids	Dry unit weight (g per cm³)	Total porosity (percent)	Hydraulic conductivity[1] (gpd per sq ft)
Granite	83+11G	2.69	1.82	32.3	43
Metasedimentary rock	86+02M	2.76	1.87	32.2	.03

[1]Repacked samples.

An increase in seepage (fig. 55) between stations 74+09 and 86+46 during July 1965 possibly indicates a connection to the surface (active zone) and a response to melt water (by increase in pressure head). A minor amount of variation in flow measured at different times is due to different personnel reading the water levels in the flumes, as well as to the varying amounts of water used in the tunneling process. Some variation may be due to leakage around the flumes.

TABLE 24. — *Relation between fracture spacing and ground-water discharge from the face of the pilot bore*

Fracture spacing (ft)	Active zone		Passive zone	
	Number of occurrences[1]	Average discharge per occurrence (gpm)[2]	Number of occurrences[1]	Average discharge per occurrence (gpm)[2]
<0.1	0	0	8	6
0.1-0.5	7	78	62	55
0.5-1	20	43	50	20
>1	13	49	10	3

[1]Only discharges >1 gpm from the face of the pilot bore are tabulated.
[2]Gallons per minute.

Water levels were measured in diamond-drill-hole 2 (1962) from the start of construction of the bore (fig. 51; table 25). The drill hole is 872 feet deep, or 72 feet deeper than the bore level, and is about 100 feet north of the tunnel line at station 96+47. As excavation of the bore approached and passed the drill hole, no noticeable water-level changes were observed. This lack of response indicates a lack of hydraulic continuity. Continued measurements then established the correlation between water level in the drill hole and recharge from spring runoff (fig. 51).

Because the water level in diamond-drill-hole 2 (1962) fluctuates seasonally but did not decline with the approach of the bore, the authors concluded that the upper part of the hole is in the active zone, and the lower part is in the passive zone. On the basis of seasonal fluctuations in water level, the contact between the two zones in the vicinity of the drill hole was estimated to be about 105-110 feet below land surface.

HYDRAULIC PROPERTIES OF CRYSTALLINE ROCK

Diamond-drill-hole 2 (1962) was slug tested on September 11, 1965. A transmissivity analysis was made by fitting the test curves to type curves (fig. 56) for wells of finite radii, as outlined by Cooper, Bredehoeft, and Papadopulos (1966). The analysis indicated a transmissivity of about 8 gpd per ft (gallons per day per foot), and a hydraulic conductivity of about 0.2 gpd per sq ft (gallons per day per square foot).

A second type of analysis was made using seasonal water-level fluctuations in diamond-drill-hole 2 (1962). The type curves of Stallman and Papadopulos (1966) for determining hydraulic diffusivity in wedge-shaped aquifers were used for analyzing the water-level fluctuations. The results of the analysis (fig. 57) indicate a diffusivity (the ratio of transmissivity to storage coefficient) of about 94,000 gpd per ft.

Samples of fault gouge from granitic rocks and from metasedimentary rocks were analyzed in the laboratory for hydraulic characteristics. The analyses (table 23) indicate a much higher hydraulic conductivity for the granite gouge than for the metasedimentary gouge.

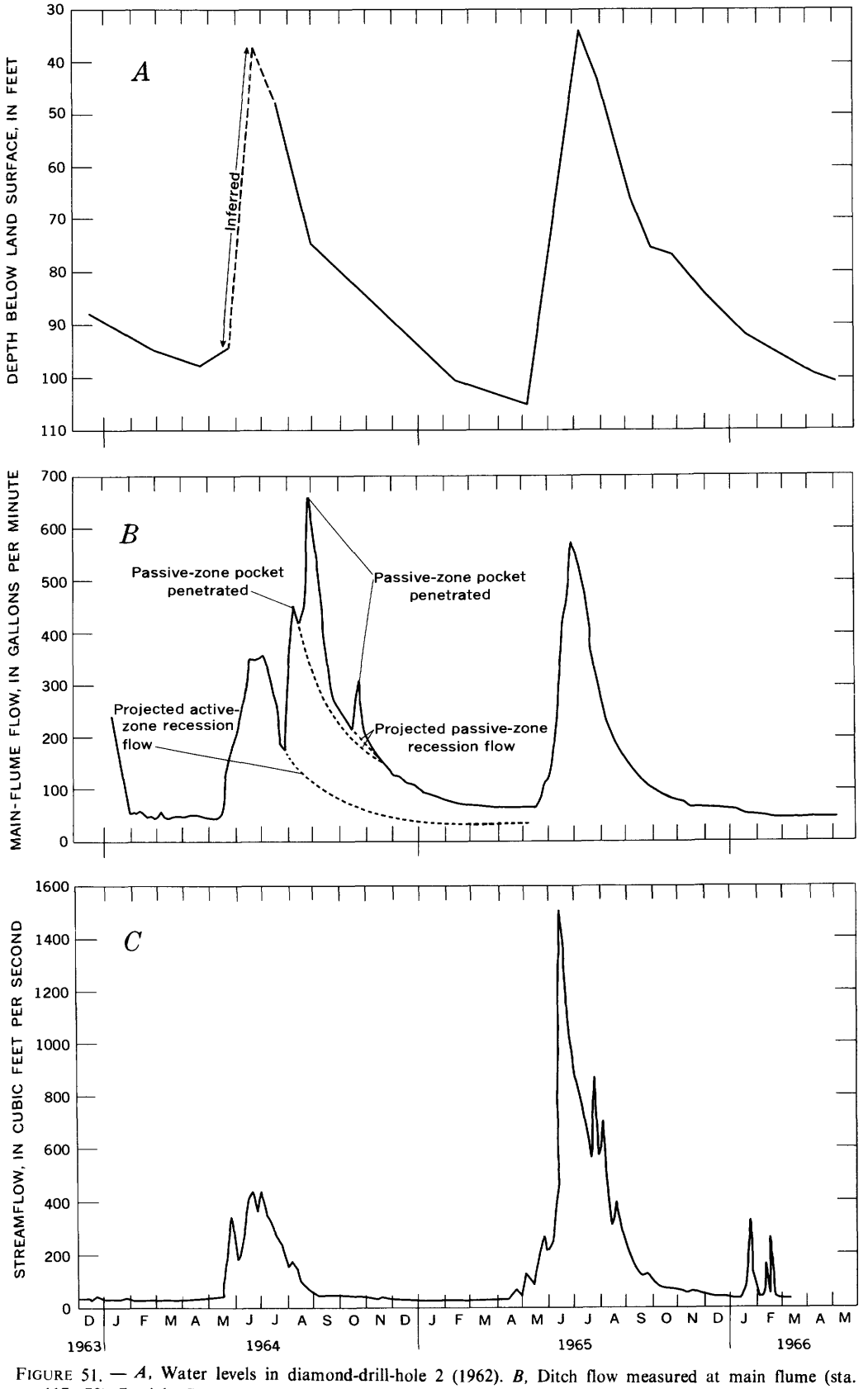

FIGURE 51. — *A*, Water levels in diamond-drill-hole 2 (1962). *B*, Ditch flow measured at main flume (sta. 117+70), Straight Creek Tunnel pilot bore. Dashed lines divide the total flow into that discharged from the active zone and that discharged from each of the three highly permeable pockets in the passive zone. *C*, Streamflow at Clear Creek near Lawson, Colo.

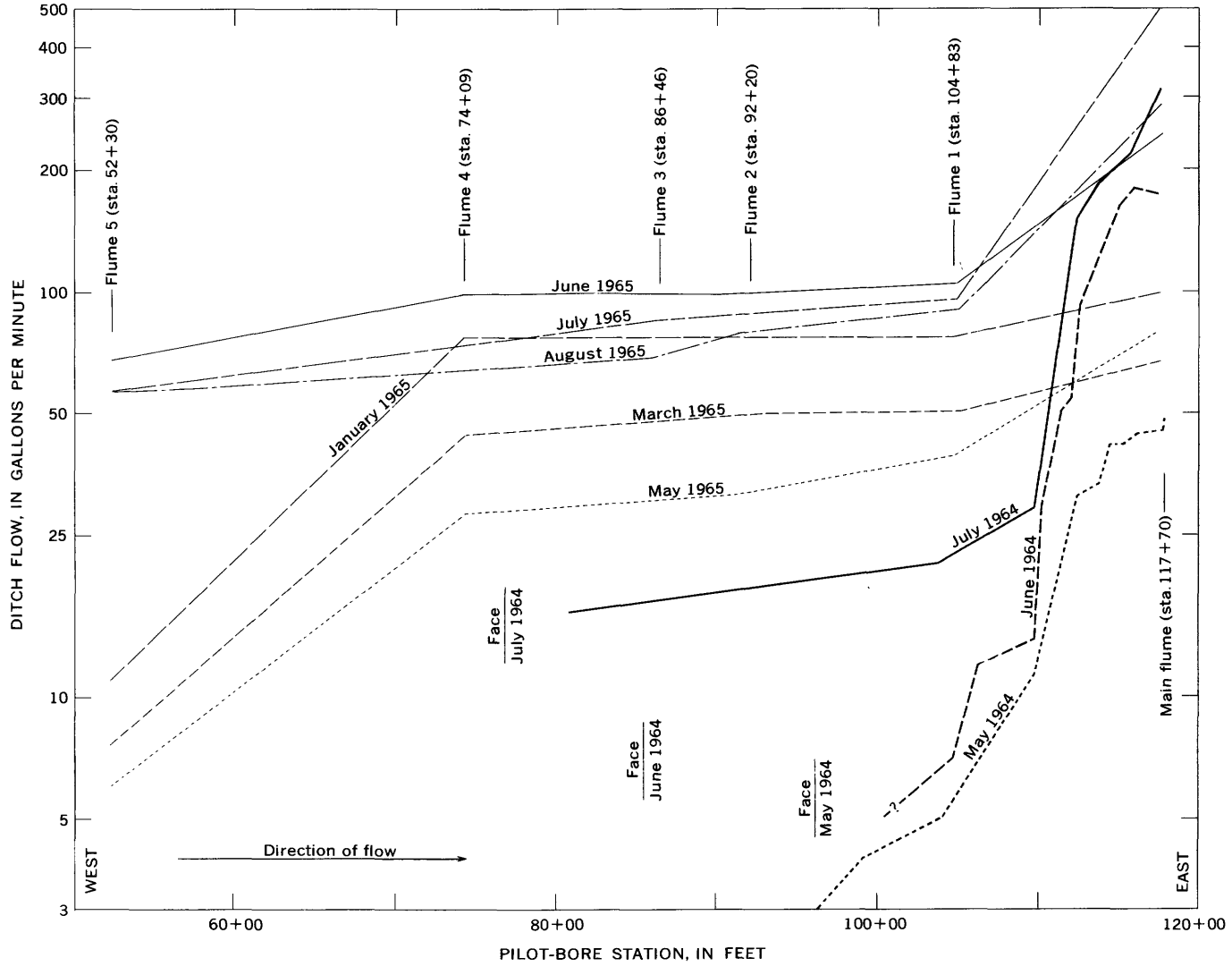

FIGURE 52. — Cumulative ditch flow at selected pilot-bore stations.

TABLE 25. — *Water-level measurements, diamond-drill-hole 2 (1962)*

[Altitude of land surface: 11,919 feet above mean sea level. Measurement data are in feet below land surface]

Date	Water level	Date	Water level
1963		*1965* — Con.	
Dec. 18	86.97	Sept. 4	59.49
23	87.45	11	64.22
		Oct. 6	75.14
1964		Nov. 3	76.28
Feb. 28	93.57	Dec. 1	82.16
Mar. 21	95.21	21	86.00
Apr. 29	96.63		
June 1	93.53	1966	
July 23	45.9	Jan. 4	88.25
Sept. 6	73.7	19	90.44
		Feb. 2	92.21
1965		Mar. 6	95.56
Feb. 20	99.9	Apr. 13	98.94
May 13	104.62	May 9	100.44
July 13	33.59	June 13	66.64
Aug. 8	43.53	Aug. 23	79.40

The hydraulic conductivity of the rock immediately surrounding the tunnel was calculated from the reduction in head through 8 feet of rock, as measured by the pressure gage at station 62+91 and the flow rate along a length of bore. The value of the hydraulic conductivity (about 50 gpd per sq ft) may not be representative of the undisturbed rock, however, because stress relief around the pilot bore may have increased the size of fracture openings.

WATER QUALITY AND GEOCHEMISTRY

The dissolved solids in the water are primarily bicarbonate and sulfate of calcium and magnesium (table 26). The dissolved-solids content of the water is low near the portals and high along the center reach of the bore. When the dissolved-solids content is below 240 mg/l (milligrams per liter), calcium is the dominant cation, and above 240 mg/l, magnesium is predominant (fig. 58). Magnesium, bicarbonate, and sulfate generally increase with an increase in dissolved solids, whereas calcium, sodium, potassium, chloride, and fluoride approach a constant value independent of dissolved-solids content (fig. 58).

Factors that influence the composition of water in contact with rock are (1) temperature and pressure of the water, (2)

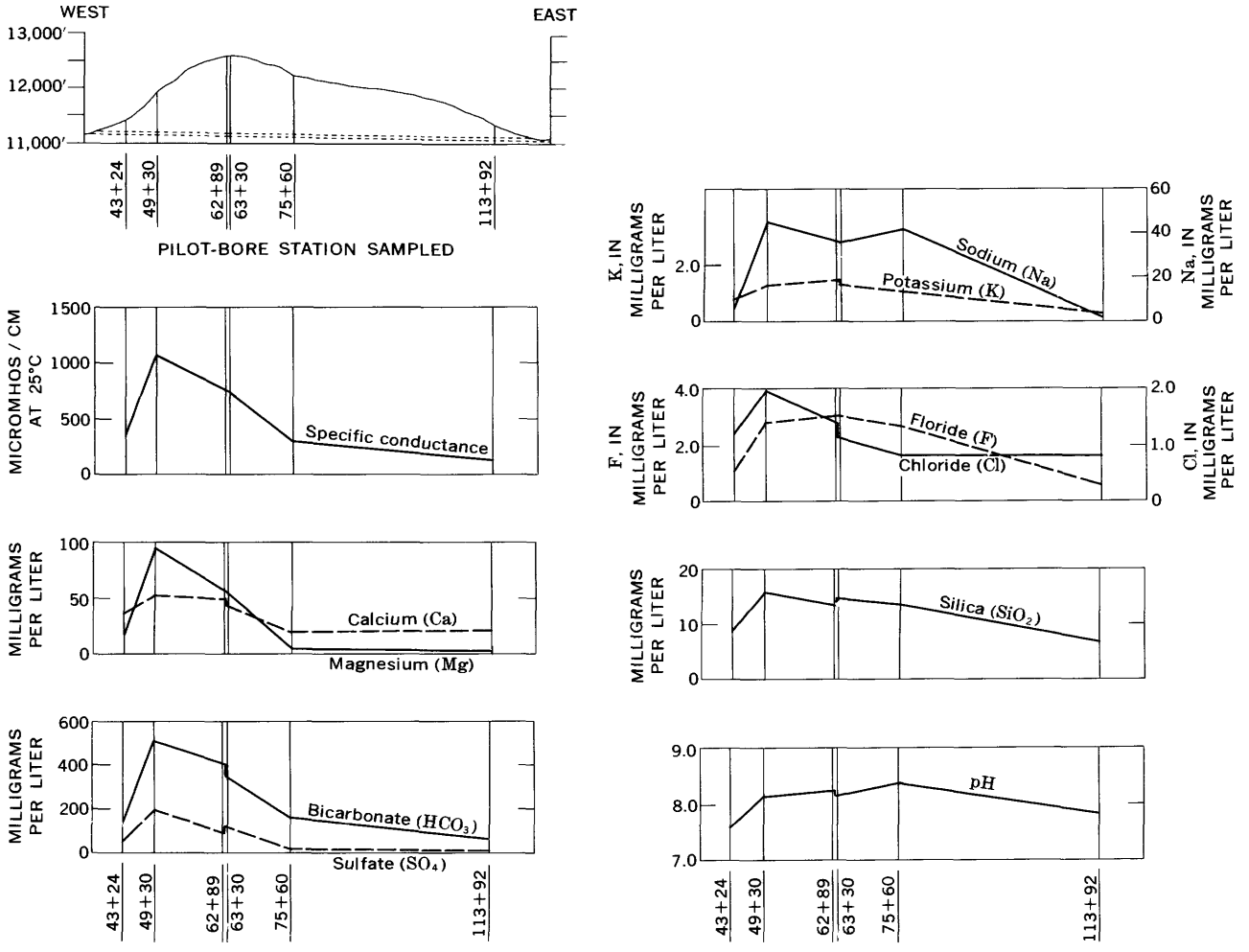

FIGURE 53. — Profiles showing quality of ground water sampled at indicated pilot-bore stations.

Eh and pH of the water, (3) original chemical composition of the water, (4) mineral composition of the rock, and (5) length of time water and rock are in contact.

The chemical composition of the ground water changes from place to place along the bore (fig. 53) as a result of the five previously named factors. Examination of these factors

TABLE 26. — *Analyses of water samples collected in the Straight Creek Tunnel pilot bore*

[Analyses by U.S. Geological Survey. Results are in milligrams per liter, except as indicated]

Station No Collection date	43+24 11-22-64	49+30 5-24-65	62+89 9-6-64	63+30 5-24-65	75+60 5-24-65	113+92 1-15-64
Silica (SiO_2)	7.8	15	13	14	13	6.8
Calcium (Ca)	36	51	50	42	18	21
Magnesium (Mg)	12	92	56	53	5.8	3.4
Sodium (Na)	3.5	43	33	34	40	1.9
Potassium (K)	.6	1.2	1.4	1.2	1.1	.3
Bicarbonate (HCO_3)	130	496	403	337	157	78
Carbonate (CO_3)	0	0	0	0	1	0
Sulfate (SO_4)	37	192	93	115	15	6.6
Chloride (Cl)	1.1	1.9	1.4	1.1	.8	.8
Fluoride (F)	.8	2.7	2.9	3.0	2.6	.6
Nitrate (NO_3)	2.9	1.2	.2	.1	.0	.6
Boron (B)	.02	.04	.00	.04	.04	.03
Dissolved solids (residue on evaporation)	165	642	442	420	177	65
Hardness as $CaCO_3$	139	507	356	321	68	66
Noncarbonate hardness as $CaCO_3$	32	100	26	45	0	2
Specific conductance (μmhos/cm at 25°C)	272	1,030	733	732	282	137
pH (laboratory)	7.5	8.1	8.2	8.1	9.3	7.8

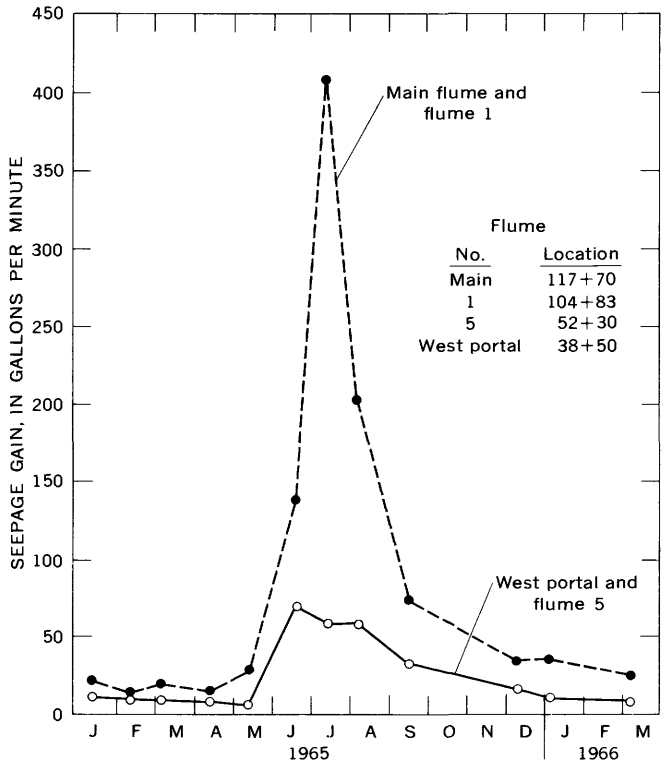

FIGURE 54. — Flow into the pilot bore from the active zone, as determined by seepage gain in ditch flow between the indicated flumes.

suggests that the major cause of the difference in chemical composition of the water is the length of time that the water and rock are in contact. Water in the active, more permeable zone moves through rock more easily and is in contact with rock for shorter periods of time than water in the passive zone and is, therefore, lower in total dissolved solids.

Excavation of the bore increased the rate of movement of water through the passive zone. This increased rate of movement is indicated by a decrease in specific conductance of passive-zone water, determined during successive measurements (fig. 59; table 21), as the drainage into the bore continued.

ENGINEERING APPLICATIONS TO TUNNEL CONSTRUCTION

The most significant engineering problems related to ground-water conditions at the Straight Creek tunnel site are the time of year and direction of tunnel construction, the mechanical behavior of the rock, and the grouting practices pertinent to tunnel construction and completion.

Tunneling through the wettest sections during their driest period and in a direction that will remove the water by the shortest route will create the least number of problems. Therefore, the tunnel alinement should intersect major water channels at nearly right angles in order to have the shortest possible length of bore in zones of large water inflow. The largest flow from the active zone occurs near the east portal, where it is >400 gpm during June and July, as compared with a flow of <75 gpm from the west portal during the same period. Low flow (approximately 50 gpm) from the active zone occurs during late winter or early spring.

Although water-bearing zones can be effectively sealed by grouting during excavation, the process is both time consuming and expensive. Allowing water-bearing zones to drain naturally proved satisfactory in the passive zone of the pilot bore. If a dry tunnel is necessary, grouting can be done after most water has drained. Grouting after such drainage is possible only because the bore is high in the watershed, because only a small part of the recharge in the watershed affects the bore, and because the permeability and storage capacity of the rock mass are low.

During the winter and early spring (1964–65), ground water entering the pilot bore at and near the east portal froze into an almost continuous mass of ice, often impeding the construction trains. This inconvenience could have been prevented by grouting the active zone in the areas susceptible to freezing. In the passive zone the rock sections having a fracture spacing of 0.1–0.5 foot are the most suitable for grouting; in the active zone, rock can be thoroughly sealed because it is porous and permeable throughout, virtually independent of the fracture spacing.

The hydrologic framework of the westbound, full-size tunnel, 100 feet north of the pilot bore, should be similar to that of the pilot bore. Possibly some of the water-bearing zones within the passive zone will be intersected by the full-size tunnel. If so, these zones will have been largely drained by the pilot bore, reducing ground-water problems. However, if the irregular permeability and the greater possibility of encountering water-bearing zones because of the larger excavation are considered, the water discharge in the tunnel may be as much as 150 percent of that in the pilot bore. This figure, only a gross estimate, is based on the ratio of the effective radii of the tunnels. The effective radii were obtained by adding the thickness (20 ft) of the stress-relieved fracture zone around the bores to the nominal radius of each tunnel. The nominal radius is about 6.5 feet for the pilot bore and 17 feet for the full-size tunnel.

CONCLUSIONS

Water in the rock surrounding the pilot bore is contained in fractures. It entered the bore by drainage of the fracture system and by interception of surface-water sources. Initial yields appear to be closely related to fracture spacing, and time-yield characteristics are a function of the extent and continuity (the storage coefficient and hydraulic conduc-

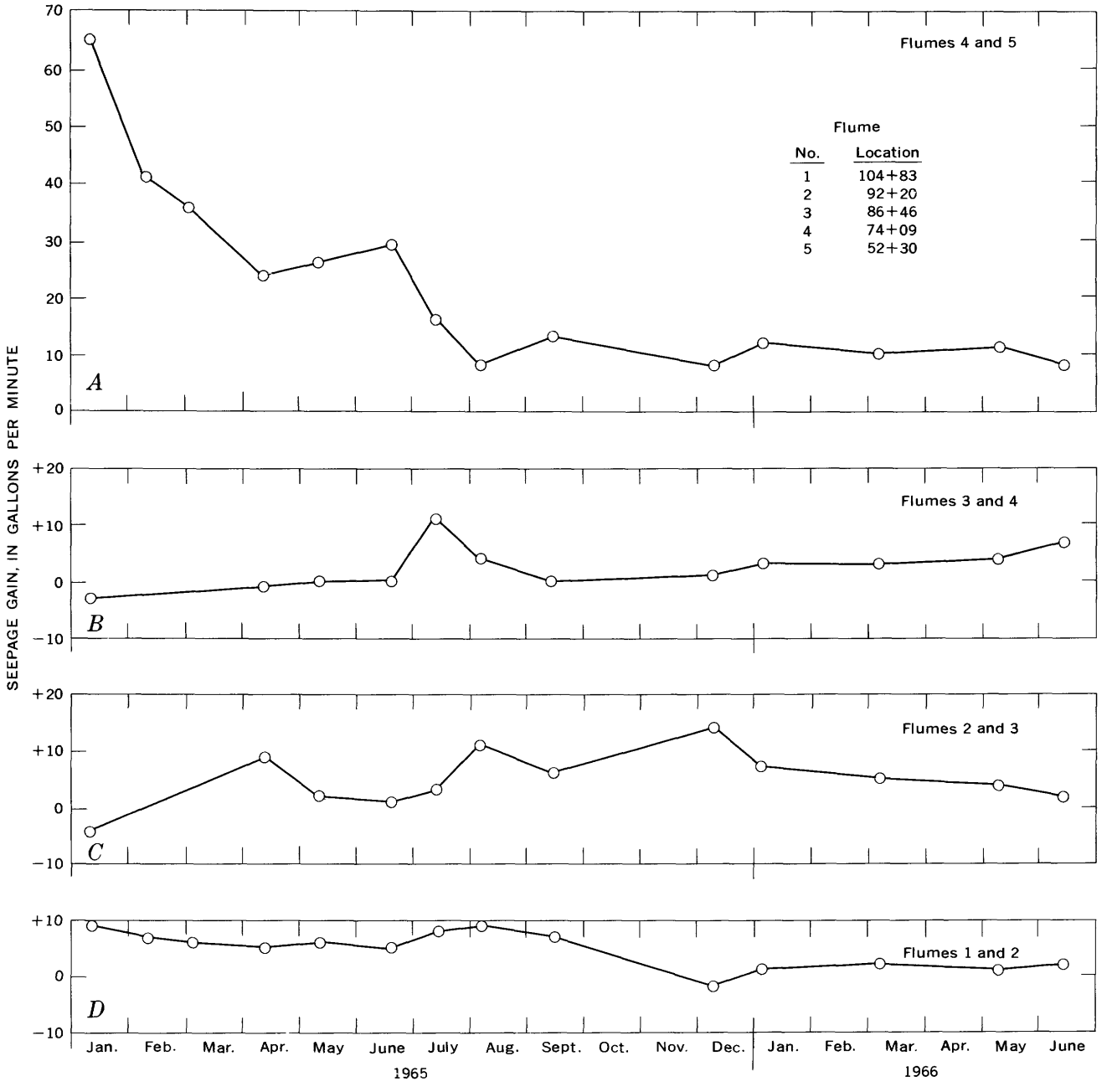

FIGURE 55. — Flow into the pilot bore from the passive zone, as determined by seepage gain in ditch flow between indicated flumes.

tivity) of the fracture system and the proximity of the recharge areas.

The occurrence of ground water in the pilot bore has the following relation to fractures:

1. Rock in shear zones, where fractures are less than 0.1 foot apart, is relatively impermeable, owing to extensive chemical and mechanical alteration.
2. Rock whose fractures are 0.1−0.5 foot apart is commonly adjacent to faults and shear zones, is the most porous, and has the greatest hydraulic continuity.
3. Rock whose fractures are 0.5−1 foot apart is usually somewhat removed from faults, is less porous, and has less hydraulic continuity.
4. Rock whose fractures are more than 1 foot apart is generally remote from faults, is relatively impermeable, and generally yields little water. Average discharge per occurrence at the tunnel face for the classifications listed above were 6, 55, 20, and 3 gpm, respectively, in the passive zone, and 0, 78, 43, and 49 gpm, respectively, in the active zone.

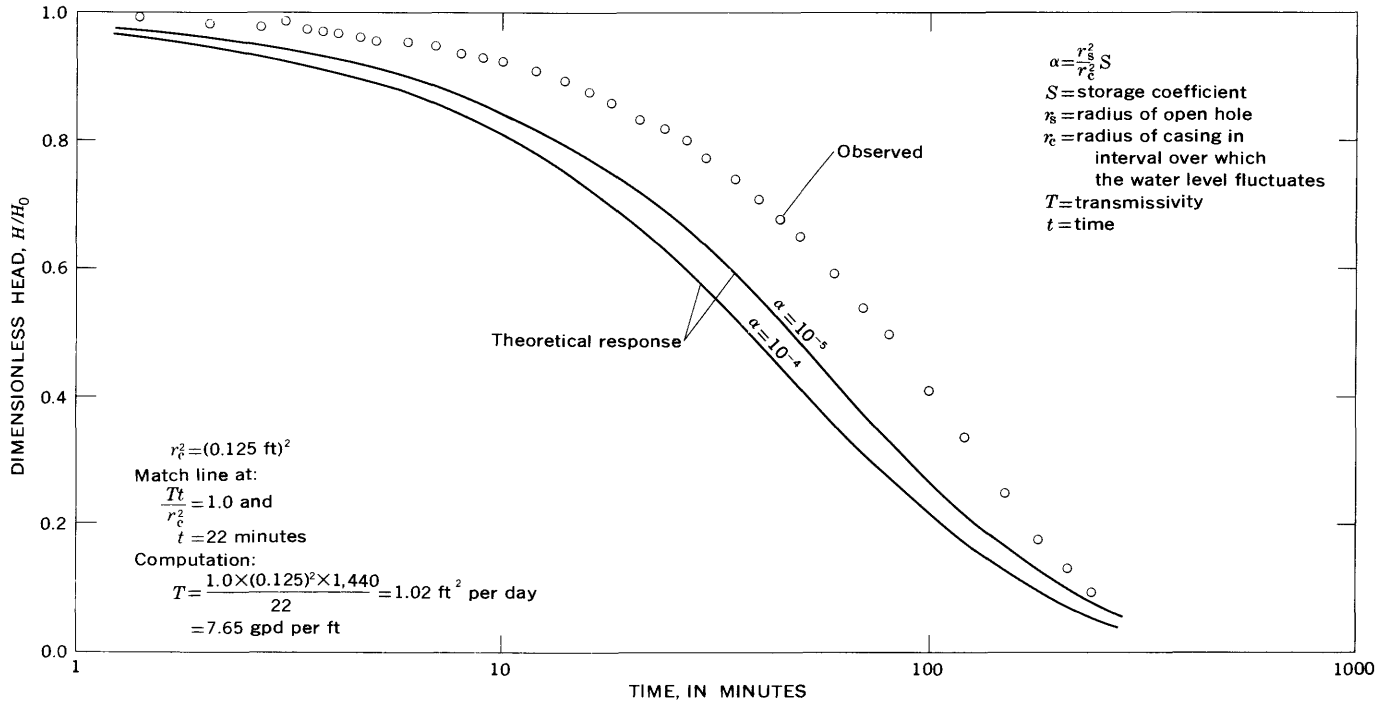

FIGURE 56. — Response curve of slug-test results for diamond-drill-hole 2 (1962).

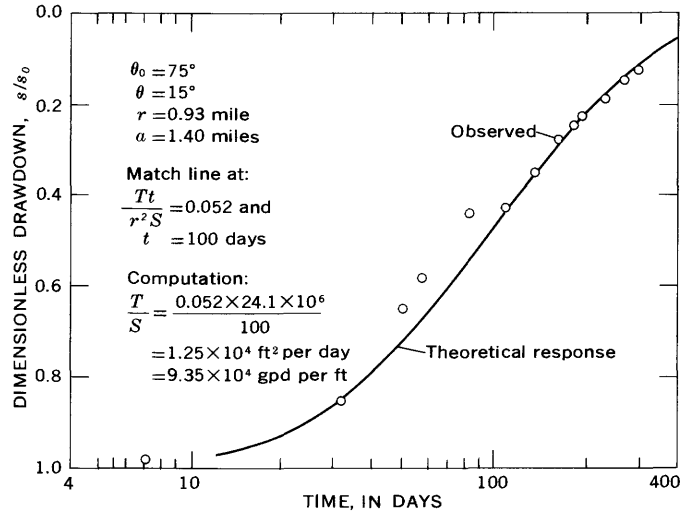

FIGURE 57. — Wedge-shaped-aquifer analysis of 1965 seasonal recessions of the water level in diamond-drill-hole 2 (1962). t, time, in days; S, storage coefficient; T, transmissivity, in gallons per day per foot.

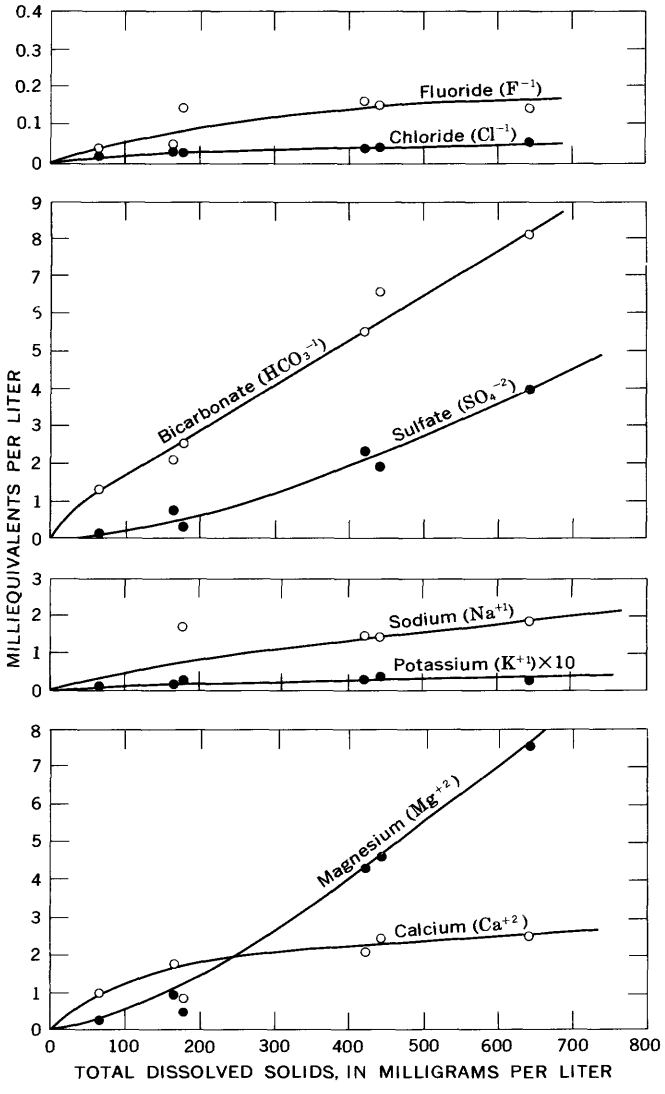

FIGURE 58. — Relation of selected elements to total dissolved solids (residue on evaporation).

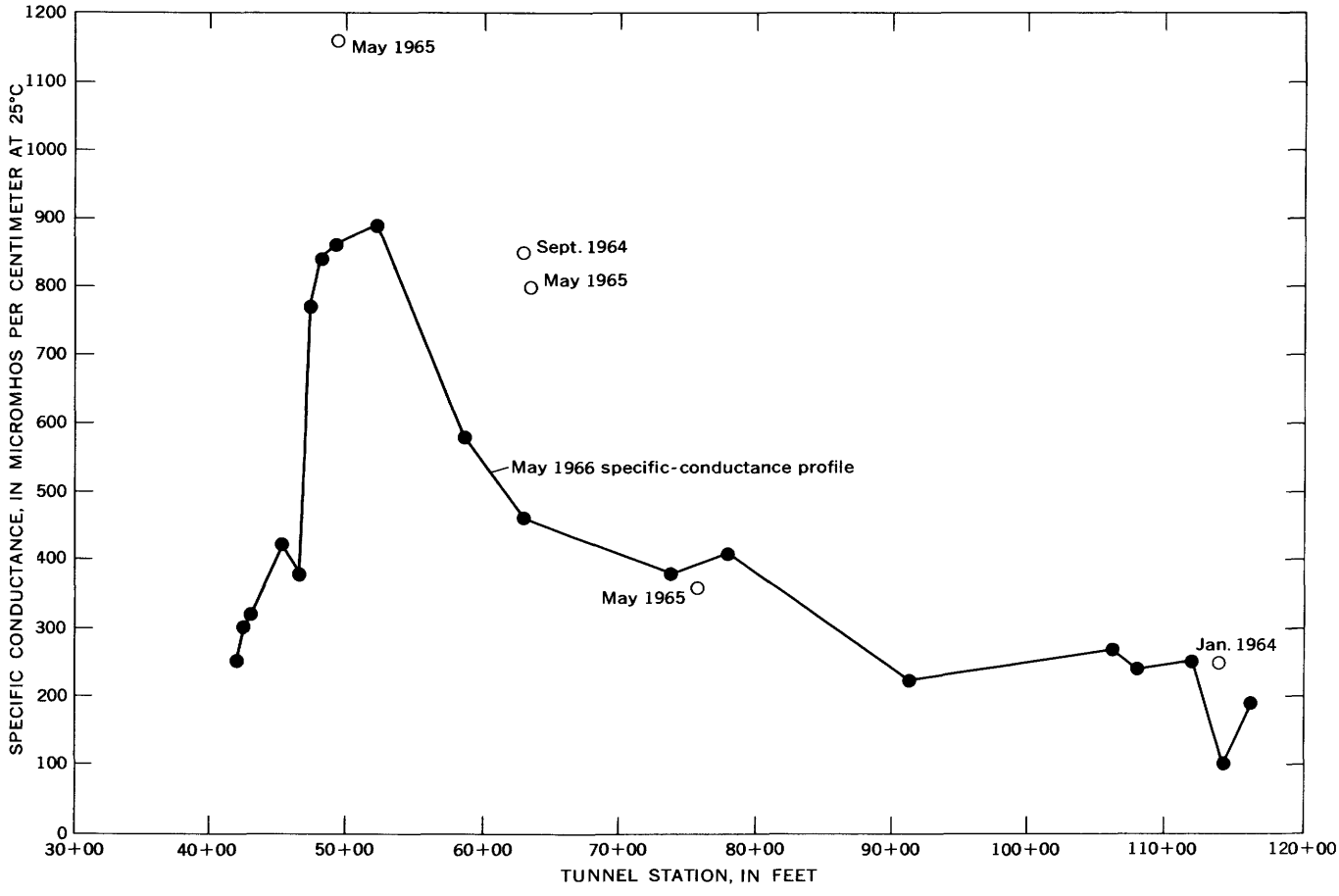

FIGURE 59. — Specific conductance of water flowing from rock fractures in the pilot bore.

Engineering Operations, Construction Practices, and Rock-Mechanics Investigations

By CHARLES S. ROBINSON, FITZHUGH T. LEE, FRED A. MATTEI, *and* BURT E. HARTMANN

ENGINEERING GEOLOGIC, GEOPHYSICAL, HYDROLOGIC, AND ROCK-MECHANICS INVESTIGATIONS OF THE STRAIGHT CREEK TUNNEL SITE AND PILOT BORE, COLORADO

GEOLOGICAL SURVEY PROFESSIONAL PAPER 815–F

ENGINEERING GEOLOGIC, GEOPHYSICAL, HYDROLOGIC, AND ROCK-MECHANICS INVESTIGATIONS OF THE STRAIGHT CREEK TUNNEL SITE AND PILOT BORE, COLORADO

ENGINEERING OPERATIONS, CONSTRUCTION PRACTICES, AND ROCK-MECHANICS INVESTIGATIONS

By CHARLES S. ROBINSON, FITZHUGH T. LEE, FRED A. MATTEI,[1] and BURT E. HARTMANN[2]

One of the objectives of the investigations of the Straight Creek Tunnel pilot bore was to determine the influence of the geologic features on the engineering design and the construction of the pilot bore. To measure the influence of the geology, particularly on the design of a tunnel, and for use in the design of the final twin-bore tunnel, a rock-mechanics measurement program was conducted during the construction of the pilot bore. This chapter describes the engineering operations and construction practices during the construction of the pilot bore, describes the procedures and instruments, and gives the results of the rock-mechanics measurement program.

ENGINEERING OPERATIONS AND CONSTRUCTION PRACTICES

The Colorado Department of Highways established a field engineering office at the east portal of the pilot bore in October 1963 adjacent to the field office of the contractor, Mid-Valley, Inc. The Colorado Department of Highways maintained an engineering staff of 11 to 12 men, supervised by F. A. Mattei, who were in charge of surveying and related tunnel-engineering duties.

The primary engineering duties consisted of maintaining the pilot bore on line and grade and measuring and recording pay items under the contract. Pay items included the volume of excavated rock, the amount of steel and wood blocking, and the amount of lagging. Highway personnel were also responsible for the enforcement of work standards required by the Department and the Bureau of Public Roads and for recommending and approving changes in engineering practices. The Highway Department staff also recorded weather data and rock-mechanics instrumentation data, made geologic sections of the pilot-bore face as the face was advanced, and generally supervised the surface and underground operations.

[1]Colorado Department of Highways, Denver, Colo.
[2]Formerly with Terrametrics, Inc.

SURVEYS

The first survey for a tunnel line from Loveland basin to the head of the Straight Creek drainage area was run by the Colorado Department of Highways in 1953 (Colorado Department of Highways, 1965). In 1956 the Colorado Department of Highways established survey monuments on each side of the Continental Divide at points near the anticipated portals of the Straight Creek Tunnel pilot bore. The services of Continental Engineers, Inc., of Denver, Colo., were contracted to prepare a topographic map of the tunnel area at a scale of 1:1,200. On the basis of this mapping, three lines were eventually chained and staked over the Continental Divide by the Colorado Department of Highways. The final alinement, the "X line," is the presently planned median centerline for the full-size twin-bore tunnel. The pilot bore is parallel to, and 47 feet south of, the X line, whose bearing is S. 89°47′20″ E.

The pilot bore was driven from east to west at an average positive grade of 1.729 percent. The centerline of the pilot bore was tied to a point on centerline just outside the east portal by backsighting on a target 1¾ miles to the east. The centerline was located in the pilot bore during construction by means of punch marks on drill-steel or steel-rail monuments cemented into the floor of the pilot bore at about 600-foot intervals. Backsights were taken on the east portal target for distances up to 6,300 feet. Beyond that distance, poor visibility limited backsights to every other monument, or distances of about 1,200 feet. The final horizontal closure was made, within 0.1 foot, on a target on centerline about 0.3 mile west of the west portal.

Horizontal distances were determined during construction by double chaining, with a 300-foot-long invar metal tape, between the centerline monuments. The horizontal distance, which was not corrected for temperature, was 2.7 feet short of the previously chained (unchecked) distance over the divide. To reconcile this error, a field equation, 38 + 99.4 Ah. = 431 + 21.0 Bk., was established at the west

FIGURE 60. — Status of east portal operations, November 14, 1963. View is to the west.

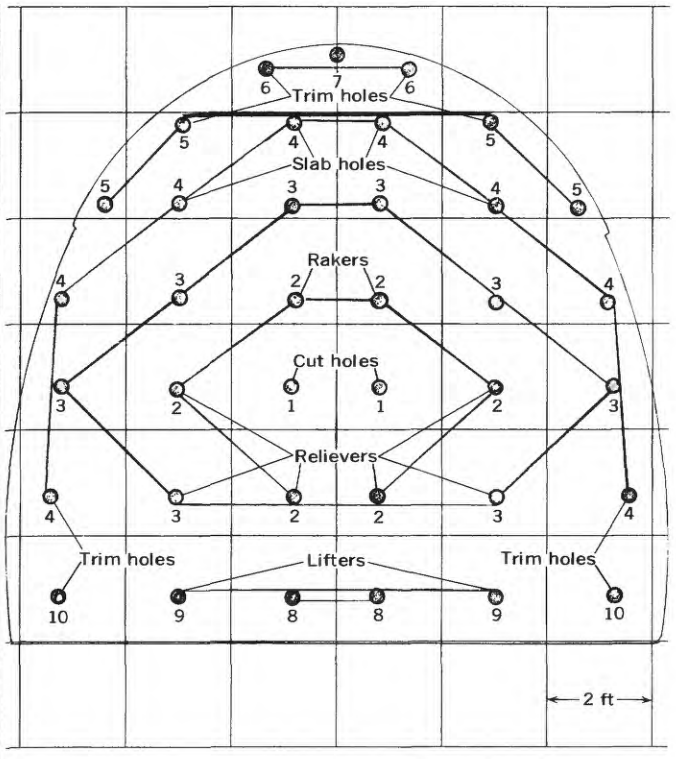

FIGURE 61. — Typical shothole pattern (37 holes), Straight Creek Tunnel pilot bore. Numbers indicate firing sequence.

portal. The original stationing was 38 + 99.4 Ah. = 431 + 23.7 Bk.

Vertical elevations were established on the same steel monuments that were used for the centerline and stationing. Vertical elevations were double checked. The elevation error of closure was 0.21 foot.

Low-order horizontal-distance control was maintained by fixing nails in plaques on the walls every 50 feet. This stationing was used by Highway Department survey teams during each shift for locating the position of the face and steel sets and for calculating the elevation of spads and foot blocks. Also, geologic wall mapping, geophysical surveys, and rock-mechanics instrumentation were referenced to these survey positions. Low-order elevation and centerline control were maintained through the use of spads placed in the back (roof) at 60-foot intervals.

EXCAVATION PROCEDURES

The pilot bore was excavated from one heading, from east to west. A mucking machine and a drill jumbo were placed on the track at the east portal and, on November 14, 1963, construction of surface facilities was begun (fig. 60). Crews worked rapidly to complete the surface installations before the heavy winter snowfalls began.

A normal pilot-bore mining cycle proceeded as follows: On the average, 37 holes, each 5 feet deep, in a pattern typical of that shown in figure 61, were drilled into the face by two drills on the top platform and two drills on the lower platform of the drilling jumbo (fig. 62). Total drilling time for 37 holes averaged 1.5 hours. The holes were loaded with dynamite, the leads were wired, and the shots were fired, typically in the sequence shown in figure 61. These operations required an average of 0.5 hour. After the

FIGURE 62. — Top platform of drilling jumbo, showing two drills in operating position at face. Colorado Department of Highways photograph.

dynamite discharge, the resultant gas and dust were exhausted from the heading area, a process which required about 15 minutes. The broken rock was then mucked and

FIGURE 63. — Muck cars and dump ramp at east portal, Straight Creek Tunnel pilot bore. Colorado Department of Highways photograph.

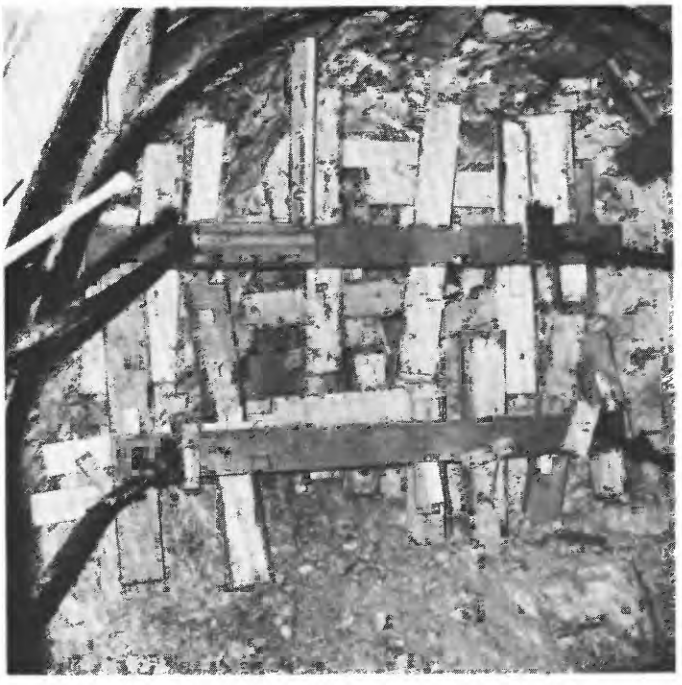

FIGURE 64. — Breast boards and jacks (note bending) in shear zone near station 105+00, Straight Creek Tunnel pilot bore. Colorado Department of Highways photograph.

loaded into muck cars by an air-operated Eimco 40−H mucker. The loaded muck cars were then pulled onto a California switch 600−800 feet back of the heading. A four- or five-car train was assembled and hauled out to the dump area (fig. 63). The side-dump cars were hauled over an eccentric movable dump ramp that elevated one side of each car, unloading it. The mucking operation usually took 1 hour to complete. A geologic section of the face was made during the time the mucking machine was being removed from the heading and while track was being laid to the face. Foot blocks were placed, and their elevation was checked with a transit. The drilling jumbo was pushed back to the heading, where it served as a platform for the installation of the steel sets. In this operation the sets were erected and bolted in place with crown bolts and tie rods, and lagging and blocking were installed as required. The flange in the crown was placed on centerline by a transit observation from centerline points. The average time for installation of the steel sets was 0.5 hour.

The average time needed for the complete mining cycle was about 4 hours, or two cycles per 8-hour shift. The average advance made during normal operation was 10 feet per shift, or 30 feet per day.

In contrast to the normal operation just described, sections in "bad ground" had to be advanced either by short rounds — drilling the bottom and air-spading the back — or by air-spading the entire face, with or without the use of breast boards (fig. 64). The average rate of advance in bad ground was 3.5 feet per shift, or 10.5 feet per day.

Figure 65 illustrates a section of tunnel in incompetent

FIGURE 65. — Squeezing ground in shear zone near station 83+50. Water level in ditch is original grade; the incompetent rock in the floor has been squeezed upward by the stresses acting across the pilot bore. Colorado Department of Highways photograph.

rock and some of the resultant construction problems that slowed the rate of advance in such rock. This section was in squeezing rock near station 83+50. The original grade was

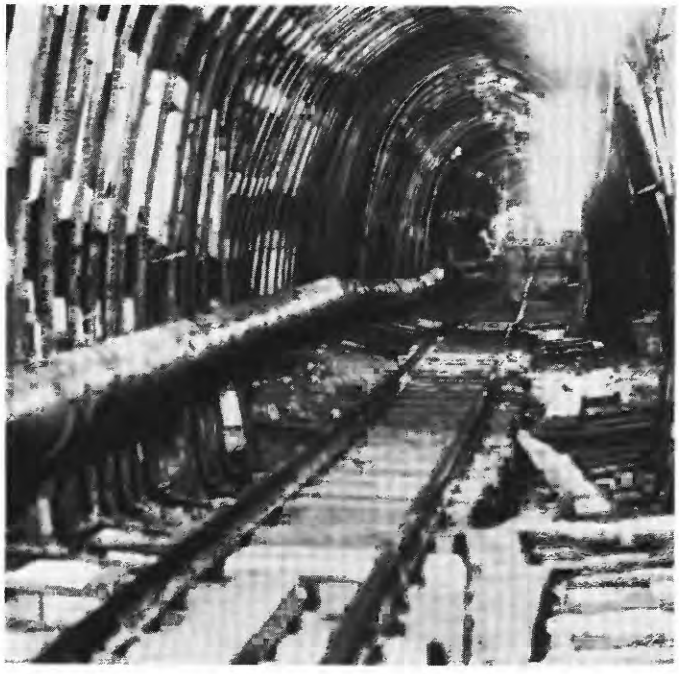

FIGURE 66. — Shear zone near station 83+50 after repair. Note irregularity and deformed condition of sets and track. Colorado Department of Highways photograph.

FIGURE 67. — Timber sets near east portal of the pilot bore. Colorado Department of Highways photograph.

approximately at the ditch-water surface. The sheared rock and fault gouge squeezed upward, forcing the track up about 2 feet. High lateral pressures deformed the steel sets inward. Figure 66 shows the irregularity and deformed condition of the sets. At this time the floor had been regraded, and additional sets with invert struts had been installed in order to withstand the high lateral pressure. This major problem might have been avoided if the initial support had been adequately and speedily blocked and lagged. Time is of great importance in preventing the inward movement of shear-zone material, which, once started, is difficult to control.

The dynamite used in excavating the pilot bore contained 50-percent nitroglycerin by weight. A rule of thumb for the amount of powder used was one stick per foot of hole drilled, or 18.7 pounds per linear foot of tunnel. Ammonium nitrate was used initially, but its use was abandoned because its tendency to absorb water made it ineffective. A total of 168,550 pounds of dynamite and ammonium nitrate was used in excavating the pilot bore. The total volume of material excavated from the pilot bore, inside the B line, was 35,203 cubic yards.

The length of the pilot bore is 8,355.0 feet, of which 2,216.1 feet (26.5 percent) is unsupported, and 6,138.9 feet (73.5 percent) is supported with timber and steel sets.

PILOT-BORE SUPPORT

Initially, the contract requirements for support in the pilot bore specified timber sets, but in December 1963, after 129 feet of the pilot bore had been supported with 8- by 12-inch timber sets (fig. 67), the Colorado Department of Highways, in the interest of speed and economy of tunneling, authorized the use of steel sets.

The first steel sets used in the pilot bore were of 4-inch I-beam, weighing 7.7 pounds per linear foot. These sets had an outside rib radius of 14 feet, 4 inches, and an outside beam (back) radius of 5 feet, 6 inches. These dimensions resulted in a set that was 11 feet high and 12 feet wide at the base. In March 1964, 6-inch H-beam steel sets, weighing 25 pounds per linear foot, were first used to replace 4-inch steel sets that were yielding under load at station 105+21 to station 106+27. The 6-inch steel sets had a radius of 14 feet 6 inches to the outside of the rib and a radius of 5 feet 8 inches to the outside of the beam (back). This set was 11 feet $1^{15}/_{16}$ inches high and 12 feet $3^{13}/_{16}$ inches across the base.

Invert struts were used only in conjunction with the 6-inch steel sets. They had a radius of 28 feet and a length of 11 feet $3^{13}/_{16}$ inches.

In June 1964 the 6-inch steel sets were modified to more nearly match the dimensions of the 4-inch steel, so that jump sets could be installed without additional excavation or removal of lagging and blocking. The modified 6-inch steel sets had a radius of 14 feet 4 inches to the outside of the rib and a radius of 5 feet 6 inches to the outside of the beam (back). The modified invert strut had a radius of 25 feet and length of 10 feet $11^{13}/_{16}$ inches. The 6-inch steel sets with invert struts were used in sections where high rock loads developed, usually in zones of squeezing ground.

The unit weights of the several steel sets were as follows:

Type of steel set	Weight (lb) per foot	Total weight (lb)
4-inch I-beam (without strut) _____	7.7	237.86
6-inch H-beam (without strut) _____	25	744.44
6-inch H-beam modified to 4-inch I-beam size (without strut) _____	25	733.20

The steel sets, in place, were somewhat heavier than these unit weights. The additional weight was due to struts, tie rods, nuts, and bolts and would vary, depending upon the set spacing and the increased length of tie rods. The total weight of steel support used in the pilot bore was approximately 1,270,000 pounds. The histogram on plate 4 shows the location, type, and amount of support used in the pilot bore.

PROGRESS

The pilot bore was driven on a three-shifts-a-day basis for periods of 12 consecutive days of work followed by 2 days off, from October 10, 1963, to July 25, 1964; then for periods of 13 consecutive days of work with 1 day off, from July 26, 1964, to October 23, 1964; and then for periods of 12 consecutive days of work with 2 days off, from October 24, 1964, until the completion of the pilot bore on December 3, 1964. The weekly progress of pilot-bore excavation is shown on plate 4. The average progress for the entire length of the pilot bore was about 142 feet per week.

FEELER HOLES

Feeler holes are holes drilled into and ahead of a tunnel face in order to test for zones of badly broken or crushed rock that might be filled with water. If these zones are located in advance of the face, it may then be possible to seal off the water by grouting and also to consolidate the broken rock prior to tunneling into the zone. The cost of feeler holes is small compared with the cost of recovering a caved face.

In the pilot bore, feeler holes were advanced with air drills to depths of 20–40 feet or more beyond the face. At least one feeler hole was drilled daily, and several were drilled if the geologic and hydrologic conditions indicated adverse conditions. In addition to their major purpose of indicating water conditions, feeler holes in the pilot bore were helpful in detecting abrupt changes in rock conditions. The lengths and locations of feeler holes in the pilot bore are shown on plate 4. A total of 9,816 feet of feeler holes was drilled in the pilot bore. Thus, for every foot of pilot-bore advance, 1.17 feet of feeler holes was drilled.

ROCK-MECHANICS INSTRUMENTATION

The overall objective of pilot-bore instrumentation was the measurement of actual rock mass behavior, including the effect of geologic discontinuities which are seldom present in laboratory-tested rock samples.

The specific objectives of the rock-mechanics instrumentation program that were accomplished are as follows:

1. Measurement of rock loads imposed on steel sets at selected locations in the pilot bore.
2. Determination of the effectiveness of the support system used in supporting the imposed rock loads and in restraining the ground movements initiated by the excavation of the pilot bore.
3. Detection of the presence or absence of progressive deformation of the rock surrounding the pilot bore, including separate measurements of individual wall, roof, and floor convergence movements, as well as total convergence measurements.
4. Location of any active fracture or opening in the rock surrounding the pilot bore that was progressively enlarging or extending and that was detected by the instrumentation used for deformation measurements described in item 3.
5. Measurement of the zone of influence around the pilot bore in which ground movements had been induced by the construction of the pilot bore.

Another original objective of the rock-mechanics instrumentation investigations was to measure the amount, direction, and inclination of any movement in the plane of any fault not exceeding 1 foot in width. Geologic conditions in the pilot bore indicated that such instrumentation would not be significant in relation to the overall scope of the investigations, and, therefore, these measurements were not made.

The mechanical behavior of a large mass of granitic rock, as in the Straight Creek Tunnel area, is governed mainly by its structural discontinuities. Joints, faults, and shear zones have low or nonexistent shear strength. The shear strength of the joints and faults and in the shear zones is strictly dependent upon friction developed along fracture surfaces. Long-term cyclic-loading tests on in place samples are necessary for valid estimates of the mechanical properties of a rock mass. The most useful tunnel measurements are those taken over a sufficient distance to include a representative sampling of the joints and other discontinuities. Representative sampling is especially important at the Straight Creek Tunnel site because most rock-mass deformations are a result of movement across or along discontinuities. The time-strain effects must be measured.

Three types of rock-mechanics instruments — load cells, borehole extensometers, and bar extensometers — were used in the Straight Creek Tunnel pilot bore; these are discussed in the following sections.

LOAD-CELL MEASUREMENTS

The most common temporary support used in tunnels in the United States is the structural steel arch. Measurements of the compressive loads on such supports provide a direct means of comparing actual rock loads with the steel-support

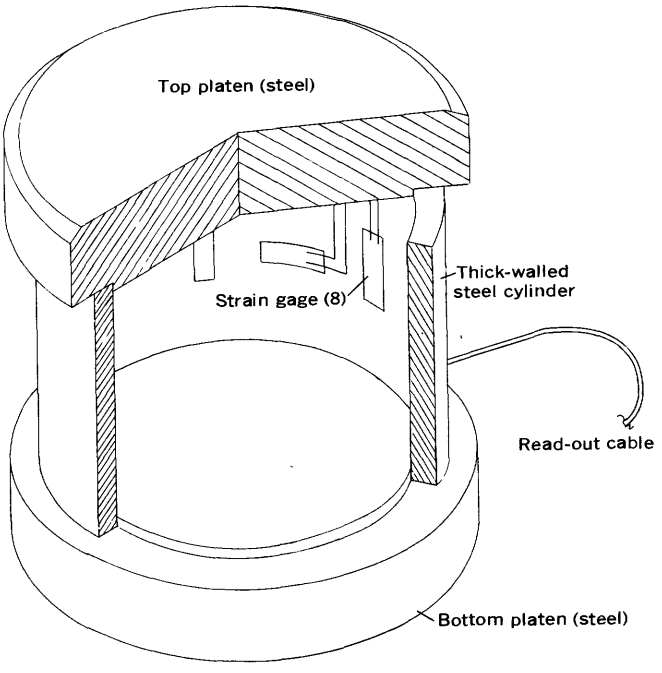

FIGURE 68. — Schematic diagram of load cell used in the Straight Creek Tunnel pilot bore.

design strength. Load cells with a load capacity equal to the yield strength of the supports were used in the present investigation. In the pilot bore, both 4- and 6-inch-diameter load cells were installed. The 4-inch-diameter cell has a normal load-design capacity of 120,000±40, and the 6-inch cell has a capacity of 300,000±100. The load cells are designed to withstand high humidity, submersion in water, blasting shocks, and general rough handling. The 4- and 6-inch cells are similar in design. Figure 68 shows the construction of a load cell used in the pilot bore. The load cells consist of a thick-walled steel cylinder with heavy steel platens sealing the ends. Eight SR−4-type strain gages are cemented symmetrically around the inside wall of the steel cylinder. The wires from the strain gages are connected to a read-out cable, which is conducted to the outside of the cell through a watertight opening. The strain gages produce an electrical response to a current that is proportional to distortion of the gage due to the applied stress. Each cell was calibrated in a press before installation. After installation in the pilot bore, the strain gages were read periodically with a hermetically sealed portable read-out unit, and the loads were calculated from the calibration charts.

Load cells were installed under the base plate of the steel sets in the pilot bore. In zones of squeezing rock, specially modified sets with invert struts were used, and additional load cells were placed in the strut and in the crown. The locations of load cells are shown in figure 69. Load cells placed under the set legs were designed to obtain the vertical-load component, and load cells placed in the crown measured the horizontal-load component. The two cells in

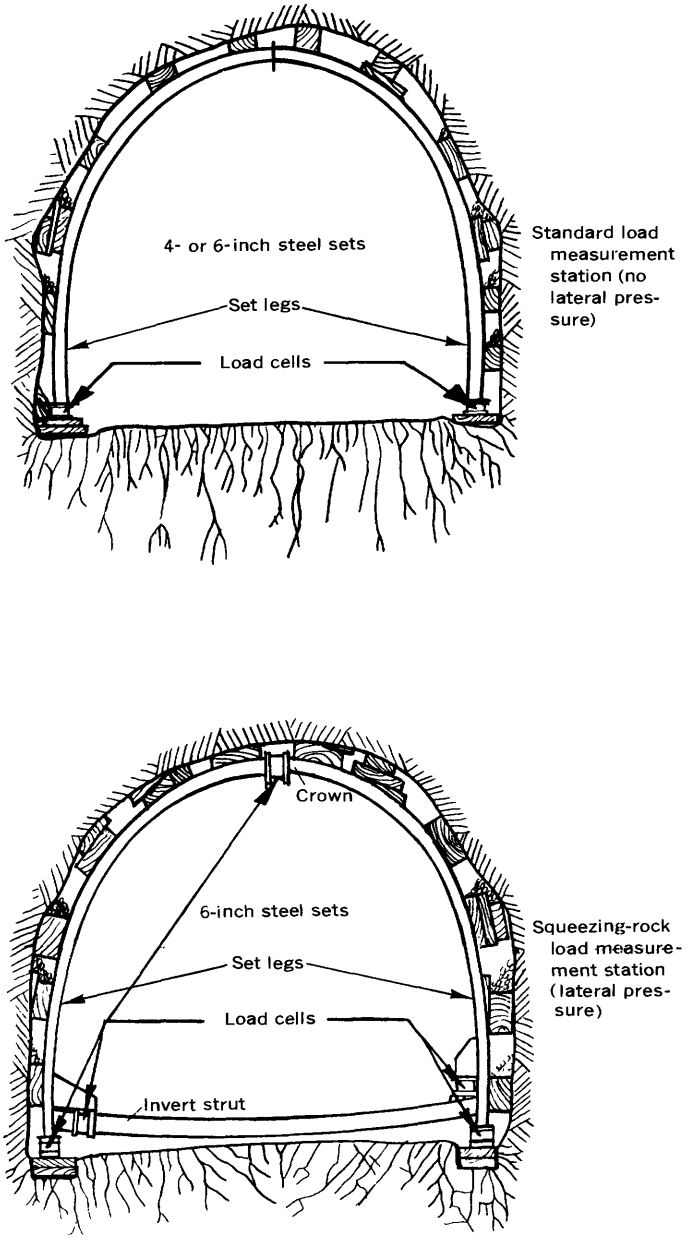

FIGURE 69. — Sketches showing typical load-cell installations, Straight Creek Tunnel pilot bore.

the invert strut are designed to measure both uplift on the strut and the horizontal-load component at invert (floor) level. Of the 37 steel sets that were instrumented with load cells, 11 contained an invert strut. The instrumented sets were at many different locations, and the information obtained reflected the entire range of geological conditions in the pilot bore. Experience has shown that it is desirable to instrument two or three consecutive sets in order to reduce the influence of nonuniform engineering-construction practice, such as blocking and lagging irregularities. This procedure also helps reduce the effect of local rock-mass anisotropy, permitting more realistic average load deter-

minations. For these reasons, six pairs of two consecutive sets and two groups of three consecutive sets were instrumented.

The vertical set loads were calculated from the equation:

$$L_v = \frac{V}{ws},$$

where

L_v = vertical load, in pounds per square foot;
V = sum of vertical loads at a specific time measured by the load cells under each leg of the set, in pounds;
w = width of tunnel opening, in feet; and
s = sum of one-half the distance between instrumented set and adjacent set on either side, in feet.

The horizontal loads for those sets that contained load cells in the crown and in the invert strut were calculated from the equation:

$$L_h = \frac{H}{hs},$$

where

L_h = horizontal load, in pounds per square foot;
H = sum of horizontal loads at a specific time measured by the load cells in the crown and between the invert strut and the set leg, in pounds;
h = height of tunnel, in feet;
s = sum of one-half the distance between instrumented set on either side, in feet.

Figure 70 illustrates a typical group of load curves from a set with instrumented crown and invert strut in squeezing ground. Figures 71–73 give the maximum and stable vertical set loads recorded by the load cells installed in the Straight Creek Tunnel pilot bore and the maximum and stable vertical rock loads calculated from the load-cell records.

Load cells were installed as close as practicable (usually within 20 ft) to the pilot-bore face at the time the steel set was installed in order to record the entire set-loading history. The use of short signal-wire lengths and a portable battery-powered read-out unit eliminated the possibility of blast damage to long signal wires and stationary read-out equipment. Load cells were normally removed after load stabilization had occurred. The time required for load stabilization varied greatly and was dependent mainly upon geological conditions and engineering-construction procedures. In the pilot bore, load-stabilization time ranged from 400 to 2,250 hours. Some instrument stations equipped with load cells were kept in operation throughout the entire period of construction. The shear zone in the vicinity of station 84+00 is typical of the extended-observation stations. Such areas required a longer time for stabilization and showed minor load readjustments long after initial load stabilization. These long-term measurements were desirable for revising design criteria for steel support and concrete lining in the enlarged bore. The amount of time (or distance from the face) required for load stabilization in the pilot bore proved to be much greater than had been estimated by applying elastic theory.

BOREHOLE EXTENSOMETERS AND ROCK-MASS MOVEMENTS

The excavation of rock material removes rock support and disturbs the rock-mass equilibrium. When rock is removed from the bore, a new condition develops, owing to the partial removal of the vertical and horizontal restraint from the rock surrounding the opening. The effects of this disequilibrium are of great concern to tunnel-construction engineers.

A primary objective of the instrumentation program was the measurement of the zone of influence around the periphery of the pilot bore throughout which ground movements (deformation) had been induced by excavation of the bore.

The movements in the rock mass surrounding the pilot bore were measured to establish where the loads on the steel supports had originated and to determine the duration and frequency of movements.

The interface between the tension (loosened) zone and the compression (compacted) zone surrounding the pilot-bore opening was termed (Fenner, 1938) the "stress-free," or "destressed," zone (fig. 76). The rock below this destressed zone must be restrained by a tunnel-support system in order to maintain a safe tunnel opening. The rock below the destressed zone may be in a state of tension, or it may contain tensile stresses within it. The jointed nature of most rock masses reduces the tensile strength and cohesion; therefore, all or part of this material must be restrained by the tunnel-support system. Strain-gradient measurements derived from multiple-position borehole extensometers at various points within the rock mass around the pilot bore established the limits of the destressed zone. This information also allowed the determination of the stress-disequilibrium time.

The length of time during which the equilibrium in the rock mass surrounding the pilot bore was disturbed depended on the rate of progress of excavation, geological conditions, and the mechanical behavior of the rock mass surrounding the opening. More competent rock-mass zones generally had a shorter equilibrium-disturbance time than did the less competent rock, inasmuch as the excavation-induced stresses were more quickly redistributed to the walls of the pilot bore in zones of competent rock. The equilibrium disturbance immediately followed the active (advancing) pilot-bore face and was characterized by extremely high support loading, which resulted from rock-mass deformations on the order of 0.2–0.5 inch of maximum movement. These small movements are normally sufficient to cause high stresses in the wall zones near the face

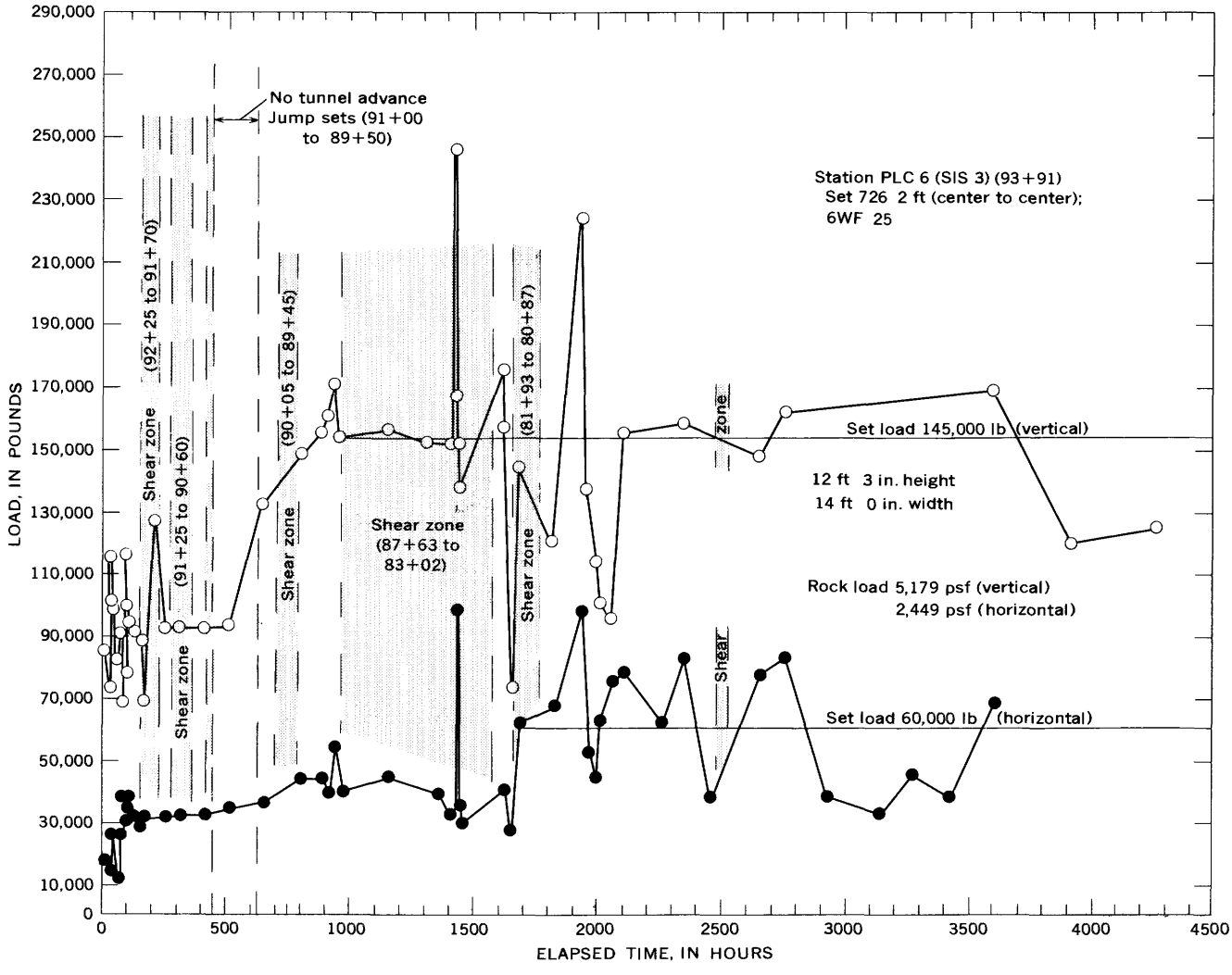

FIGURE 70. — Typical load-history curves.

of the pilot bore. Rock movements ceased, for all practical purposes, when the load formerly supported by the excavated-rock material was transferred to the walls and steel sets. However, the disturbed rock contained in the loosened zone was in a new equilibrium condition that was commonly highly unstable. Certain construction practices — such as stopping excavation at the face, reblocking, and replacement of steel sets — triggered new episodes of rock movement in which rock loads exceeded previous maximum loads.

The geometric shape of the tunnel opening also influences the amount of material in the loosened zone. The effect on the tunnel-support system of irregularities in the tunnel cross section, perhaps due to overbreak or underbreak, can be monitored by borehole extensometers. Multiple-position borehole extensometers, which made measurements soon after each advance of the pilot-bore face, yielded information regarding the formation and location of the tension-compression-zone interface, thus allowing the monitoring of stabilization or failure trends as the excavation proceeded.

Most present knowledge regarding rock-mass behavior during tunnel construction has come from the analysis of measurements obtained from single- and multiple-position borehole extensometers. Single-position extensometers are useful primarily in the analysis of the total rock-surface extension or contraction and the restoration of rock-mass stability. These simple extensometers provide information on two separate points within a borehole. The point at the bottom of the borehole was assumed to be fixed, although this was not always true. The point at the collar of the hole was assumed to move in reference to the point at the bottom of the hole.

Although single-position instruments have yielded valuable information, the recently developed multiple-position borehole extensometers yield much more useful data from a single borehole. Figure 74 shows the construction of an eight-position multiple-anchor borehole extensometer. Measurements made with this extensometer are particularly useful in boreholes in a tunnel roof (back) zone. This type of placement can determine the dimension and

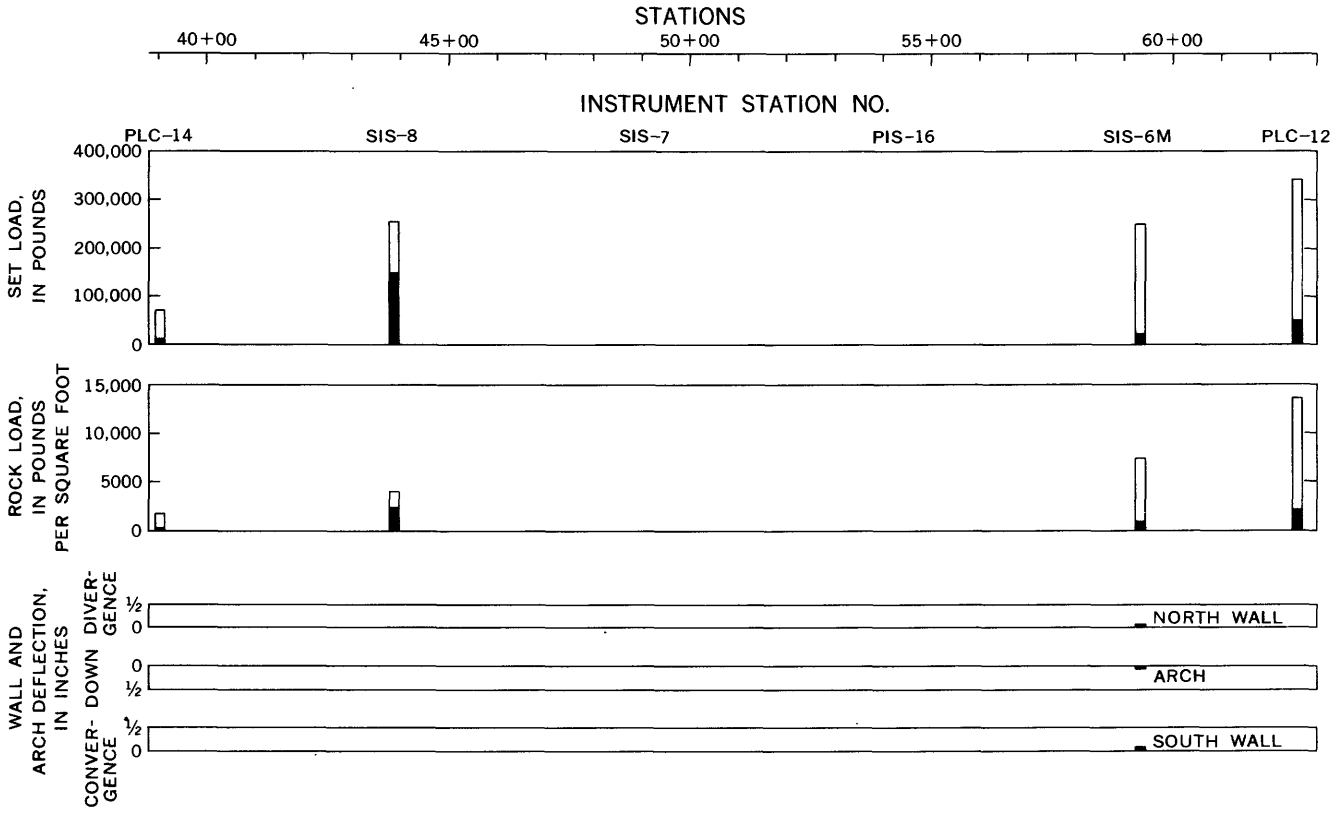

FIGURE 71. — Maximum and stable loads and convergence measurements, station 39+00 to 65+00. Data from Terrametrics, Inc. Black bar, stable load; open bar, maximum load. Instrumentation stations include prop-load (PLC), single-position borehole extensometers and prop-load cells (PIS), and multiple-position borehole extensometers and prop-load cells (SIS).

shape of the tension zone by analyzing a series of strain gradients obtained as the face advances. Rock loads can be estimated from these data, and the measurements of the extent of the loosened zone can also be used to calculate the maximum potential rock loads for use in the design of the tunnel lining. The degree of stabilization of the surrounding rock mass after stress redistribution can readily be determined at all eight points.

The multiple-position borehole extensometer used in the pilot bore by Terrametrics, Inc., provides eight fixed points and a sensing head that can measure remotely, to an accuracy of at least 0.001 inch, the axial relation of the anchors to the sensing head (fig. 74). Measurements taken successively with time and face advance provide the basis for plotting rock-mass strain gradients. Major faults and shear zones penetrated by the instrumented borehole can also be located. All movements are measured in relation to the sensor head by means of wire under tension connected to each anchor. The instrument system consists of a special spring-wedge anchor, high-modulus stainless steel wire, and instrument housing for supporting flat-blade cantilever springs for each wire and anchor. The cantilever blades apply a continuous tension to the movement wire. Cantilever deflection is measured by a transducer, here a bonded SR−4 strain gage, attached to the cantilever. The measurement range of the instrument can be changed by varying the cantilever length and the modulus of elasticity of the wire. Some minor nonelastic deformation occurs in the wire, but the amount can be readily calculated and included in the instrument-calibration factor prior to calculation of anchor displacement. The instrument-calibration factor is based on the design characteristics of the cantilever spring, the strain gages, and the stainless steel wire used. After installation of the extensometer, a null reading is taken with a portable read-out unit — the same read-out unit used for the load cells — and is used for reference for future readings. After installation, the relative motion of any two anchors can be obtained by simple subtraction of the results of two successive sets of readings.

Borehole extensometers were installed at 24 locations in the pilot bore (figs. 71−73). Generally, one 25-foot vertical hole and two 25-foot horizontal holes were drilled as close to the face as possible (usually within 50 feet); however, because of unfavorable geologic conditions, some holes were less than 25 feet long. At later stages in the instrumentation program, one hole was drilled vertically and two or more holes were drilled 30°−60° from the vertical. The drilling, by percussion drills on the drilling jumbo, was done at the

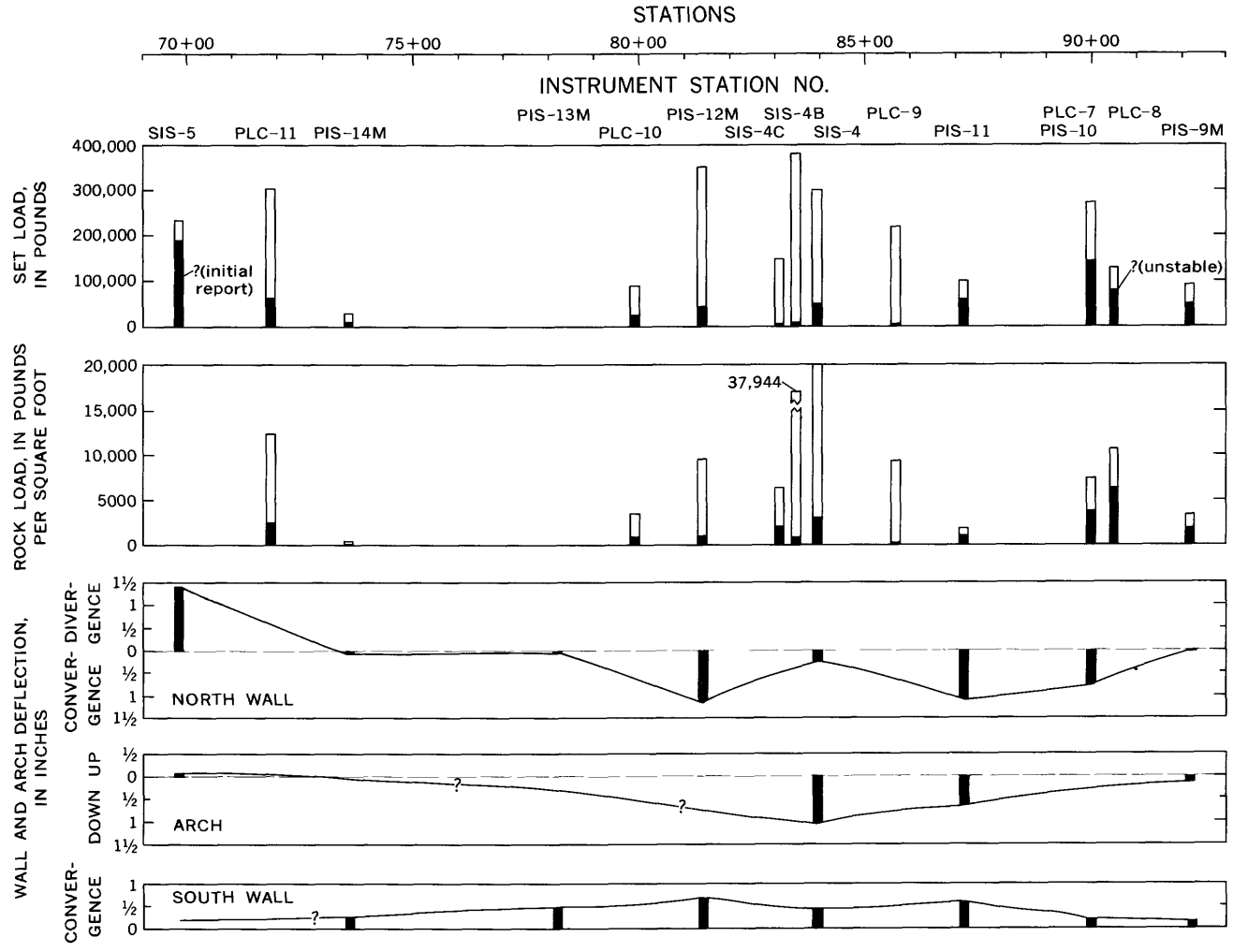

FIGURE 72. — Maximum and stable loads and convergence measurements, station 65+00 to 93+00. Data from Terrametrics, Inc. Black bar, stable load; open bar, maximum load. Sta. PIS15M, no data. Instrumentation stations include prop-load cells (PLC), single-position borehole extensometers and prop-load cells (PIS), and multiple-position borehole extensometers and prop-load cells (SIS).

end of the swing shift (4 p.m. to 12 p.m.) on Saturday nights, and the borehole extensometers were installed as soon as was practical after drilling had been completed. Measurements were taken on the borehole extensometers until the surrounding rock mass became stabilized. Some extensometers were maintained in service until construction of the pilot bore was completed.

Of the 24 borehole-extensometer stations, single-anchor extensometers were used at 12 stations, and multiple-anchor extensometers at 12 stations. Figure 75 is a typical graph of the strain-rate-change curves of a set of single-anchor extensometers with time and figure 76 is a typical graph of the strain distribution at a multiple-anchor extensometer station. Table 27 gives the total roof and wall deflection at each multiple-anchor borehole-extensometer station in the pilot bore at the time of load stabilization or at the last reading made.

TABLE 27. — *Depth of maximum wall and roof deflection at multiple-position borehole-extensometer stations*

[Leaders (_ _) indicate no data collected]

Station	Deflection (ft)		Station	Deflection (ft)	
	Wall	Roof		Wall	Roof
114+53	20	18	73+58	_ _	6
104+83	25	20	69+81	_ _	22
93+90	25	_ _	65+94	_ _	6
92+20	_ _	18	59+35	20	21
83+93	_ _	20	49+27	_ _	24
81+41	_ _	11	43+87	27	18

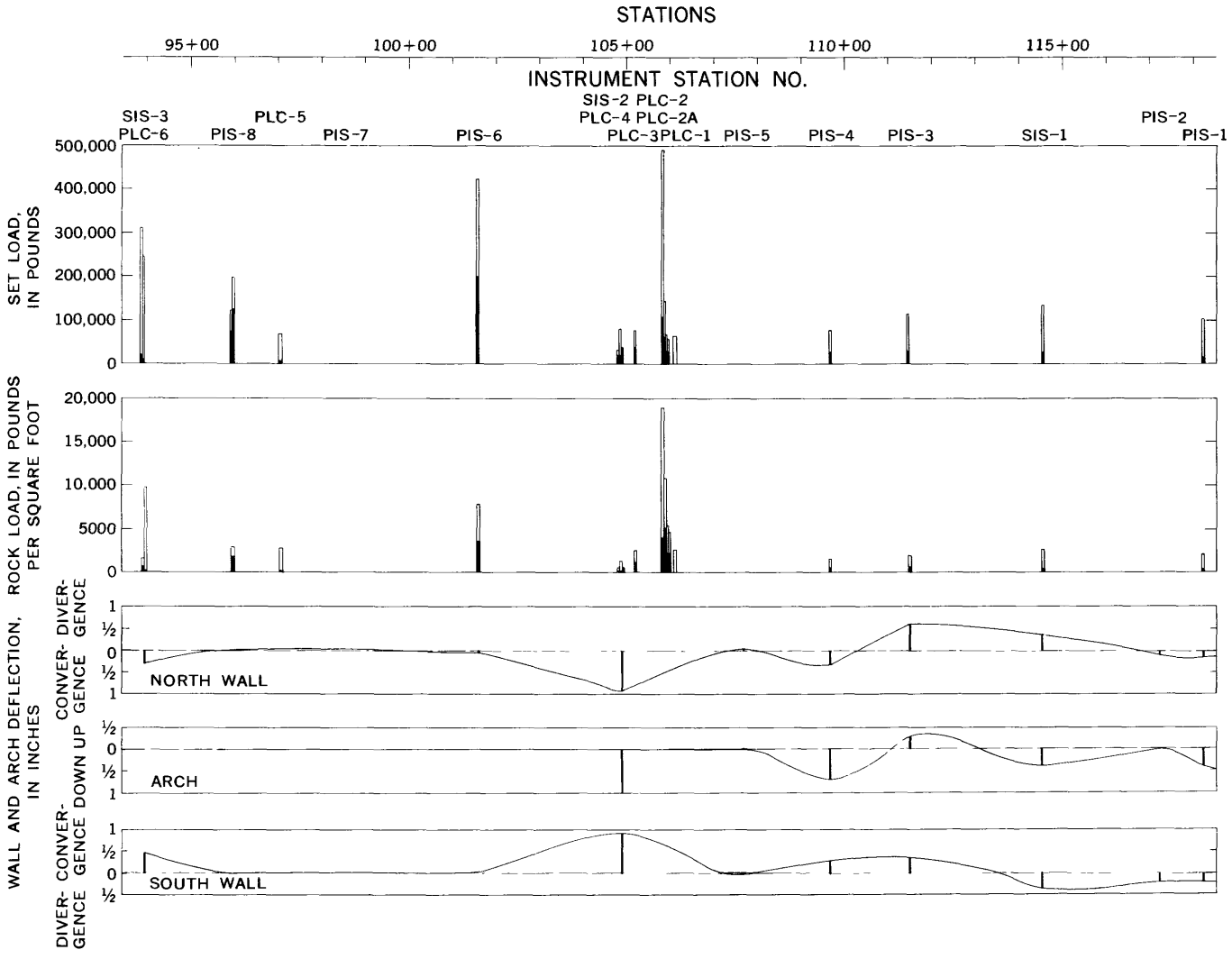

FIGURE 73. — Maximum and stable loads and convergence measurements, station 93+00 to 120+00. Data from Terrametrics, Inc. Black bar, stable load; open bar, maximum load. Instrumentation stations include prop-load cells (PLC), single-position borehole extensometers and prop-load cells (PIS), and multiple-position borehole extensometers and prop-load cells (SIS).

BAR EXTENSOMETERS

Bar or rod extensometers, among the earliest rock-mechanics equipment used in underground excavations, are simply constructed and relatively inexpensive. Measurements are made with a calibrated bar between reference points — short rock bolts or steel pins set in the rock in pairs opposite each other. One pair is set in the roof and floor and the other pair in opposite walls of the tunnel. A stainless steel ball or cap is threaded on the rock bolts or steel pins. The bar extensometer consists of an adjustable, calibrated bar, generally of stainless steel, that has known thermal expansion characteristics and is fitted with a micrometer dial. The bar length is approximately equal to the tunnel diameter. Convergence or divergence of the tunnel walls may be detected by shortening or lengthening, respectively, of the bar.

Eight instrument stations in the pilot bore were equipped with bar-extensometer pins. Measurements made periodically during the construction of the tunnel were considered to be accurate to ±0.03 inch.

Although bar-extensometer measurements of pilot-bore geometric changes had originally been planned for the entire length of the bore, this instrumentation was discontinued after about 3,000 feet because the measurement

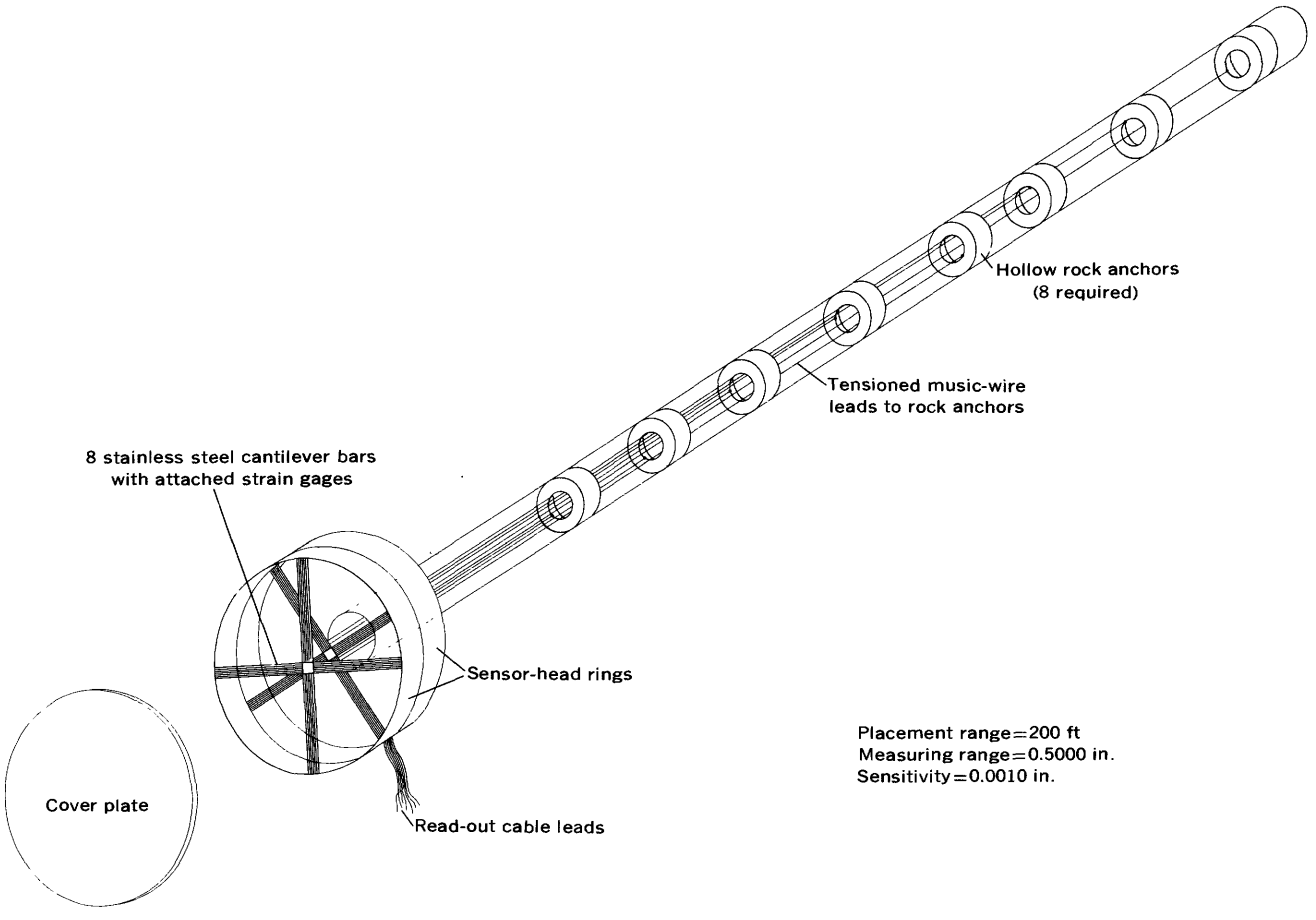

FIGURE 74. — Eight-position multiple-anchor borehole extensometer of the type used in the Straight Creek Tunnel pilot bore.

reproducibility of the instruments over the time interval required was considered to be too erratic. Data on significant changes in tunnel geometry that had been noted with the bar extensometer, it was believed, could have been obtained as easily and as accurately with an engineering pocket tape, graduated to 0.01 foot. Because the measuring points are on rock surfaces, the apparent changes in tunnel diameter may be due entirely to surficial joint-block movement, unrelated to the rock-mass behavior at depth. In general, the borehole-extensometer measurements were much more reliable and significant.

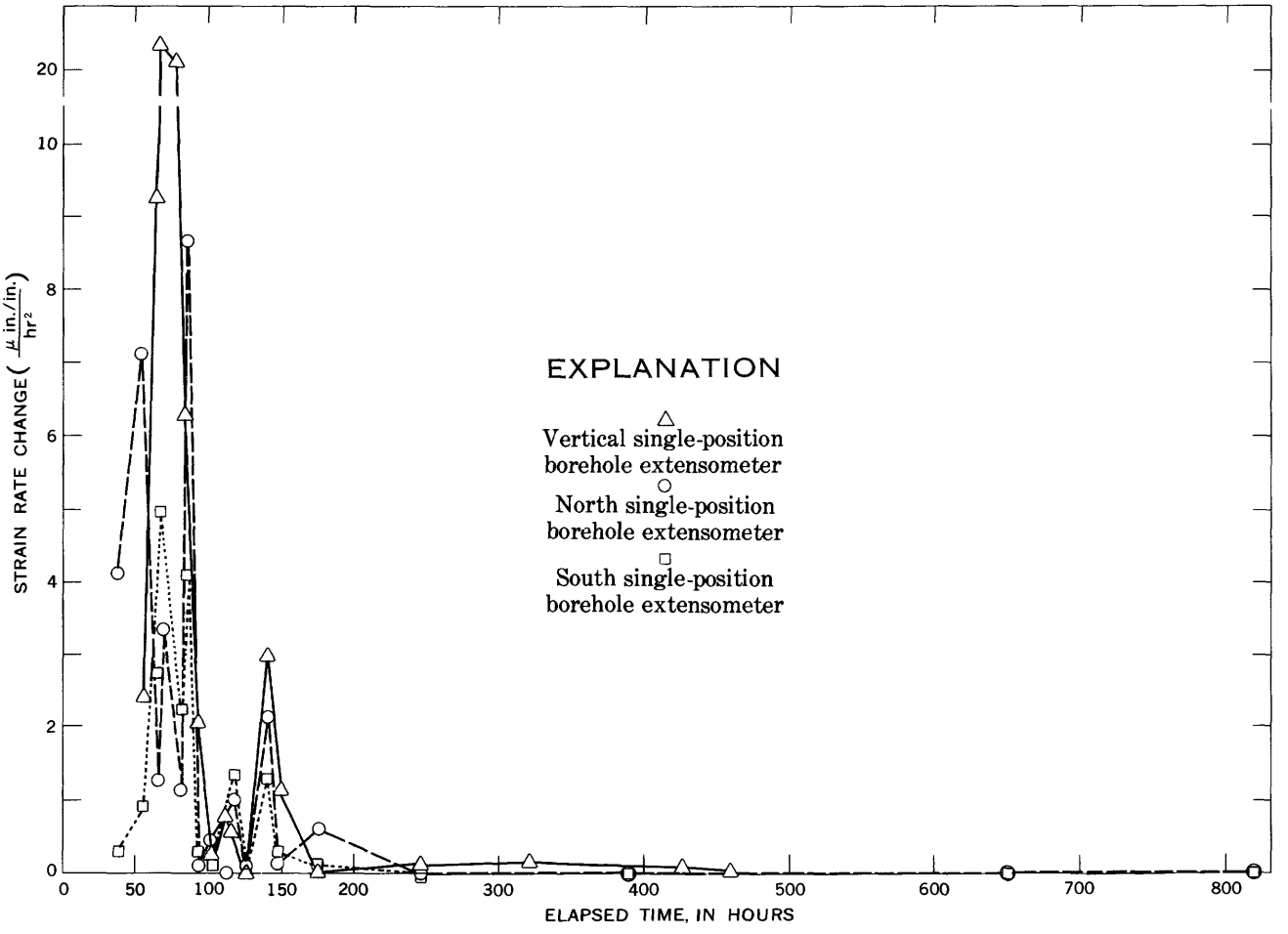

FIGURE 75. — Typical strain-rate-change curves from a single-position borehole-extensometer station, PIS11, located at 87+17. Stability was attained in 245 hours, after an advance of 192 feet (average advance rate 0.78 ft per hr).

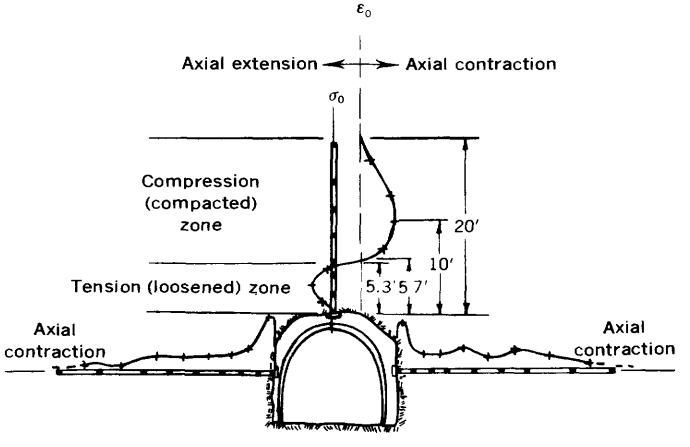

FIGURE 76. — Typical strain-distribution curves from a multiple-position borehole-extensometer station, showing stress-strain zones in walls and roof of pilot bore. ϵ_0, no strain change; σ_0, zero stress. Axial contraction indicates compressive stress; axial extension indicates tensional stress.

Statistical Analysis of Rock Loads

By JOHN F. ABEL, JR., *and* FITZHUGH T. LEE

ENGINEERING GEOLOGIC, GEOPHYSICAL, HYDROLOGIC, AND ROCK-MECHANICS INVESTIGATIONS OF THE STRAIGHT CREEK TUNNEL SITE AND PILOT BORE, COLORADO

GEOLOGICAL SURVEY PROFESSIONAL PAPER 815–G

STATISTICAL ANALYSIS OF ROCK LOADS

By JOHN F. ABEL, JR., and FITZHUGH T. LEE

As the pilot-bore investigation progressed it became evident that a computer would be invaluable in handling the large mass of geologic, geophysical, and engineering-construction data that was accumulating. The need for a computer was also recognized from the preliminary finding that measured rock loads had no simple correlation with geology and construction practices. Although it seemed reasonably obvious that fracture spacing, alteration, and several construction variables were the major factors responsible for the variation in loads imposed on the steel sets, it was believed that other, more subtle variables contributed to the measurements and should be analyzed. Statistical techniques were therefore initiated with the hope of establishing a valid conceptual and mathematical model (equation) for predicting rock loads in the Straight Creek Tunnel pilot bore. The findings of Abel (1967, p. 15–69) are reported here in a modified, somewhat condensed form, inasmuch as he had started a similar program, which utilized similar data and methods, as part of his doctoral dissertation at the Colorado School of Mines. A close collaboration between us during and after the period of pilot-bore construction assured mutual confidence in the findings.

ROCK LOAD

Rock load is an engineering-design concept related to the uniform load acting on the area of tunnel walls and roof that is supported by an individual steel set. As such, it is a measure not of load, but of pressure, in pounds per square foot. The set load, which is measured, does not indicate the area of the tunnel roof that is supported by an individual set. The use of the term "rock load" for a rock pressure originated with Terzaghi (1946, p. 47), who stated that "the term rock load indicates the height of the mass of rock which tends to drop out of the roof." This height of rock results in a rock load — actually a rock pressure, in pounds per square foot — which the steel sets are designed to support. The term "rock load" is used in this report in its commonly accepted meaning of rock loading pressure. This use is made for clarity in understanding by the engineers and geologists who work in the field of tunnel-support design and construction.

Rock load can be determined by measuring the set load, estimating the area of the roof supported by the set, estimating the density of the rock mass, and calculating the height of a column of rock that would result in the measured set load. In practice, where the density of the rock mass is so variable, as in the Straight Creek pilot bore, the calculated rock load, in pounds per square foot, is used without calculating the equivalent-height rock column. This method for determining rock load is shown in figure 77.

ROCK-LOAD HISTORY

The rock-load history for a typical set in the Straight Creek Tunnel pilot bore follows a definite pattern. This pattern is related to the mechanism of transfer of the vertical and horizontal rock loads from the rock in the advancing pilot-bore face to the rock in the roof, walls, and floor. This pattern is described as follows:

1. The steel set supports are placed and blocked close to the load-bearing face. These blocking loads are negligible (3,000–7,000 lb) compared to peak (as much as 700,000 lb) or stable set (as much as 550,000 lb) loads.
2. As the pilot-bore face is advanced away from the instrumentation station by the blasting of successive rounds, the support effect of the face decreases, and the horizontal and vertical rock load is progressively transferred from the face to the rock adjacent to the station.
3. The rock in the walls of the pilot bore strains in response to the application of this load; as a result, the roof lowers, and the walls deflect.
4. The steel supports attempt to prevent the deformation of the rock mass resulting from the transfer of the vertical and horizontal rock loads.
5. The steel sets are plastically deformed or the blocking is crushed by this transfer of rock loads. This deformation is a result of the disparity between the load-carrying capacity of the steel set or of the blocking and the load-carrying capacity of the rock removed from the pilot bore.

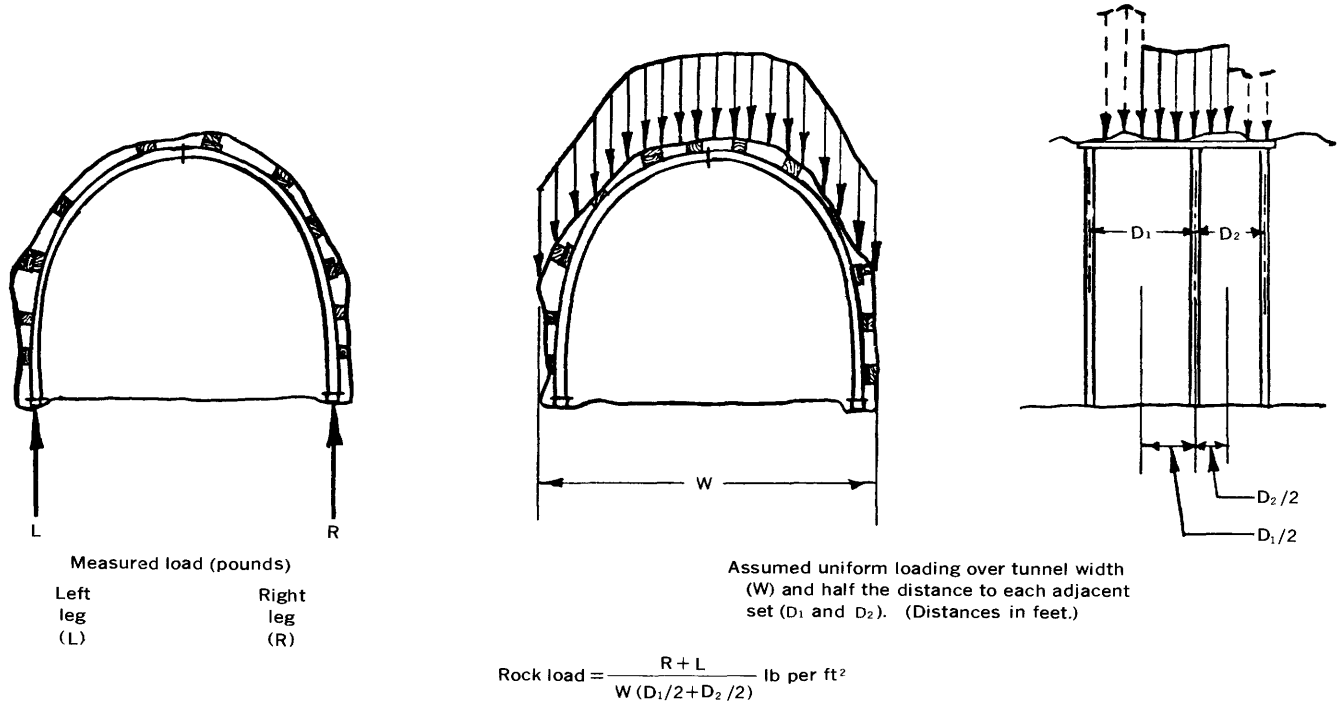

FIGURE 77. — Bases for rock-load calculation.

6. A period of peak loading results from the increased load on the sets as the strain of the adjacent rock mass increases. When the plastic yield stress of the steel is reached, or when a part of the blocking crushes, this set overload is removed. This cycle of overload and release may be repeated many times during the period of dynamic load transfer and rock strain. The magnitude of each set overload peak is different because each cycle of steel-set plastic deformation or of failure in the blocking changes the set loading configuration. The set loading configuration, in turn, determines the total vertical and horizontal rock loads the set can carry before yielding.
7. When dynamic rock strains cease or become negligible, the set loads reach an initial stabilization.

Steel sets cannot be economically designed to take the place of the rock removed. They should be designed for the stable loads determined from a load-history curve; peak loads are not the critical factor. A steel set (1) should continuously support the loosened rock above and to the sides of a tunnel, and (2) should yield, or the blocking points should crush, under a set overload, yet still support the loosened rock. A rigid steel set, on the other hand, is not designed to yield under peak loading; therefore, either the blocking is crushed or the steel set is plastically deformed, which can result in collapse of the steel set and loss of the opening.

The load-history curves (fig. 70) plotted from pilot-bore data illustrate that the preceding seven-point description of rock-load response is a simplification of a more complex set of conditions. The stable load, which occurred at the time of initial rock-strain stabilization, was subject to later changes, many of which were apparently related to the penetration of shear zones by the pilot bore.

When the pilot bore penetrated a major shear zone, a set-load response resulted along the tunnel for distances of as much as 2,500 feet. This load response moved progressively down the pilot bore, away from the face. It passes through unsupported sections and was recorded by instruments monitoring sets on the far side. Other conditions that apparently affected the stable set loads were (1) blast damage to one set that triggered set-load readjustment on nearby sets, (2) set replacement or reblocking that reactivated set loads for great distances along the pilot bore, particularly where the set replacement or reblocking was in a shear zone, (3) sudden failure of blocking or lagging at one point in a shear zone that resulted in changes in nearby set loads, and (4) removal of rock from a shear zone, in an attempt to relieve set loads, that resulted in futher set-load adjustments. Also, some rock-strain and set-load responses may have been triggered by vibrations. Blasting vibrations were probably significant near the pilot-bore face, but the muck train was the major source of vibrations at greater distances from the pilot-bore face.

The set-load histories (fig. 70) show that most of the foregoing conditions resulted in heavier set loads because of the fact than any rock-mass adjustment adjacent to the pilot

bore necessarily involved a progressive deterioration of that adjacent rock mass.

The conclusion to be drawn from the analysis of set-load response is that the entire tunnel-support structure was affected by the changes in lithology and tunneling practice described previously. Changes in set loads at one point in the tunnel resulted in load adjustments up and down the pilot bore. The extent of these adjustments depended on the proximity and magnitude of the initiating condition, on the geologic conditions, and on the in-situ stress field.

CALCULATION OF ROCK LOADS

The length of tunnel supported by any one steel set was estimated to be half the distance to the adjacent steel set on each side. The method of estimation used introduces a dispersion in the rock loads calculated from the measured set loads. The load borne by a steel set and, therefore, the area supported by this steel set are controlled partly by the way the set is blocked. As it was not economically feasible to determine the load applied to the set at each blocking point, it was not possible to critically define this important parameter. The influence of this variable can be seen in part by comparing the set loads in figure 78. Three adjacent 4-inch I-beam (7.7 lb per ft) steel sets are shown. The only major variations apparent for these sets were the set loads and the number of blocking points. The effectiveness of the individual blocking points is the probable explanation for the variations in the calculated rock loads. Given a sufficient number of measurements of set loads, this dispersion of individual rock loads should be compensated for, and, in fact, such a compensation occurred.

Rock load, in pounds per square foot, is the dependent variable in the statistical model that was developed. Once the rock load is known or predicted, the set spacing can readily be specified by using the elastic-steel-design charts by Proctor and White (1946, p. 219–232).

OBSERVATIONS USED

Of the 44 instrument stations for which the geologic and construction parameters were available, only 33 stations were used in developing the statistical model of rock load. Eleven stations were rejected for the following reasons:

1. The last station in the pilot bore, near the west portal, was located in talus and morainal material; therefore, the geologic parameters were not applicable to it.
2. Five stations were rejected because the dependent variable — rock load — did not stabilize during the period of measurement.
3. Two stations were rejected because the sets were jump sets. A jump set, installed long after excavation, is used between two sets already in place to prevent destruction of the original sets by loads greater than those predicted at the time of excavation and construction. The area supported by a jump set cannot be estimated accurately if the original sets are of different size than the jump sets, and (or) if the original sets are still carrying some of the rock load.
4. Two stations were rejected because of changes in their configuration after installation. At one station an invert strut was placed only on the instrumented set and not on the adjacent sets; this probably prevented a meaningful estimate of the area supported by that set. At the other station, the steel set was severely damaged by blasting. The load carried by that set was clearly anomalous to similar undeformed sets.
5. One set was rejected because its invert strut was deformed by the rock load and later had to be replaced. The pilot bore had been completed and the

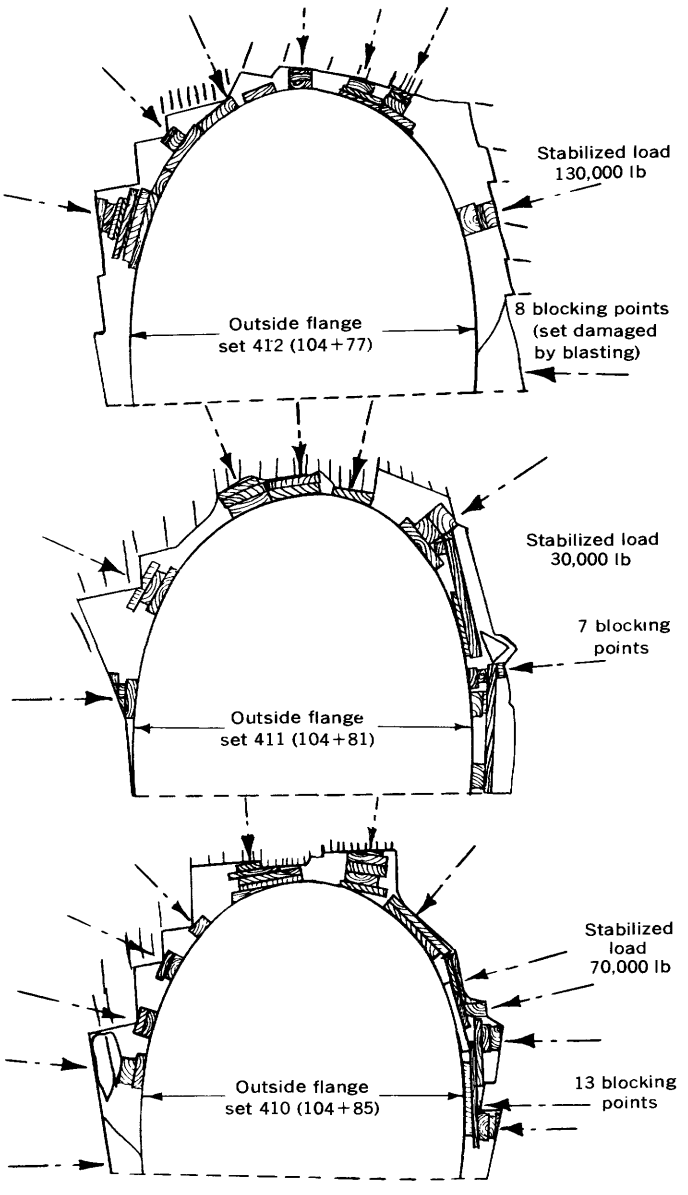

FIGURE 78. — Typical blocking diagrams.

load cells had been removed before a stable set load could be determined after replacement.

Table 28 presents the stabilized rock loads and data for other variables for all 44 instrument stations in the Straight Creek Tunnel pilot bore. Seven of the instrument stations were located where no steel sets were installed, but, inasmuch as other instrumentation was used at these stations and all the geologic variables were determined, they are included in the rock load analysis. They are important as a limiting condition for any such analysis. Of the 44 stations, 17 used 4-inch I-beam (7.7 lb per ft) steel sets, and 20 used instrumented 6-inch wide flange (25 lb per ft) steel sets, eleven of which included invert struts, which permitted the measurement of horizontal, as well as vertical, rock loads.

TABLE 28. — *Rock loads and geologic and construction data*

[Leaders (_ _ _) indicate no data collected]

Station[1]	Rock load[2] (psf)	Fracture spacing (ft)	Alteration (percent)	Water condition (percent of greatest inflow)	Average fracture dip (degrees)	Rock type (granite = 0, metasedimentary rocks = 1)	Degree of faulting (percent of most intense faulting)	Distance to nearest fault (ft)	Thickness of nearest fault or shear zone (ft)	Depth from surface (ft)	Steel section modulus[3] (in.^{3})	Number of effective blocking points	Horizontal rock load (psf)
118+24	256	0.60	10	20	60	0.10	20	2	2.00	140	3.0	6	_ _ _
117+21	0	1.20	0	10	70	.10	10	5	.10	170	0	0	_ _ _
114+53	450	1.00	5	40	70	.00	0	23	2.00	270	3.0	8	_ _ _
111+48	452	.70	5	20	50	.80	40	2	1.50	400	3.0	6	_ _ _
109+66	487	.80	0	10	85	.10	40	10	.10	480	3.0	8	_ _ _
107+65	0	1.60	0	10	70	.10	20	5	.50	550	0	0	_ _ _
105+82	7,308	.05	75	100	45	.80	100	0	80.00	630	16.8	14	2,708
105+80	7,692	.05	75	100	45	.80	100	0	80.00	630	16.8	14	7,708
105+18	1,538	.30	5	20	75	.10	40	17	6.00	660	3.0	10	_ _ _
104+85	1,334	1.00	5	0	60	.10	40	3	.50	670	3.0	13	_ _ _
104+81	524	1.00	5	0	60	.10	40	3	.50	670	3.0	7	_ _ _
104+77	2,267	1.00	5	0	60	.10	40	3	.50	670	3.0	8	_ _ _
101+59	3,056	.70	10	0	80	.20	40	14	4.00	750	3.0	13	_ _ _
101+55	481	.70	10	0	80	.20	40	14	4.00	750	3.0	9	_ _ _
98+58	0	.70	0	10	75	.80	50	10	3.50	800	0	0	_ _ _
97+05	2,955	.50	10	20	40	.80	50	15	.20	840	16.8	9	1,231
95+96	2,500	.80	5	10	90	.20	50	25	.20	860	3.0	11	_ _ _
95+92	1,389	.80	5	10	90	.20	50	25	.20	860	3.0	7	_ _ _
93+91	5,179	.10	25	20	50	.20	50	11	1.0	880	16.8	12	2,449
93+89	7,143	.10	25	20	50	.20	50	11	1.00	880	16.8	12	2.449
92+21	1,538	.20	50	0	55	.20	50	47	1.50	900	3.0	7	_ _ _
92+19	1,154	.20	50	0	55	.20	50	47	1.50	900	3.0	10	_ _ _
90+50	4,878	.20	10	0	60	.90	40	16	1.00	920	16.8	12	_ _ _
89+99	4,354	.20	50	60	50	.90	40	2	1.00	930	16.8	11	3,590
87+19	1,226	.30	25	20	50	.20	50	3	.80	970	16.8	11	_ _ _
85+66	3,077	.20	50	20	60	.20	70	9	.80	990	16.8	8	12,000
83+93	10,270	.10	75	0	85	.40	70	0	[4]99.99	1,010	16.8	12	38,043
83+89	54,660	.10	75	0	85	.40	70	0	99.99	11010	16.8	18	22,860
83+47	23,580	.05	75	10	85	.40	70	0	99.99	1,020	16.8	16	23,510
83+10	4,656	.20	75	10	85	.40	70	0	99.99	1,030	16.8	12	4,082
81+41	1,333	.10	25	0	70	.40	60	8	4.00	1,040	16.8	11	_ _ _
79+92	1,320	.30	5	60	65	.70	50	18	1.00	1,050	3.0	8	_ _ _
78+17	0	.70	0	20	60	.70	20	28	1.00	1,070	0	0	_ _ _
73+58	1,100	.50	5	0	50	.10	20	22	1.50	1,230	3.0	13	_ _ _
71+83	4,000	.50	25	20	60	.10	40	17	6.00	1,280	16.8	14	_ _ _
69+81	2,747	.40	5	60	60	.10	20	79	1.00	1,320	16.8	14	_ _ _
65+94	0	1.00	5	10	50	.05	10	10	1.50	1,400	0	0	_ _ _
62+59	4,314	.10	10	20	75	.10	20	7	.10	1,450	16.8	12	_ _ _
59+35	1,333	.70	5	20	75	.05	20	38	.10	1,340	3.0	13	_ _ _
54+60	0	.80	0	10	60	.05	10	254	.02	1,120	0	0	_ _ _
49+27	0	.80	5	10	85	.00	20	54	.30	710	0	0	_ _ _
43+89	3,787	.50	5	60	60	.20	40	4	2.50	260	16.8	9	_ _ _
43+84	7,857	.50	5	60	60	.20	40	4	2.50	260	16.8	8	_ _ _
39+05	1,127	.10	0	10	0	.05	80	0	50.00	20	16.8	9	_ _ _

[1]Italicized station numbers indicate data at that station were not used.
[2]Rock load at time of initial stabilization.
[3]Steel section modulus, in inches^3, is defined as I/C, where I = moment of inertia, in inches^4, and C = distance from centroid, in inches.
[4]Severely sheared area consisting of several shear zones grading into each other.

GEOLOGIC AND CONSTRUCTION VARIABLES

Twelve variables were investigated in addition to the dependent variable, rock load. They include four construction variables: depth of the pilot bore from the surface, steel section modulus, number of effective blocking points. Eight geologic variables were examined: average fracture spacing, percentage of alteration, water condition, average fracture dip, rock type, degree of faulting, distance to the nearest fault or shear zone, and thickness of the fault or shear zone.

Certainly not every possible geologic or construction parameter in the pilot bore was determined. Parameters that cannot be measured rapidly at the face during tunneling are of little value in controlling installation of tunnel support. Selection of the geologic parameters was governed by experience in other tunnels, ease of measurement, and by an intuitive feeling for the effect on tunnel mechanics. Of the eight geologic variables, only three — water condition, degree of faulting, and thickness of nearest fault or shear zone — were significant to the development of an acceptably precise rock-load-prediction model. These facts seem to justify the limited selection of variables.

The interrelationships between the supposedly independent variables measured in the pilot bore were determined by a correlation analysis (table 29).

DESCRIPTION OF VARIABLES

The geologic and construction variables investigated were assumed to be independent prior to the correlation analysis. These variables — average fracture spacing, percentage of alteration, water condition, average dip of the fractures, rock type, degree of faulting, distance to the nearest fault or shear zone, thickness of the nearest fault or shear zone, depth of the pilot bore from the surface, and a composite variable representing the steel support — were determined as follows:

The average fracture spacing was reported for each station. The spacing was determined in the pilot bore by laying a tape along the south wall of the tunnel and counting the number of fractures intersected by the tape between the instrumented set and the adjacent sets. After measuring on the north wall and the roof of the pilot bore at several stations, as well as along the south wall, it was decided that a determination of fracture spacing based on only one line would be sufficient. The number of fractures counted proved to be approximately the same on each line.

The percentage of alteration was determined by estimating the percentage of alteration of the constituent mineral grains by examination with a hand lens.

The water condition was determined at the time of instrument placement by use of the following arbitrary quantification scale: 0 = dry, 20 = damp, 40 = wet, 60 = dripping, 80 = shower, 100 = water issuing from fractures or drill holes in a steady stream (as much as 300 gpm).

The average dip of the fractures was determined for each station and represents a weighted average of fractures exposed in the pilot bore at the station.

The rock types encountered in the Straight Creek Tunnel pilot bore showed many combinations of gneiss and granite, as described in chapter B. The abundance of both rock types at each station was quantified by assigning the value of zero to the granite and a value of 1 to the gneiss. The rock-type information was obtained from the maps, at a scale of 1 inch = 50 feet, described previously.

The degree of faulting was derived from the 1-inch- to 100-foot-scale maps (Robinson and Lee, 1965). The following arbitrary scale was used: 0 = no faulting or shearing, 10 = minor shearing or faulting, 20 = minor to moderate, 40 = moderate, 60 = moderate to intense shearing and faulting, 80 = intense, and 100 = shear zone.

The distance to the nearest fault or shear zone was

TABLE 29. — *Correlation coeficients for the Straight Creek Tunnel pilot bore*

[A positive correlation coefficient indicates that as the one variable increases, the other increases; a negative correlation coefficient indicates that as the one variable increases, the other decreases]

	Alteration (percent)	Water condition	Average fracture dip	Rock type	Degree of faulting	Distance to nearest fault or shear zone	Thickness of nearest fault or shear zone	Depth from surface	Steel section modulus plus blocking points
Average fracture spacing	−0.689	−0.282	+0.203	−0.394	−0.626	+0.131	−0.424	−0.429	−0.778
Alteration (percent)		+0.214	−0.030	+0.334	+0.780	−0.216	+0.757	+0.210	+0.598
Water condition			−0.424	+0.373	+0.297	−0.085	+0.260	−0.179	+0.374
Average fracture dip				−0.316	−0.075	−0.031	+0.153	+0.069	−0.189
Rock type					+0.502	−0.244	+0.305	+0.049	+0.281
Degree of faulting						−0.369	+0.643	+0.090	+0.587
Distance to nearest fault or shear zone							−0.196	+0.278	−0.326
Thickness of nearest fault or shear zone								+0.075	+0.455
Depth from surface									+0.363

measured directly from the 1-inch- to 100-foot-scale geologic maps. The measurement made is the distance back, along the pilot-bore axis, from the station to the fault. The irregularity of attitudes of the fault surfaces made difficult an accurate estimate of the distance from the various instrument stations to the nearest fault. The distance was measured from the station to the near side of the fault zone, where the fault intersects the pilot-bore wall at shoulder height.

The measurement of the width or thickness of the nearest fault or shear zone involved similar problems, due to the variations in structure. The reported fault width is the apparent width of the fault or shear zone measured along the pilot-bore axis. The thicknesses were taken from the 1-inch- to 100-foot-scale maps (Robinson and Lee, 1965).

The depth from the surface was scaled from the 1-inch- to 100-foot-scale pilot-bore section (Robinson and Lee, 1965).

The steel support variable represents the sum of the section modulus of the steel and the number of effective set blocking points. This composite variable proved very significant in the rock-load model. The section modulus represents the stiffness of the steel in the direction of bending. The number of effective blocking points was determined from the blocking-point diagram. To be considered effective, a blocking point had to present a direct line for load application from the rock to the outer flange of the steel. This technique was arbitrary, but, as explained previously, it was not economically feasible to measure the loads carried by each blocking point of each blocking point of each instrumented set.

STATISTICAL ASSUMPTIONS

The application of statistical methods to the analysis of the effect of geologic and construction variables on rock loads requires that the samples, or observations, be unbiased and independent of all other samples. That this condition was approximately true in the pilot bore is supported by two facts. First, the surface and underground geologic mapping (Robinson and Lee, 1962, 1965) indicated that the occurrence of metasedimentary rocks is about 24 percent and of granite is about 75 percent. The distribution of rock types at the instrument stations is about 28 percent metasedimentary rocks and about 72 percent granite. Second, the instrument stations were installed at the end of the work week (usually on Sunday mornings); therefore, the stations were located independently of any measured geologic or construction variables.

The application of statistical methods to this problem also requires the specification of the degree of mathematical model variation permitted. The first, and most basic, restriction is that all the variables must be continuously variant, or that no discontinuities may exist. The interdependence between the dependent and the various independent variables was assumed to be such that only one maximum and one minimum could exist in the various interrelationships. The other types of interdependence permitted were linear variations and continuous nonlinear variations in one direction across the range of observations.

Regression analyses were performed using both logarithmic terms, with very low values substituted for observed values of zero, and the more refined interaction variables (Miesch and Connor, 1968). The use of logarithmic terms biased the results because it did not permit the consideration of the condition where supports were placed when the rock was actually self-supporting. For practical reasons, simple second-order interaction variables (XY), which produced a less complex, but slightly less accurate, rock-load-prediction model (968 psf (pounds per square foot) standard deviation of the rock-load residuals versus 917 psf), were not used in the rock-load model. Under the difficult working conditions at a tunnel heading, where such rock-load models are to be used to select steel set size and spacing, all but the most essential mathematical manipulations should be eliminated. Because of the inaccuracy involved in estimating the area of wall and roof supported by any instrumented set, the construction of a more complex mathematical model that is rigidly tied to the observed dependent variable cannot be justified. Only an acceptable (95-percent confidence level) estimate of rock loads, not an exact fit of the sample data, is desired. The method presented here permits the geologist to enter a nomograph with the value of each geologic variable and rapidly select the spacing for the next steel set to be installed at the tunnel heading. This method is an improvement over present practice, in which the walking boss or lead miner looks at the exposed rock and estimates the set spacing.

CORRELATION-COEFFICIENT ANALYSIS

The calculated correlation coefficients between the various geologic and construction variables measured at each station made it possible to determine probable interrelationships. Probability must enter into the determination of interdependence because any two sets of 33 random numbers can exhibit varying degrees of purely random correlation. In this correlation analysis, the significant levels of correlation could be explained by random occurrence in only 1 out of 20 data sets (95-percent confidence level), 1 out of 100 data sets (99-percent confidence level), or 1 out of 1,000 data sets (99.9-percent confidence level).

The correlations between each of the geologic and construction variables and the dependent rock-load variable (table 30) show that only the depth of the pilot bore and the distance to the nearest fault are not related to the rock loads. All the other variables were significantly (95-percent confidence level) related to rock load. Not all these variables entered the statistical model because of interrelationships among the variables. For example, the close correlation between degree of faulting and percentage of

TABLE 30. — *Correlation between rock load and geologic and construction variables*[1]

Acceptance region (33 observations) (r = correlation coefficient)	Confidence level (percent) and required correlation coefficient
$+0.346<r<-0.346$	95 ($r>0.346$)
$+0.445<r<-0.445$	99 ($r>0.445$)
$+0.549<r<-0.549$	99.9 ($r>0.549$)

Function of rock load (RL)	Average fracture spacing	Percentage of alteration	Water content	Average fracture dip	Rock type	Degree of faulting or shearing	Distance to nearest fault[2]	Thickness of nearest fault or shear zone	Depth from surface[2]	Steel section modulus	Number effective blocking points	Steel section modulus plus blocking points
RL^3	−0.713	+0.545	+0.557	−0.271	+0.224	+0.615	−0.304	+0.398	+0.016	+0.797	*+0.867*	*+0.932*
RL^2	*−.715*	+.578	+.645	−.306	+.284	+.639	−.282	+.478	+.014	*+.834*	+.793	+.914
RL^1	−.650	*+.595*	+.763	−.350	+.367	*+.640*	.242	+.612	−.050	+.810	+.601	+.812
$RL^{1/2}$	−.524	+.569	*+.800*	*−.360*	*+.389*	+.610	−.211	+.714	−.113	+.677	+.416	+.640
$RL^{1/3}$	−.445	+.538	+.781	−.345	+.372	+.599	−.192	*+.738*	−.215	+.579	+.338	+.539

[1]Values in italic type represent the highest correlation for each variable.
[2]Not related to rock load.

alteration explains why only one of these two variables was used in the rock-load-model equation. The degree of faulting explained so much of the influence of the percentage of alteration on rock loads that subsequent inclusion of the percentage of alteration in the model equation did not significantly reduce the variance in the predicted dependent variable rock load.

The correlation analysis pointed to certain specific conclusions:

1. The most significant variable influencing set loads was the composite construction variable of steel section modulus plus blocking points.
2. The geologic variables that have a relationship to rock load, in the order of importance, are as follows: Amount of water entering the tunnel heading, thickness of the nearest fault zone, average fracture spacing, degree of faulting or shearing, percentage of alteration, rock type, and average fracture dip.

REGRESSION ANALYSIS

A multiple linear stepwise regression analysis was made, to predict rock loads with acceptable accuracy, by using the "final" stable rock-load data from the pilot bore. These final values for rock load were obtained after construction practice and geologic conditions at the tunnel face had ceased to exert influence on the set loads. The rock loads used in the analysis were, in general, higher than the initial stabilization rock loads. The final stable rock loads included the increases that resulted from subsequent penetration of shear zones by the tunnel and from resupport operations carried on in sections of tunnel where load failure or other unexpected load transfer occurred.

The multiple linear stepwise regression method was developed by Efroymson (1960). Use of this method produces a partial correlation matrix after each regression step. Thus, at the end of each step, the independent variable having the highest partial correlation with the remaining part of the unexplained variable is entered into the computation of the new regression equation. When the independent variable is entered into the new regression equation, the standard error of the predicted dependent variable and the squared multiple correlation coefficient (r^2) are produced. Normally, after a few regression steps the decrease in standard error became smaller than the precision of variable measurement.

A perfect statistical fit of a sample of 33 observations can be developed with an equation of 31 terms. Such a complex perfect fit of the sample, however, probably would not produce a better prediction of rock load for the other 2,000+ uninstrumented sets in the pilot bore because it would be too rigidly tied to the sample data. This relates to the previously discussed problem of blocking-point effectiveness and supported-area estimation.

The final stable rock-load prediction equation is

$$\text{Rock load, in pounds per square foot} = 218 + 911\,(W)^{1/2} - 1{,}386\,(W)^{1/3} + 42\,(DF) - 6{,}117\left(\frac{DF}{100}\right)^3 + 201\,(TNSZ)^{1/2} - 3{,}094\,(TNSZ)^{1/3} - 261\,(SB) + 35\,(SB)^2 - 1\,(SB)^3,$$

where

W = water condition, in percentage of highest inflow;
DF = degree of faulting and shearing, in percentage of most intense shearing;
TNSZ = thickness of nearest fault or shear zone, in feet; and
SB = steel section modulus, in cubic inches, plus number of effective blocking points.

The squared multiple correlation coefficient of this equation was 0.84. The standard deviation of the residuals was 917 psf.

The final test of any predictive tool, such as regression modeling, is to see how good a job it does in practice. The ideal test of a regression model would be to collect additional samples and check the error in prediction of rock load. This was not possible in the Straight Creek Tunnel pilot bore. A less satisfactory method, used to test the validity of a regression model, consists of successively

reducing the number of data stations and comparing the new residuals of prediction against those for the total sample model. The test used was the equality of variance test ($F = S_1^2/S_2^2$, where F is the Fisher statistic, and S_1^2 and S_2^2 are the residual variances for all 33 stations.

This test indicates the anticipated difference (at the 95-percent confidence level) in sample variances for equal-size samples drawn from an infinitely large population. The rock-load model required data from the first 13 stations, or approximately 2,000 feet of the 8,350-foot-long pilot bore, to produce a regression equation equal (at the 95-percent confidence level) to the one produced with all 33 data stations. Figure 79 shows the results of this analysis.

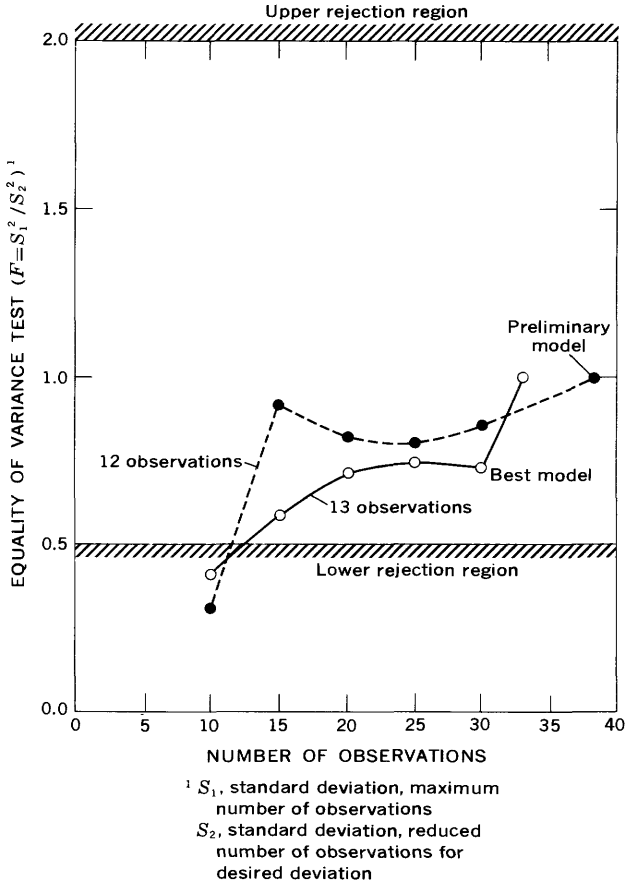

FIGURE 79. — Required number of observations for rock-load analysis (95-percent confidence).

Another advantage of the model is that it indicates the amount of rock load that could be supported by the rock mass itself. There is an indication that predicted rock loads of 550 psf probably are self-supporting in the pilot bore. Larger tunnels under the same geologic conditions probably would not be self-supporting at the same rock-load level. A rock load that is self-supporting for a small tunnel should be related by some unknown inverse function of relative increase in dimensions for a larger tunnel.

SAMPLE NOMOGRAPH SOLUTION

From the rock-load prediction equation, a set of nomographs was computer generated. These nomographs (figs. 80–82) show the controlling mechanism of rock load in the pilot bore. A set of sample geologic and construction conditions is analyzed to illustrate this mechanism:

Steel section modulus, 16.8 in.^{3} (6-in. wide flange, 25 lb per ft).
Number of effective blocking points, 11.
Relative water condition, 60 (dripping).
Degree of faulting and shearing, 40 (moderate).
Thickness of nearest fault or shear zone, 1.0 ft.

Using figure 80 with section modulus (16.8), effective number of blocking points (11), and the relative water condition (60), the first cumulative rock load equals 4,800 psf (pounds per square foot).

Using figure 81 with the first cumulative rock load (4,800 psf) and the degree of faulting and shearing (40), the second cumulative rock load equals 6,100 psf.

Using figure 82 with the second cumulative rock load (6,100 psf) and the thickness of nearest fault or shear zone (1.0), the predicted rock load equals 5,000 psf. This compares with a measured rock load of 4,354 psf.

Once the rock load has been estimated, the standard set-spacing design of Proctor and White (1946, p. 219–224, or table 1, p. 238) can be used. For the sample data presented and the estimated rock load of 5,000 psf, figure 83 (a graphical representation of Proctor and White's tabular data) indicates a design set spacing of 3.5 feet.

CONCLUSIONS

The following conclusions concerning rock behavior, construction procedures, and geologic influences in the pilot bore can be made on the basis of the rock-load analysis:

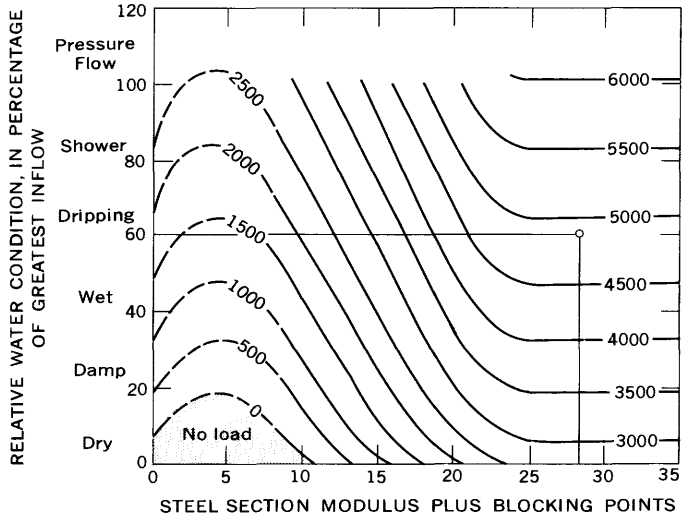

FIGURE 80. — First cumulative load, in pounds per square foot, in relation to water condition and steel modulus plus blocking points.

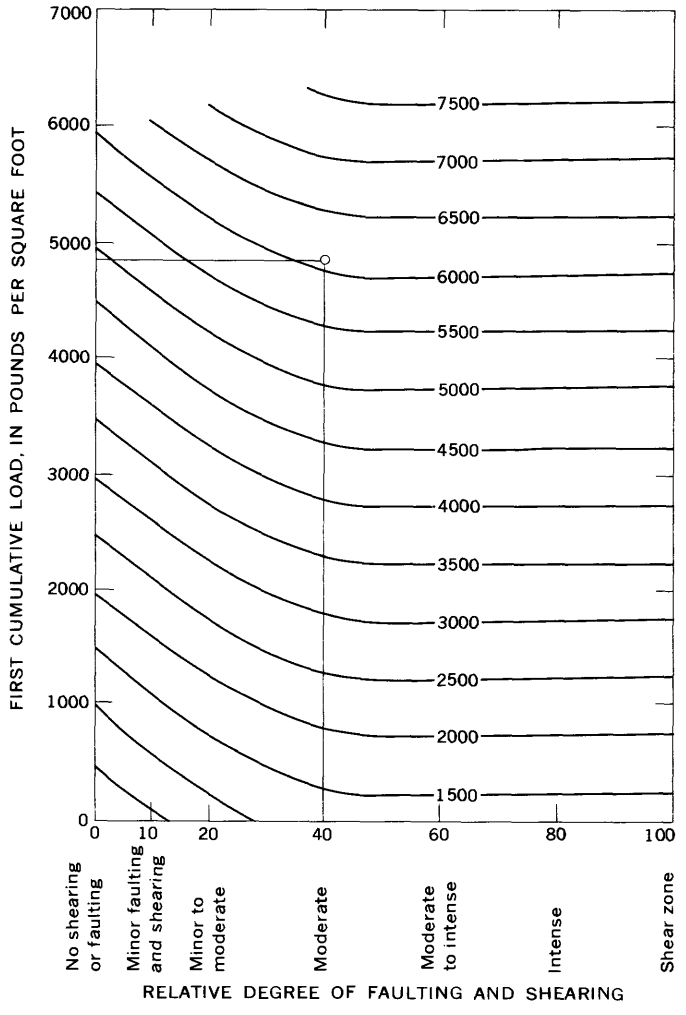

FIGURE 81. — Second cumulative load, in pounds per square foot, in relation to first cumulative load and degree of faulting and shearing.

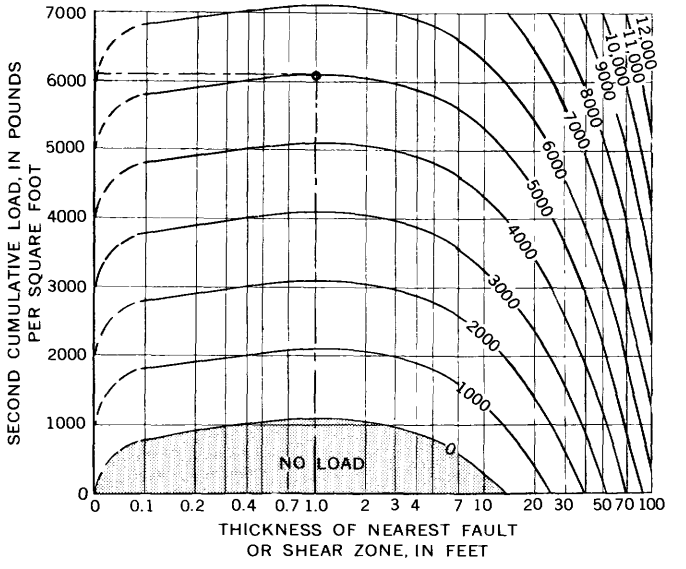

FIGURE 82. — Predicted rock load, in pounds per square foot, in relation to second cumulative load and thickness of nearest fault or shear zone.

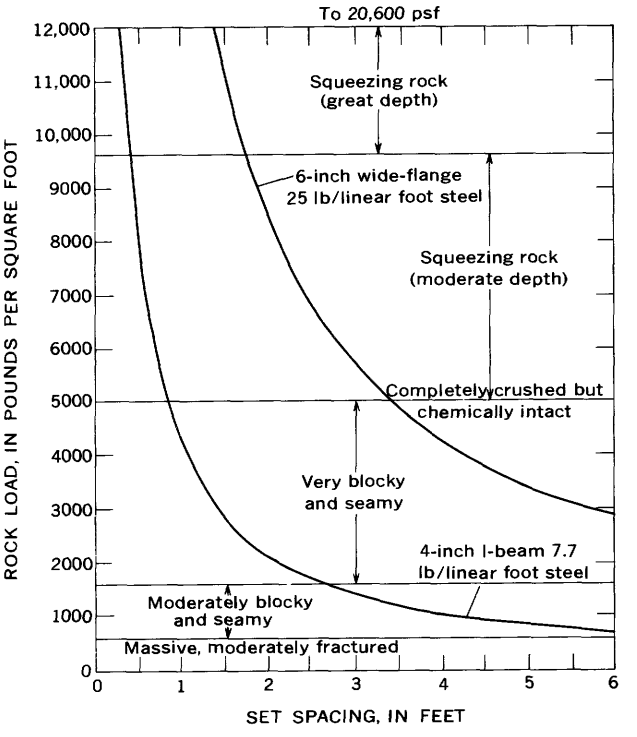

FIGURE 83. — Selection of set spacing based on rock load. Data from Proctor and White (1946, p. 219–224): 14-foot-diameter tunnel; 24-inch spacing of blocking points; elastic design, 24,000 pounds per square inch fiber stress.

1. The rock loads increase almost linearly with any increase in the quantity of water entering the pilot bore (fig. 80).
2. In the pilot bore, where the degree of faulting and shearing reaches the level designated as "moderate," the rock loads are not influenced by that variable (fig. 81). A possible explanation of this phenomenon may lie in particle "unlocking." Once a rock mass has been subjected to moderate shearing, further shearing and consequent reduction in particle size should not (and apparently does not) result in additional rock loads. In this regard, Hurr and Richards (chap. E of the present report) found that the greatest water flows in the pilot bore issued from moderately fractured rock, rather than from the more intensely altered, central part of a shear zone. Heavy rock loads develop under such a combination of geologic conditions. The greater the water flow, the greater the permeability indicated for the rock mass at that location. The existence of this condition in granitic and metasedimentary terrain suggests that there should be open fractures for some distance into the rock surrounding the pilot-bore walls. Blasting and subsequent rock adjustment probably were effective in opening many fractures. Such an open-fracture system could allow easy downward movement of fracture blocks, creating, at least in some places, high loads on the steel supports.

3. The number of blocking points strongly influences the set load. Great care must be used in the blocking of sets to insure that the load-carrying capacity of the set is fully utilized.
4. There is an optimum spacing of blocking points for the steel sizes used in the pilot bore (fig. 79) which results in maximum set loads and set efficiency. Closer spacing does not increase the load-carrying capacity of a set, and wider spacing does not make full use of that capacity. The optimum spacing is 17 inches for the 4-inch I-beam (7.7 lb per ft) steel and 46 inches for the 6-inch wide-flange (25 lb per ft) steel. The resulting spacing over radius of gyration ratios ($1/r$), in direction of least stiffness of the steel section, was 28.8 for the 4-inch I-beam (7.7 lb per ft) steel sets and 30.3 for the 6-inch wide-flange (25 lb per ft) steel sets. This spacing indicates that column loading is the controlling factor between blocking points.
5. There is an indication that several supported sections of the pilot bore could have remained unsupported if barring-down had been performed at intervals after excavation.

Rock-mechanics instrumentation, geologic mapping, and statistical-research techniques, in combination, can produce an accurate estimate of any desired tunnel design parameter. The primary problem is to determine the significance of inelastic geologic conditions on the ideal elastic approximations of tunnel mechanics. The secondary problem is to determine the influence of construction practices on any desired design parameter.

The significance of the design-parameter model developed here is in the verification of the safety of a tunnel structure. The rock-load-prediction model permits the continuous control of steel support size and spacing at a tunnel heading. The use of a model makes it possible to eliminate unnecessary supports and prevents the placement of inadequate supports that later require expensive additional support.

Use of the design-parameter model for estimating necessary tunnel support could be extended to other types of support, such as rock bolts or concrete, and, with additional information, to more complicated underground excavations. Any rock-excavation operation can be aided by knowledge of the conditions that control the response of the rock mass adjacent to the excavation. The more complicated the underground operation, the greater the potential value of such a program. Underground powerhouse-support design should be an area of particularly fruitful application of this method.

The next logical use for this method of tunnel-mechanics research would be to define the effect of increasing the size of the opening. This should prove to be a simple extension of the model presented in this report. The procedure would consist of developing statistical rock-load models for three or more sizes of openings. A curve could then be drawn to relate the rock loads for specific geologic and construction variables of the size of opening. The type of chart envisioned is shown in figure 84.

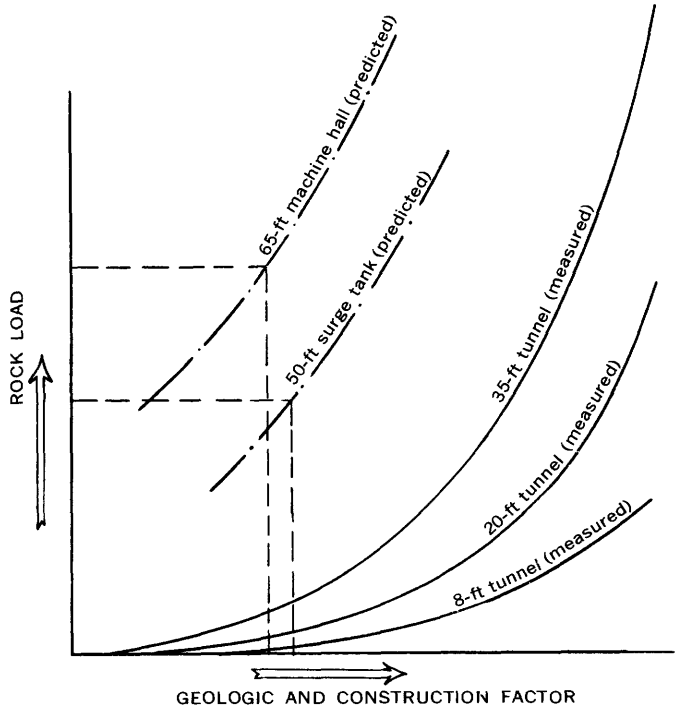

FIGURE 84. — Relation of rock load and geologic and construction factor to size of underground opening

Each tunnel, however, is unique; the geologic and construction conditions that control the inelastic part of the response of the adjacent rock mass will vary with each location. If sufficient measurements at enough different locations in any tunnel are available, a model for rock loads can be constructed for that tunnel. The development of a unified model covering all possible geologic and construction conditions will require the collection of data from several different tunnels. Even such a unified model would not eliminate the necessity of verifying the load predictions by measurement in any new tunneling operation.

SUMMARY

During the construction of the Straight Creek Tunnel pilot bore set loads were measured with load cells. The geologic conditions and construction practices at each load-cell station were determined and recorded, and, by means of stepwise regression, their relative significance upon the measured rock loads was determined that the rock loads at the Straight Creek Tunnel pilot bore would have to be carried by the steel tunnel supports were controlled by the following factors: (1) Average fracture spacing, (2) percen-

tage of alteration, (3) relative ground water condition, (4) relative degree of faulting and shearing, (5) average dip of the fractures, (6) rock type, (7) thickness of the nearest fault or shear zone, and (8) size and placement of the steel sets. Elastic theory alone cannot apply because a set load is, in itself, evidence of inelastic rock-mass response.

By using the statistical model, a description was formulated of the mechanism by which rock loads are controlled by geologic conditions in the rock mass adjacent to the tunnel walls and by construction practices. The model also made possible the accurate estimate of rock loads at intermediate positions between the instrument stations, where rock-load measurements were not made.

Summary of Investigations

By CHARLES S. ROBINSON *and* FITZHUGH T. LEE

ENGINEERING GEOLOGIC, GEOPHYSICAL, HYDROLOGIC, AND ROCK-MECHANICS INVESTIGATIONS OF THE STRAIGHT CREEK TUNNEL SITE AND PILOT BORE, COLORADO

GEOLOGICAL SURVEY PROFESSIONAL PAPER 815–H

ENGINEERING GEOLOGIC, GEOPHYSICAL, HYDROLOGIC, AND ROCK-MECHANICS INVESTIGATIONS OF THE STRAIGHT CREEK TUNNEL SITE AND PILOT BORE, COLORADO

SUMMARY OF INVESTIGATIONS

By CHARLES S. ROBINSON and FITZHUGH T. LEE

PRECONSTRUCTION INVESTIGATIONS

The preconstruction investigations began in July 1962 with the detailed geologic mapping of about 6 square miles in the vicinity of the proposed pilot bore. Particular attention was given to the percentage of different rock types, the attitude of the foliation of the rock, the attitude and spacing of faults and joints, and the degree and amount of rock alteration.

Rocks in the area were found to consist of about 75 percent granite and 25 percent metasedimentary rocks, which occur as inclusions in the granite. The granite is medium to fine grained and consists of about equal amounts of quartz, potassium feldspar, and plagioclase feldspar, and 5–15 percent biotite. Small pods and dikes of pegmatite, mainly of quartz and potassium feldspar, were mapped with the granite. The metasedimentary rocks consist of various generally fine grained biotite-rich gneisses. Common types in the area are biotite-quartz-microcline gneiss, biotite-quartz-plagioclase gneiss, hornblende-biotite-plagioclase gneiss, and sillimanitic biotite-plagioclase gneiss.

In the granite, much of the biotite has been partially altered to chlorite, and the plagioclase feldspar has been slightly altered to sericite. The granite is extensively altered only in or adjacent to the shear zones and faults. In nearly all extensively altered outcrops, biotite and some hornblende in the metasedimentary rocks are commonly altered to chlorite. In and adjacent to the faults and shear zones, the metasedimentary rocks are extensively altered and form a green plastic clay in which the foliation, although contorted considerably, is still recognizable.

Foliation in the granite is distinct in most outcrops. It results from a subparallel orientation of the potassium feldspar grains. In the metasedimentary rocks, foliation is due to the parallelism of mica grains. Foliation trends northeast and dips steeply to the northwest or to the southeast.

Dikes of Tertiary age range in maximum dimension from a few feet to about 1,000 feet. These rocks have a fine-grained to aphanitic groundmass containing phenocrysts of augite and plagioclase and variable smaller amounts of biotite, quartz, and magnetite.

The bedrock throughout much of the area is mantled by surficial deposits as much as 50 feet thick. These consist of swamp and morainal deposits at lower altitudes in the valleys and consist of colluvial deposits of soil, talus, and landslides on the upper slopes.

Geologic structures are often the major factors in increasing the cost of tunnel construction above the estimated cost. Accordingly, during surface mapping and drill-core study, attention was concentrated on foliation, joints, faults, and shear zones. In the granitic rocks foliation is not a principal direction of weakness and should not significantly affect the engineering properties of the rock. In the metasedimentary rocks, however, the foliation is a major direction of weakness; those layers composed predominantly of biotite or chlorite are much weaker than those composed predominantly of quartz and feldspar. Faults and shear zones are numerous in the mapped area, which is within a wide zone of shearing related to the Loveland Pass fault zone. The distinction between faults and shear zones is based only on width; faults are elongate areas of crushed rock 5–50 feet wide, and shear zones are elongate areas >50 feet wide. The faults and shear zones consist of rock showing various degrees of crushing or shearing. The zones are gradational, with the intensity of shearing decreasing outward from the center of each zone. Near the margins, the rock consists of slivers <0.1–1 inch wide, bounded by slickensided shear planes. Where the shearing was more intense, the rock has been crushed to a coarse to fine sand and the shear planes are <0.01–0.5 inch apart, and they lie in all directions. Where the most shearing occurred — accompanied by alteration — the material consists of clay (fault gouge) and variable amounts of quartz and (or) feldspar grains. The gouge usually does not occur near the center of the sheared zone but is nearer one margin than the other, most commonly adjacent to the footwall of

the zone. The gouge occurs as disconnected pods of clay and sand that are elongated parallel to the trend of the fault or shear zone. The faults and shear zones vary in width within short distances and pinch and swell, and some end abruptly against relatively unbroken rock. Some shear zones contain blocks of rock, as much as about 100 feet in maximum dimension, that are relatively unsheared, although they are surrounded by intensely sheared rock. The shear zones and faults, because of their general discontinuity in most places, could be projected with certainty for only short distances. Most of the faults and shear zones trend N. 20° E. to N. 50° E. and dip about 75° E. or W. Most of the fractures recorded as joints have had some movement; joint surfaces commonly display some form of alteration, gouge, or slickensides. The condition and attitude of the joint surfaces, as well as the maximum, minimum, and average distance between joints in each set, were recorded. In general, joints strike in any direction and dip 45°–90° in any direction. The surface mapping showed that the average minimum distance between fractures was 0.98 foot, the average maximum distance was 2.5 feet, and the average distance was 1.5 feet.

Two core holes, about equally spaced between the proposed pilot-bore portals, were drilled to determine geologic conditions in the vertical dimension. The attitude of fractures in the core was measured in relation to the strike of the foliation. From the drilling it was determined that the average minimum distance between fractures in the core, regardless of rock type, was 0.11 foot, the average maximum distance was 0.68 foot, and the overall average distance was 0.25 foot. The presence of smaller fracture spacings in the core relative to the surface fracture spacings was largely due to the tendency for only the more competent (least fractures) rocks to crop out.

Geophysical investigations consisted of resistivity, radioactivity, and gamma-ray density logging of the drill holes and of seismic and resistivity profiles at the surface along, and at right angles to, the proposed tunnel line. The resistivity logging supplemented the geologic logging and was used primarily to determine or confirm zones of shearing, particularly where core recovery had been poor. The radioactivity and gamma-ray density logs helped determine relative values for the amount of shearing and alteration; natural-radiation logs were useful for rock-type determination in intervals of poor recovery. Preconstruction surface seismic and resistivity surveys were of only limited success; this information was valuable primarily for estimating the amount of surficial material that had to be removed near the east portal.

Laboratory investigations were conducted continuously in coordination with the geologic and geophysical field investigations. The mineralogy, porosity, grain density, dry bulk density, and saturated bulk density were determined for surface and drill-core samples. The elastic properties of selected samples were measured by dynamic and static methods. Compressive and shear strengths were determined under various confining pressures. Correlation was established between compressive strength and the mineralogy of the samples. The swelling properties of fault gouge were investigated, and the results indicated that high swell pressures were not anticipated in the pilot bore. This information was important in the design of an efficient pilot-bore-support system.

GEOLOGIC AND ENGINEERING PREDICTIONS

The data from the geologic, geophysical, and laboratory investigations were used to construct a predicted geologic section along the proposed tunnel line. In constructing the geologic section, no effort was made to project individual rock units, faults, or shear zones to tunnel level. Rather, the different zones of the average spacing between fractures, as determined at the surface, were projected to tunnel level, on the basis of the average dip of faults and shear zones as measured from the surface and from the drilling data. These projected zonal boundaries were gradational and indefinite, and the location of each zone was based on the projection of statistical values. The length and position of these zones of different rock competencies were expected to be in error by as much as 50 percent, but the percentage of the several rock-condition categories was expected to be correct within less than 25 percent. This gave a reasonable basis for calculation of engineering data necessary for estimating, in advance of construction, the overall cost of construction of the pilot bore.

The engineering data calculated for estimating the cost of construction of the pilot bore were the rock loads, spacing of support sets and lagging, the location of feeler holes, areas possibly requiring grouting, and areas of ground-water flows.

Rock loads were based on the assumptions that the pilot bore, outside the timbers, would be about 10.5 feet wide and 11.5 feet high, and that the rates of driving the pilot bore and of installing supports (both factors affect the rock load) would be as efficient as possible. Under these conditions the rock load would be primarily the result of geologic conditions. A maximum load of about 5,900 pounds per square foot was calculated.

Rock pressure, fracture spacing, and the amount of fault gouge or clay alteration products, although considerably interrelated, were expected to vary from place to place. The total effect of these geologic variables on pilot-bore construction was expressed, more or less quantitatively, by the amount of support that might be required. Estimates of support were regarded as a measure of the severity of geologic conditions, and not as an attempt to formulate definitive engineering design requirements. The principal factor then that would influence the amount of support was the fracture spacing. In the most severely fractured areas, where wide

zones of fault gouge were expected, the need for invert struts was anticipated.

The approximate location was given for feeler holes in advance of the face to test for zones of highly fractured rock that might be filled with water. The use of grout was forecast where heavy water inflow was expected. Sections of the bore to be tested by feeler holes and sections to be grouted were predictions only. In practice, and as stipulated, rock conditions at the face were to be continually and carefully observed, and if there was any indication of a possible water-bearing zone ahead of the face, the rock was to be tested by feeler holes. It was emphasized that the cost of feeler holes is low in comparison with the cost of recovering a caved face. The amount of ground water that might be encountered depended upon the porosity and permeability of the rock and the height of the overlying water table. The porosity of the rock, as determined, depended primarily on the average distance between fractures, calculated for each interval of the pilot bore, and on the percentage of faults and shear zones for the particular interval. The permeability of the rock depended primarily on the size and interconnection of the fractures. These factors were determined from field and laboratory investigations, water-flow data in other tunnels, and test data from wells in similar rocks. The average amount of ground water that was expected was based on an assumed advance rate of the heading of 1,000 feet per month. Maximum initial flows from faults or shear zones were estimated at about 1,000 gpm (gallons per minute). This flow was expected to decrease rapidly within 5–10 days. The maximum flow from the portal was estimated at about 500 gpm. Projecting this rate beyond the completion of the pilot bore, the flow at the portal was expected to decrease to about 300 gpm within 2 weeks and to about 100 gpm within 1 year.

INVESTIGATIONS DURING CONSTRUCTION

During construction of the pilot bore, begun in November 1963 and completed in December 1964, geological, geophysical, rock-mechanics, and laboratory investigations were made.

The pilot bore was mapped geologically at various scales, and throughout its length samples were taken for various purposes. Walls of the bore were mapped at a scale of 1:600. On these maps were recorded rock type; attitude of the foliation, joints, faults, and shear zones; percentage of mineral alteration in the wallrock; fracture spacing; and occurrence of ground water. Geologic sections, at a scale of 1:24, were made of the pilot bore face at about 800 stations. In support of the geophysical and rock-mechanics investigations, the geology of one wall or the other was mapped at 1:60 for 50 feet or more on each side of a geophysical or instrument station.

Rock samples for petrographic analysis were systematically collected during the geologic mapping. Samples of altered wallrock and fault gouge were collected for determination of swelling pressures and mineralogy. Chip samples were collected 5 feet on each side of instrument stations for size and mineral analyses. Blocks of wallrock about 1 foot in largest dimension were collected and cored in the laboratory for the determination of elastic properties by dynamic and static tests.

As the construction of the pilot bore progressed, and as the results of the geophysical effort was made to determine the geologic and engineering conditions influencing these results. It became apparent that the categories of fracture spacing, as determined from surface mapping (<0.1–0.5 ft, 0.5–1 ft, and 1–3 ft), were not definitive enough. Underground, the fracture-spacing categories were changed to <0.1 foot, 0.1–0.5 foot, 0.5–1 foot, and >1 foot. The instrumentation and geophysical work also dictated the need for mapping the percentage of wallrock alteration and for sampling for size and mineral analyses.

Geophysical investigations were undertaken in the pilot bore to determine whether geophysical instruments and techniques could be used effectively to define the physical conditions around the pilot bore, and whether these conditions could be correlated with the results of the instrumentation and the construction practices used in the pilot bore. Resistivity and seismic-velocity measurements were made at selected points along the walls of the pilot bore. A correlation analysis was made between resistivity and velocity values and economic and engineering parameters: time rate of construction, cost of construction per foot, rock quality, set spacing, percentage lagging and blocking, type of steel support used, height of tension arch, and vertical load. The correlation coefficients from this analysis ranged from 0.8 to nearly 1.0 in absolute value, which indicates that correlation among these parameters exists. Comparison of surface and underground geophysical measurements indicated that reasonably accurate predictions are possible from surface measurements. Greater accuracy and more detailed information would have been obtained if predictions had been based on geophysical logging measurements made in feeler holes drilled ahead of the working face. Inasmuch as the cost of geophysical surveys is small in comparison with tunnel-construction costs, the predictive capability of these surveys should be desirable for reducing construction costs by increasing construction efficiency.

Ground-water investigations included the recording of water flows near the portal and at different intervals within the pilot bore. Where possible, initial water flows were recorded from the face, from fractures in the walls, and from feeler holes. The water level in a drill hole at the surface above the tunnel was periodically recorded. The specific conductance of the water in the pilot bore was measured at many points, and water samples for chemical analysis were taken from different points in the tunnel. The pilot bore was divided into active and passive ground-water

zones. In the active zone, near both portals, the ground-water flows were in direct response to the precipitation and runoff at the surface. In the passive zone, in the central part of the tunnel, the ground-water flows were initially large, but these flows decreased rapidly and were not appreciably affected by the annual precipitation and runoff.

The pilot bore was instrumented for the purpose of measuring the loads on the supports and for the determination of strain rates and total strain around the pilot bore. Two types of instruments were installed at 44 instrument stations: electronic load cells and borehole extensometers. The load cells were placed between the legs of the sets and the foot blocks, and at a few stations they were also placed in horizontal positions in the crown of the sets and between the legs and the invert struts to measure horizontal loads. The borehole extensometers, which were of single- and multiple-anchor types, were placed in boreholes, generally 25 feet deep, drilled into the roof and walls of the pilot bore. To better understand the load distribution on the sets, the position of the wooden blocking and lagging placed between the instrumented sets and the roof and walls was mapped at a scale of 1:24. From the load-cell and extensometer data it was possible to calculate: The total maximum and stable loads, in pounds; the maximum and stable geologic rock loads, in pounds per square foot; the wall and arch deflections, in inches; and the height of the tension arch, in feet; and to relate these factors to the geologic conditions and the engineering practices in the pilot bore.

Comparison of Predictions and Findings

By CHARLES S. ROBINSON *and* FITZHUGH T. LEE

ENGINEERING GEOLOGIC, GEOPHYSICAL, HYDROLOGIC, AND ROCK-MECHANICS INVESTIGATIONS OF THE STRAIGHT CREEK TUNNEL SITE AND PILOT BORE, COLORADO

GEOLOGICAL SURVEY PROFESSIONAL PAPER 815–I

COMPARISON OF PREDICTIONS AND FINDINGS

By CHARLES S. ROBINSON and FITZHUGH T. LEE

One of the main purposes of the Straight Creek Tunnel project was to evaluate a statistical method of compiling surface geologic information and predicting geologic and engineering data at tunnel depth.

The predictions were based on a pilot bore 8,050 feet long, 10.5 feet wide, and 11.5 feet high, supported by timber sets. As a result of a landslide at the east portal, the east portal was relocated about 150 feet to the south, and the portal grade was lowered about 16 feet. This lengthened the pilot bore to about 8,350 feet. Also, during construction, a change was made to steel sets which were used for most of the bore, and the diameter of the pilot bore, outside the steel, averaged about 13 feet. Two types of steel sets were used: 4-inch I-beam weighing 7.7 pounds per foot and 6-inch H-beam weighing 25 pounds per foot.

GEOLOGIC MEASUREMENTS

The geologic features predicted were the percentage of pilot-bore length that would be in the different rock types; the percentage that would be in the different categories of fracture spacing; the percentage that would be in faults or shear zones; and the attitudes of the faults and shear zones, joints, and foliation.

ROCK TYPES

The findings in the pilot bore of 75.4 percent granite, 23.8 percent metasedimentary rocks, and 0.8 percent diorite dikes agree well with the predicted 75 percent granite and 25 percent metasedimentary rocks (table 31). The results show that the surface and drill-hole data were adequate to define the rock-type percentages at pilot-bore depth.

FRACTURE SPACING

The fracture-spacing categories as defined on the surface were modified in the underground mapping, as explained in chapter C. The fracture-spacing categories given in table 31 are a combination of the surface and underground systems. The purpose of the combining was to put the predictions and findings in comparable form. The analysis of the pilot-bore data revealed that fracture spacing does not always provide an adequate basis for predicting rock behavior from an engineering standpoint. When the average size of a block of rock exceeds about 0.5 foot, the rock loads that develop are more dependent of the nature of the surface of the fracture than on the size of the blocks or the spacing of the fractures. Loads were found to increase greatly with an increase in rock alteration. The largest loads usually developed in the shear zones, where the rock had been ground to the size of fine sand or smaller, most of the minerals had been altered to clay minerals, and the zone was damp. A better determination of fracture spacing, perhaps by the geophysical methods, taking into account the amount of alteration, is needed.

FAULTS AND SHEAR ZONES

Underground, only those faults and shear zones greater than 1 foot wide were used to calculate the sum of the widths of the faults and shear zones. The prediction, however, was based on surface faults and shear zones greater than 5 feet wide. The change in criterion was made because the pilot bore could be mapped with more precision than was possible on the surface. The prediction that 51 percent of the total length of the pilot bore would be in faults and shear zones is considered well within the limits of mapping accuracy for the measured 49 percent.

ATTITUDES OF FAULTS AND SHEAR ZONES

In the 6-square-mile mapped area, the strike or trend of 284 faults and shear zones wider than 5 feet was measured, but the dip could be measured on only 74. Of the 284 faults, 24.7 percent had a strike or trend between N. 20° E. and N. 50° E., and 44.8 percent between N. 20° E. and N. 80° E. The average dip of the 74 faults was 75° either southeast or northwest. Underground, the attitude of 120 faults and shear zones wider than 1 foot was measured. Two maximums were defined, one representing faults that strike about N. 45° E. and dip 40°–60° SE. and one representing faults that strike about N. 20° E. and dip about 75° SE.

These figures seem to compare favorably with the predictions when it is considered that there is only 4.0 percent outcrop at the surface in the 6-square-mile area and that the pilot bore is essentially a linear feature across the area but has 100-percent rock exposure. The prediction that no fault or shear zone wider than 5 feet would follow the tunnel for considerable distance was upheld. Rock loads are related to the apparent angle of the dip of the faults and shear zones. The maximum loads developed where the apparent dip of the faults and shear zones was about 45°. The loads were less where the dips were greater or less than 45°. The data also indicated that the width of a fault or shear zone must equal about one-half the diameter of the pilot bore before any effect on the loads could be noticed. Better methods are needed, again perhaps geophysical methods, for defining the widths and attitudes of faults and shear zones at the surface.

TABLE 31. — *Comparison of predictions and findings in the Straight Creek Tunnel pilot bore*

	Prediction	Findings
Geologic measurements[1]		
Rock type (percentage of pilot-bore length):		
Granite	75.0	75.4
Metasedimentary rock	25	23.8
Diorite dikes	Minor	.8
Fracture spacing (percentage of pilot-bore length):		
<0.1–0.5	40.1	38.7
0.5–1	49.3	42.6
>1 ft	10.6	18.7
Faults and shear zones (percentage of pilot-bore length)	51	49
Faults and shear zones, principal ranges in trend or attitude (Surface, >5 ft wide; pilot bore, >1 ft wide):		
Strike	N. 20°–50° E.	N. 45° E., N. 20° E.
Dip	75° NW. or SE.	75° SE., 40°–60° SE.
Joints, principal range and average attitude:		
Strike	180°	180°
Dip	45°–90°	8°–90°
Average dip	60°	45°
Foliation, principal range:		
Strike	N. to N. 30° E.	N. 10°–60° E.
Dip	60°–90° SE. or NW.	10°–50° SE.
Statistical maximums:		
Foliation		
Strike	N. 15° E.	N. 45° E.
Dip	65° SE. or 70° NW.	30° SE.
Joints:		
Strike	N. 30° E.	----------
Dip	75° NW.	----------
Average dip	60°	30°
Engineering measurements		
Rock loads (psf):		
Predicted maximum rock load calculated from Terzaghi (1946) on 10.5- × 11.5-ft pilot bore	5,900	----------
Predicted maximum rock load recalculated from Terzaghi (1946) on 13- × 13-ft pilot bore	6,970	----------
Calculated geometric midpoint for maximum stable geologic rock load from measurements in pilot bore, 13 × 13 ft	----------	6,300
Average final swell pressure (psf) of altered rock and gouge	[2] 2,233	[3] 1,727
Ground water (gpm):		
Maximum initial flow from any section	1,000	750
Maximum cumulative flow at east portal	500	800
Flow at east portal 2 weeks after completion of pilot bore	300	130
Construction practices[4]		
Set spacing (percentage of pilot-bore length):		
1-ft centers	1.6	2
2-ft centers	23	22
3-ft centers	40	30
5-ft centers	35	20.9
Invert struts	1.4	8
Total number of sets	2,691	2,059
Total number of invert struts	113	210
Lagging and blocking (footage in pilot bore):		
100–67 percent lagged and blocked	1,731	1,456
66–34 percent lagged and blocked	3,659	2,447
33–0 percent lagged and blocked	2,660	4,447
Feeler holes (linear feet)	2,905	9,816
Grout (linear feet of pilot bore)	403	0
Construction costs[5]		
Estimated cost (bid by Mid-Valley, Inc.)	$1,300,000	----------
Actual cost	----------	$1,400,000

[1]Predictions based on 4.0 percent outcrop.
[2]Average of 6 samples.
[3]Average of 29 samples.
[4]Predictions based on pilot-bore length of 8,050 ft; findings based on pilot-bore length of 8,350 ft.
[5]Values are rounded.

ATTITUDES OF JOINTS

The prediction that the joints in the pilot bore would strike in any direction was confirmed by the mapping of the pilot bore. The predicted attitude of joints in the pilot bore based on the surface information included a maximum representing joints with attitudes of N. 80°–90° E., 65°–75° NW. which was 2.5 percent of 838 joints. The joints of this maximum were considered to be probably related to the N. 70°–80° E. fault directions but the maximum was not considered significant from an engineering point of view. The joints in the pilot bore gave minor maximums of N. 70°–80° E., 60°–75° NW., and N. 40°–50° W., 40°–50° SW., but in general for engineering purposes the joints can be considered to strike in any direction and to dip from 8° to 90°. The average dip of 60° determined at the surface was high compared to the average dip of 45° determined in the pilot bore. For the pilot-bore analysis, the attitudes of the joints on the walls and on the heading faces were compiled separately, which resulted in considerably different contour-diagram configurations. On the walls, relatively fewer joints having a N. 45° E. strike and northwest dip were recorded, whereas on the faces fewer joints having a N. 20° E.–N. 30° W. strike and northwest or southwest dip were recorded. This comparison suggests that what is considered a significant joint, and so recorded, depends on the trend of the surface in the tunnel being mapped in relation to the attitude of the joint and the direction of the tunnel. About four times as many joints were measured on the faces as on the walls because of the scale of mapping and the number of faces mapped.

ATTITUDES OF FOLIATION

The strike of the foliation at the surface agrees closely with that in the pilot bore, as predicted, but the dip at the surface is considerably higher than in the pilot bore. The dip at depth may actually be less than at the surface, but another possible explanation of the difference lies in the number of measurements made in the granite in relation to the number of measurements made in the metasedimentary rocks; the measurements of both were combined in the compilations. Data from the surface mapping represent 161

measurements in granite and 28 in metasedimentary rocks; data from the pilot bore mapping represent 93 measurements in granite and 113 in metasedimentary rocks. Also, in the pilot bore, the relation of the surface of measurement to the attitude of the foliation (as with the joints) probably influences the number of observations made. The attitude and degree of foliation, even in the more schistose rocks, had only a minor influence on rock loads.

ENGINEERING MEASUREMENTS

ROCK LOADS

The maximum predicted rock load of 5,900 psf (pounds per square foot) was based on the preliminary design of a 10.5- by 11.5-foot pilot bore utilizing a modification of the formula of Terzaghi (1946). The final pilot bore, however, averaged about 13 feet in diameter. Using the same formula, the predicted maximum rock load for this size tunnel would be 6,970 psf.

The results of the instrumentation of the pilot bore required a modification of Terzaghi's method for calculating the stress around a tunnel.

It is known that as the face advances away from a point, a maximum load develops at that point, which — after a period of time — drops off to a stable load. The time for, and the magnitude of, the development of the maximum load, the time required for the load to stabilize, and the magnitude of the stable load are dependent upon geologic conditions, construction practices, and the dimensions of the tunnel. It is possible within certain limits to determine the part of the load that is the result of the construction practices and the part that is the result of geologic conditions (Robinson and Lee, 1965).

That part of the load that is the result of the geologic conditions is termed the geologic load, and that part that is the result of the construction practices is termed the construction load. The geologic conditions were divided into three categories depending upon a range in fracture spacing and a range in the percentage of alteration. The range in the geologic loads for each geologic category was calculated from the results of the instrumentation. From this range in geologic loads a geometric midpoint for each geologic category was calculated. The geometric midpoint is that geologic load that multiplied by or divided by a factor will give the range in loads for the geologic category. For the pilot bore, the geometric midpoint for the most difficult geologic conditions — where the maximum loads developed — was 6,600 psf with a factor of 1.5. The range in geologic loads for the most difficult geologic conditions was 4,400–9,900 psf. As a result of the most difficult geologic conditions and the construction practices, the maximum load that developed in the pilot bore was about 20,000 psf. Probably the calculated geometric midpoint for the worst geologic conditions most closely fits the theory as developed by Terzaghi (1946).

FINAL SWELL PRESSURE OF FAULT GOUGE

It was assumed that weathering and ground water would not appreciably change the clay mineralogy of fault gouge and altered rock at the surface and that the final swell pressures of this material in the pilot bore would be about the same. The average final swell pressure of 29 samples collected from the pilot bore was 1,727 psf which compares favorably with an average final swell pressure of 2,233 psf based on six samples from the surface. The assumption that the final swell pressures of samples from the surface would be about the same as for samples from the tunnel therefore seems valid.

GROUND-WATER FLOWS

The figures for the predicted and for the actual maximum flow from the portal have little significance. The principal authors, in their original calculations and predictions, did not account for the time of year and the influence of spring runoff. The normal ground-water flow from the portal increased on the order of 7.5 times as a result of the spring runoff.

The predicted flow from the portal 2 weeks after completion of the tunnel was based on a constant rate of advance of the tunnel of 1,000 feet per month. The average rate for the tunnel was about 610 feet per month. At this rate of advance, the estimated flow would have been about 183 gpm. These figures, although comparable, are meaningless because the influence of the spring runoff was not considered, and if the tunnel had been completed in the spring, the measured flow at the portal would have been greater than the predicted flow.

All the water flow predictions were based on an interpretation of the porosity and permeability of the faults and shear zones, which were estimated too high. In the pilot bore, the faults and shear zones had relatively low permeability and were essentially dry when intersected by the pilot bore. The principal water flows came from relatively competent rock with open joints, most of which were beyond the limits of the faults and shear zones.

CONSTRUCTION PRACTICES

The predictions of the spacing of sets, lagging and blocking, feeler holes, and amount of grout were, of course, empirical because actual requirements can be determined only at the time of construction. It was believed that such predictions would be of value in estimating the cost of construction. Geologic conditions alone do not determine construction requirements. Other factors, some of which have been discussed in relation to the geologic load, also exert an influence.

SET SPACING

In the pilot bore, the sets were not uniformly spaced, particularly where jump sets were added. For the purpose of comparison with the prediction, spacings of 0.5 foot to 1.5

feet are combined and compared with 1 foot, 1.5 to 2.5 with 2 feet, 2.5 to 4.5 with 4 feet, and 4.5 and greater with 5 feet.

The predicted and actual spacing of sets agree well when all the factors that influence support are considered, plus the fact that the length of the tunnel was increased by approximately 300 feet. The total number of sets calculated from the predicted spacing was 2,691. The actual number used was 2,059.

It was predicted that 1.4 percent of the pilot-bore length would require struts on 1-foot centers, or 113 struts. The contractor used struts for 8.0 percent of the pilot-bore length, or 210 struts, but these were on 1- to 3-foot centers.

LAGGING AND BLOCKING

The predictions for lagging and blocking specified the sections of the pilot bore that would require blocking only, blocking and lagging along the arch, and blocking and lagging along the arch and walls. In practice, it was more convenient to record the percentage of blocking and lagging around the walls and arch. The predicted figures have been converted to percentages for comparative purposes and are shown in table 31.

FEELER HOLES

The drilling of feeler holes was recommended in the preconstruction report (Robinson and Lee, 1962), and the approximate areas in which they might be advisable were indicated. In practice, the Colorado Department of Highways and the contractor considered it advisable to keep at least one feeler hole about 40 feet in advance of the face for most of the length of the pilot bore, a decision in which the authors concurred. For that reason, there is a considerable difference — on the order of almost 4 times — between the predicted number of linear feet of feeler holes and the footage actually drilled. Most of the feeler holes, however, did not intersect broken, water-saturated ground, which was their purpose. From an economic and safety point of view, however, they were advisable, for they gave the contractor a better idea of the ground in advance of the face and allowed him to plan more economically and more confidently such things as lengths of round and supplies (sets, timber, and so forth) needed in the pilot bore.

GROUT

It was predicted that it might be economic to grout certain types of ground in advance of the face, as determined by feeler holes. The purpose of the grout is to consolidate the ground and seal off water and thereby reduce the amount of support required and reduce the difficulty of driving through that section. The alternative is the used of closely spaced steel supports and forepoling. The choice of methods is made by the contractor and his employer, and they decided that grout was not needed in the pilot bore.

COST

The pilot bore was holed through during the first week of December 1964, and cleanup work was completed in January 1965. The total cost of construction of the pilot bore was approximately $1,400,000, which compares favorably with the contractor's bid of $1,300,000.

CONCLUSIONS

The accuracy of a geologic projection depends on the understanding of the structural elements of the geology, the amount of time available for surface examination, the time and money for physical exploration involving drill holes, the application of geophysical techniques, and the knowledge and experience of the geologists. The Straight Creek Tunnel project has established that geology can be treated statistically to predict the kinds and percentages of different geologic conditions at depth, and that engineering requirements can be equated with predicted geologic conditions to provide a sound basis for estimating probable cost of construction. This should benefit both the design engineer and the contractor who, having a prior knowledge of the conditions underground, can more confidently design and construct the underground structure. Savings accrue as confidence increases. All the materials necessary for the job could be ordered in advance, rather than piecemeal as the excavation proceeds. The labor force could be scheduled well in advance, allowing the contractor to more efficiently plan his activities.

The failures of some of the predictions of the project have shown those fields in which there is not adequate geologic and engineering knowledge. Continued research in the prediction of geologic conditions and engineering behavior of rock masses at the depth of a tunnel should make possible more accurate predictions and thus reduce the cost of construction, particularly by reducing the amount required for contingencies.

The Straight Creek Tunnel project was conducted in an area with a relatively small number of geologic variables, which in part accounts for its success. It is believed, however, that a similar approach can be equally successful when applied to the projection of geology to depth in any geologic environment if the structural framework of the geology is properly analyzed and thoroughly understood.

GLOSSARY OF TUNNEL TERMS

The following definitions, most of which are used in the report, may be useful to the reader unfamiliar with mining terminology. Some definitions are the authors'; the others were taken from Terzaghi (1946) and from L. A. Warner, E. E. Wahlstrom, and C. S. Robinson, (unpub. information).

Abutment. The area of concentration of ground stress that has been deflected by an opening or by a zone of more yielding ground.

"A" line. The line within which there shall be no steel or timber support.

Arch. Curved roof of an underground openring. The portion of the tunnel above the centerline.

Arching tendency. Tendency of incompetent or moderately competent rocks to form an arch above an underground opening by caving. Commonly the arch assumes the shape of a Gothic arch in cross section.

Air drill. A rock drill driven by compressed air.

Air hammer; air spade. A pneumatic hammer or spade.

"B" line. The line within which no unexcavated material, tamped fill, lagging, spiling, crown bars, spreaders, collar braces, or wall plates shall remain.

Back. Roof of a tunnel or mine.

Bar. A drilling, tamping, or prying rod.

Barring down. Removing loose rocks in the roof of a mine (or tunnel) by means of a bar.

Bench. (1) A level layer worked separately in a mine (or tunnel). (2) A ledge left, in tunnel construction work, on the edge of a cutting in earth or in rock.

Bid items. Items of work listed in contract documents and serving as the basis for bids by the contractor.

Blasthole. A hole for a blasting charge.

Blocking. Wood blocks placed between steel supports and walls or the arch of a tunnel to provide support and maintain alinement of ribs.

Breastboards. Wood planking placed temporarily at tunnel heading to contain incompetent rock.

Broken ground. Incompetent, shattered rock.

Bulkhead. A solid crib used to support a very heavy roof, face, or wall.

Cap. A piece of timber or plank placed horizontally above and between the posts of a timber set.

Cave; cave-in. The partial or complete collapse of a mine or tunnel.

Center cut; center shot. The boreholes, drilled to include a wedge-shaped piece of rock, which are fired first in a heading, tunnel, drift, or other working place.

Centerline. The line at the center of the finished concrete lining of circular cross section of the tunnel.

Change order. Order issued to define procedures or items of work not covered in contract documents, or order to change the provisions expressed in the original contract documents.

Charge. The explosive loaded into a borehole for blasting.

Collar. The mouth or opening of a borehole.

Collar brace. Wood or steel brace placed between or on top of steel sets to maintain alinement.

Competent rock. Rock that will stand with little or no support in underground openings.

Contract drawings. Drawings included in the contract documents.

Contract specifications. Specifications for various items of construction included in the contract documents.

Core drill. A diamond drill or other hollow drill for securing cores.

Cover. The total thickness of strata overlying the underground workings; overburden.

Cribbing. (1) Close timbering, as the lining of a shaft. (2) The construction of cribs of timber and earth or rock to support the roof.

Crown bar. Steel rail or heavy wood plank placed on top of steel set or sets nearest heading and projecting forward to tunnel heading. Provides temporary support of rock in arch until additional steel sets and lagging can be installed closer to the heading.

Crown tree; crown. (1) A piece of timber set on props to support the mine roof. (2) Crown also refers to roof of tunnel.

Cut holes. The first round of holes fired in a tunnel or shaft. They are placed so as to force out a cone-shaped core in the center of the heading and relieve the burden on the second round of shots.

Ditch. An artificial watercourse, flume, or canal to convey water away from tunneling operations.

Entry. An underground passage used for haulage or ventilation, or as a manway.

Extensometer. Instrument used for measuring small deformations, deflections, or displacements.

Face. *See* Heading.

False set. A steel or timber set placed temporarily to expedite a tunneling operation, as, for example, a spiling operation.

Fan. A revolving machine to blow air into a mine (pressure fan, blower) or to draw it out (suction fan).

Feeler hole. Hole drilled from tunnel heading or elsewhere to test geologic conditions beyond heading or in rocks adjacent to an underground opening.

Floor. That part of any underground excavation upon which one walks or upon which a track is laid.

Foot block. Wood block serving as a support at the base of a steel rib. Block on which ribs are erected.

Force account (extra work order). Order issued to contractor to perform work not originally described in the contract documents.

Forepoling. *See* Spiling.

Full-face method. A method of tunneling or drifting whereby the whole area of the face is blasted out each round.

Grout. Mixture of cement, water, and, for special purposes, various additives. Pumped into fractured rock to fill voids, seal off water flows, and increase strength.

Gunite. Mixture of water, sand, and cement sprayed on exposed rock to provide a protective coating.

Heading. The working face at the limit of penetration of the tunnel.

Incompetent rock. Rock that will not stand in underground openings without support.

In situ. In its natural position or place.

Invert. The portion of the tunnel below the centerline. The bottom, or floor, of a tunnel.

Invert section. The section of the tunnel below the centerline or spring line.

Jump set. Steel or timber set placed between existing sets to provide additional support.

Lagging. Wood planking or blocks placed above and on sides of steel ribs to contain broken rock and to prevent its fall into an underground opening.

Left rib. The steel rib on the left side of the tunnel (as one faces the tunnel heading).

Load. Weight of surrounding rock on tunnel supports.

Load cell. Instrument placed in or under tunnel support to measure the rock load on the support.

Muck. Disaggregated rock formed by blasting operation or by the free flow of incompetent material into an underground opening.

Mucking machine. The machine used to load broken rock for haulage out of underground excavations.

Opening. An entrance to a mine or tunnel.

Overbreak. Rock removed from outside the payline as defined in the specifications. Generally expressed as the percentage of material removed in a cross-sectional area relative to the area within the payline. Also may be expressed as a volume percent.

Payline. The line beyond which the contractor shall not be paid for excavation. Excavation outside of the payline is done at the contractor's expense.

Permanent support. The concrete lining of the tunnel. Steel and timber supports are regarded as temporary supports.

Pilot bore (tunnel). A small tunnel driven before a main tunnel to determine its grade and direction, as well as to determine underground conditions.

Popping rock. Stressed rock that fails with explosive violence and ejects rock fragments with high velocity.

Post. A mine timber fastened between the roof and floor and standing vertically, or nearly so.

Relief holes. Boreholes that are loaded and fired for the purpose of relieving

or removing part of the burden of the charges to be fired in the main blast.

Rib. A curved steel segment comprising half of a steel set or support.

Rib shot. A shot in the face next to a rib.

Right rib. The steel rib on the right side of the tunnel (as one faces the tunnel heading).

Rock bolt. Steel bolt split at the bottom and inserted into a drilled hole in rock to support the rock. Head of bolt is forced against a steel plate next to the rock to make bolting action more effective.

Rock load. The pressure on tunnel supports due to weight of overlying rock mass.

Roof. The upper portion of a tunnel, especially the part of the tunnel immediately above the centerline.

Round. Volume of rock removed in one drilling and blasting cycle.

Running ground. Clayey or sandy aggregate, commonly water saturated, that flows freely into underground excavations.

Set. A timber or steel frame for supporting the sides of a tunnel, shaft, or other excavation.

Shift. The length of time a miner works in 1 day — 8 hours in this report.

Shot. A charge or blast.

Slabbing. The development and falling of thin fragments of rock from the surfaces of an underground opening.

Soft ground; heavy ground. Rock above underground openings that does not stand well and requires strong support.

Spalling rock. A rock mass under stress that yields thin slabs or wedges of rock by progressive failure. Slabs commonly form parallel to walls or the arch of an opening in rock.

Spiling. Pointed steel bars or rails, or wood planks or logs driven into the tunnel heading to support incompetent rock until supports can be placed. Generally, the spiling is driven above and beyond the supports nearest the heading or on top of and beyond a false set.

Splitting rock. A rock mass under stress that breaks and ejects small fragments with considerable velocity.

Spring line. The line across or parallel to the tunnel above which the steel ribs are bent to a radius of curvature different from that below it. Longest horizontal dimension between steel ribs. May or may not coincide with centerline.

Spreader. Wood section placed between sets to maintain tension on tie rods or preserve alinement.

Squeezing ground. Incompetent material, generally clayey, that behaves plastically under stress and tends to close the tunnel opening.

Station. Distance from zero point, measured in hundreds and fractions of feet. For example, station 105+06.5 is 10,506.5 feet from station 0+00.

Steel rib. One of the segments of bent structural steel bolted to another rib to form a steel support (set) in a tunnel.

Steel set. Steel support consisting of two ribs bolted or welded together. May include a strut across the invert of the tunnel.

Stem; stemming. The inert material used on top of a charge of powder or dynamite to contain the explosion within the rock mass.

Strain gage. An instrument for measuring the expansion or compression occurring parallel to a surface of a body and over a known gage length, which can then be converted into strain.

String. A series of well-drilling tools arranged for lowering into the hole.

Strut. Steel or timber segment placed between steel ribs across tunnel invert to provide additional strength. Bolted or welded to bottom extensions of ribs.

Support. Any fabricated structure — steel, wood, or concrete — placed to prevent failure of rocks around underground openings.

Swelling ground. Rock that swells after being exposed, usually because of hydration of clay minerals in an altered rock.

Temporary support. Support placed to support tunnel rocks until permanent supports can be installed. Steel and timber supports generally are regarded as temporary.

Tension arch (destressed zone). Height of rock mass in roof of underground opening that tends to move toward opening in response to gravity forces.

Tie rod. Steel rod threaded at both ends. Used as a connection between adjacent steel sets to hold sets in place and provide strength in the direction of the tunnel.

Timber. Any of the wooden props, posts, bars, collars, lagging, and so forth, used to support mine workings.

Timber lagging. Timber planks placed on sides and on top of steel sets to contain exposed rocks between the sets and to transmit loads to the steel sets.

Topheading. A small tunnel opening ahead of the full-size opening. Used to probe and place temporary supports in exceedingly incompetent or wet sections of tunnel.

Tunnel. An approximately horizontal underground passage open at both ends.

Tunnel face. *See* Heading.

Tunnel section. Outline of tunnel as measured at right angles to centerline, or any portion of the tunnel measured parallel to the direction of the tunnel.

Tunnel supports. Wood, steel, or concrete structures placed to prevent collapse or failure of tunnel rocks.

Wall. The side of a tunnel or mine working.

Wedge. Wooden wedge used to hold lagging or steel supports in place.

Working face. The heading being excavated by drilling and blasting.

ANNOTATED BIBLIOGRAPHY OF REPORTS ON THE STRAIGHT CREEK TUNNEL PILOT BORE, 1960–68

This section contains a short statement of contents of reports pertaining to the Straight Creek Tunnel project and was prepared to aid readers in acquiring additional historical or collateral information.

Abel, J. F., Jr., 1965, Tunnel instrumentation: Mines Mag., v. 55, no. 1, p. 20–23.

The purpose and capabilities of the pilot-bore rock-mechanics instruments are explained. The zones in a tunnel where rock and steel set failures occur are related to the zone of dynamic strain near the advancing face. Both the rock around the opening and the steel sets afford confinement and support for the rock loads and must be considered in the design of a tunnel support system. The extent of the dynamic rock strain zone is a function of the rock structure, as well as of the construction practices at any given instrumentation station in the pilot bore.

Abel, J. F., Jr., 1966, Statistical analysis of tunnel supporting loads: Am. Inst. Mining, Metall., and Petroleum Engineers Trans., v. 235, p. 288–301.

By means of stepwise multiple-regression analyses, Abel determined the geologic, engineering, and construction variables that most significantly affected rock loads in the Straight Creek Tunnel pilot bore. In the order of their relative significance, the geologic variables were degree of faulting, percentage of alteration, water conditions, distance to nearest fault, and average joint spacing. Significant engineering and construction variables were steel-section modulus and number of effective blocking points. The depth of the pilot bore variable had no statistical significance.

Abel, J. F., Jr., 1967, Tunnel mechanics: Colorado School Mines Quart., v. 62, no. 2, 88 p.

This publication is Abel's doctoral thesis submitted to the Colorado School of Mines (1966). Elastic model response to a single opening and the author's photoelastic plane stress models are briefly described. Computer analyses of set loads, rock strains, geologic conditions, and construction

practices demonstrated the inelastic behavior of the rock mass surrounding the Straight Creek Tunnel pilot bore. Statistical models based on the computer analyses allow prediction of construction and engineering parameters for other tunnels.

Carroll, R. D., Scott, J. H., and Cunningham, D. R., 1966, Elastic moduli of granitic rock from in situ measurements of seismic velocity, *in* Geological Survey research 1966: U.S. Geol. Survey Prof. Paper 550–C, p. C25–C28.

Measurements in the pilot bore were made using a linear array of accelerometers along the walls. A recognizable shear-wave arrival on a number of records allowed elastic moduli to be calculated. Consistent shear-wave generation with repeated shooting was not obtained even though numerous shot hole orientations were tried. A section of relatively unfractured granite was selected for these initial tests. Average dynamic values were calculated to be compressional-wave velocity, 17,800 fps; shear wave velocity, 8,900 fps; Young's modulus, 7.6×10^6 psi; shear modulus, 2.8×10^6 psi; bulk modulus, 7.6×10^6 psi; and Poisson's ratio, 0.33.

Drake, R. E., 1967, A surface-subsurface measurement of an anomaly in the vertical gradient of gravity near Loveland Pass, Colorado: Riverside, California Univ. unpub. M.A. thesis.

Results of surface and pilot-bore measurements of the vertical gradient of gravity indicate a vertical anomaly, ranging from +0.4 to +3.7 percent, which probably represents rock density changes between the surface and the pilot bore.

Grosvenor, N. E., and Abel, J. F., Jr., 1966, Measurement on the pilot bore for the Straight Creek Tunnel, *in* Rock mechanics: Highway Research Rec. 135 (Natl. Research Council–Natl. Acad. Sci. Pub. 1379), p. 27–34.

The results of load cell and borehole extensometer instrumentation in the pilot bore showed that as the face advances away from an instrumented station, the load increases until the face is a certain distance from the station. This distance is dependent upon rock conditions, advance rate, and method of support installation. Rock-strain–time plots were used in assessing the adequacy of pilot-bore support. The pattern of decreasing strain rate was a primary indication of approaching stability. Measured radial strains were similar to those anticipated by elastic theory, and these data are directly applicable to roof support (rock bolt) design.

Hartmann, B. E., 1966, Rock-mechanics instrumentation for tunnel construction: Wheat Ridge, Colo., Terrametrics, Inc., 153 p.

Borehole extensometer and load-cell measurements from the Straight Creek Tunnel pilot bore in different structural environments illustrate rock-mass behavior around underground excavations. Data from instruments can be utilized to provide confidence in tunnel design and to control safety factors.

Hurr, R. T., and Richards, D. B., 1966, Ground-water engineering of the Straight Creek Tunnel (pilot bore), Colorado: Assoc. Eng. Geologists Eng. Geology Bull. v. 3, nos. 1, 2, p. 80–90.

Ground-water flows in the pilot bore were directly related to rock-fracture density and distance from the portals. The two near-portal zones are called the active zones, where rates of flow vary with the season. A passive zone was located in the central rock mass between the portals, where water issues at a more constant rate.

Lee, F. T., and Nichols, T. C., Jr., 1966, Rupture phenomena in the Silver Plume Granite, Colorado, *in* Geological Survey research 1966: U.S. Geol. Survey Prof. Paper 550–C, p. C29–C33.

Fractures, slickensides, and gouge produced during laboratory compressive testing of cylinders of Silver Plume Granite obtained from surface and pilot bore samples resembled fractures noted in the granite during surface and subsurface mapping in the Straight Creek area. Formation of gouge and slickensides in the laboratory is believed to be due primarily to energy release, rather than to movement and granulation. It is suggested that fault displacements in granitic terrane should be examined in the light of these findings.

Nichols, T. C., Jr., and Lee, F. T., 1966, Preliminary appraisal of applied rock mechanics research on Silver Plume Granite, Colorado, *in* Geological Survey research 1966: U.S. Geol. Survey Prof. Paper 550–C, p. C34–C38.

A program of laboratory testing was conducted to determine elastic and physical properties of Silver Plume Granite samples, some of which were obtained from the Straight Creek area. Data derived from the tests were used to relate deformation to the structure, fabric, and mineralogy of the rock. Results showed that strong lineations, foliations, joints, faults, and mineralogic variations are related to deformation and failure of the rock. The physical behavior of a rock, as determined in the laboratory, is significant to the engineer when it can be related to the behavior of the rock in the field.

Pavlo, E. Lionel, Engineering Co., 1960, Interstate highway location study, Dotsero to Empire Junction [Colorado]: Colorado Dept. Highways State Proj. HPS–1–(20), 38 p.

This report gives the results of a feasibility study for locating the best highway tunnel route through the Continental Divide west of Denver. It is established that an overland route across the Continental Divide meeting interstate highway standards cannot be constructed. The Straight Creek route was selected over several other tunnel routes on the basis of lower cost, greater road-user benefit, shorter tunnel and total route length, fewer major structures, shorter length of maximum grades, better alinement, and better utilization of construction stages. The estimated cost for the first bore of the dual highway tunnel (including pilot bore) was $28,792,000.

Richards, D. B., 1963, Engineering geology of the proposed Straight Creek Tunnel, Clear Creek and Summit Counties, Colorado: Colorado School of Mines unpub. M.S. thesis T–982, 131 p.

An early study of rock units and structural features of the Straight Creek Tunnel area in which the author recommended a preferred route alinement based on geologic conditions at the surface. He also considered the feasibility of a surface crossing of the Continental Divide in the Straight Creek area.

Robinson, C. S., Carroll, R. D., and Lee, F. T., 1964, Preliminary report on the geologic and geophysical investigations of the Loveland basin landslide, Clear Creek County, Colorado: U.S. Geol. Survey open-file report, 5 p.

The Loveland Basin landslide in June 1963 threatened the east portal of the proposed pilot bore. Geologic, geophysical, and engineering studies made prior to pilot-bore construction were successful in providing a three-dimensional definition of the slide that was useful for designing methods of stabilizing the slide. Geophysical and geologic data indicated that the movement of the landslide was probably taking place along a slip zone, from a few inches to possibly as much as 40 feet thick, at the base of the landslide.

Isopach and structure contour maps prepared from the geological and geophysical data indicated that the volume and mass of landslide material above the slip zone was 270,000 cubic yards weighing 567,000 tons, and that the volume and mass of the landslide to the base of the slip zone was 770,000 cubic yards weighing 1,600,000 tons. It is believed that in any

sudden failure of the landslide, the volume and mass of material involved would be in amounts between these figures.

Robinson, C. S., and Lee, F. T., 1962, Geology of the Straight Creek Tunnel site, Clear Creek and Summit Counties, Colorado, and its predicted effect on tunnel construction: U.S. Geol. Survey open-file report, 43 p.

This report presents the preliminary results of geologic and geophysical research at the surface over the proposed Straight Creek Tunnel. The results are interpreted and, primarily on the basis of statistical analyses, predictions are made as to the probably geologic conditions at the depth of the tunnel and how these conditions may influence the engineering design of the pilot bore. Methods of compilation of data and the accuracy of predictions are discussed.

The report was furnished to the Colorado Department of Highways prior to construction of the pilot bore, so that prospective bidders on the pilot bore might be appraised of the geologic and hydrologic conditions to be expected.

Robinson, C. S., and Lee, F. T., 1964a, Engineering geology of Straight Creek Tunnel site, Colorado, *in* Symposium on soil exploration, Atlantic City, N.J., 1963: Am. Soc. Testing and Materials Spec. Tech. Pub. 351, p. 17–28.

A statistical three-dimensional model of the geology at the depth of the tunnel was developed on the basis of field and laboratory information. From this model predictions were made as to probable rock load, spacing of sets, areas to be tested by feeler holes, amount of grout, average flow of water as the heading is advanced, and the maximum initial flow of water that might be expected within any interval of the pilot bore.

Robinson, C. S., and Lee, F. T., 1964b, Geologic research at the Straight Creek Tunnel site, Colorado: Highway Research Rec. 57 (Natl. Acad. Sci–Natl. Research Council Pub. 1241), p. 18–34.

Detailed surface geologic mapping was combined with drill-hole and geophysical information to prepare a statistical model of the geology at the depth of the proposed pilot bore. From this model it was possible to calculate the probable rock loads, spacing of sets, spacing of lagging, probable sections of the bore that should be tested by feeler holes, probable amount of grout required to seal badly broken ground that was highly saturated with water, probable amount of water that would flow from the portal as the face advanced, and probable initial amount of water expected to flow from a fault zone within any interval of the pilot bore.

Robinson, C. S., and Lee, F. T., 1965, Preliminary report on the engineering geology of the Straight Creek Tunnel pilot bore, Clear Creek and Summit Counties, Colorado: U.S. Geol. Survey open-file report, 33 p.

This report was for the Colorado Department of Highways to be used in planning and design of the final highway tunnel and to illustrate the relative success of the various research methods and of the preconstruction predictions.

Laboratory tests on samples from the most severely altered rock show that the high loads in the pilot bore were primarily the result of squeezing, rather than swelling, ground. It was possible to define those intervals in the final bores that would probably require maximum support, intermediate support, and minimum support, and to define the range in loads to be expected in each supported interval as a result of the geologic conditions. It was estimated that the ground-water flows from the final bores probably would not exceed 500 gpm during periods of spring and summer runoff (May–August) and that the average flow would probably be on the order of 100–150 gpm.

Robinson, C. S., and Lee, F. T., 1967, Results of geologic research at the Straight Creek Tunnel pilot bore, Colorado: Highway Research Rec. 185 (Natl. Acad. Sci.–Natl. Research Council–Natl. Acad. Eng. Pub. 1516), p. 9–19.

Results of geologic investigations made prior to and during construction of the pilot bore were compared with predictions. Agreement was good on the following: Rock type, fracture spacing, faults and shear zones, strike of joints and foliation, rock loads, final swell pressure of fault gouge, set spacing, and lagging and blocking. Not in good agreement were dip of joints and foliation, placement of feeler holes, and amount and type of grout needed. Ground-water flows agreed with the predictions, but for reasons different from the basis of prediction. Water came from relatively unfractured rock, rather than from faults and shear zones. Also, the flow from the portal was found to be dependent upon the time of year.

Scott, J. H., and Carroll, R. D., 1967, Surface and underground geophysical studies at Straight Creek Tunnel site, Colorado: Highway Research Rec. 185 (Natl. Acad. Sci.–Natl. Research Council–Natl. Acad. Eng. Pub. 1516), p. 20–35.

Seismic refraction and electrical resistivity measurements were made on the surface above and in the pilot bore before, during, and after construction. Underground measurements were interpreted to obtain the seismic velocity and electrical resistivity of rock behind the disturbed layer surrounding the bore. These velocity and resistivity values were correlated statistically with the following economic and engineering parameters: Time rate of construction, cost of construction per foot, rock quality, set spacing, percentage lagging and blocking, type of steel support required, height of tension arch, and vertical rock load. The quality of these correlations ranged from 0.8 to nearly 1.0 in absolute value. Surface seismic measurements revealed the presence of three distinct layers of rock approximately parallel to the surface. The deepest layer has an average velocity of 16,400 feet per second, similar to the average velocity of rock in the pilot bore behind the disturbed layer. Estimates of engineering and economic parameters based on these velocities were reasonably accurate.

Electrical resistivity measurements from surface and drill holes were used to estimate the average resistivity of zones of rock at pilot-bore level. These estimates are less accurate than those based on seismic velocity. The discrepancies between actual values and estimates based on resistivity indicate that the resistivity of rock in the immediate vicinity of the pilot bore was generally lower than the average resistivity of the large volumes of rock that influenced the surface resistivity measurements.

Scott, J. H., Lee, F. T., Carroll, R. D., and Robinson, C. S., 1968, The relationship of geophysical measurements to engineering and construction parameters in the Straight Creek Tunnel pilot bore, Colorado: Internat, Jour. Rock Mechanics and Mining Sci., v. 5, p. 1–30.

Seismic refraction and electrical resistivity measurements made along the walls of the pilot bore during and after construction showed good correlation with rock condition. A low-velocity and high-resistivity layer exists in the disturbed rock surrounding the excavation. The electrical resistivity and the seismic velocity of rock at depth, the thickness of the rock in the low-velocity layer, and the relative amplitude of seismic energy correlated well with the following important tunnel construction parameters: Height of the tension arch, stable vertical rock load, rock quality, rate of construction and cost per foot, percentage of lagging and blocking, set spacing, and type and amount of steel support required.

The authors concluded that parameters of interest in tunnel construction could be predicted from geophysical measurements made in feeler holes drilled ahead of an advancing face. The predictions might be based on cor-

relations established either during the early stages of construction or from geophysical surveys in other tunnels of similar designs in similar geologic environments.

Terrametrics, Inc., 1964, Rock mechanics instrumentation, Straight Creek Tunnel pioneer bore: Monthly Repts, to Colorado Dept. Highways, Jan.–Nov.

Basic data from all pilot-bore rock-mechanics instrumentation are given in these reports. In addition, rock and steel support behavior are interpreted.

Tippetts-Abbett-McCarthy-Stratton, Engineers, 1965, Research investigations and studies to establish the ventilation requirements for the Straight Creek Highway Tunnels, Colorado, Project No. 170–3(13)212: New York, Rept. prepared for Colorado Dept. Highways and Bur. Public Roads, 149 p.

The ventilation of a vehicular tunnel at an altitude of 11,000 feet presents a difficult problem because human tolerance to carbon monoxide exposure is significantly decreased at high altitudes, and emission of carbon monoxide by vehicles increases appreciably. Physiological effects of exposure to carbon monoxide at high altitudes have been noted and studied. Prior to this study information on the emission of carbon monoxide by gasoline engines has been generally limited to tests of vehicles operating at low altitudes. Ventilation of the Straight Creek Tunnel required the development of wholly new design criteria. In addition to carbon monoxide investigations, this report contains preliminary tunnel section designs, cost estimates, and proposed portal structures. The predesign cost estimate for construction of the first of the two bores was $39,500,000 (exclusive of pilot bore).

REFERENCES CITED

Abel, J. F., Jr., 1965, Tunnel instrumentation: Mines Mag., v. 55, no. 1, p. 20–23.

_____1966, Statistical analysis of tunnel supporting loads: Am. Inst. Mining, Metall. and Petroleum Engineers Trans., v. 235, P. 288–301.

_____1967, Tunnel mechanics: Colorado School Mines Quart., v. 62, no. 2, 88 p.

American Society for Testing and Materials, 1952, Tentative method of test for fundamental transverse and torsional frequencies of concrete specimens, *in* 1952 book of ASTM standards, Pt. 3: p. 1072–1075.

Carroll, R. D., Scott, J. H., and Cunningham, D. R., 1966, Elastic moduli of granitic rock from in situ measurements of seismic velocity, *in* Geological Survey research 1966: U.S. Geol. Survey Prof. Paper. 550–C, p. C25–C28.

Colorado Department of Highways, 1965, Engineering and construction report of Straight Creek pilot tunnel: 44 p.

Cooper, H. H., Jr., Bredehoeft, J. D., and Papadopulos, I. S., 1966, Response of a finite-diameter well to an instantaneous charge of water: Water Resources Research, v. 3, no. 1, p. 263–269.

Davis, S. N., and Turk, L. J., 1963, Some hydrologic characteristics of crystalline rocks: Palo Alto, Calif., Hazelton–Nuclear Science Corp., HNS–38, 32 p.

Drake, R. E., 1967, A surface-subsurface measurement of an anomaly in the vertical gradient of gravity near Loveland Pass, Colorado: Riverside, California Univ. M.A. thesis.

Efroymson, M. A., 1960, Multiple regression analysis, *in* Ralston, Anthony, and Wilf, Herbert, eds., Mathematical methods for digital computers: New York, John Wiley & Sons, Inc., p. 191–201.

Fenner, R. 1938, Untersuchungen zur Erkenntnis des Gebirgsdruckes: Glückauf, v. 74, p. 681–695, 705–715.

Fyfe, W. S., Turner, F. J., and Verhoogen, John, 1958, Metamorphic reactions and metamorphic facies: Geol. Soc. America Mem. 73, 259 p.

Grosvenor, N. E., and Abel, J. F., Jr., 1966, Measurement on the pilot bore for the Straight Creek Tunnel, *in* Rock mechanics: Highway Research Rec. 135 (Natl. Research Council–Natl. Acad. Sci. Pub. 1379), p. 27–34.

Harrison, J. E., and Moench, R. H., 1961, Joints in Precambrian rocks, Central City–Idaho Springs area, Colorado: U.S. Geol. Survey Prof. Paper 374–B, 14 p.

Harrison, J. E., and Wells, J. D. 1956, Geology and ore deposits of the Freeland-Lamartine district, Clear Creek County, Colorado: U.S. Geol. Survey Bull. 1032–B, p. 33–127.

_____1959, Geology and ore deposits of the Chicago Creek area, Clear Creek County, Colorado: U.S. Geol. Survey Prof. Paper 319, 92 p.

Hartmann, B. E., 1966, Rock-mechanics instrumentation for tunnel construction: Wheat Ridge, Colo., Terrametrics, Inc., 153 p.

Hedge, C. E., 1968, Precambrian geochronology of the central Front Range, Colorado [abs.]: Geol. Soc. America Spec. Paper 115, p. 423.

_____1970, Whole-rock Rb-Sr age of the Pikes Peak batholith, Colorado, *in* Geological Survey research 1970: U.S. Geol. Survey Prof Paper 700–B, p. B86–B89.

Howell, B. F. Jr., 1959, Introduction to geophysics: New York, McGraw-Hill Book Co., 399 p.

Hurr, R. T., and Richards, D. B., 1966, Ground-water engineering of the Straight Creek tunnel (pilot bore), Colorado: Assoc. Eng. Geologists Eng. Geology Bull., v. 3, nos. 1, 2, p. 80–90.

Jaeger, J. C., 1962, Elasticity, fracture and flow with engineering and geological applications: 2d ed., New York, John Wiley & Sons, Inc., 208 p.

Jamieson, J. C., and Hoskins, Hartley, 1963, The measurement of shear-wave velocities in solids using axially polarized ceramic transducers: Geophysics, v. 28, no. 1, p. 87–90.

Knechtel, M. M., and Patterson, S. H., 1952, Bentonite deposits of the Yellowtail district, Montana and Wyoming: U.S. Geol. Survey Circ. 150, 7 p.

Kujundžić, Bratislav, and Čolić, Bratislav, 1959, Determination of the elastic modulus of rocks and of the depth of the disaggregated zone in hydraulic pressure tunnels by means of the seismic-refraction method: Belgrade, Yugoslavia, Inst. Hydraulic Eng. Trans., no. 8.

Lambe, T. W., 1960, The character and identification of expansive soils: Federal Housing Adm. Tech. Studies Rept. FHA–701, 46 p.

Lee, F. T., and Nichols, T. C., Jr., 1966, Rupture phenomena in the Silver Plume Granite, Colorado, *in* Geological Survey research 1966: U.S. Geol. Survey Prof. Paper 550–C, p. C29–C33.

Lovering, T. S., 1928, Geology of the Moffat Tunnel, Colorado: Am. Inst. Mining Metall. Engineers Trans., v. 76, p. 337–346.

_____1935, Geology and ore deposits of the Montezuma quadrangle, Colorado: U.S. Geol. Survey Prof. Paper 178, 119 p.

Lovering, T. S., and Goddard, E. N., 1950, Geology and ore deposits of the Front Range, Colorado: U.S. Geol. Survey Prof. Paper 223, 319 p.

McKinstry, H. E., 1948, Mining geology: New York, Prentice-Hall, 680 p.

Miesch, A. T., and Connor, J. J., 1968, Stepwise regression and nonpolynominal models in trend analysis: Kansas Geol. Survey Computer Contr. 27, 40 p.

Mitchell, L. J., 1954, Dynamic testing of materials: Highway Research Board 33d Ann. Mtg., Proc., p. 242–258.

Moench, R. H., 1964, Geology of Precambrian rocks, Idaho Springs district, Colorado: U.S. Geol. Survey Bull. 1182–A, 70 p. [1965].

Moench, R. H., Harrison, J. E., and Sims, P. K., 1962, Precambrian folding in the Idaho Springs–Central City area, Front Range, Colorado: Geol. Soc. America Bull., v. 73, no. 1, p. 35–58.

Nichols, T. C., Jr., and Lee, F. T., 1966, Preliminary appraisal of applied rock mechanics research on Silver Plume Granite, Colorado, *in* Geological Survey research 1966: U.S. Geol. Survey Prof. Paper 550–C, p. C34–C38.

Pavlo, E. Lionel, Engineering Co., 1960, Interstate Highway location study, Dotsero to Empire Junction [Colorado]: Colorado Dept. Highways State Proj. HPS–1–(20), 38 p.

Peterman, Z. E., Hedge, C. E., and Braddock, W. A., 1968, Age of Precambrian events in the northeastern Front Range, Colorado: Jour. Geophys. Research, v. 73, no. 6, p. 2277–2296.

Pirson, S. J., 1963, Handbook of well log analysis for oil and gas formation evaluation: Englewood Cliffs, N.J., Prentice-Hall, 326 p.

Plouff, Donald, 1961, Gravity profile along Roberts Tunnel, Colorado, *in* Short papers in the geologic and hydrologic sciences: U.S. Geol. Survey Prof. Paper 424–C, p. C263–C265.

Proctor, R. V., and White, T. L., 1946, Rock tunneling with steel supports: Youngstown, Ohio, Commercial Shearing & Stamping Co., 271 p.

Reichmuth, D. R., 1968, Point load testing of brittle materials to determine tensile strength and relative brittleness, Chap. 7, *in* Status of practical rock mechanics — Symposium on Rock Mechanics, 9th, Golden, Colo., 1967, Proc.: New York, Am. Inst. Mining, Metall., and Petroleum Engineers, P. 134–160.

Richards, D. B., 1963, Engineering geology of the proposed Straight Creek Tunnel, Clear Creek and Summit Counties, Colorado: Colorado School Mines unpub. M.S. thesis T–982, 131 p.

Robinson, C. S., Carroll, R. D., and Lee, F. T., 1964, Preliminary report on the geologic and geophysical investigations of the Loveland basin landslide, Clear Creek Country, Colorado: U.S. Geol. Survey open-file report, 5 p.

Robinson, C. S., and Lee, F. T., 1962, Geology of the Straight Creek Tunnel site, Clear Creek and Summit Counties, Colorado, and its predicted effect on tunnel construction: U.S. Geol. Survey open-file report, 41 p.

———1964a, Engineering geology of Straight Creek Tunnel site, Colorado, *in* Symposium on soil exploration, Atlantic City, N.J., 1963: Am. Soc. Testing and Materials Spec. Tech. Pub. 351, p. 17–28.

———1964b, Geologic research at the Straight Creek Tunnel site, Colorado: Highway Research Rec. 57 (Natl. Acad. Sci.–Natl. Research Council Pub. 1241), p. 18–34.

———1965, Preliminary report on the engineering geology of the Straight Creek Tunnel pilot bore, Clear Creek and Summit Counties, Colorado: U.S. Geol. Survey open-file report, 34 p.

———1967, Results of geologic research at the Straight Creek Tunnel pilot bore, Colorado: Highway Research Rec. 185 (Natl. Acad. Sci.–Natl. Research Council–Natl. Acad. Eng. Pub. 1516), p. 9–19.

Robinson, C. S., Lee, F. T., Moore, R. W., Carroll, R. D., Scott, J. H., Post, J. D., and Bohman, R. A., 1972, Geological, geophysical, and engineering investigations of the Loveland basin landslide, Clear Creek County, Colorado, 1963–65: U.S. Geol. Survey Prof. Paper 673, 41 p.

Roman, Irwin, 1960, Apparent resistivity of a single uniform overburden: U.S. Geol. Survey Prof. Paper 365, 99 p.

Scott, J. H., and Carroll, R. D., 1967, Surface and underground geophysical studies at Straight Creek Tunnel site, Colorado: Highway Research Rec. 185 (Natl. Acad. Sci.–Natl. Research Council–Natl. Acad. Eng. Pub. 1516), p. 20–35.

Scott, J. H., Lee, F. T., Carroll, R. D., and Robinson, C. S., 1968, The relationship of geophysical measurements to engineering and construction parameters in the Straight Creek Tunnel pilot bore, Colorado: Internat. Jour. Rock Mechanics and Mining Sci., v. 5, p. 1–30.

Sims, P. K., Drake, A. A., Jr., and Tooker, E. W., 1963, Economic geology of the Central City district, Gilpin County, Colorado: U.S. Geol. Survey Prof. Paper 359, 231 p.

Sims, P. K., and Gable, D. J., 1964 Geology of the Precambrian rocks, Central City district, Colorado: U.S. Geol. Survey Prof. Paper 474–C, 52 p.

Stallman, R. W., and Papadopulos, I. S., 1966, Measurement of hydraulic diffusivity of wedge-shaped aquifers drained by streams: U.S. Geol. Survey Prof. Paper 514, 50 p.

Terrametrics, Inc., 1964, Rock mechanics instrumentation, Straight Creek Tunnel Pioneer bore: Monthly Repts. to Colorado Dept. Highways, Jan,–Nov.

Terzaghi, Karl, 1946, Introduction to tunnel geology *and* Rock defects and loads on tunnel supports, *in* Proctor, R. V., and White, T. W., Rock tunneling with steel supports: Youngstown, Ohio, Commercial Shearing & Stamping Co., p. 15–99.

Tippetts-Abbett-McCarthy-Stratton, Engineers, 1965, Research investigations and studies to establish the ventilation requirements for the Straight Creek Highway Tunnels, Colorado, Proj. No. I70–3(13)212: New York, Rept. prepared for Colorado Dept. Highways and Bur. Public Roads, 149 p.

Tweto, Ogden, and Sims, P. K., 1963, Precambrian ancestry of the Colorado mineral belt: Geol. Soc. America Bull., v. 74, no. 8, p. 991–1014.

Wahlstrom, E. E., 1962, Geological aspects of construction of the Harold D. Roberts Tunnel: Soc. Mining Engineers Trans., v. 223, no. 3, p. 291–303.

———1964, The validity of geologic projection — A case history: Econ. Geology, v. 59, no. 3, p. 465–474.

Wahlstrom, E. E., and Hornback, V. Q., 1962, Geology of the Harold D. Roberts Tunnel, Colorado — West portal to station 468+49: Geol. Soc. America Bull., v. 73, no. 12, p. 1477–1498.

Wahlstrom, E. E., and Kim, O. J., 1959, Precambrian rocks of the Hall Valley area, Front Range, Colorado: Geol. Soc. America Bull., v. 70, no. 9, p. 1217–1244.

Wahlstrom, E. E., Robinson, C. S., and Nichols, T. C., Jr., 1968, Swelling of rocks in faults in the Roberts Tunnel, Colorado: Geol. Soc. America Eng. Geology Case Histories, no. 6, p. 83–89.

Wahlstrom, E. E., Warner, L. A., and Robinson, C. S., 1961, Relation of supports to geology in the Harold D. Roberts Tunnel, Colorado, *in* Short papers in the geologic and hydrologic sciences: U.S. Geol. Survey Prof. Paper 424–B, p. B303–B306.

Wantland, Dart, 1964, Geophysical measurements of rock properties in situ, *in* State of stress in the Earth's crust — Internat, Conf., Santa Monica, Calif., 1963, Proc.: New York, Elsevier Publishing Co., p. 408–448.

Warner, L. A., and Robinson, C. S., 1967, Geology of the Harold D. Roberts Tunnel, Colorado — Station 468+49 to East Portal: Geol. Soc. America Bull., v. 78, no. 1, p. 87–119.

Warrick, R. E., Hoover, D. B., Jackson, W. H., Pakiser, L. C., Jr., and Roller, J. C., 1961, The specification and testing of a seismic-refraction system for crustal studies: Geophysics, v. 26, no. 6, p. 820–824.

Wells, J. D., Sheridan, D. M., and Albee, A. L., 1964, Relationship of Precambrian quartzite-schist sequence along Coal Creek to Idaho Springs Formation, Front Range, Colorado: U.S. Geol. Survey Prof. Paper 454–O, 25 p.

Wilson, J. H., and Boyd, J., 1932, Report on geophysical investigation along the Blue River diversion tunnel line, Summit County, Colorado: Prepared for Board of Water Commissioners, City and County of Denver, Colo., Sept. 1932.

Wuerker, R. G., 1956, Annotated tables of strength and elastic properties of rocks: Am. Inst. Mining Metall. Engineers, Petroleum Branch, Paper 663–G, 12 p.

Zohdy, A. A. R., 1965, The auxiliary point method of electrical sounding interpretation, and its relationship to the Dar Zarrouk parameters: Geophysics, v. 30, no. 4, p. 644–660.

INDEX

[Italic page numbers indicate major references]

☆ U.S. GOVERNMENT PRINTING OFFICE: 1974—543-583/84